"Inhibitors of cytochrome P450 enzymes CYP17 and 17β-HSD3: their role in the treatment of hormone-dependent prostate and breast cancer"

A thesis submitted in the partial fulfilment for the degree of

Doctor of Philosophy

at

KINGSTON UNIVERSITY LONDON

BY

AMMARA ABDULLAH

JULY 2012

Dedicated to my Father

(May his soul rest in peace)

DECLARATION

This thesis entitled "Inhibitors of cytochrome P450 enzymes CYP17 and 17β-HSD3: their role in the treatment of hormone-dependent prostate and breast cancer" is based upon the work conducted by the author in the School of Pharmacy and Chemistry at Kingston University London. All of the work described here is original unless otherwise acknowledged in the text or by references. None of the work has been submitted for another degree in this or any other universities.

TABLE OF CONTENTS

LIST OF FIGURES

LIST OF TABLES

ACKNOWLEDGEMENT

Thanks to Almighty Allah, the most beneficial and the most merciful who made all things possible.

It would not have been possible to write this thesis without the help and support of the kind people around me and therefore I would like to express my greatest gratitude to the people who have helped and supported me throughout my project.

Above all, I would like to thank my parents for their support and encouragement at all times. I want to pay a special thanks to my dad who is although no more with us but his undivided support and interest inspired me and encouraged me to go my own way to fulfil his and my dream, without whom I would be unable to complete my project. My mother, brothers and sister have given me their unequivocal support throughout, as always, for which my mere expression of thanks likewise does not suffice.

I am grateful to my Director of Studies, Dr. Nicholas Freestone for his continuous support, motivation and enthusiasm. I want to pay the deepest gratitude to my co-supervisors, Dr. Andrew Snabaitis and Dr. Francesca Arrigoni for their good advice, novel ideas and great help and support which has been invaluable. Their guidance helped me in all time of research and writing of this thesis. I could not have imagined having a better supervisory team for my Ph.D. without these people. Their encouragement, insightful comments and throughout support has made the hardest things easier for me during the last three years.

I am also thankful to Dr. Imran Shahid and Dr. Siamak Soltani Khandanani for providing their novel synthesised compounds for my research project. I also want to acknowledge Mr. Richard Harris and Wai Yee Lee, for their help during my initial work in the Nuclear Sciences laboratory. I also want to thank Dr. Michael Tsuang in FC201 laboratory for his help.

Many thanks to Dr. Alan Seddon and Prof. Tony Walker, from the School of Life Sciences, to allow me to use the facilities in their laboratories. I am also very grateful to Prof. Helmout Modjtahedi for providing me with the human prostate and breast cancer cell lines.

I would like to acknowledge the University of Karachi and the Higher Education Commission (HEC) of Pakistan for the financial support and awarding me with an overseas scholarship that provided the necessary financial support for this research. I also thank Mr. Tariq Aziz, the Project Director, University of Karachi, whose support and assistance were of great help during the accomplishment of my degree.

I am thankful to all my friends and colleagues in EM213 especially Dr. Abdul Waheed, Dr. Siamak Soltani, Syeda Amena Shah and Salah Breidi for providing a stimulating and fun filled environment in Kingston. I would also like to acknowledge Jason Cranfield for his help in the editing of this thesis.

My deepest and heartiest gratitude goes to two great ladies; Elena and Khatebeh, in my life who were always beside me during the happy and hard moments to push me and motivate me. Their moral support, love and care helped me overcome setbacks and stay focused. I have no words to pay my special thanks to Elena whose useful comments and suggestions in this thesis were of great help. I greatly value her friendship and I am lucky to have her in my life.

Last, but not least, my uncles, Dr. Saqib Masood and Mr. Tahir Mehmood whose endless support and encouragement always created a new passion inside me.

ABSTRACT

Androgens play an important role in the initiation and progression of hormone-dependent prostate and breast cancer. These types of cancers can be treated by androgen ablation therapy. However, androgen ablation is associated with short (2-3 years) remission of the disease. Therefore therapies that inhibit the systemic biosynthesis of androgens, by targeting the P450 enzymes (CYP17 and 17-βHSD type 3) which catalyse androgen biosynthesis, may represent a rational approach in the treatment of androgen-dependent cancer. Inhibitors of the enzyme CYP17: ketoconazole and liarozole, have been shown to decrease tumour cell adhesion to the endothelium and expression of adhesion molecules. The adhesion of cancer cells to the endothelium is an important preliminary event that underlies cancer metastasis.

Within the this study, the development of assays for the enzymes; CYP17 and 17β-HSD3 and the evaluation of a series of compounds which were designed to inhibit these enzymes have been considered. The preliminary screening of the compounds showed good inhibition of 17α-OHase and 17, 20 lyase components of the CYP17 enzyme in comparison to the reference drug, ketoconazole (KTZ). The IC_{50} of compounds 31, 34, 38, 41, 48 and 51 and KTZ was calculated as 14.40 μM, 5.82 μM, 0.18 μM, 1.35 μM, 1.21 μM, 0.50 μM and 5.65 μM respectively. However, only a few of the compounds designed to inhibit 17β-HSD3 showed ap potent inhibitory activity. Compound 132 showed the highest percentage inhibition (40.51 ± 0.14%) of 17β- HSD3 activity when compared to the reference drugs, 7-hydroxy flavone (12.90 ± 0.31%) and biacalein (13.66 ± 0.31%). CYP17 inhibitors did not have any cytotoxic effect on human cancerous and non-cancerous cell lines. The adhesion of DU145, PC3 and MCF7 to a non-stimulated HUVEC monolayers was decreased from 100 ± 0.01% cell adhesion to 60.93 ± 3.95%, 65.79 ± 9.39% and 65.12 ± 4.04% by compounds 38, 48 and 51 respectively in the absence of tumour necrosis factor alpha (TNF-α). Similarly, compounds 38, 48 and 51 showed the highest anti-adhesion effect of DU145 on stimulated HUVEC monolayers (69.85 ± 4.08%), PC3 (74.26 ± 5.42%) and MCF7 (68.98 ± 2.51%) cells respectively. Flow cytometry and immunostaining of intracellular adhesion molecules showed that CYP17 inhibitors did not have any effect on the expression of ICAM-1.

In conclusion, the synthesised compounds were found to be good inhibitors of the CYP17 enzyme with no cytotoxic and better anti-adhesion effects when compared to KTZ. Thus, these compounds can be further investigated as a therapeutic strategy against hormone-dependent prostate and breast cancer.

CHAPTER 1: GENERAL INTRODUCTION

1.1. Cancer

Cancer is the leading cause of death worldwide (Iiizumi, *et al.,* 2007; Jemal *et al.,* 2011). In 2008, approximately 12.7 million cancer cases and 7.6 million cancer deaths were reported worldwide. Breast cancer in women and lung cancer in men are the most frequently diagnosed cancers and the leading cause of cancer death. However in economically developed countries prostate cancer, in males, is a more frequent cause of cancer than lung cancer (Jemal *et al.,* 2011). In the United Kingdom, approximately 28% of all deaths are caused by cancer; as such there were 157,000 cancer deaths reported in the UK in 2010. Prostate and breast cancers are the second most leading cause of cancer deaths in men and women respectively after lung cancer. In 2010, about 10,721 (13% of total cancer cases) men and 11,556 (15%) women were diagnosed with prostate and breast cancer respectively. (Cancer Research UK, 2012).

Cancer is a group of diseases in which cells lose control of their growth which leads to uncontrolled cell division and loss of cell specificity (Eales *et al.*, 1997). Each cancer has four main features; (i) excessive cell proliferation, (ii) loss of tissue specific characteristics, (iii) invasiveness and (iv) metastasis

The progression of a normal cell towards a neoplastic (cancerous) state depends on the cell acquiring some characteristic features, also called "hallmark capabilities" of cancer (Figure 1.1). The hallmarks of cancer are comprised of six biological capabilities and include (i) sustaining proliferative signalling, (ii) evading growth suppressors, (iii) resisting cell death, (iv) enabling replicative immortality, (v) inducing angiogenesis, and (vi) activating invasion and metastasis which lead to genome instability. The escape of the immune system and reprogramming of energy metabolism are two other potential hallmarks of cancer. The resistance of cell death or apoptosis and an unrestrained cell proliferation are the two major hallmarks of cancer progression (Hanahan and Weinberg, 2000; Hanahan and Weinberg, 2011).

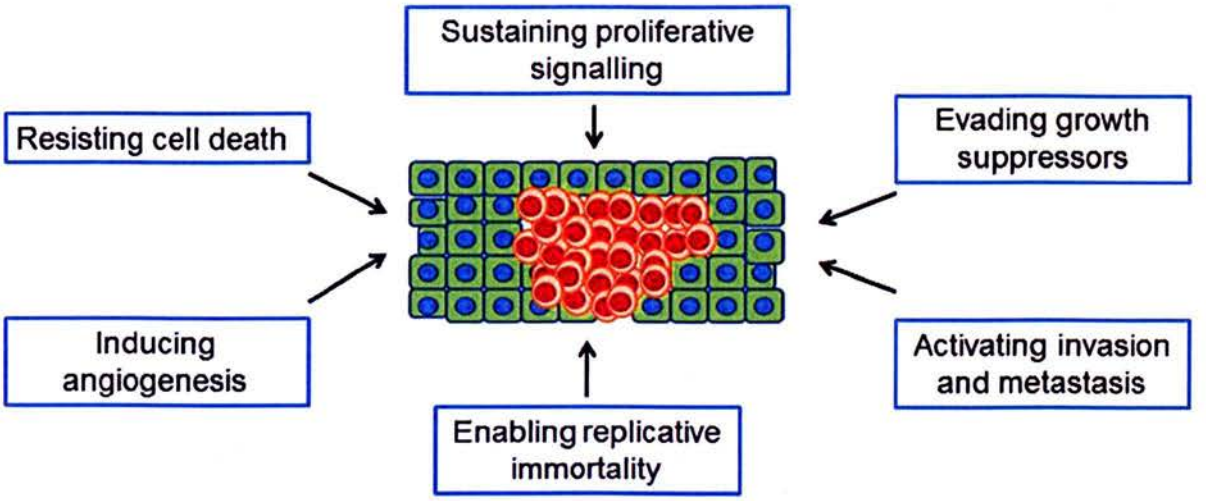

Figure 1.1: ***Hallmarks of cancer which a normal cell adopts to differentiate into a neoplastic (cancer) cell*** *(Adapted from Hanahan and Weinberg, 2011).*

1.2. Abnormalities in cell cycle leads to development of cancer

Defects in cell cycle regulation can result in cancerous growth and developmental abnormalities (Maddika *et al.,* 2007). The cell cycle in eukaryotes is divided into five phases; G_1-phase, S-phase, G_2-phase, M-phase and G_0-phase. In the G_1-phase the cell is preparing for DNA synthesis, and has diploid (2n) chromosomes. In the subsequent S-phase, DNA duplication occurs and at the end of this phase the DNA content has reached 4n. In the G_2-phase cells prepare for cell division. In the M-phase, mitosis occurs that results in the formation of two daughter cells. G_0 is a quiescent phase where cells are not actively cycling. To control the proliferation of cells, there are some control mechanisms that regulate the cell cycle. The key regulator proteins which allow the transition from one cell cycle phase to another are called cyclin-dependent kinases (CDKs). CDKs are a family of serine/threonine protein kinases which are activated at specific points during the cell cycle (Collins and Garrett, 2005).

Proteins that are involved in the control of the G_1 to S phases have been shown to be inactive in a majority of cancers. However, the inactivity of proteins that control the G_2 to M phases is less common. Any defect or abnormality in these cell cycle regulator pathways results in the uncontrolled proliferation of the cell and hence tumour formation.

Different stimuli such as DNA damage, hypoxia, and oncogene activation enhance intracellular signal transduction pathways. p53, one of the CDKs, acts as a transcription factor, integrates signals from various pathways and initiates various cellular responses that can lead to cell-cycle arrest, senescence, differentiation, DNA repair, apoptosis, and inhibition of angiogenesis. Genes encoding P*53* and BCL-2 play important key roles in apoptosis (Maddika *et al.*, 2007).

1.3. Molecular basis of cell cycle progression

Cancer occurs when the genetic information within the cell has been mutated. As a result of these mutations, the genes which control cell growth and survival have an enhanced effect whereas the genes which suppress these effects are repressed. However there are also some epigenetic (non-mutational) factors which are also responsible for cancer.

Proto-oncogenes and tumour suppressor genes are the two genes involved in the formation and progression of cancer. The mutation of proto-oncogenes gives rise to oncogenes which are responsible for uncontrolled cell division, enhanced survival and dissemination. The gene-specific mutation, gene amplification and fusion of two different genes can activate the oncogenes that have an enhanced biological activity. Tumour suppressor genes are involved in the inhibition of cell proliferation and apoptosis (Harrington, 2011).

The imbalance between cell growth and programmed cell death (or apoptosis) is the main cause of carcinogenesis (Vara *et al.*, 2004). Several signalling molecules play a critical role in controlling cell growth and cell death. Disregulation of the molecular mechanisms controlling cell cycle progression is a hallmark of cancer. Some of the important signalling mechanisms are described overleaf (Figure 1.2).

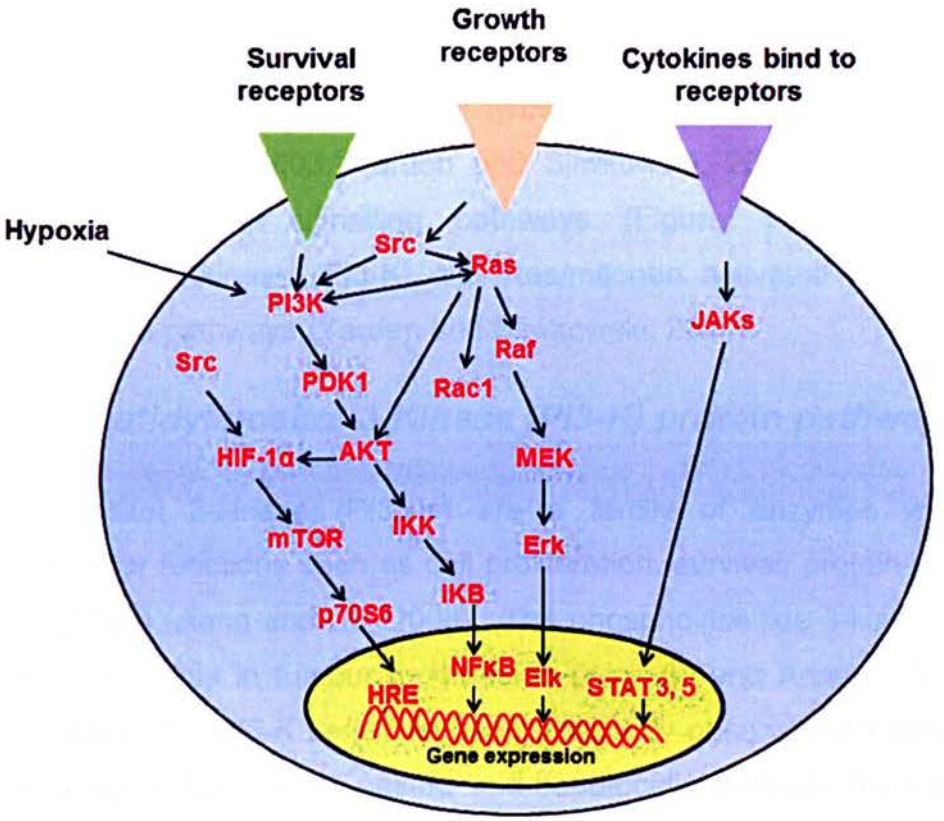

Figure 1.2: ***Schematic illustration of signal transduction pathways involved in tumour progression. All these pathways activate the transcription of proteins responsible for cell proliferation and survival.***

1.3.1. Epidermal growth factor receptor (EGFR) pathway

Growth factor peptides and their receptors are involved in cell proliferation, differentiation and survival (Yarden and Sliwkowski, 2001).

The epidermal growth factor receptors (EGFR) initiate the intracellular signalling that directs the behaviour of epithelial cells and tumours of epithelial cell origin (Herbst, 2004). EGFR belongs to a family of tyrosine kinase receptor proteins and is also known as HER-1 or c-erbB-1. EGFR is a 170-KD glycoprotein that consists of an extracellular receptor domain, a trans-membrane region, and an intracellular domain with tyrosine kinase function (Herbst, 2004; Yarden and Sliwkowski, 2001).

EGFR are of four different types: EGFR-1, EGFR-2, EGFR-3 and EGFR-4. Binding of ligands such as epidermal growth factor (EGF), transforming growth

factor (TGF-α), heparin-binding EGF-like growth factor, (HB-EGF), amphiregulin (AR), betacellulin (BTC), epiregulin (EPR), and epigen to receptors leads to dimerisation and auto-phosphorylation of tyrosine residues within tyrosine kinase receptors (Harris *et al.,* 2003; Yarden and Sliwkowski, 2001). This triggers a cascade of intracellular signalling pathways (Figure 1.2) such as the phosphatidylinositol-3-kinase (PI3-K) and Ras/mitogen activated protein kinase (MAPK) dependent pathways (Yarden and Sliwkowski, 2001).

1.3.2. Phosphatidylinositol-3-Kinase (PI3-K) protein pathway

Phosphatidylinositol 3-kinases (PI3-Ks) are a family of enzymes which are involved in cellular functions such as cell proliferation, survival, protein synthesis, and tumour growth (Jiang and Liu, 2008). The phosphoinositide 3-kinase (PI3-K) plays an important role in tumour progression (Wojtalla and Arcaro, 2011). The over-expression of the *PI3-K* gene has been frequently observed in many human cancers such as ovarian, breast, gastric, and hepatocellular carcinoma (Lee *et al.,* 2005).

Phosphatidylinositol 3-kinases have been classified into three major subfamilies according to their structure and substrate specificity. Class I PI3-Ks are activated by cell surface receptors and consist of two subfamilies, Class IA and Class IB, based on the associated adaptors (Cantley, 2002). Class IA PI3-Ks can be activated by receptor tyrosine kinases (RTKs) and Class IB PI3-Ks by G-protein-coupled receptors (GPCRs). Class I PI3-Ks are involved in the production of phosphatidylinositol 3,4-bisphosphate [PI(3,4)P2] and phosphatidylinositol 3,4,5-trisphosphate [PI(3,4,5)P3] from phosphatidylinositol-4,5-bisphosphate [PI-(4,5)-P2] (Engelman and Cantley, 2006; Hennessy *et al.,* 2005). Class I PI3-Ks are involved in a number of cellular functions including cell growth, proliferation, and survival (Jiang and Liu, 2008). Class II PI3-Ks consist of PIK3C2α, PIK3C2β and PIK3C2γ isoforms. Class II PI3-Ks can also be activated by tyrosine kinase receptors, cytokine receptors and integrins (Urso *et al.,* 1999). The class III PI3-Ks are involved in the regulation of mammalian target of rapamycin (mTOR) protein synthesis in response to cellular stress. The mTOR is involved in cell growth and differentiation (Cantley, 2002).

Activation of EGFR protein tyrosine kinase receptors leads to auto-phosphorylation of Tyr992, Tyr1068, and Tyr1173 which leads to allosteric activation of the catalytic subunit within PI3-K. PI3-K directly bind to phosphotyrosine residues (Tyr992, Tyr1068, and Tyr1173) of EGFR receptors. (Vara *et al.*, 2004; Sordella *et al.*, 2004). This causes the release of a secondary messenger (PIP3) (Figure 1.2). The PIP3 initiates a subset of signalling proteins including phosphoinosititde-dependent kinase- 1 (PDK1) and protein kinase B/Akt (Vara *et al.*, 2004).

1.3.3. Protein Kinase B (PKB)/ Akt pathway

Akt mediates the activation and inhibition of several targets, resulting in cellular survival, growth and proliferation through various mechanisms (Bianco *et al.*, 2006; Vara *et al.*, 2004). Akt, known as protein kinase B (PKB), is a serine threonine protein kinase. Akt interacts with PIP3 (Figure 1.2) following activation by growth factor receptors (Bianco *et al.*, 2006). Akt phosphorylates and regulates mammalian target of rapamycin (mTOR) which controls cell growth and proliferation (Sansal and Sellers, 2004; Bjornsti and Houghton, 2004).

1.3.4. p21Ras protein pathway

The growth factor receptors, cytokines (IL-2, IL-3) and hormones (insulin, insulin-like growth factor-IGF) activate small GTPase proteins in the cell, one of which is known as Ras or retrovirus-associated DNA sequences. The activated Ras is bound to GTP whereas the inactive form is GDP-bound. The activated GTP-bound Ras (Figure 1.2) transmits a signal to the Raf-1 protein which further activates several downstream effector pathways that mediate cell proliferation and suppression of apoptosis (Shields *et al.*, 2000).

1.3.5. Janus Kinase (JAK) protein pathway

Cytokines released by cells bind to cell surface receptors. This causes an oligomerisation and activation of the Janus kinase (JAK) family of tyrosine kinases. Activated JAKs (Figure 1.2) phosphorylate STATs (signal transducers and activators of transcription) which then dimerise and subsequently migrate to the nucleus where they regulate gene transcription (Valentino and Pierre, 2006).

1.3.6. Src protein pathway

Src is a tyrosine kinase protein that plays a major role in the regulation of cell proliferation, differentiation, migration, adhesion, invasion and angiogenesis. It is called Src after the name of a Rous sarcoma virus (Lieu and Kopetz, 2010). Binding of a ligand to growth factor receptors and integrins and cellular stress activates Src and it undergoes auto-phosphorylation of tyrosine at position 416 (Roskoski, 2005). This leads to the activation of several downstream signalling pathways that include PI3-K/Akt, Ras/Raf/MAPK, and STAT3/STAT5B pathways (Lieu and Kopetz, 2010).

1.3.7. Protein Kinase C (PKC) pathway

PKC belongs to a class of serine–threonine kinases encompassing at least 12 closely related isozymes. Activation of cell surface receptors, such as EGFR and platelet-derived growth factor receptor (PDGFR), triggers the phospholipase C to produce diacylglycerol (DAG) which binds and activates PKC (Mackay and Tweleves, 2003). PKC then activates the downstream pathways which include extracellular related kinase 1/2 (ERK 1/2), glycogen synthase kinase-3 beta (GSK-3β) and nuclear factor kappa beta (NFκB). The activities of these downstream pathways are involved in cell proliferation and cell survival. (Koivunen *et al.,* 2006).

1.4. Metastasis of cancer

Most cancer patients die because of the spreading of malignant cells from the primary tumour to distant sites of the body, a process called metastasis (Geiger and Pepper, 2009). It is a multi-step process during which malignant cells escape from the primary site and enter into the blood or lymph vessels and then disseminate to organs distal to the primary tumour (Park *et al.*, 2009).

All the steps of metastasis (Figure 1.3) are connected through a series of adhesive interactions, invasive processes and responses to chemotactic stimuli (Brooks *et al,* 2010). The different steps of metastasis are defined by Chambers *et al.* (2002) and Fidler (2003) as follows:

- Angiogenesis which is defined as the development of new blood vessels around tumour cells.

- Detachment and escape of cancer cells from the primary tumour
- Tumour cell invasion and migration
- Intravasation of tumour cells into the blood or lymphatic vessels
- Adhesion of tumour cells to the endothelial cells of the blood capillaries that surrounds the target organ
- Extravasation of tumour cells from blood vessels to tissues for secondary growth
- Formation of secondary tumour

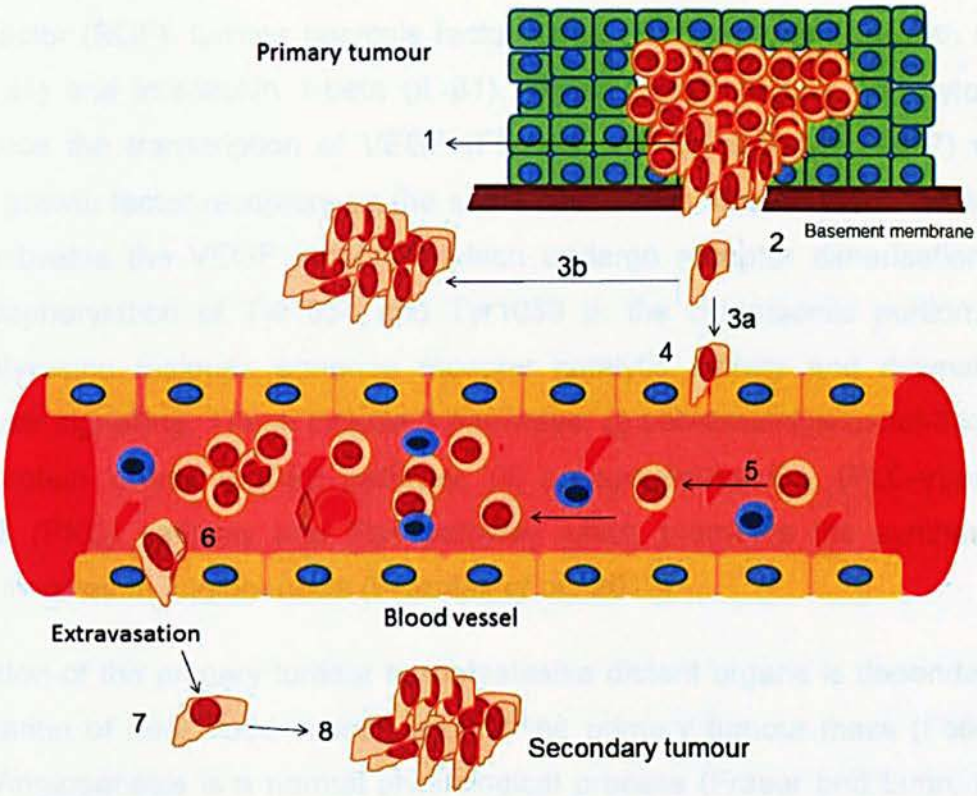

Figure 1.3: ***The metastatic cascade****. (1) Cells in the primary tumour undergo epithelial mesenchymal transition (EMT) (2) that is followed by degradation of basement membranes and remodeling of the extracellular matrix (ECM). (3a) Tumour cells invade surrounding tissue as single cells (3b) or collectively (4). Tumour cells intravasate into newly formed vessels. (5) Tumour cells are transported through the vasculature (6) and arrest in a capillary bed where they extravasate. (7) Extravasated tumour cells can stay dormant for years (8) but some disseminated cells grow out to a secondary tumour / macro metastasis (Adapted from Geiger and Peeper 2009).*

1.4.1.Angiogenesis

Tumour cells cannot obtain oxygen and nutrients by diffusion, after they have grown more than $1mm^3$ in size. As a result of this, many tumour cells secrete angiogenic factors such as vascular endothelial growth factor (VEGF) which stimulate the formation of vessels around the tumour. This process is called angiogenesis (Ferrara, 2002).

The process of angiogenesis is initiated by hypoxia. As a result of hypoxia, hypoxia inducible factor (HIF-α) translocates to the nucleus where it binds with HIF-β and forms HIF which interacts with the transcription site of DNA and induces VEGF expression (Forsythe *et al.,* 1996). Tumour cells secrete other growth factors and cytokines such as platelet-derived growth factor (PDGF), epidermal growth factor (EGF), tumour necrosis factor alpha (TNF-α), tumour growth factor β1(TGF-β1) and interleukin 1-beta (IL-β1). These growth factors and cytokines also induce the transcription of VEGF (Ferrara and Davis-Smyth, 1997) which binds to growth factor receptors on the same cells which secrete them. Binding of VEGF activates the VEGF receptors which undergo receptor dimerisation and auto-phosphorylation of Tyr1054 and Tyr1059 in the cytoplasmic portion. The phosphotyrosine residues enhance receptor catalytic activity and downstream intracellular signalling. These include 3 pathways: (i) phosphatidylinositol-3-kinase (PI3-K)/protein kinase B (Akt) pathway, (ii) phospholipase C-γ (PLC-γ)/protein kinase C (PKC) pathway and Ras pathway which promotes the synthesis of proteins involved in angiogenesis (Wozniak *et al.,* 2012).

Progression of the primary tumour to metastasise distant organs is dependent on the formation of new blood vessels around the primary tumour mass (Folkman, 2006). Angiogenesis is a normal physiological process (Fraser and Lunn, 2000; Reynolds and Redmer, 2001) which is normally under the control of angio-inhibitory and pro-angiogenic factors (Brooks *et al.,* 2010). Loss of these control mechanisms causes inappropriate angiogenesis in the case of many diseases including cancer (Folkman, 1995). The newly formed tumour vessels have an abnormal branching pattern with thin and leaky walls (McDonald and Baluk 2002) that provide a network for the metastatic spread of tumour cells to distant organs (Yano *et al.,* 2003).

1.4.2. Detachment of cells from the primary tumour

The next step in metastasis is the detachment of tumour cells from the primary tumour mass. Cadherins are a large family of adhesion molecules that are responsible for tight intercellular adhesion interactions. The cytoplasmic domain of cadherins interacts with the actin proteins in the cytoskeleton of cells via α- β- and γ- catenins whereas the extracellular domain binds to the cadherin of another cell. Cadherins maintain the tight intercellular interaction between tumour cells (Angst *et al.,* 2001); however the cadherin expression in the primary tumour is altered resulting in the loss of cell-cell adhesion (Brooks *et al.,* 2010). The loss or down-regulation of E-cadherin has been reported in cancers of the breast *in vivo* (Perl *et al.,* 1998) and prostate (Richmond *et al.,* 1997). This suggests that loss of tumour cell to cell adhesion in the primary mass is a consequence of reduced cadherin expression resulting in the disaggregation and dissemination of tumour cells (Brooks *et al.,* 2010).

1.4.3. Invasion and migration of tumour cells

The metastatic process requires the increased migratory and invasive capabilities of tumour cells. There are two different patterns by which tumour cells invade the surrounding tissue; single cell invasion and collective cell invasion.

Single cell invasion is the movement of isolated and dispersed tumour cells whereas in collective cell invasion, a group of cancerous cells displaces the healthy surrounding cells (Figure 1.3) (Yilmaz *et al.*, 2007; Christiansen and Rajasekaran, 2006). A single tumour cell either adopts an elongated mesenchymal morphology or crawls in an amoeboid manner (Brooks *et al.,* 2010). This mesenchymal morphology of tumour cells depends on a process called epithelial-mesenchymal transition or EMT (Christofori, 2006). The cells that undergo EMT become resistant to anoikis; which is a programmed cell death because of lack of contact between the cell and endothelial cell matrix, and therefore are less sensitive to cytotoxic drugs (Box *et al.*, 2010).

For the migration, tumour cells have to cross the barriers of collagen and elastic structures in the interstitial tissues and basement membrane (Beitz and Calabresi, 1993). The basement membrane is a specialised form of the extracellular matrix

which is 50-100nm thick and located at extracellular surfaces of both epithelial cells and capillary endothelial cells. During normal circumstances, the basement membrane is impermeable to cells and macromolecules, but it becomes permeable during metastasis (Brooks *et al.,* 2010). There are different protease enzymes which are responsible for the degradation of the extracellular matrix. These include serine thiol-proteases (Reich *et al.,* 1988), urokinase type plasminogen activator (uPA) (Dano *et al.,* 2005), metalloproteinases (Deryugina and Quigley, 2006) and cathepsins (Brooks *et al.,* 2010). It has been shown that movement of cancer cells is not always protease dependent. Cancer cells may also squeeze between and around the collagen fibres (Sahai, 2007). The endothelial cells of the lymphatic system have loose intercellular junctions; therefore it is potentially easier for tumour cells to enter into lymph compared to blood vessels (Brooks *et al.,* 2010).

Integrins are essential for cell migration and invasion because they regulate intracellular signalling pathways to control cell migration. During migration, cells are constantly making and breaking integrin contacts which activates intracellular signalling pathways. These pathways typically involve auto-phosphorylation of focal adhesion kinase (FAK) causing it to bind growth-factor-receptor-bound protein 2 (GRB2) and activate Ras protein. Activated Ras activates the Rac and phosphatidylinositol 3-kinase (PI3-K) pathway (Figure 1.2). These pathways subsequently lead to gene transcriptional activity and alterations in integrin affinity for ligand/cytoskeleton alterations (Hood and Cheresh, 2002).

1.4.4. Intravasation of tumour cells to surrounding tissue

After the tumour cell detaches from the primary mass it intravasates into blood and the lymphatic system. During intravasation, tumour cells come in contact with the tumour associated microvasculature (Spano *et al.,* 2012). The tumour cells invade and traverse across the basal lamina of the endothelium and then migrate between the endothelial cells of the blood capillaries (Quigley and Armstong, 1998; Sahai, 2005). Tumour-associated macrophages (TAMs) have been shown to guide tumour cells to the blood vessels and sites of intravasation via a paracrine interaction between carcinoma cells and macrophages (Wyckoff *et al.*, 2007). The intravasated tumour then releases neoplastic cells into the blood which disperse to

all tissues of the body via the circulatory system (Quigley and Armstong, 1998). In the blood circulation, the tumour cells come in contact with platelets, leukocytes and vascular endothelium. These interactions protect the tumour cells from the immune system (Brooks *et al.*, 2010).

1.4.5. Adhesion of tumour cells to endothelial cells

The adhesive properties of tumour cells are critical parameters for the development of metastasis (Price and Thompson, 2002). The interaction of malignant cells from the primary tumour to the endothelial cells of the blood vessels is one of the important preliminary events that cause metastasis (Geng 2003; Haddad *et al.*, 2010).

Adhesion of cancer cells to endothelial cells has been described as one of the fundamental molecular steps that lead to intravasation of tumour cells into blood or lymphatic vessels (Laubli and Borsig, 2010). The extravasation of circulating tumour cells in the host organ also depends on adhesive interactions between endothelial cells and cancer cells (Figure 1.4) (Gout and Huot, 2008).

Al-Mehdi *et al.* (2000) used intravital videomicroscopy to observe the adhesion of tumour cells to blood capillaries in intact mouse lung. Tumour cells were transfected with green fluorescent protein (GFP) and injected into a mouse. Most of the tumour cells were found attached to the endothelium of blood capillaries. They also found that tumours proliferate before extravasation (Al-Mehdi *et al.*, 2000). This suggests that the tumour cells interact with the endothelial cell to facilitate cell proliferation and prevent programmed cell death (Iiizumi *et al.*, 2007). Chotard-Ghodsnia *et al.* (2007) have also developed an *in vitro* model of fluorescent labelled tumour cells interacting with endothelial cell membranes (Chotard-Ghodsnia *et al.*, 2007). In this study, HT 29 LMM colorectal carcinoma cells were also found to interact with the pulmonary vascular endothelium a few minutes after these cells were injected into male Sprague-Dawley rats in an intra-vital *in-situ* study. (Gassmann *et al.*, 2010). The study also reports that a tumour cell has the specificity to metastasise towards a specific organ. The metastasis of tumour cells towards a specific organ has been explained by "the seed and soil" theory proposed by Paget (1889) which states that a secondary tumour is

established only if the microenvironment of the target site ("the soil") is compatible with the properties and requirements of the disseminated tumour cell ("the seed") (Paget, 1889).

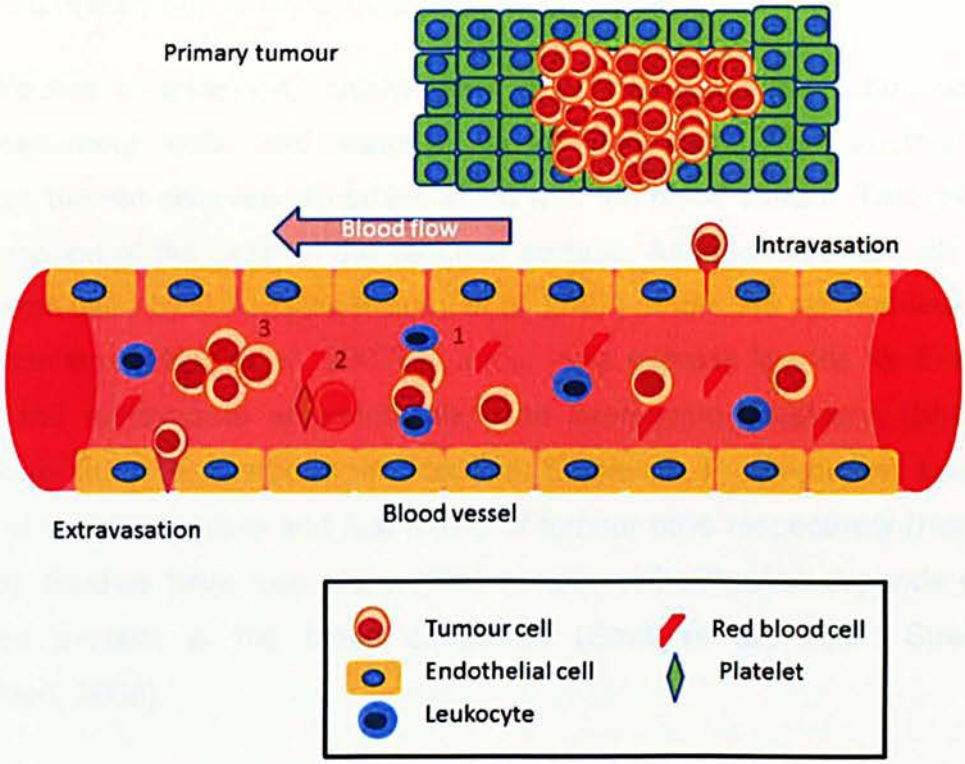

Figure 1.4: ***Cancer cell interaction with the endothelium of blood capillaries before intravasation and extravasation.*** *Cancer cells escape from the primary site and enter into the blood circulation via their interaction with endothelial cells of the blood capillary. 1) Tumour cells attached to the leukocytes 2) tumour cells attached to the platelets and 3) the tumour cells grow in the blood circulation of the capillary bed and then attach to the endothelium to disseminate to far organs.*

1.4.5.1. Leukocyte-endothelial cell interaction as a model to study tumour cell interaction

Leukocyte interaction with endothelial cells has been used as a model to study tumour cell interaction with the endothelium (Hashimoto *et al.,* 2004; Sheikh *et al.,* 2005; Cinamon *et al.,* 2004; Al-Mehdi *et al.,* 2000). Leukocytes escape the blood circulation in order to reach the tissue sites of inflammation, infection or injury while tumour cells are disseminated by the circulation for the development of metastatic tumours (Strell and Entschalden, 2008). Similar to neutrophil extravasation at sites of inflammation, tumour cells initially adhere to the

endothelium forming loose interactions via adhesion molecules before rolling and finally forming firm attachments, prior to diapedesis and extravasation of cells. The tumour cells adhere to the endothelial cells of blood vessels in the same way as leukocytes do because many cancer cells express similar adhesion molecules that are also expressed on the leukocytes. (Iiizumi *et al.*, 2007).

In the process of adhesion, initially there is a very loose interaction between leukocytes/tumour cells and vascular endothelial cells. Due to this loose interaction, tumour cells are still pulled along with the blood stream. This results in a rolling motion of the cells on the vascular surface. Although tumour cells mimic mechanisms used by leukocytes (Iiizumi *et al,* 2007) others are still non-leukocyte-like mechanisms (Miles *et al.,* 2008). Tumour cells express ligands for E-selectin and roll and extravasate at endothelial sites expressing E-selectin (Strell and Entschalden, 2008). It has been reported that E-selectin, P-selectin and L-selectin mediate slow, intermediate and fast rolling of tumour cells respectively (Hanley *et al.,* 2006). Studies have also shown that tumour cell adhesion depends on the leukocytes present in the blood circulation (Strell *et al.*, 2007; Strell and Entschalden, 2008).

During the rolling step, integrins on leukocytes are activated and then bind to their counterparts on the endothelial cells (Strell and Entschalden, 2008). Chemokines are the most powerful physiological activators of integrin-mediated adhesion (Constantin *et al.,* 2000). Expression of integrins was also reported on the tumour cell surface of human melanomas and sarcomas but the process in tumour cells is not as yet clearly defined as in leukocytes (Strell and Entschalden, 2008).

1.4.5.2. Molecular pathways leading to cell adhesion

The process of cancer cell adhesion is regulated by cancer cells themselves through intracellular signals that regulate the binding affinity of matrix proteins (Basson, 2007). These pathways involve activation of focal adhesion kinase (FAK) and Src activation. These signals are stimulated by increased extracellular pressure and laminar or non-laminar shear stress (Thamilselvan and Basson, 2007).

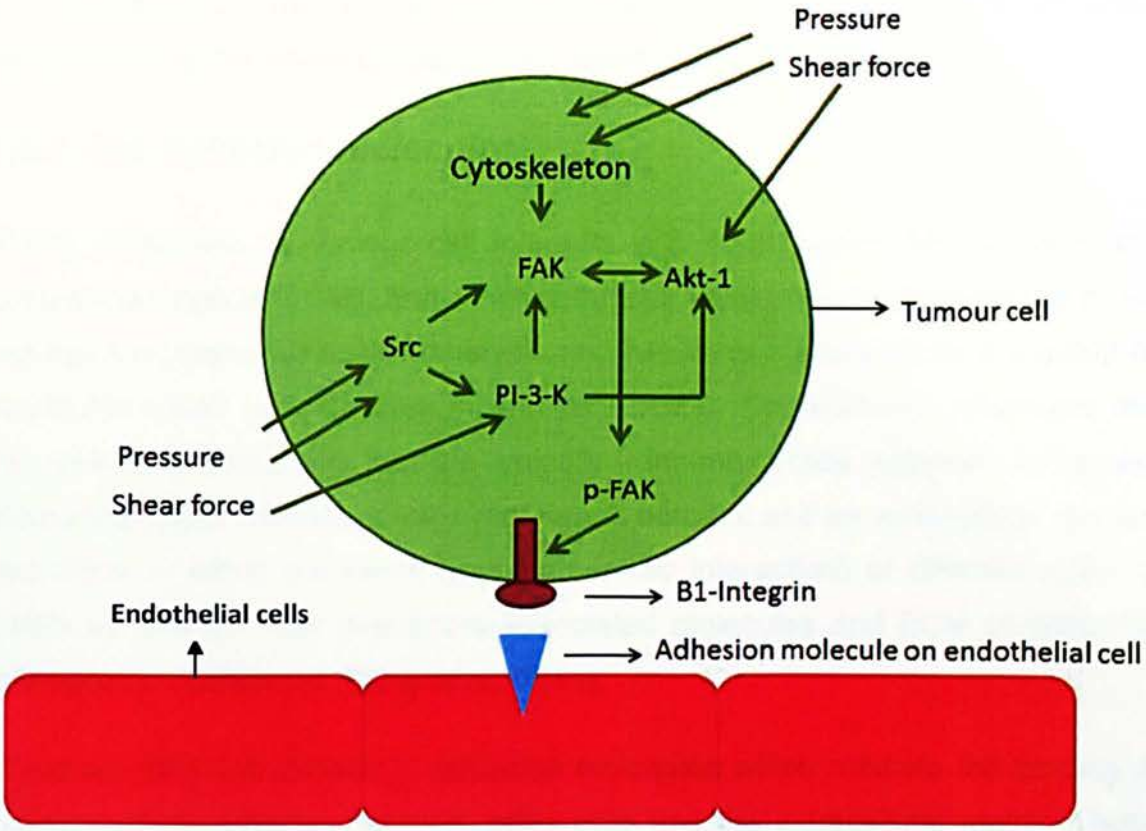

Figure 1.5: ***FAK cascade that regulates cell adhesion.*** *The external pressure on the cell activates Src, PI3-K and Akt1 proteins. The cytoskeleton transfers signals of extracellular shear force to focal adhesion kinase (FAK). The Src and PI3-K, together with FAK, activate Akt-1. This results in the phosphorylation of FAK and subsequent increase in integrin binding affinity for the substrates.*

The microenvironment of tumours is characterised by a state of hypoxia, low extracellular pH and high glycolysis which produce a stressful environment around the tumour cell (Brahimi-Horn and Pouyssegur, 2006). The Src protein and cytoskeleton of the cell is an active sensor for the external forces (Thamilselvan and Basson, 2005). Cellular stress activates Src and it undergoes auto-phosphorylation of tyrosine at position 416. This leads to the activation of several downstream pathways that include PI3-K/Akt, Ras/Raf/MAPK, and STAT3/STAT5B pathways (Lieu and Kopetz, 2010). The signalling molecules Src and PI3-K interact with focal adhesion kinase (FAK) in a complex manner which results in the activation of Akt (Basson 2008). PI3-K and Akt are also activated by extracellular pressure (Thamilselvan and Basson, 2007). These events increase the proportion of phosphorylated FAK, resulting in FAK activation associates with β1-integrin heterodimers, increasing integrin binding affinity for substrate (Figure

1.5). Binding of β1-integrin induces the activation of kinases within focal adhesion complexes and the whole cascade starts again (Basson, 2008).

1.4.6. Cell adhesion molecules

During metastasis, a tumour cell interacts with neighbouring tumour cells, the extracellular matrix (ECM), and other cell types within the microenvironment. An important regulator for such homotypic and heterotypic interactions is a group of molecules called cell adhesion molecules (CAMs). Cell adhesion molecules are cell surface glycoproteins that are typically trans-membrane receptors composed of an intracellular domain, a trans-membrane domain, and an extracellular domain that binds to either the same type (homophilic interaction) or different types of CAMs as well as other membrane-associated molecules and ECM components (heterophilic interaction) (Feng *et al.,* 2011).

There are different classes of adhesion molecules which mediate the binding of tumour cells to adjacent tumours, other cells and the extracellular matrix. These include; (i) vascular cell adhesion molecule-1 (VCAM-1), (ii) intracellular adhesion molecule -1 (ICAM-1) (immunoglobulin super-families), (iii) cadherins, (iv) integrins and (v) selectin (Bogenrieder and Herlyn, 2003; Haass *et al.*, 2005 Park, 2009). Cancer patients have been reported as having increased levels of ICAM-1 and VCAM-1. These increased levels correlate with the tumour progression (Gallicchio *et al.*, 2008).

1.4.6.1. Cadherins in cell adhesion

There are two classes of cadherins: classical and non-classical (Cavallaro and Christofori, 2004). Classical cadherins are Ca^{2+}-dependent transmembrane adhesion molecules. They are involved in homophilic cell to cell interactions. E-cadherin and N-cadherin are two such classical cadherin proteins (Cavallaro and Christofori, 2004; Kilsdonk *et al.,* 2010).

Most cadherins are single-span trans-membrane proteins. They have an extracellular domain that contains variable numbers of Ca^{2+} binding 110 amino acid repeats known as cadherin domains (CADs). These domains are responsible for homophilic interactions (Koch *et al.,* 2004). The intracellular C-terminal domain

binds to catenin and modulates the actin cytoskeleton in the adherent junctions (Halbleib and Nelson, 2006).

Cadherins are a large family of adhesion molecules that are responsible for tight intercellular adhesion interactions (Angst *et al.,* 2001). Epithelial tumours often lose E-cadherin partially or completely as they progress toward malignancy (Christofori and Semb, 1999). Loss of E-cadherin expression leads to disruption of cell to cell contact. This results in increased dissociation, motility and dispersal of cells and hence tumour metastasis (Golias *et al.,* 2005; Brooks *et al.,* 2010). Loss of cell to cell adhesion of the tumour cells in the primary mass, due to loss of cadherin, results in the disaggregation and dissemination of tumour cells (Brooks *et al.,* 2010).

1.4.6.2. Integrins in cell adhesion

Intergrins are heterodimeric transmembrane glycoproteins that facilitate cell-cell and cell-extracellular matrix (ECM) adhesion. They regulate intracellular signalling (Schwartz *et al.,* 1995; Takagi, 2007; Paschos *et al.,* 2009). Integrins are involved in an adhesive function and the link between the extracellular matrix and actin cytoskeleton is maintained by integrins (Rathinam and Alahari, 2010). There are 24 different types of integrins, each comprised of different α and β sheets. They consist of a large extracellular transmembrane and a short cytoplasmic domain (Hynes, 2002; Paschos *et al.,* 2009). They are expressed on the surface of epithelial cells, leukocytes, platelets and tumour cells (Takagi, 2007). Integrins play an important role in each step of the cancer metastasis process including; adhesion, migration and invasion (Schneider *et al.,* 2011).

1.4.6.3. Selectins in cell adhesion

Selectins are a family of three membrane-bound calcium-dependent (C-type) lectins. They mediate the interactions of leukocytes, platelets and the endothelium (Laubli and Borsig 2010; Brooks *et al.,* 2010). Cancer cell seeding requires specific interactions with the local microenvironment that leads to tumour cell adhesion, extravasation and outgrowth in target organs (Kannagi *et al.,* 2004). Selectins mediate the initial tethering of leukocytes during the extravasation process and are involved in the transition from fast to slow rolling before the

leukocytes firmly adhere to endothelial cells (McEver, 2002). They interact with carbohydrate ligands on cancer cells (Laubli and Borsig, 2010; McEver, 1997). L-selectins are present on all myeloid cells, resting T-cells and some activated memory T-cells. P-selectin is expressed in endothelial cells of the lung, choroid plexus, megakaryocytes and thrombocytes. P-selectin is stored within the Weibel-Pallade bodies of endothelial cells or alpha-granules of platelets. E-selectin is expressed exclusively on activated endothelial cells (Kansas, 1996). Selectins are the adhesion molecules that cause leukocyte trafficking and haemostasis and are involved in the progression of many diseases such as cancer (McEver, 2002; McEver, 1997). In response to an inflammatory stimulus (e.g. TNF-α or IL-1β) E-selectin synthesis can be induced within 2-6 hours (Kansas, 1996).

1.4.6.4. Immunoglobulin-like cell adhesion molecules (Ig-CAMs)

Immunoglobulin superfamily molecules are expressed in a wide variety of cell types, including cells of the nervous system, leukocytes, epithelial and endothelial cells. Ig-CAMs exert both homophilic/heterophilic interactions and are associated with cytoskeletal proteins via intracellular signal transduction pathways (Cavallaro and Christofori, 2004).

This class of adhesion molecules are membrane proteins which are organised into β-pleated sheets. The structure of these protein molecules is defined by one or more immunoglobulin folds with two cysteine residues separated by 55-75 amino acids which are arranged as two anti-parallel β-pleated sheets. Ig-CAMS consist of a large extracellular N-terminal domain, a trans-membrane helical segment and a cytoplasmic tail (Vaughn and Bjorkman, 1996; Cavallaro and Christofori, 2004).

Alterations of cell adhesion molecule expression in the immunoglobulin superfamily also appear to play a critical role in invasion and metastasis (Skubitz, 2002). The Ig-CAMs include the intracellular adhesion molecule-1 (ICAM-1) and vascular cell adhesion molecule-1 (VCAM-1). The expression of these molecules is up-regulated as a result of inflammation in the body (Hanlon *et al.,* 2002). Both of these adhesion molecules play a role in tumour cell adhesion to the vascular endothelium, which facilitates the extravasation of tumour cells and finally the development of metastasis. The understanding of these adhesion mechanisms

and the interference in these processes can be used as a better tool for anti-cancer and anti-metastatic therapy (Hanlon *et al.,* 2002).

1.4.6.4.1. VCAM-1

VCAM-1 is a 110 KDa glycoprotein that is a widely distributed protein. It is expressed on the surface of macrophages, dendritric cells, and epithelial cells and on the surface of stimulated endothelial cells (Ding *et al.,* 2003). VCAM-1 binds to α4β1 integrin, which is constitutively expressed on lymphocytes, monocytes and eosinophils and mediates α4β1 integrin-dependent rolling-type adhesion (Chen *et al.,* 1999). It regulates leukocyte attachment and extravasation at sites of inflammation (Buul and Hordijk, 2004). Inflammatory cytokines and leukocyte attachment increases endothelial expression of VCAM-1, activates signalling cascades, results in endothelial retraction and passage of leukocytes through the endothelial barrier (Slack-Davis *et al.,* 2009).

VCAM1 mediates tumour cell adhesion to vascular endothelial cells thus promoting the metastatic process (Byrne *et al.,* 2000). VCAM-1 is involved in tumour progression and metastasis (Ding *et al,* 2003; Lu *et al,* 2011; Slack-Davis *et al,* 2009).

1.4.6.4.2. ICAM-1

Intercellular adhesion molecule-1 (ICAM-1) belongs to the immunoglobulin superfamily of adhesion molecules. It is a transmembrane glycoprotein and is composed of five extracellular IgG-like domains and a short cytoplasmic tail (Dymicka-Piekarska and Kemona, 2009).

Non-cancerous human tissues have some expression of ICAM-1. According to one study, low levels of ICAM-1 were found in human testes and thyroid while the cerebellum, parathyroid, pituitary tissues, adrenal gland and tonsils have slightly higher expression of ICAM-1. The spleen was reported to have the highest level of ICAM-1 expression. ICAM-1 expression was absent in the non-cancerous cerebrum, peripheral nerves, pancreas, ovary, breast, uterus, cervix, prostate, lung, larynx, bone marrow, striated muscle, heart, mesothelium, esophaghus, small intestine, colon and liver (Hayes and Siegel, 2009).

ICAM-1 levels were found to be significantly higher in advanced or metastatic stages of breast cancer (Hanlon *et al.,* 2002), gastric cancer, patients with liver metastasis and papillary thyroid carcinoma (Buitrago *et al.,* 2011). Hayes and Siegel have examined a broad range of both normal and malignant human tissue samples to determine the expression patterns of ICAM-1 and its association with tumour progression. ICAM-1 levels were also found up-regulated in colorectal, breast, lung, pancreas and renal cancers (Hayes and Siegel, 2009).

ICAM-1 can be used as a biomarker to assess the progression and prognosis of tumours (Buitrago *et al.,* 2011).

1.4.7. Extravasation of tumour cells to secondary sites

The process of extravasation is defined as the movement of tumour cells from blood vessels to tissues to initiate secondary metastatic outgrowth (Spano *et al.,* 2012). It is a highly dynamic process that involves the adhesion of tumour cells to the endothelium and intravascular cell migration along the luminal surface of the vascular wall (Stoletov *et al.,* 2010). Circulating tumour cells use adhesion molecules, such as selectins or intercellular adhesion molecules (ICAMs) to interact with endothelial cells (Spano *et al.,* 2012).

The binding of tumour cells to endothelial cells results in the release of cytokines and chemokines that attract macrophages. This also causes the upregulation of adhesion molecules; such as ICAM-1 on the tumour cell surface. The macrophages also produce cytokines and attract polymorpho-nuclear leukocytes (PMNs) which interact with the tumour cells through the ICAM-1 present on the tumour cell surface. The binding of PMNs and tumour ICAM-1 allows PMNs to release elastases that digest the endovascular and endolymphatic barriers hence allowing tumour cells to easily migrate through the endothelial cell barrier (Roland *et al.,* 2007).

Huh *et al* (2010) have also shown that the neutrophils facilitate cancer cell extravasation. They demonstrated that cancer cells secrete interleukin-8 (IL-8) which attracts neutrophils that promote tumour cell attachment to the vascular endothelium. The interactions between endothelial cells and cancer cells, assisted

by a release of cytokines, are the major event in extravasation (Spano *et al.*, 2012).

1.4.8. Formation of secondary tumours

The metastasis of cancer is not a random process and involves tumour cells from the primary site disseminate to a specific organ (Geiger and Peeper, 2009). The observations from different studies led to the formation of "seed and soil hypothesis" (Section 1.4.5). The endothelial cells of the vessels in different organs express different adhesion molecules which are specific to that organ (Ruoslahti and Rajott, 2000). Tumour cells with corresponding receptors can adhere to the vascular bed and form a secondary tumour (Geiger and Peeper, 2009).

1.5. Prostate cancer

Prostate cancer is a malignant tumour that consists of cells from the prostate gland. Initially, it is a slow growing cancer and asymptomatic, but as the tumour progresses, it begins to metastasise throughout the body (Payne and Hales, 2004) to organs such as the lung, liver and also bone (Payne and Hales, 2004). Prostate cancer is the most common cancer in men. It is the second commonest cause of cancer death in men after lung cancer and is mostly observed in men of 50-80 years of age (Penning *et al.*, 2008). In 2010, 40,841 new cases of prostate cancer were reported per 100,000 of population in the UK resulting in 10,721 deaths (Cancer research UK, 2012).

1.5.1. Sign and symptoms of prostate cancer

The symptoms of prostate cancer are similar to those of prostatitis and benign prostate hyperplasia (BPH). Early prostate cancer has no signs, however in later stages; the cancer shows a few symptoms (Schiller, 2010) such as:

- Frequent urination and difficulty in starting and maintaining a steady stream of urine
- Painful urination and increased urination at night
- Blood in the urine

- Advanced prostate cancer can spread to other parts of body. The most common symptoms are bone pain such as in the vertebrae, pelvis or ribs.

1.5.2. Risk factors for prostate cancer

In one study, follow-up data from health professionals showed that there are a few factors that have a high impact on prostate cancer incidence (Giovannucci *et al.*, 2007). These include:

- Age: Prostate cancer is very common in men after 50 years of age
- Race: Prostate cancer is more common in African–Americans.
- Diet: High total energy intake, α-linolenic acid and calcium are associated with an increased risk.
- Family history, smoking and being taller and having a higher BMI are other risk factors of prostate cancer.

1.5.3. Mechanism of androgen-dependent prostate cancer

Androgens are involved in the development, growth and maintenance of prostate cells and as such they have been implicated as having a causative role in prostatic diseases such as benign prostate hyperplasia (BPH) as well as prostate cancer (Luu-The *et al.,* 2008).

In the case of androgen-dependent prostate cell growth, androgen receptors play an important role as mediators of cell growth. The direct effects of testosterone and dihydrotestosterone are mediated via binding to the androgen receptor. The androgen receptor is a member of the steroid hormone receptor family of ligand-activated transcription factors (Evans, 1988). Testosterone is secreted primarily by the testes and is bound to albumin and sex-hormone-binding globulin (SHBG), with a small fraction dissolved freely in serum (Feldman and Feldman, 2001). When testosterone enters into the prostate cell (Figure 1.6), it is converted into dihydrotestosterone by the enzyme, 5α-reductase. Dihydrotestosterone is the most active hormone which stimulates the growth of hormone-dependent prostate tumours via its interaction with the androgen receptor (Day *et al.,* 2008) in the

cytoplasm. The androgen receptor has three domains; (i) ligand binding domain, (ii) transcriptional binding domain and (iii) DNA-binding domain. The binding of dihydrotestosterone to the androgen receptors causes a conformational change in receptors which causes the auto-phosphorylation of serine 81 residue. The receptor undergoes dimerisation, and subsequently translocates into the nucleus (Settlur and Rubin, 2005; Feldman and Feldman, 2001). The androgen and receptor complex binds to the androgen-response elements within the upstream promoter region of androgen-dependent genes. The androgen-receptor complex along with several co-activators and co-repressors leads to transcriptional activation and modulation of an RNA polymerase II transcription complex that can regulate the expression of androgen-regulated genes (Cano *et al.,* 2007; Feldman and Feldman, 2001).

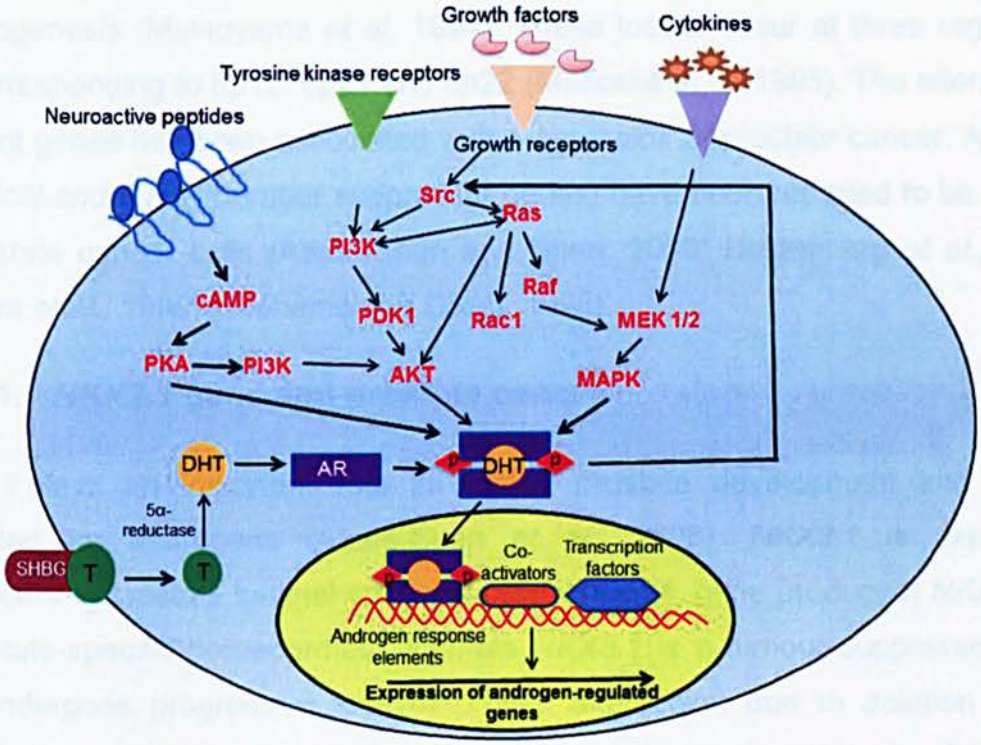

Figure 1.6: ***Role of androgens in the progression of prostate cancer.*** *The testosterone is bound to sex-hormone binding globulin (SHBG) in the blood circulation. It diffuses into the prostate cell where it is converted into dihydrotestosterone (DHT) by the enzyme 5α-reductase. The DHT activates the androgen receptors (AR) forming an androgen-receptor complex which translocates into the nucleus where it binds to the androgen response elements of DNA. Binding of different growth factors and cytokines to cell membrane receptors activates different signalling pathways that results in the translocation of the androgen-receptor complex into the nucleus which leads to transcription of different proteins involved in cell proliferation.*

Binding of different growth factors, cytokines and neuroactive peptides leads to the activation of cytoplasmic kinases (PKA, PI3-K) and second messengers (cAMP) which further activates their downstream signalling pathways. As a result of these pathways, the phosphorylated androgen receptors translocate to the nucleus. Several co-activators and co-repressors are involved in the assembly of the basal transcription machinery complex regulating androgen receptor activity (Koochekpour, 2010). Inoue and Ogawa (2011) have suggested that the androgen-androgen receptor complex activates Rac1 and Src which contributes to androgen-dependent cell proliferation.

1.5.4. Genes involved in prostate cancer development

The loss of specific regions of chromosome 8p has been reported in early prostate carcinogenesis (Matsuyama *et al,* 1994). These losses occur at three regions of 8p, corresponding to 8p12, 8p21 and 8p22 (Macoska *et al.* 1995). The alteration in different genes has been associated with progression of prostate cancer. *NKX3.1, p53, Bcl2 and PTEN* (tumour suppressor genes) have been reported to be altered in prostate cancer cells (Abate-Shen and Shen, 2000; Heidenberg *et al.,* 1995; Vlietstra *et al.,* 1998; Maehama and Dixon, 1998).

1.5.4.1. *NKX3.1* gene and prostate cancer

NKX3.1 plays an important role in normal prostate development and is up-regulated by androgens (Abate-Shen *et al.,* 2008). *NKX3.1* is expressed specifically in prostate luminal epithelial cells. NKX3.1, gene product of *NKX3.1*, is a prostate-specific homeoprotein whereas *NKX3.1* is a tumour suppressor gene that undergoes progressive loss of protein expression due to deletion of the 8p21.2 region. This results in prostate cancer progression to hormone-independence and metastasis (Swalwell *et al.,* 2002; Bowen *et al.,* 2000). Loss of function of *NKX3.1* contributes to prostate carcinogenesis (Abate-Shen *et al.,* 2008; Possner *et al.,* 2007).

1.5.4.2. *TP53* gene and prostate cancer

TP53 is a tumour suppressor gene whose inactivation is one of the main causes of cancer initiation (Aylon and Oren, 2011). *TP53* is a transcription factor which

induces G1 arrest of the cell cycle, apoptosis and DNA-repair (Maddika *et al.,* 2007). The *TP53* gene is located on chromosome 17 and is expressed in response to various stress signals such as DNA damage (Okumura *et al.,* 2011; Oldenburg *et al.,* 2011). Immunocytochemical studies have revealed that *TP53* is mutated in advanced stages of prostate cancer, as well as in recurrent and metastatic disease (Bookstein *et al.,* 1993; Effert *et al.,* 1992; Heidenberg *et al.,* 1995).

1.5.4.3. *BCL-2* gene and prostate cancer

BCL-2 regulates cell proliferation by preventing apoptosis. It is involved in the molecular biology of a wide range of human cancers. *BCL-2* affects neoplastic cell proliferation by preventing apoptosis (Catz and Jhonson, 2003). Over-expression of *BCL-2* in prostate carcinoma cells causes resistance to apoptosis (McDonnell *et al.,* 1992).

1.5.4.4. Phosphatase and tensin homologue *(PTEN)* gene and prostate cancer

PTEN is a tumour-suppresor gene which is found on chromosome 10. It suppresses cell growth by promoting apoptosis. It arrests the cell cycle at the G_1 phase and inactivation of *PTEN* results in activation of kinase signalling pathways which leads to uncontrolled cell proliferation (Okumura *et al.,* 2011). *PTEN* plays an important role in the initiation of prostate cancer. It mainly functions as a lipid phosphatase and targets phosphatidylinositol 3, 4, 5-trisphosphate (PIP-3). By dephosphorylating PIP-3, PTEN down-regulates the Akt/PKB signalling pathway that promotes cell survival and inhibits apoptosis (Maehama and Dixon, 1998).

1.5.5. Development of androgen-independent prostate cancer

In the androgen-independent pathway, prostate cancer cells grow in an androgen-depleted environment through different mechanisms which include androgen receptor gene amplification, androgen receptor gene mutations, involvement of co-regulators, ligand-independent activation of the androgen receptor, and the involvement of tumour stem cells (Chen *et al.,* 2004; Feldman and Feldman , 2001).

The amplification of the androgen receptor gene causes the increased production of androgen receptors which are sensitive to low levels of androgens (Gregory *et al.,* 2001). The mutation of the androgen receptor gene allows the androgen receptors to bind non-androgenic steroid molecules as well as anti-androgens and results in the activation of receptors. Some non-steroid molecules activate the androgen receptors by ligand-independent mechanisms (Chen *et al.,* 2004; Feldman and Feldman, 2001). Deregulated growth factors, including insulin-like growth factor, keratinocyte growth factor, and epidermal growth factor, and cytokines, including IL-6, have been shown to directly phosphorylate and activate the androgen receptor (Culig *et al.,* 1994). There are a number of co-activators and co-repressors which are involved in signalling intermediaries between the androgen receptor and the transcriptional machinery. Alterations in the balance between co-activators and co-repressors have been shown to influence androgen receptor activation (Feldman and Feldman, 2001).

1.5.6. Metastasis of prostate cancer to the bones

During the early stages of prostate cancer, some of the malignant cells remain confined to the prostate gland which later disseminate to the surrounding stroma. The tumour cells become more aggressive and start spreading to nearby organs such as the seminal vesicles and bladder. The newly formed vessels around the tumour help the tumour cells to reach the blood stream and metastasise (Koutsilieris, 1995). Most of the prostate cancer cells when entered into blood vessels will die because of two mechanisms; mechanical stress of vascular transportation and the host immune defence system (Rosol *et al.,* 2003). However some prostate cancer cells escape these two mechanisms because they circulate in the form of aggregates either with other tumour cells or with platelets. The prostate cancer cells escape the host immune system by down-regulating the expression of class I major histocompatibility complex (Bander *et al.,* 1997).

The reason why prostate cancer cells metastasise to bone has been explained by two theories. The first theory is "the seed and soil" theory proposed by Paget (1889) (Section 1.4.5). The second theory is based on the presence of a network of veins called Baston Plexus that drains the lower vertebral column pelvic girdle which receives blood from the prostate (Batson, 1967). A large number of tumour

cells were found at the interconnection between the Batson plexus and the bone marrow spaces of the vertebral column (Ghossein *et al.,* 1995). Compared to the endothelium of other organs, prostate cancer cells attach more efficiently to the bone endothelium with the help of adhesion molecules that include integrins, selectins and intracellular adhesion molecules (Lehr and Pienta, 1998). After binding to the endothelium of the bone-marrow, the prostate cancer cells produce proteases and traverse the basement membrane of the microvessels. Finally the tumour cells extravasate into the microenvironment (Koutsilieris, 1995).

1.5.7. Therapies for prostate cancer

There are two therapies for prostate cancer which have been reported to date. These are:

a) Surgical castration; including orchidectomy, which is the removal of the testicles and prostactomy, which is the removal of all or part of the prostate glands.

b) Chemical castration or hormonal therapy (Antonarakis *et al.,* 2010).

1.5.8. Hormonal therapy for prostate cancer

Gonadotrophin-releasing hormone (GnRH, also known as LHRH) is a 10-amino acid polypeptide. It is released in pulses from the hypothalamus under the feedback control of circulating androgens and oestrogens. GnRH further acts on the cells of the anterior pituitary gland which results in secretion of luteinising hormone (LH) and follicle-stimulating hormone (FSH). These two hormones then release testosterone (Figure 1.7) from the leydig cells of the testes (Marieb, 2003; Tammela, 2004) which accounts for 90% of the total testosterone in the body. Testosterone and dihydrotestosterone (DHT) are two androgens that are involved in the development, growth and maintenance of prostate cells. They have been implicated in prostatic diseases such as benign prostate hyperplasia (BPH) as well as prostate cancer (Luu-The *et al.,* 2008).

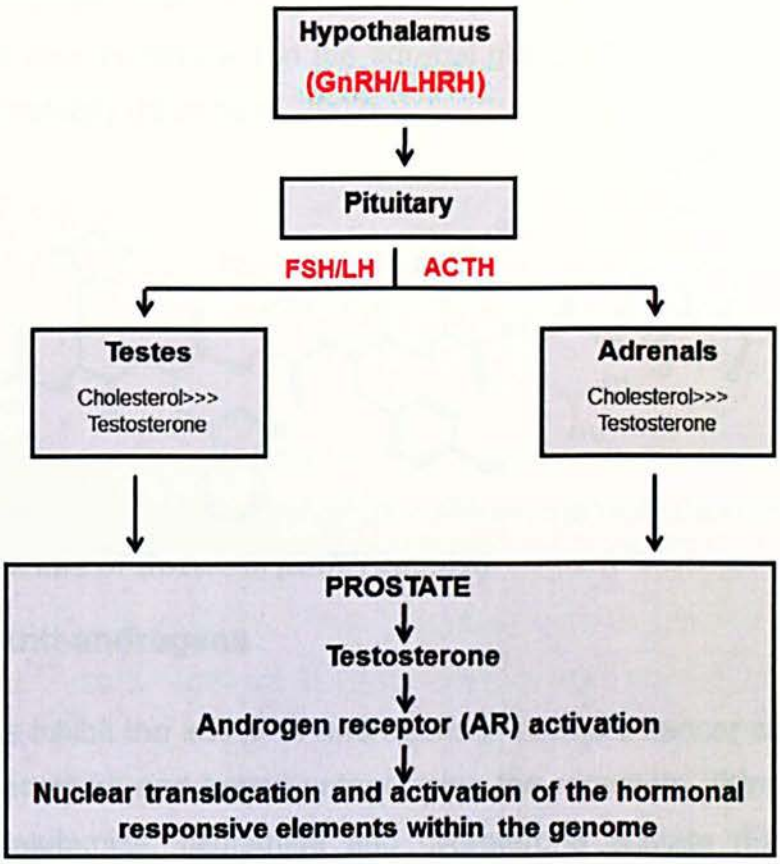

Figure 1.7: ***The hypothalamic-pituitary-gonadal axis in prostate cancer progression.*** *The GnRH/LHRH from the hypothalamus stimulates the release of FSH and LH from the pituitary that acts on the testes. The testosterone from the testes and adrenal gland acts on prostate cells where they bind to androgen receptors (adapted from Abraham and Staffurth, 2011).*

1.5.8.1. Luteinising hormone releasing hormone (LHRH) agonists

LHRH agonists include goserelin (Figure 1.8), leuprolide and triptorelin. These compounds increase the release of luteinising hormone (LH) from the pituitary gland which interacts with steroidal receptors present on the interstitial leydig cells of the testes. This leads to the synthesis and further release of testosterone (Figure 1.4). High levels of testosterone result in a negative feedback loop which inhibits the release of further LHRH from the hypothalamus as well as the release of LH from the pituitary. As a result of this, there is a dramatic decrease in the synthesis and release of testosterone from the Leydig cells. In the initial stages, this treatment results in adverse symptoms due to a large increase in testosterone levels. After sometime, however, the LHRH receptors become less responsive as a result of which androgen production is suppressed (Tammela, 2004).

Unfortunately, these drugs only affect testicular androgen production. Since androgens are also synthesised in the adrenal glands, tumour stimulation cannot be blocked completely (Hartmann, 2002).

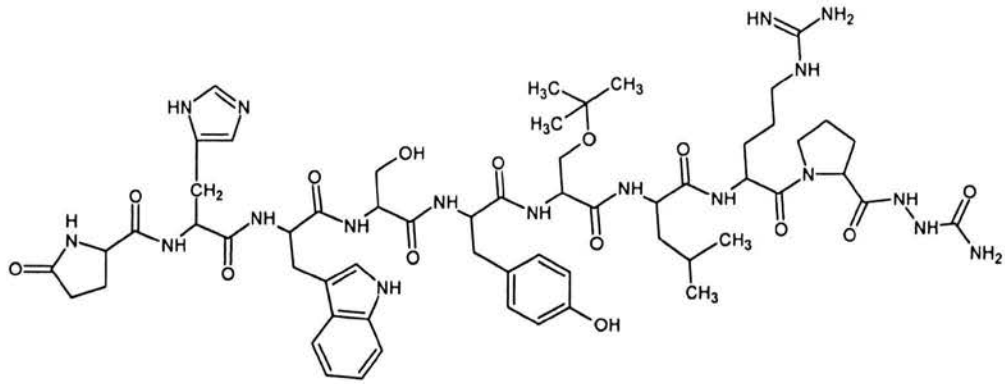

Figure 1.8: Structure of Goserelin (LHRH agonist)

1.5.8.2. Anti-androgens

Anti-androgens inhibit the action of androgens in prostate cancer cells by binding to androgen receptors and hence antagonising the receptors. (Kim *et al.,* 2002). Flutamide, bicalutamide, nilutamide and cyproterone acetate (Figure 1.9) are examples of anti-androgens (Wirth *et al.,* 2007). Anti-androgens may be weakly agonistic in prostate cancer cells with mutated or over-expressed androgen receptors. The mutated androgen receptors can recognise them as ligands (Chen *et al.,* 2004).

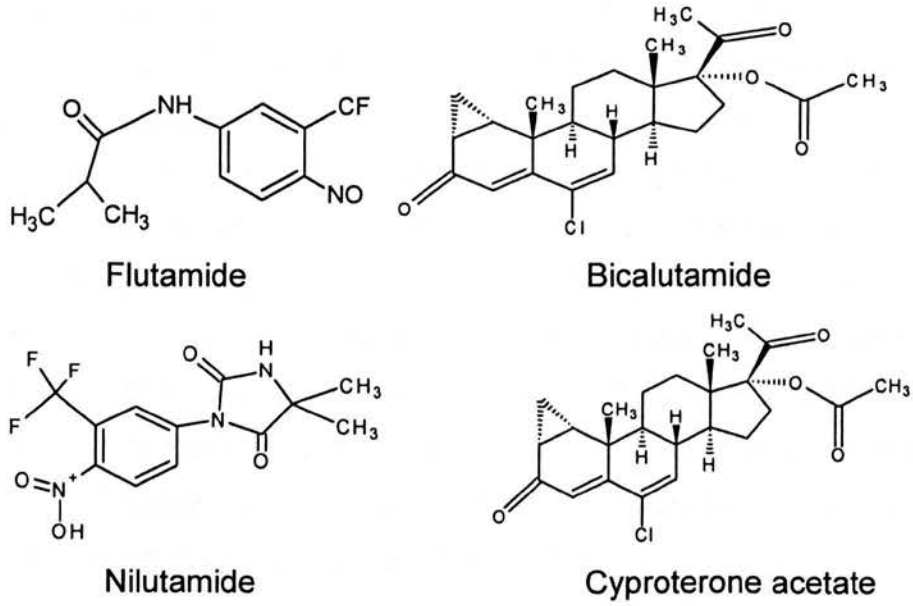

Figure 1.9: Examples of anti-androgen compounds

1.5.9. Steroid hormones biosynthesis

Two of the major families of enzymes involved in steroid hormone metabolism are: the cytochrome P450 and the reductase families (Hakki, 2006). The cytochrome P450 family of enzymes is a group of haem containing proteins that absorb light at a maximum wavelength of 450nm and are membrane bound enzymes. They are either associated with the mitochondrial membrane or with the endoplasmic reticulum (Payne and Hales, 2004).

The cytochrome P450 enzymes are involved in the bioconversion of cholesterol to other steroids (Figure 1.10) and important endogenous biomolecules. Furthermore they are considered to be important biological targets in androgen-dependent diseases (Bruno and Njar, 2007). These enzymes are classified as mixed function oxidases or monooxygenases as they incorporate one atom of oxygen into the substrate whilst the other oxygen atom from the oxygen molecule is reduced to water (Equation 1.1) (Mason, 1957).

$$RH + O_2 + NADPH + H^+ \rightarrow ROH + H_2O + NADP^+$$

Equation 1.1: Enzymatic reaction for cytochrome P450 monooxygenase

The two cytochrome P450 enzymes which are targeted as a therapeutic strategy for hormone-dependent prostate cancer are cytochrome P450 17α-Hydroxylase, 17/20 lyase (CYP17) and cytochrome P450 17 β-hydroxysteroid dehydrogenase type 3 (17β-HSD3) (Yap *et al.,* 2008; Day *et al.,* 2009). The enzyme CYP17 catalyses the conversion of progesterone or pregnenolone to androstendione (Akhtar *et al,* 2011) which is further converted to testosterone by the action of the enzyme 17β-HSD 3 (Laplante and Poirier, 2008). Testosterone is then further converted to dihydrotestosterone by an enzyme called 5α- reductase (Figure 1.6). Both testosterone and dihydrotestosterone bind to and activate the androgen receptor (AR), but dihydrotestosterone shows a higher affinity for these receptors. Dihydrotestosterone also dissociates from the androgen receptors much more slowly than its precursor (Aggarwal *et al.,* 2010).

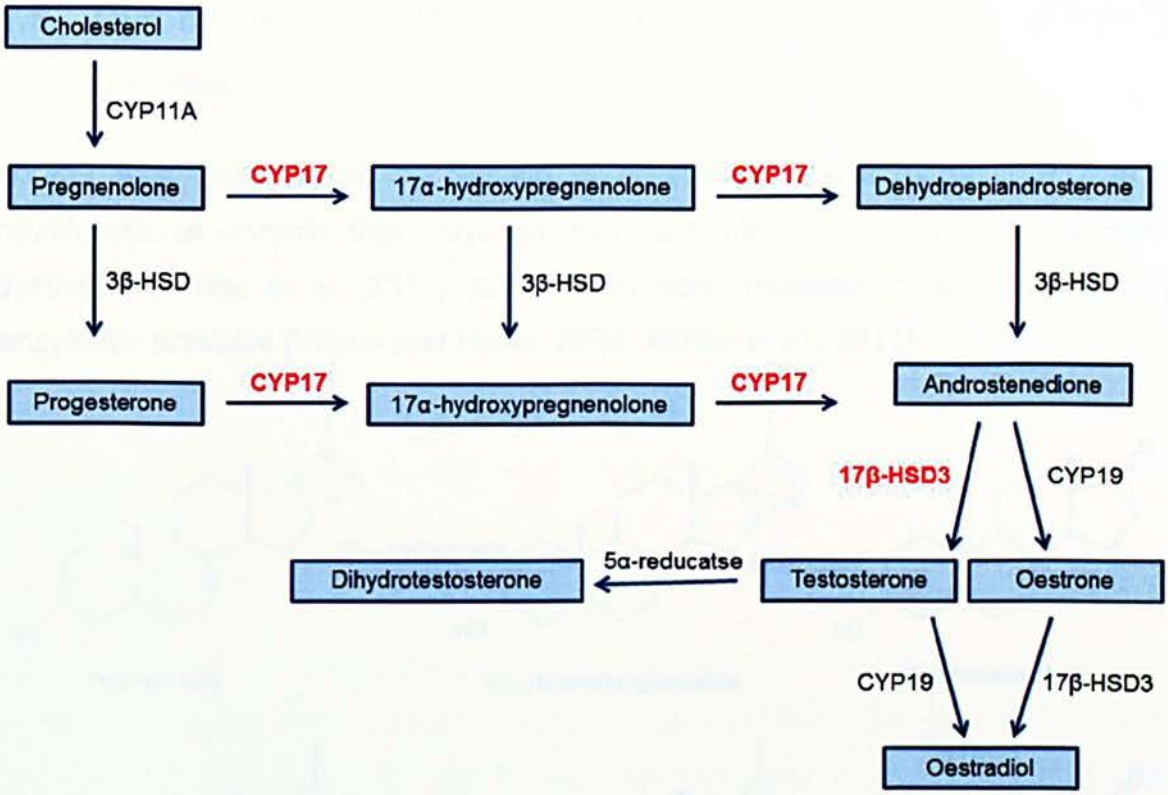

Figure 1.10: ***Steroid hormone synthesis.*** *The enzyme CYP17 has two enzymatic roles: hydroxylation of C (17) of progesterone and pregnenolone and the lysis of the bond between C (17) and C (20) of 17-hydroxy substrates (modified from Payne and Hales, 2004).*

1.6. Cytochrome P45017α-hydroxylase / 17, 20-lyase (CYP17) enzyme

CYP17 was first isolated by Nakajin *et al.* (1981). The enzyme CYP17 is a multifunctional enzyme that plays an important role in corticoid and oestrogen synthesis (Akhtar *et al.,* 2011). CYP17 has been reported to have two distinct enzymatic activities (Payne and Hales, 2004; Akhtar *et al.,* 2011).

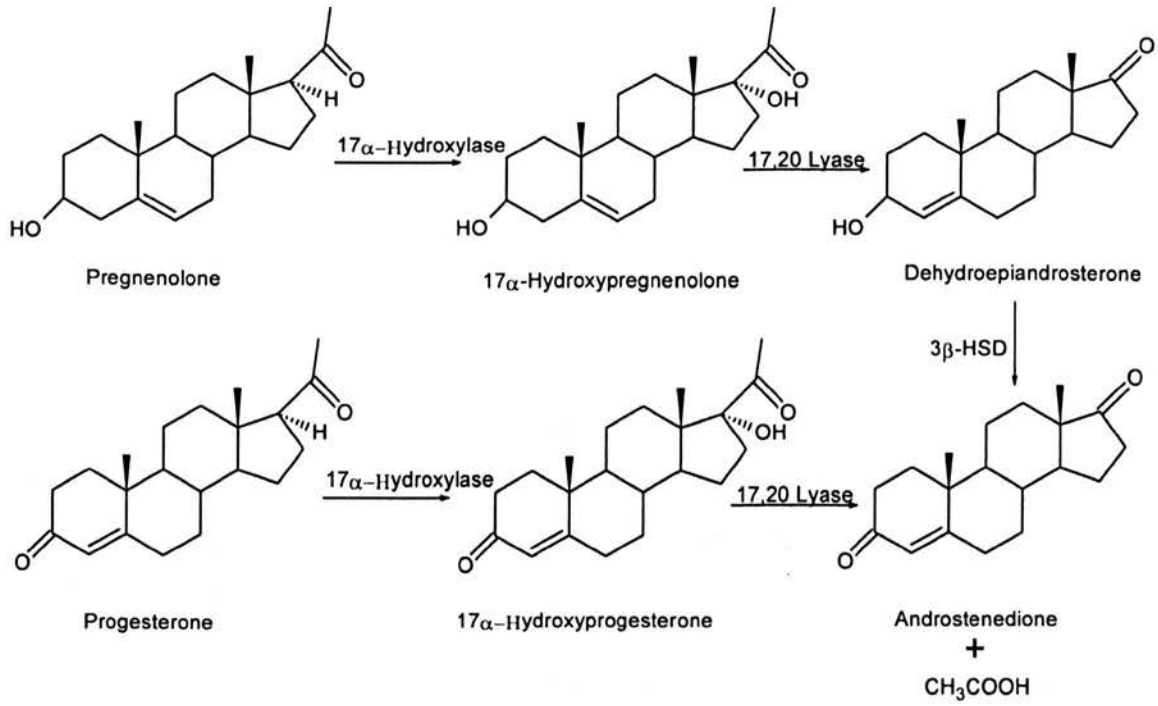

Figure 1.11: ***Reaction catalysed by the enzyme CYP17*** *(Ahmed, 1999). The enzyme has two catalytic activities; 17α-OHase that hydroxylates the carbon 17 of the substrate and lyase which cleaves the bond between carbon 17 and carbon 20 of the substrate.*

The 17α-hydroxylase (17α-OHase) component of the enzyme (Figure 1.11) catalyses the hydroxylation of the C (17) position of progesterone and pregnenolone and the 17, 20 lyase (lyase) component catalyses the cleavage of the bond between C (17) and C (20) of 17α-hydroxyprogesterone and 17α-hydroxypregnenolone (17α-OHP) (Akhtar *et al.,* 2011; Bruno and Njar, 2007) which are further converted into the most potent androgen, dihydrotestosterone. Both of these components of CYP17 have a single binding site for the substrate (Auchus and Miller, 1999). The activity of CYP17 requires NADPH and cytochrome P450 reductase (Potter *et al.,* 1995).

1.6.1. Structure of CYP17

CYP17 is a cysteinatohaem enzyme in which the amino acid cystiene is attached to the haem moiety (Haider *et al,* 2010). CYP17 is a membrane bound enzyme and therefore the crystal structure of CYP17 has not been reported (Zurek *et al.,* 2006). However the crystal structure of other P450 enzymes is being used to construct a homology model of it (Haider *et al.,* 2010).

Ahmed (2004) has reported the substrate–haem complex (SHC) approach to construct an SHC for the 17α-OHase and lyase components of this enzyme which has been used to derive the overall model in the study of the binding of some steroidal and non-steroidal inhibitors.

Different studies have reported a similar model for CYP17 according to which the enzyme has a two lobed substrate binding pocket in which the C (17) and the D-ring of the substrate are positioned over the haem moiety. During the hydroxylation reaction the A-ring is in the first lobe of the pocket which moves to the second lobe during the 17, 20 lyase reaction (Hakki and Bernhardt, 2006). However Auchus and Miller have reported a monolobal active-site cavity in the CYP17 structure (Auchus and Miller, 1999).

Pechurskaya and colleagues (2008) engineered a soluble form of the usually membrane-bound human CYP17 which was then used as a subject for crystallization of the haem protein. They reported a computer model of the tertiary structure of the haem protein and have also identified the surface hydrophobic amino acid residues.

Using the UniProt database system, the amino acid sequence for rat, mouse and human CYP17 were aligned (Figure 1.12) and 62.40% homology was found between the three species. Rat and mouse CYP17 enzymes have 507 amino acids whereas the human CYP17 has 508 amino acids. The amino acid cysteine at position 442 in rat and mouse CYP17 and position 443 in human CYP17 binds to an iron atom which forms a covalent bond with inhibitors of CYP17.

```
Rat     1    MWELVGLLLLILAYFFWVKSKTPGAKLPRSLPSLPLVGSLPFLPRRGHMHVNFFKLQEKY   60
Mouse   1    MWELVGLLLLILAYFFWPKSKTPNAKFPRSLPFLPLVGSLPFLPRRGHMHANFFKLQEKY   60
Human   1    MWELVALLLLTLAYLFWPKRRCPGAKYPKSLLSLPLVGSLPFLPRHGHMHNNFFKLQKKY   60
             *****.**** ***:** * : * ** *:**  ************:**** ******:**

Rat     61   GPIYSLRLGTTTTVIIGHYQLAREVLIKKGKEFSGRPQMVTQSLLSDQGKGVAFADAGSS  120
Mouse   61   GPIYSLRLGTTTAVIVGHYQLAREVLVKKGKEFSGRPQMVTLGLLSDQGKGVAFADSSSS  120
Human   61   GPIYSVRMGTKTTVIVGHHQLAKEVLIKKGKDFSGRPQMATLDIASNNRKGIAFADSGAH  120
             *****:*:**.*:**:**:***:***:****:*******.*  : *:: **:****:.:

Rat     121  WHLHRKLVFSTFSLFKDG-QKLEKLICQEAKSLCDMMLAHDKESIDLSTPIFMSVTNIIC  179
Mouse   121  WQLHRKLVFSTFSLFRDD-QKLEKMICQEANSLCDLILTYDGESRDLSTLIFKSVINIIC  179
Human   121  WQLHRRLAMATFALFKDGDQKLEKIICQEISTLCDMLATHNGQSIDISFPVFVAVTNVIS  180
             *:***:*.::**:**:*  *****:**** .:***:: ::: :* *:*  :* :* *:*.

Rat     180  AICFNISYEKNDPKLTAIKTFTEGIVDAIGDRNLVDIFPWLTIFPNKGLEVIKGYAKVRN  239
Mouse   180  TICFNISFENKDPILTTIQTFTEGIVDVLGHSDLVDIFPWLKIFPNKNLEMIKEHTKIRE  239
Human   181  LICFNTSYKNGDPELNVIQNYNEGIIDNLSKDSLVDLVPWLKIFPNKTLEKLKSHVKIRN  240
              **** *::: ** *..*:.:.***:*  .. .***:.***.***** ** :* :.*:*:

Rat     240  EVLTGIFEKCREKFDSQSISSLTDILIQAKMNSDNNNSCEGRDPDVFSDRHILATVGDIF  299
Mouse   240  KTLVEMFEKCKEKFNSESLSSLTDILIQAKMNAENNNTGEGQDPSVFSDKHILVTVGDIF  299
Human   241  DLLNKILENYKEKFRSDSITNMLDTLMQAKMNSDNGNAGPDQDSELLSDNHILTTIGDIF  300
             . *  ::*: :*** *:*::.: * *:*****::* *:   :* .::**.***.*:****

Rat     300  GAGIETTTTVLKWILAFLVHNPEVKKKIQKEIDQYVGFSRTPTFNDRSHLLMLEATIREV  359
Mouse   300  GAGIETTSSVLNWILAFLVHNPEVKRKIQKEIDQYVGFSRTPSFNDRTHLLMLEATIREV  359
Human   301  GAGVETTTSVVKWTLAFLLHNPQVKKKLYEEIDQNVGFSRTPTISDRNRLLLLEATIREV  360
             ***:***::*::* ****:***:**:*: :**** *******::.**.:**:********

Rat     360  LRIRPVAPMLIPHKANVDSSIGEFTVPKDTHVVVNLWALHHDENEWDQPDQFMPERFLDP  419
Mouse   360  LRIRPVAPLLIPHKANIDSSIGEFAIPKDTHVIINLWALHHDKNEWDQPDRFMPERFLDP  419
Human   361  LRLRPVAPMLIPHKANVDSSIGEFAVDKGTEVIINLWALHHNEKEWHQPDQFMPERFLNP  420
             **:*****:*******:*******:: * *.*::*******:::**.***:*******:*

Rat     420  TGSHLITPTQSYLPFGAGPRSCIGEALARQELFVFTALLLQRFDLDVSDDKQLPRLEGDP  479
Mouse   420  TGSHLITPTPSYLPFGAGPRSCIGEALARQELFIFMALLLQRFDFDVSDDKQLPCLVGDP  479
Human   421  AGTQLISPSVSYLPFGAGPRSCIGEILARQELFLIMAWLLQRFDLEVPDDGQLPSLEGIP  480
             :*::**:*: ***************** *******:: * ******::* ** *** * * *

Rat     480  KVVFLIDPFKVKITVRQAWMDAQAEVSI  507
Mouse   480  KVVFLIDPFKVKITVRQAWKDAQVEVSI  507
Human   481  KVVFLIDSFKVKIKVRQAWREAQAEGSI  508
             ******* *****.***** :**.* **
```

Figure 1.12: ***Amino acid sequence alignment of CYP17 in different organisms.*** *The identical amino acids are highlighted in grey. The metal binding site in the amino acid sequence is highlighted in blue.*

1.6.2. Mechanism of action of CYP17

The CYP17 reaction involves hydroxylation at the 17α position of progesterone or pregnenolone via an "oxygen rebound" mechanism involving ferryl oxene as the active oxygenating species (Figure 1.13). The hydroxylation step is followed by the C17, 20-lyase reaction in which the carbon–carbon bond is oxidatively cleaved to yield a ketosteroid and acetic acid, subsequently leading to the formation of the androgens dehydroepiandrosterone and androstenedione (Denisov *et al.,* 2005).

The active site of CYP17 contains the amino acid cysteine which is attached to a haem molecule (Nebel, 2006). The iron (Fe) of the haem in the resting state is Fe^{III} (Akhter *et al.,* 1994). The substrate RH binds to the Fe^{III} of the enzyme and after various steps, an iron peroxide (Fe^{III} –O-O$^-$) intermediate is produced (Akhtar *et al,* 1982) which is further converted to a ferrexy radical species (Fe^{IV} –O$^{\bullet}$) by accepting two protons from neighbouring amino acids (Akhtar *et al.,* 1994; Lee-Robichaud *et al.,* 1998).

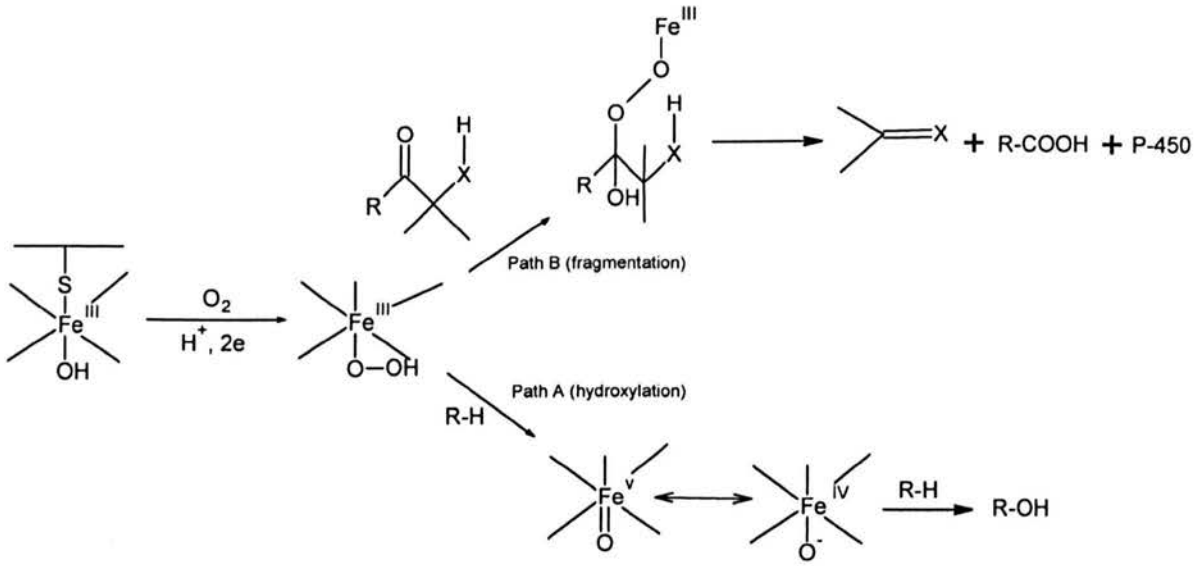

Figure 1.13: Different iron species involved in the hydroxylation of substrate *(Akhtar et al, 1997)*

The ferrexy radical species abstracts the hydrogen atom at the C (17) position of the substrate. This results in the hydroxylation of the iron of the haem and radical formation at the C (17) position of the substrate. The radical now attacks the hydroxyl group attached to the iron of the haem moiety and hence the hydroxylation step is completed (Figure 1.13 and 1.14) (Akhtar *et al.,* 1997).

The lyase step of the CYP17 activity involves the attacking of another iron peroxo anion species (Fe^{III} –O-O$^-$) on the C (20) carbonyl moiety of the hydroxylated substrate (i.e. 17α-OHP). This results in the production of intermediates which leads to the production of an acetate group and dihydrotestosterone (Figure 1.14) (Lee-Robichaud *et al.,* 1998; Swinney and Mak, 1994)

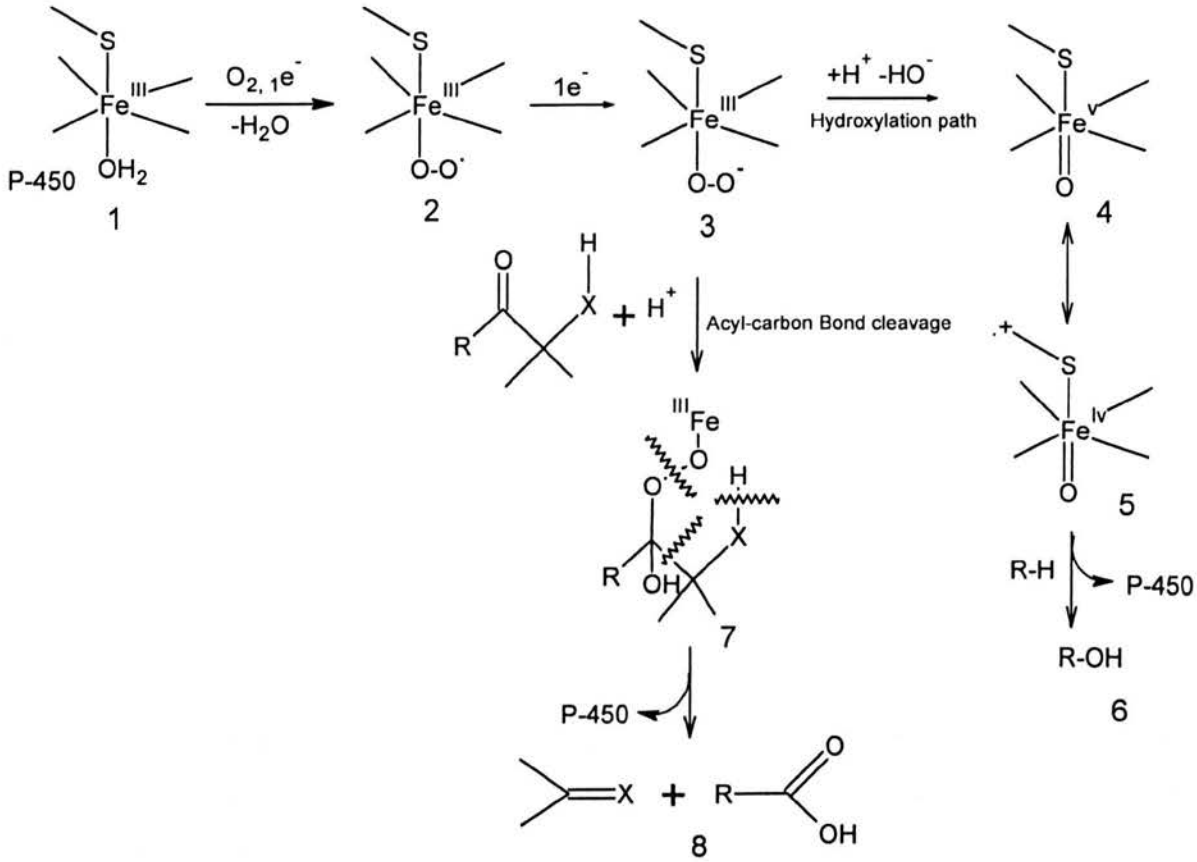

Figure 1.14: ***Chemical reaction for the hydroxylation and lyase component of CYP17*** *(Akhtar et al., 2011)*

1.6.3. Inhibitors of CYP17

Androgens are responsible for the growth, development and maintenance of the prostate (Payne and Hales, 2004). Inhibitors of CYP17 in the androgen synthetic pathway have been shown to have a beneficial role in the treatment of prostate cancer (Ahmed, 1999).

Since CYP17 is a membrane bound enzyme, the crystal structure of the enzyme is still unknown (Zurek *et al.,* 2006; Moreira *et al.,* 2007). Design of inhibitors has been based on information including docking and molecular modelling techniques, and the substrate haem complex approach. (Vasaitis *et al.,* 2011; Lewis and Lee-Robichaud, 1998; Armutlu, 2009; Ahmed, 2004). Inhibitors of CYP17 can be divided into two categories: non-steroidal and steroidal. These inhibitors can be further sub-divided as reversible or irreversible.

1.6.4. Non-steroidal inhibitors of CYP17

Non-steroidal inhibitors of CYP17 have been based on the ABC rings of the steroidal backbone and variation in substituent at the C (3) and the C (17) position of the natural substrate. These inhibitors coordinate with the haem residue of CYP17. Azole, pyridyl and phenylamine-based compounds are examples of non-steroidal inhibitors which have been studied to date (Leroux, 2005).

1.6.4.1. Azole based compounds as non-steroidal inhibitors of CYP17

Ketoconazole (KTZ) (Figure 1.15) is the most important member of the azole based compounds. Moreira *et al.* (2007) have reported an IC_{50} value of 47nM for KTZ against CYP17. The discovery of KTZ led to the development of other imidazole and triazole derivatives. It has been previously used in the first line treatment of patients with advanced prostate cancer; however, due to its non-selectivity for other P450 enzymes and number of significant side effects, it is used as secondary hormonal therapy along with surgery (Trachtenberg and Zadra 1988; Moreira *et al,* 2007). All imidazole compounds form a dative covalent bond with haem iron and inhibit the enzyme (Shahid *et al.,* 2008). Other azole based compounds, econazole and miconazole (Figure 1.15) were shown to have an IC_{50} of 0.3 μM (Mason *et al.,* 1987) against CYP17 while bifonazole was found to be more potent possessing a K_i value of 56.5 nM against the lyase component (Ayub and Levell, 1987).

1.6.4.2. Pyridyl derivatives as non-steroidal inhibitors of CYP17

The mode of action of pyridyl derivatives compounds is similar to azole-based compounds. Superimpositioning studies reveal that these compounds are good mimics of the natural substrate (Laughton *et al.,* 1990). These pyridyl derivatives (Figure 1.16) are susceptible to the action of esterases. Compound **1** (Laughton *et al.,* 1990) has been shown to have an IC_{50} of 2.7μM and 2μM against lyase and 17α-OHase activity of rat CYP17 respectively. However, other pyridyl derivatives (compound **2** and **3**) were shown to be more potent against the human CYP17 enzyme. Compound **2** showed an IC_{50} of 1.8 nM and 3.3 nM while compound **3** was found to possess an IC_{50} value of 2.7 nM and 8.8 nM against the human lyase and 17αOHase components respectively (Chan *et al.,* 1996).

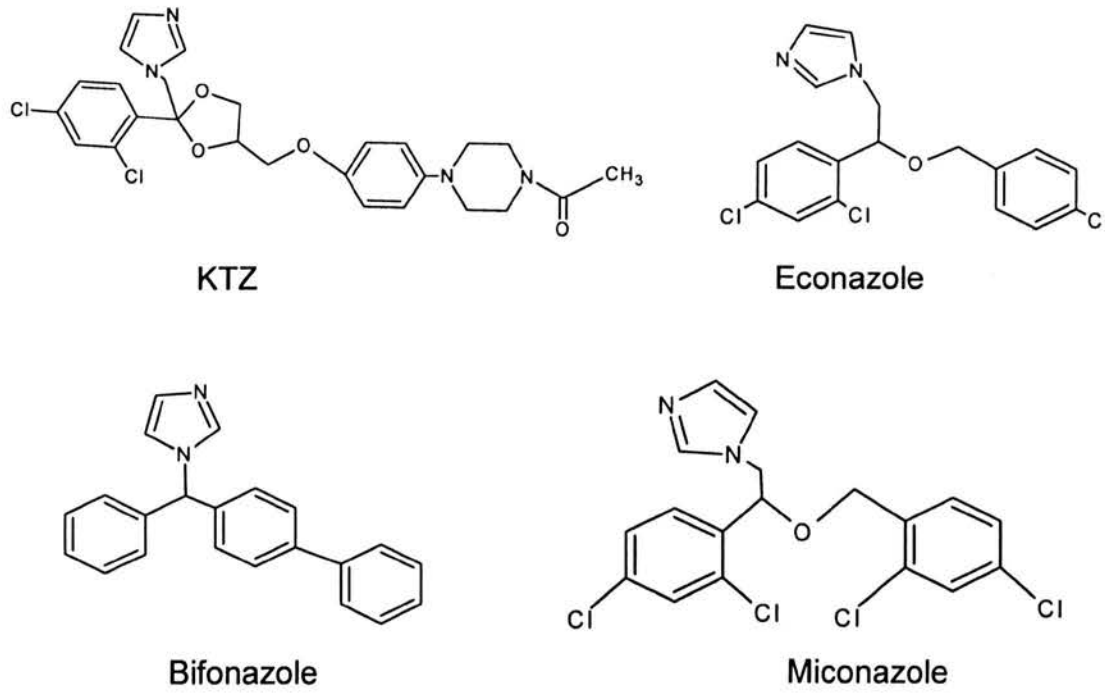

Figure 1.15: Examples of azole-based inhibitors of CYP17

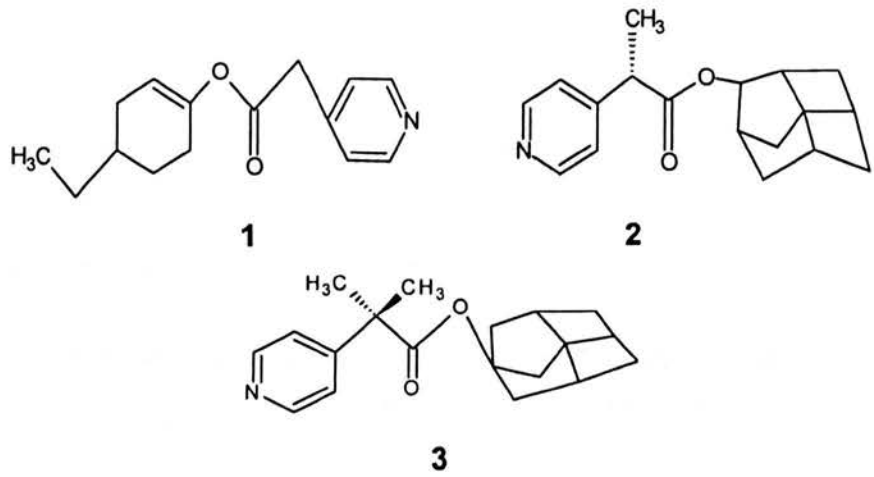

Figure 1.16: Examples of pyridyl-based inhibitors of CYP17

1.6.4.3. Phenylamine-based compounds as non-steroidal inhibitors of CYP17

A number of phenylamine-based compounds have been evaluated for their inhibitory action against other cytochrome P450 enzymes such as aromatase beside CYP17 enzyme. Compounds based upon a pyrrolidine-2, 5-dione ring system containing an aniline ring system have been previously reported as weak inhibitors of CYP17 (Ahmed *et al.,* 1995). They have been shown to possess a similar mode of action as the azole-based compounds, that is, the phenylamine

nitrogen atom donates a lone pair of electrons to the Fe^{3+} at the centre of the haem, and as such, these compounds possess reversible inhibition. The IC_{50} of compounds **4**, **5** and **6** (Figure 1.17) synthesised by Ahmed *et al* (1995) have been found to be 88 μM, 95 μM and 89 μM against the CYP17 enzyme, respectively.

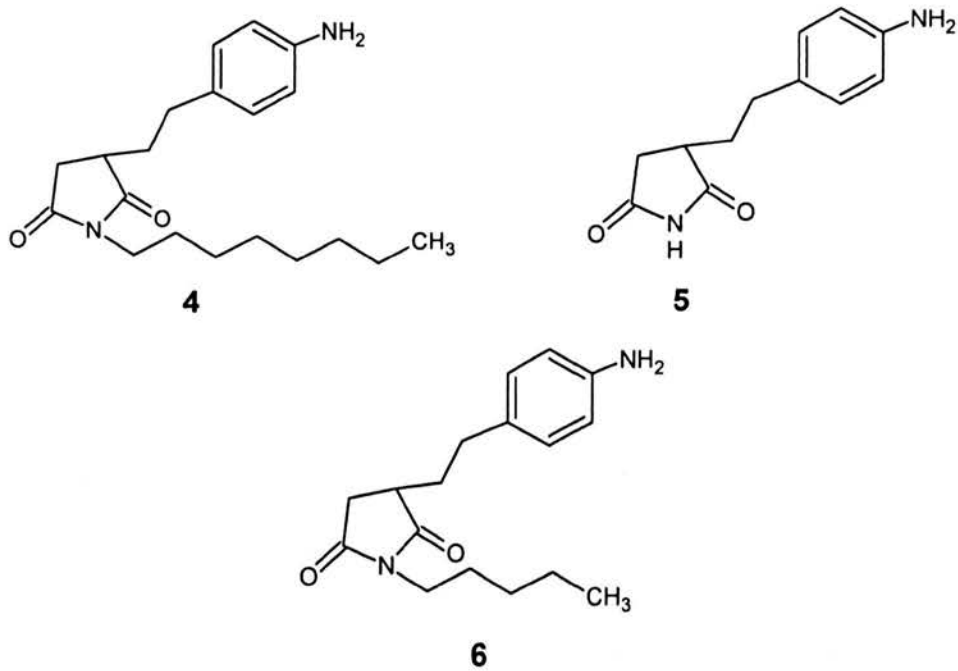

Figure 1.17: Examples of phenylamine-based inhibitors of CYP17 *(Ahmed et al., 1995)*

1.6.5. Steroidal inhibitors of CYP17

Steroidal inhibitors are designed to mimic the natural substrates of the enzyme at the active site. Natural substrates are usually modified at the C (17) or C (20) positions of the steroid backbone.

1.6.5.1. Irreversible (mechanism-based) inhibitors as steroidal inhibitors of CYP17

The irreversible inhibitors of CYP17 contain a specific group that undergoes covalent binding with the active site of the enzyme, making it impossible for the substrate to bind to the active site. Compounds **7** and **8** (Njar *et al.,* 1996) were tested against 17α-OHase and found to have IC_{50} values of 0.21 μM and 1.2 μM respectively (Figure 1.18). Abiraterone acetate (Figure 1.18) is one of the examples of this class of inhibitors and has been shown to be very useful as a secondary hormone therapy in clinical trials. Abiraterone decreases levels of

prostate specific antigens in patients with hormone dependent prostate cancer (Pezaro *et al,* 2011; Attard *et al.,* 2009).

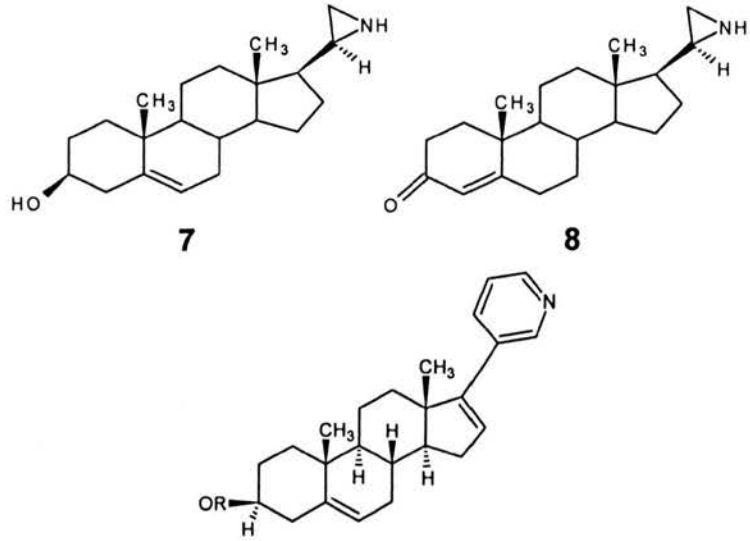

Figure 1.18: Examples of irreversible steroidal inhibitors of CYP17

1.6.5.2. Reversible inhibitors as steroidal inhibitors of CYP17

As with the mechanism-based inhibitors, these substrate analogue inhibitors have structural similarity to the natural substrate, however, they bind reversibly to the active site of the enzyme. A number of reversible steroidal inhibitors have been developed (Figure 1.19) including compound **9** and **10** which have been shown to possess IC_{50} values of 8 nM and 7 nM respectively (Nnane *et al.,* 1999).

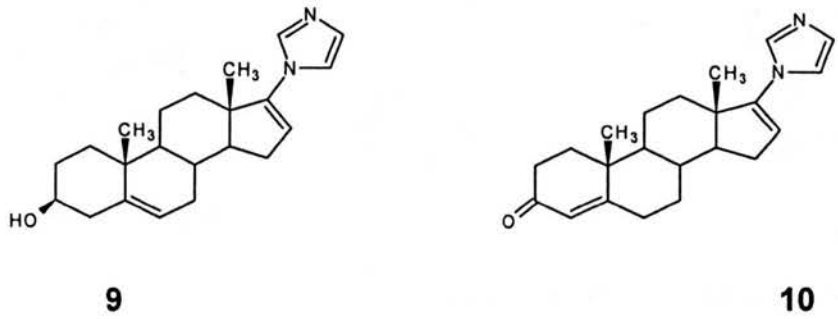

Figure 1.19: Examples of some steroidal azole-based inhibitors of CYP17

1.6.6. Mechanism of action of inhibitors of CYP17

Inhibitors of CYP17 can be divided into class I and II types and this classification is based on the binding of the inhibitor to the active site of the enzyme (Vasaitis *et al.,* 2011). Type I inhibitors displace water as the sixth ligand of the iron (Fe) haem

and thus allow the Fe to exist in a penta-coordinate state (Schenkman *et al.*, 1972). Type II competitive inhibitors interact as the sixth ligand with the haem atom and with amino acid residues closer to the haem site (Jefcoate, 1978). The most commonly studied type II inhibitors contain a nitrogen heteroatom (Vasaitis *et al.*, 2011).

The inhibitors of CYP17 contain a functional group which is mostly a nitrogen bearing heterocycle that is capable of forming a coordinate bond with the haem iron of the enzyme (Figure 1.20) (Shahid *et al.*, 2008; Haider *et al.*, 2003). Based on this proposed mechanism, the medicinal chemistry research group at Kingston University has synthesised some potential CYP17 inhibitors that interact with the enzyme's active site in the same manner.

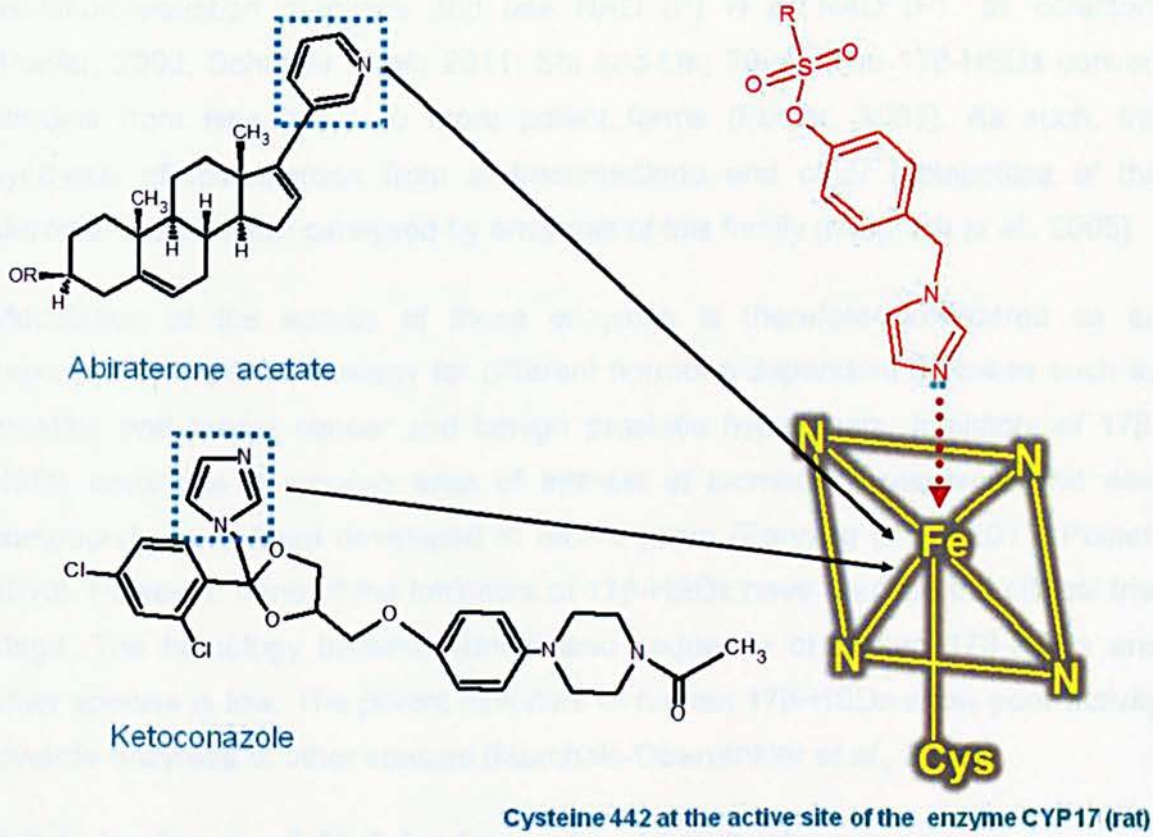

Figure 1.20: ***Mode of action of CYP17 inhibitors.*** *The nitrogen atom of pyrimidine and imidazole rings (highlighted in the square box) of abiraterone acetate and ketoconazole respectively forms a dative covalent bond with the iron atom of the haem moiety of the enzyme active site. The iron atom is attached to cysteine 442 of the rat CYP17. The synthesised compounds (red) interact with the enzyme in a similar manner.*

1.7. Cytochrome P450 17 β-hydroxysteroid dehydrogenases (17β-HSDs)

The 17β-HSD is a group of enzymes which are involved in the synthesis of the most active androgens and estrogens in the steroidal cascade (Prehn *et al.,* 2009).

There are different substrates for 17β-HSD enzymes which include steroids, bile, fatty acids, retinols and xenobiotics. They are of different types and are differentiated from each other on the basis of their localisation to sub-cellular levels, cofactors and spatio-temporal patterns of tissue expression (Lukacik *et al.,* 2006).

The enzymes 17β-HSDs are dehydrogenase/reductase enzymes which catalyse oxidation-reduction reactions and use NAD (P) H or NAD $(P)^+$ as cofactors (Poirier, 2003, Schuster *et al.,* 2011; Shi and Lin; 2004). The 17β-HSDs convert steroids from less active to more potent forms (Poirier, 2003). As such, the synthesis of testosterone from androstenedione and other metabolites of the steroidal cascade are catalysed by enzymes of this family (Mindnich *et al.,* 2005).

Modulation of the activity of these enzymes is therefore considered as an important therapeutic strategy for different hormone-dependent diseases such as prostate and breast cancer and benign prostatic hyperplasia. Inhibitors of 17β-HSDs constitute a growing area of interest in biomedical research, and new compounds have been developed in recent years (Penning *et al.,* 2011; Poirier, 2010). However, none of the inhibitors of 17β-HSDs have reached the clinical trial stage. The homology between amino acid sequence of human 17β-HSDs and other species is low. The potent inhibitors of human 17β-HSDs show poor activity towards enzymes of other species (Marchais-Oberwinkler *et al., 2011).*

1.7.1. Isoforms of 17 β-hydroxysteroid dehydrogenase

There are 14 isoforms of 17β-HSD which have been identified (Marchais-Oberwinkler, 2011). All of them are short chain dehydrogenases/reductases apart from HSD type 5 (Pletnev and Duax, 2005; Vihko *et al.,* 2006). The functions of the different 17β-HSD isoforms are listed in the table overleaf (Table 1.1).

Type	Gene	Function	Disease-association
1	HSD17β1	Steroid (oestrogen) synthesis	Breast and prostate cancer, endometriosis
2	HSD17β2	Steroid (oestrogen, androgen, progestin) inactivation	Breast and prostate cancer, endometriosis
3	HSD17β3	Steroid (androgen) synthesis	Prostate cancer, Pseudohermaphroditism in males
4	HSD17β4	Fatty acid β-oxidation, steroid (oestrogen, androgen) inactivation	D-specific bifunctional protein-deficiency, prostate cancer
5	AKR1C3	Steroid (androgen, oestrogen, prostaglandin) synthesis	Breast and prostate cancer
6	HSD17β6	Retinoid metabolism, 3α-3β-epimerase.	-
7	HSD17β7	Cholesterol biosynthesis, steroid (oestrogen) synthesis	Breast cancer
8	HSD17β8	Fatty acid elongation, steroid inactivation, oestrogens, androgens	Polycystic kidney disease
9	HSD17β9	Retinoid metabolism	-
10	HSD17β10	Isoleucine, fatty acid, bile acid metabolism, steroid (oestrogen, androgen) Inactivation	X-linked mental retardation MHBD deficiency, Alzheimer's deficiency
11	HSD17β11	Steroid (oestrogen, androgen) inactivation, lipid metabolism	-
12	HSD17β12	Fatty acid elongation, steroid (oestrogen) synthesis	-
13	HSD17β13	-	-
14	HSD17β14	Steroid (oestrogen, androgen) Inactivation, fatty acid metabolism	Breast cancer, prognostic marker

Table 1.1: Different types of human 17β-hydroxysteroid dehydrogenases *(adapted from Marchais-Oberwinkler, 2011)*

1.8. 17 β-hydroxysteroid dehydrogenase 3 (17β-HSD3)

17β-HSD3 is excessively present in leydig cells of the testes, seminal vesicles and prostate tissue. Therefore, this enzyme is involved in the synthesis of testosterone in both gonadal and non-gonadal tissues (Vicker *et al.,* 2009). In the presence of NADPH, the enzyme 17β-HSD3 reduces the C19 steroid α4-androstene-3, 17-dione to testosterone (Figure 1.21) (Laplante and Poirier, 2008) which is further converted into dihydrotestosterone by the action of the reductase enzyme. Dihydrotestosterone stimulates the growth of hormone-dependent prostate tumours via its interaction with the androgen receptor (AR). (Day *et al.,* 2008)

Studies have shown that expression of 17β-HSD3 mRNA is increased over 30-fold in cancerous prostate biopsies (Koh *et al.,* 2002; Maltais *et al.,* 2011). The involvement of 17β-HSD3 in the synthesis of potent androgens therefore presents a new target to treat prostate cancer and other androgen-dependent diseases (Vicker *et al.,* 2009)

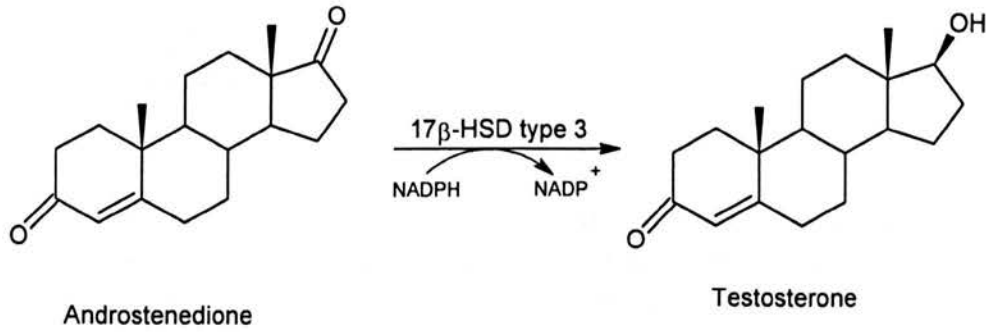

Figure 1.21: Reaction catalysed by 17β-HSD3

1.8.1. Structure of 17β-HSD3

17β-HSD3 is a membrane bound protein (Vicker *et al.,* 2009). The enzyme is bound through an N-terminal transmembrane domain to the endoplasmic reticulum (Lukacik *et al.,* 2006).

Using the UniProt database system, the amino acid sequence for rat, mouse and human 17β-HSD3 were aligned (Figure 1.22) and 67.74% homology was found between the three species. The rat, mouse and human 17β-HSD3 enzymes have 306, 305 and 310 amino acids respectively. The active site of 17β-HSD3 contains

a tyrosine amino acid at position 195 in rat and mouse and at position 199 in humans.

```
Rat     1    ----MEQFLLSVGLLVCLVCLVKCVRFSRYLFLSFCKALPGSFLRSMGQWAVITGAGDGI   56
Mouse   1    ----MEKLFIAAGLFVGLVCLVKCMRFSQHLFLRFCKALPSSFLRSMGQWAVITGAGDGI   56
Human   1    MGDVLEQFFILTGLLVCLACLAKCVRFSRCVLLNYWKVLPKSFLRSMGQWAVITGAGDGI   60
                 :*:::: .**:* *.**.**:***: ::* : *.** ******************

Rat     57   GKAYSFELARHGLNVVLISRTLEKLQVISEEIERTTGSRVKVVQADFTREDIYDHIEEQL  116
Mouse   57   GKAYSFELARHGLNVVLISRTLEKLQTIAEEIERTTGSGVKIVQADFTREDIYDHIKEHL  116
Human   61   GKAYSFELAKRGLNVVLISRTLEKLEAIATEIERTTGRSVKIIQADFTKDDIYEHIKEKL  120
             *********::**************:.*: *******  **::*****::***:**:*:*

Rat     117  KGLEIGVLVNNVGMLPNLLPSHFLSTSGESQSVIHCNITSVVKMTQLVLKHMESRRRGLI  176
Mouse   117  EGLENGILVNNVGMLPSFFPSHFLSSSGESQNLIHCNITSVVKMTQLVLKHMESRRKGLI  176
Human   121  AGLEIGILVNNVGMLPNLLPSHFLNAPDEIQSLIHCNITSVVKMTQLILKHMESRQKGLI  180
              *** *:*********.::*****.:  * *.:**************:*******::***

Rat     177  LNISSGVGVRPWPLYSLYSASKAFVCTFSKALNVEYRDKGIIIQVLTPYSVSTPMTKYLN  236
Mouse   177  LNISSGAALRPWPLYSLYSASKAFVYTFSKALSVEYRDKGIIIQVLTPYSISTPMTKYLN  236
Human   181  LNISSGIALFPWPLYSMYSASKAFVCAFSKALQEEYKAKEVIIQVLTPYAVSTAMTKYLN  240
             ****** .: ******:******** :*****. **: * :********::** ******

Rat     237  TSRVTKTADEFVKESLKYVTIGAETCGCLAHEILAIILNLIPSRIFYSSTTQRFLLKQFS  296
Mouse   237  N-KMTKTADEFVKESLKYVTIGAESCGCLAHEIIAIILNRIPSRIFYSSTAQRFLLTRYS  295
Human   241  TNVITKTADEFVKESLNYVTIGGETCGCLAHEILAGFLSLIPAWAFYSGAFQRLLLTHYV  300
             .  :************:*****.*:********:* :*. **:  ***.: **:**.::

Rat     297  DYLKSNISNR  306
Mouse   296  DYLKRNISNR  305
Human   301  AYLKLNTKVR  310
              *** * . *
```

Figure 1.22: ***Amino acid sequence alignment of 17β HSD3 in different organisms.*** *Identical amino acids are highlighted in grey. The binding site is highlighted in green and the active site of the enzyme is highlighted in red.*

It has not been possible to isolate the crystal structure of this protein as the crystallisation process can disrupt the tertiary structure. Different homology models are being constructed to understand the active site of this molecule which can then be used to design drugs against this enzyme. Competitive inhibitors from Schering-Plough and Bristol-Myers Squibb (BMS) have been docked into these models (Vicker *et al.,* 2009).

1.8.2. Mechanism of action of 17β-HSD3

All types of 17β-HSDs have a common chemical mechanism. They either transfer a hydride from NADPH to a ketosteroid or a hydride from hydroxysteroid to NAD^+ which is accompanied by a proton shift for charge equalisation (Marchais-Oberwinkler *et al.,* 2011). HSDs catalyze the direct transfer of a hydride ion from

the C4 position of a reduced nicotinamide cofactor to the acceptor carbonyl of the steroid substrate. To facilitate this hydride transfer there is polarization of the acceptor carbonyl at the active site. This polarization may lead to the generation of a partial or full carbonium ion (Figure 1.23) (Penning, 1996).

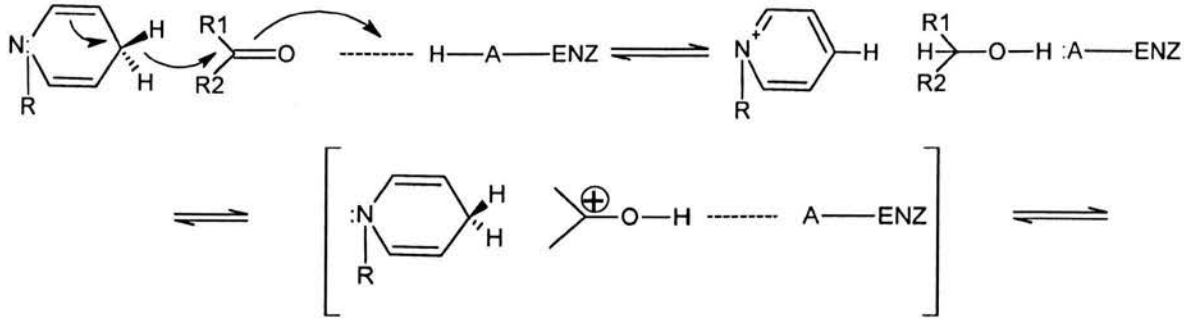

Figure 1.23: ***Catalytic mechanism for HSDs.*** *Polarization of the acceptor carbonyl with the formation of a formal carbonium ion is shown in parenthesis. ENZ=enzyme, H-A=general acid at the enzyme active site, R1 and R2=components of the steroid nucleus (Penning, 1996).*

Three conserved amino acid residues of 17β-HSDs i.e. Ser142, Tyr155 and Lys159 which are also known as the "catalytic triad" and a water molecule are essential for the catalytic process (Puranen *et al.,* 1994). An additional conserved water molecule is stabilized by an H-bond interaction with an asparagine residue. This forms a "catalytic tetrad" which has also been reported to play a critical role in the enzymatic process for HSDs (Figure 1.24) (Filling *et al.,* 2002).

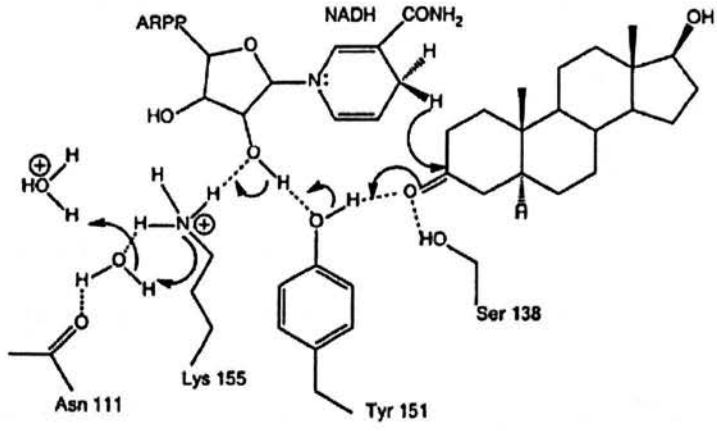

Figure 1.24: ***Reduction reaction mechanism of 17β-HSD involving NADH and the steroid substrate (5α-androstane, 3-one, 17ol)*** *(Filling et al., 2002) where ARPP is the adenosine ribose pyrophosphate moiety of NADH.*

1.8.3. Inhibitors of 17β HSD 3

The 3D-structure of the protein has facilitated drug design against the activity of the enzyme (Marchais-Oberwinkler, 2011). Several inhibitors of 17β-HSD have been reported to date. The natural substrate, androstenedione, has been modified at the 3β position to synthesize two different derivatives as steroidal inhibitors of this enzyme. These include tertiary amines and carbamates. The sulphonamide derivative possessed strong inhibitory activity (IC_{50} = 6 nM) against 17β-HSD3 (Maltais *et al.,* 2011).

There are different non-steroidal inhibitors of 17β-HSD3. Fink *et al.* (2006) has reported a series of dibenzazocine-based compounds as potent inhibitors of 17β-HSD3. Compounds that have a pyridine ring in their structure were found to be potent inhibitors of 17β-HSD 3 (IC_{50} = 14nM) in a cell- based assay (Harada *et al.,* 2012). The substrate androstenedione was incubated with human 17β-HSD3 expressing HeLa cells that convert androstenedione into testosterone. Some other non-steroidal compounds e.g. 7-hydroxyflavone and baicalein (IC_{50} = 9.0 and 9.3 mM respectively) (Figure 1.25) were also reported to inhibit 17β-HSD3 (Le Lain *et al.,* 2001).

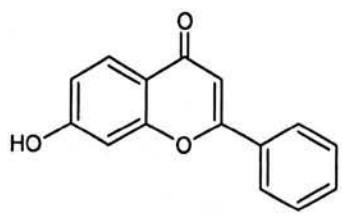

7-Hydroxyflavone

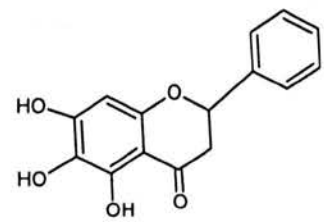

Baicalein

Figure 1.25: Structure of inhibitors of 17β-HSD3

1.8.4. Pharmacological inhibition of 17β-HSD3

The design and development of inhibitors of specific 17β-HSD enzymes for the treatment of various disorders, including steroid-dependent diseases such as breast and prostate cancer and endometriosis, has been progressed greatly in recent years (Day *et al.,* 2008).

Pittaway (1983) first and then Lombardo *et al.* (1993) demonstrated the inhibition of 17β-HSD3 activity by steroids which are structurally very similar to the substrate androstenedione. These studies indicated that a non-aromatic A-ring and C17 carbonyl group were important for inhibition (Day *et al,* 2008)

Inhibitors of 17β-HSD3 that act as pseudo-substrates (structurally similar to the natural substrate) are known as mechanism-based (irreversible) inhibitors. These inhibitors interact with the enzyme active site by forming a potent electrophile, which can alkylate the active site residue leading to irreversible enzyme inhibition (Penning *et al.,* 1997). The reversible HSD inhibitors are based on a number of different pharmacophores (Penning *et al.,* 2011; Schuster *et al.,* 2011).

The homology model showed that the substrate binding site in the protein is highly hydrophobic in nature. Vicker *et al.* (2009) have suggested that the inhibitors may potentially form pi–pi interactions and other hydrophobic interactions with amino acid residues such as Val213 and Leu252. The homology model is used as a tool in structure-based drug design by docking potential target molecules to discover novel 17β-HSD3 inhibitors (Vicker *et al.,* 2009).

1.8.5. Clinical trials for the new treatment options for patients with metastatic castration-resistant prostate cancer (CRPC).

Those prostate cancer patients who are resistant to surgical castration have been clinically defined into three groups; asymptomatic or minimally symptomatic, symptomatic and metastatic.

Patients who are asymptomatic and have not yet received chemotherapy are often treated with second line hormonal therapy such as anti-androgens (flutamide, bicalutamide, nilutamide, cyproterone acetate), ketoconazole, or diethylstilbestrol. These agents have been reported to decrease prostate specific antigens (PSA) but there has not been any Phase III clinical trials performed for these agents (Higano, 2012)

Docetaxel and prednisone are used for the treatment of patients with symptomatic prostate cancer. The patients in the third disease state consist of patients who have been treated with docetaxel previously. (Rosenberg *et al.,* 2007). Docetaxel and prednisone were tested in two Phase III clinical trials; TAX (Taxotere) 327 and

SWOG (Southwest Oncology group) 9916 (Tannock *et al.*, 2004; Petrylak *et al.*, 2004). Docetaxel was shown to increase the patient's life expectancy by approximately 2–2.4 months as well as an improvement in the quality of life. Mitoxantrone has been used in practice and in clinical trials as second-line chemotherapy, because of its known palliative benefits (Rosenberg *et al.*, 2007).

In April 2010, the FDA approved sipuleucel-T for the treatment of asymptomatic or minimally symptomatic men with metastatic castration-resistant prostate cancer (CRPC) (Higano, 2012). Sipuleucel-T is an active cellular immunotherapeutic designed to stimulate an immune response to the tumour antigen (Higano *et al.*, 2009)

In June 2010, the FDA approved Cabazitaxel (in combination with prednisone) for the treatment of metastatic prostate cancer based on the Phase III TROPIC trial. Cabazitaxel is a novel semi-synthetic taxane (De Bono *et al.*, 2010). Cabazitaxel was found to be more potent than docetaxel in preclinical models (Attard *et al.*, 2006). Cabazitaxel is now the second chemotherapeutic agent that has shown survival advantage in metastatic CRPC after prior docetaxel therapy. The combination of cabazitaxel and prednisone has been approved by health authorities around the world, including the European Union, Canada, South Korea, and many countries in South America (Higano, 2012)

Radium-223 (Alpharadin®) is a radiopharmaceutical that delivers high energy, short range irradiation that induces double-stranded DNA breaks with lower penetration to surrounding tissues that showed a survival benefit in those patients who were treated with radium-223. It has been studied extensively in preclinical animal models, phase I, phase II and phase III ALSYMPCA (Alpharadin in symptomatic prostate cancer) clinical trials (Henriksen *et al.*, 2002; Nilsson *et al.*, 2005; Nilsson *et al.*, 2007).

Abiraterone acetate is an oral agent that inhibits the cytochrome P450 CYP17 enzyme and blocks androgen production in the testes, prostate and adrenal glands. The results of the global Phase III COU-AA-301 (Cougar Biotechnology-Abiraterone acetate) trial presented in October 2011 reported that patients who had received docetaxel prior to treatment with abiraterone and prednisone, had prolonged survival rates (Higano, 2010).

Patients treated with abiraterone and prednisone had prolonged survival so were given the combination of abiraterone and prednisone instead of prednisone alone. The FDA approved the combination of abiraterone and prednisone for men who were previously treated with docetaxel in April 2011. A second Phase III COU-AA-302 trial, conducted in men with metastatic CRPC prior to receiving docetaxel has been conducted and data is currently being compiled (Higano, 2012).

TAK-700 which is also known as orteronel, is another CYP17 inhibitor that is in two Phase III trials; one in pre-docetaxel and the other one in a post-docetaxel setting. These trials are based on promising Phase II data (Higano, 2012).

Ketoconazole (KTZ), a weaker and non-specific inhibitor of CYP17 has been used in phase II clinical trials in combination with docetaxel (Pond *et al.*, 2012). The results showed that the patients treated with KTZ following docetaxel-based chemotherapy showed the worst outcomes as when compared to the patients who were not exposed to KTZ.

1.9. Androgens and breast cancer

Breast cancer is the most common cancer among women and still the most common cause of death in women between 35 and 55 years of age (Harbeck *et al.*, 2010). Sex hormones play important roles in both the development and progression of breast cancer (Henderson *et al.*, 1985). Oestrogens are synthesised in the ovaries of premenopausal women as well as the adipose tissue of post and pre-menopausal women. In the adipose tissues, the cholesterol is converted to progesterone and pregnenolone which are further converted by the enzyme CYP17 into androgens. The androgens are then aromatised to estrogens (Simpson, 2003; Chumsri *et al.*, 2011; Abraham and Staffurth, 2011).

Both endogenous and exogenous oestrogens produce their effects via interaction with steroid receptors. Steroid receptors are members of a nuclear receptor family which are ligand-responsive transcription factors. Oestradiol in the blood circulation enters into the cell by passive diffusion (Figure 1.26) and binds to the steroid receptor in the cytosol. Binding of oestradiol activates the intracellular steroid receptor which allows the receptors to undergo dimerisation. The hormone-receptor complex then subsequently translocates into the nucleus where it binds to

promoter regions of DNA, called oestrogen responsive elements (EREs). The receptor-DNA complex associates with co-activators and other transcriptional factors. This results in the synthesis of proteins involved in cell growth and survival (Murphy and Watson, 2002; Katchy *et al.,* 2012). The mechanism is similar to androgen-dependent prostate cancer (Section 1.5.3).

The aromatisation of testosterone has been shown to stimulate the growth of hormone-dependent breast cancer cells (Sonne-Hasnen and Lykkesfeldt, 2005). The studies have shown that androgens are involved in the progression of hormone-dependent breast cancer (Secreto *et al.*, 2009, Missmer *et al.,* 2004; Rossouw *et al.,* 2002). Proposed mechanisms of androgens include a direct effect on epithelial cell proliferation or indirect effect as a precursor for oestrogen synthesis (Kotsopoulos and Narod, 2005). The high levels of androgens and oestrogens in the circulation have been associated with breast cancer in post and menopausal women (Eliassen and Hankinson, 2007, Kaaks *et al.,* 2005; Dorgan *et al.,* 2010; Eliassen *et al.,* 2006; Kaaks *et al.,* 2005). Dihydrotestosterone, the most potent androgen in the body has been reported to stimulate cell proliferation *in vitro* of both oestrogen receptor positive and oestrogen receptor negative human breast cancer cells (Lin *et al.,* 2009). Androgens have been reported to increase the growth and proliferation of breast cancer cells via the stimulation of androgen receptors (Liao and Dickson, 2002).

Moreover, androgen receptors have been shown to play an important role in the proliferation of breast cancer cells (Yeh *et al.,* 2003) and are present on the surface of 25-82% of breast cancer cells, which lack oestrogen and progesterone receptors (Hu *et al.,* 2011; Schover, 2008; Agoff, 2003; Bayer-Garner and Smoller, 2000). Androgen receptors interact with oestrogen receptor elements of the promoter region gene of oestrogen-dependent genes, which cause the transcription of genes involved in cell growth and proliferation (Peters *et al.,* 2009).

Inhibitors of androgen synthesis can also be proposed as one of the strategies to treat breast cancer. In the this study, the compounds which have been synthesised against the enzyme CYP17 have also been tested against a breast cancer cell line, to determine if they have a similar effect to that found in the prostate cancer cell lines.

1.9.1. Signs and symptoms of breast cancer

Tiredness, loss of appetite and weight loss are the general symptoms like every other cancer. The following are symptoms which give a more specific indication of breast cancer.

- Lump in the breast or the nearby armpit
- Change in the shape of nipple (red or scaly nipple)
- Non-bloody or bloody discharge from nipple
- Change in the size or shape of the breast
- An itchy, red, scaly, warm or swollen breast (Ogden, 2004)

1.9.2. Risk factors for breast cancer

Breast cancer is common in developed countries. The main risk factors for breast cancer are older age, family history of breast cancer, being overweight (postmenopausal diseases only), alcohol, late pregnancy, hormonal replacement therapy, hormonal contraceptives, early menarche and late menopause (Murray 2009).

1.9.3. Genetic changes in breast cancer

Gene mutation is one of the main causes of breast cancer. These genes can be divided into "high risk" and "low-moderate risk" genes. The high risk breast cancer genes include *BRCA1, BRCA2, PTEN, TP53, LKB1/STk11* and CDH1 while the low-moderate risk genes include *CHEK2, TGFβ1, CASP8* and *ATM* (Oldenburg *et al.,* 2007).

BRCA1 and *BRCA2* genes are tumour suppressor genes. The products of these genes are responsible for the repair of DNA double strand breaks, control of the cell cycle and transcription. The *BRCA1* gene is present on chromosome 17 and consists of 24 exons whereas the *BRCA2* gene is present on chromosome 13 and consists of 27 exons. Mutation in both genes can occur on any part of the gene (Murray, 2009). Mutations in *BRCA1* have been related to increased risk of breast cancer (Okumura *et al.,* 2011). The risk of breast cancer varies with the position of the mutation within the gene sequence. For *BRCA1* and *BRCA2* genes, mutations in the central region of genes are associated with lower breast cancer risk as

compared to the outer regions (Thompson and Easton, 2001). The mutation in *BRCA1* and *BRCA2* genes are not only associated with the high risk of developing breast cancer, but other types of cancer as well (Oldenburg *et al.*, 2011).

In breast cancer cells, *TP53* genes transcribe different variants which are expressed differentially. The abnormal expression of the *p53* isoforms results in the loss of tumour- suppressor activity in breast cancer (Okumura *et al.*, 2011; Oldenburg *et al.*, 2011). Somatic mutations in *TP53* are reported in 20–60% of human breast cancers (De Jong *et al.*, 2005).

The *PTEN* gene has been found mutated in many cases and plays an important role in the pathogenesis of sporadic breast cancer (Okumura *et al.*, 2011; Carracedo *et al.*, 2011). Inactivation of *PTEN* results in activation of kinase signalling pathways which leads to uncontrolled cell proliferation (Okumura *et al*, 2011). Women carrying a *PTEN*-mutation have a 25–50% (2–4-fold) increase in lifetime breast cancer risk (Oldeburg *et al.*, 2011).

1.9.4. Treatment of breast cancer

Breast cancer can be treated in a variety of ways.

a) Surgery

Two major surgical treatments for breast cancer are lumpectomy and mastectomy. Lumpectomy is the removal of cancerous tissue and a small amount of adjacent tissue with overlying skin left in place. Mastectomy is the removal of the entire breast and some lymph nodes (Lynda, 2004).

b) Radiotherapy

c) Chemotherapy

d) Hormonal therapy (Pujol *et al*, 1998) which involves blocking oestrogen receptors with drugs such as tamoxifen (TAM) and suppressing oestrogen synthesis with LHRH analogues. LHRH agonists provide an effective additional class of agents for the treatment of premenopausal women with hormone-sensitive breast cancer (Cuzick *et al.*, 2007)

1.9.5. Hormonal therapy for breast cancer

More than two thirds of breast cancers give positive immunohistochemical staining for the oestrogen receptor (ER), so hormonal therapies are the backbone of treatment for the large majority of patients with breast cancer (Del-Re *et al,* 2011). In pre-menopausal women, oestrogen levels can be reduced by chemical ablation (Abraham and Staffurth, 2011), also known as hormonal therapy. This can be achieved in various ways.

a) Permanent interruption of ovarian functions with oophorectomy or radiotherapy (Mastro *et al.,* 2011). Oophorectomy is the surgical removal of an ovary or both ovaries. Oophorectomy is a good strategy to treat breast cancer but it has a few negative consequences such as menopause, infertility and increased risk of osteoporosis and coronary artery disease. Oophorectomy is irreversible (Puhalla, 2009).

b) Temporary suppression of oestrogen using GnRH or LHRH agonists (e.g. Goserelin)

c) Anti-oestrogen therapy (e.g. Tamoxifen) (Figure 1.27).

d) Aromatase and other enzyme inhibitors (Anastrozole, Letrozole etc) (Mastro *et al.*, 2011).

1.9.5.1. GnRH or LHRH agonists

As described earlier (Section 1.5.8), the hypothalamus produces LHRH in pulses which stimulate the pituitary to release gonadotropins, which then stimulate oestrogen production in the ovaries (Abraham and Staffurth, 2011) (Figure 1.26). Synthetic LHRH agonists have higher affinity for the LHRH receptors than endogenous LHRH and therefore the continuous stimulation results in subsequent down-regulation of pituitary LHRH receptors. As a result of this disruption in the hypothalamic–pituitary– ovarian axis, the oestrogen levels decrease within 2–3 weeks reaching the postmenopausal range (Limonta *et al.*, 2001).

LHRH agonists used for the treatment of breast cancer are similar to those used for prostate cancer treatment and include goserelin (Figure 1.8), triptorelin, and

leuprolide (Tammela, 2004; Pauhalla *et al.,* 2009). The effect of these agents is reversible and hence preserves fertility. They also limit the adverse effects of menopause such as osteoporosis (Puhalla *et al.,* 2009).

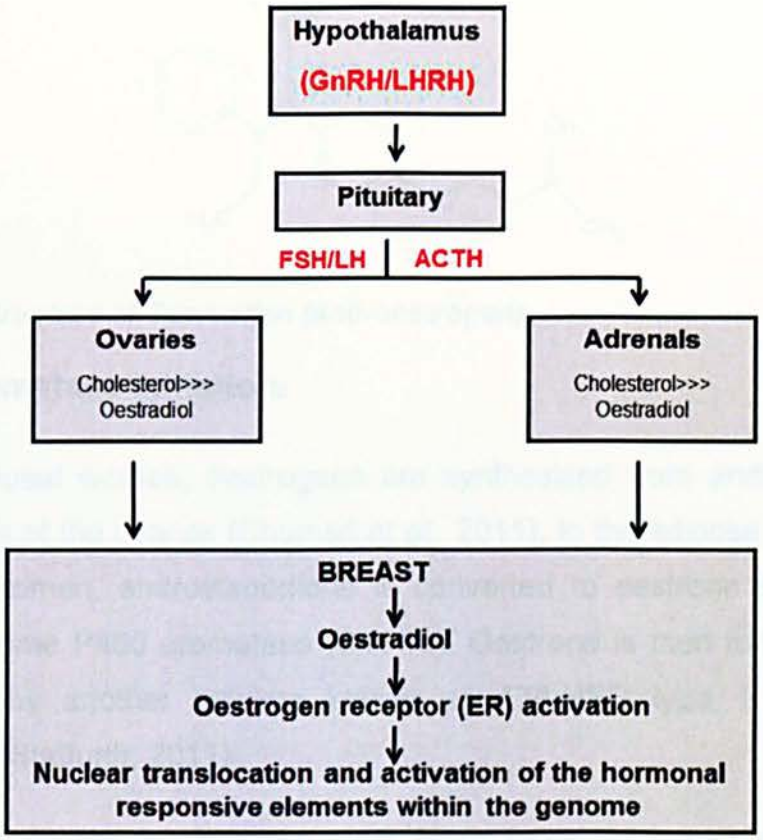

Figure 1.26: The hypothalamic-pituitary-gonadal axis in breast cancer progression. *The GnRH/LHRH from the hypothalamus stimulates the release of FSH and LH from the pituitary that acts on ovaries. The Oestradiol from the ovary and adrenal act on breast cells where they bind to oestrogen receptors (adapted from Abraham and Staffurth, 2011).*

1.9.5.2. Anti-oestrogens

The ER-positive breast tumours are dependent on oestrogen signalling for their growth and replication and they can be treated by anti-oestrogen therapy with either tamoxifen or an aromatase inhibitor. However, ER-negative tumours do not respond to anti-oestrogen therapy (Del-Re *et al.,* 2011). Tamoxifen (Figure 1.27) is known as an anti-oestrogen because it blocks oestrogen receptors (Singh *et al.,* 2011, Abraham and Staffruth, 2011). Tamoxifen is an anti-oestrogen used in the treatment of oestrogen receptor positive breast cancer in premenopausal women (Colleoni *et al.,* 2006). Tamoxifen has been reported to decrease the relapse rate

by half and the mortality rate by one third (Stearns *et al.,* 2003; Abraham and Staffurth, 2011).

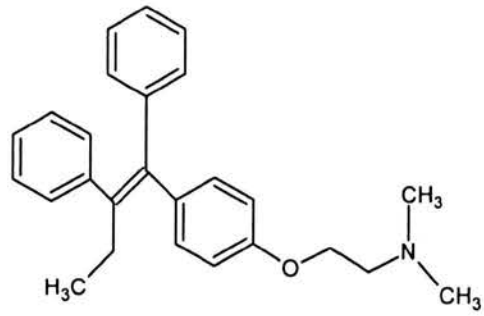

Figure 1.27: Structure of Tamoxifen (anti-oestrogen)

1.9.5.3. Aromatase inhibitors

In premenopausal women, oestrogens are synthesised from androgens by the granulosa cells of the ovaries (Chumsri *et al.,* 2011). In the adipose tissue of post-menopausal women, androstenedione is converted to oestrone by an enzyme called cytochrome P450 aromatase (CYP19). Oestrone is then further converted to oestradiol by another enzyme known as 17β-HSD type 1 (Figure 1.10) (Abraham and Staffurth, 2011).

High levels of aromatase enzyme have been found in breast cancer tissues (Kristensen *et al,* 2000). This is why aromatase inhibition is one of the main strategies for the treatment of breast cancer (Harada, 1997). In the post-menopausal woman, aromatase inhibitors are also used for the treatment of ER-positive breast cancer (Singh *et al.,* 2011).

Since the aromatisation of androgen substrates is the terminal and rate limiting step in oestrogen biosynthesis (Brodie, 1987), inhibitors of the aromatase enzyme have been used as a treatment for hormone-dependent breast cancer (Brueggemeier, 2004). There are two different kinds of inhibitors of aromatase enzyme according to their mechanism of action and structure.

a) Type-I inhibitors: These are steroidal in nature that bind to the substrate-binding site of the enzyme and their action is irreversible (Miller, 1997). Examples of these compounds are exemestane and aminogluthetethimide (Figure 1.28) (Lonning *et al.,* 2000).

b) Type-II inhibitors: These are competitive reversible inhibitors. They are non-specific and can target other steroid-metabolising enzymes. They are azoles in structure (Miller, 1997). Examples of these compounds include anastrozole (Howell *et al.,* 2003) and letrozole (Keam and Scott, 2006).

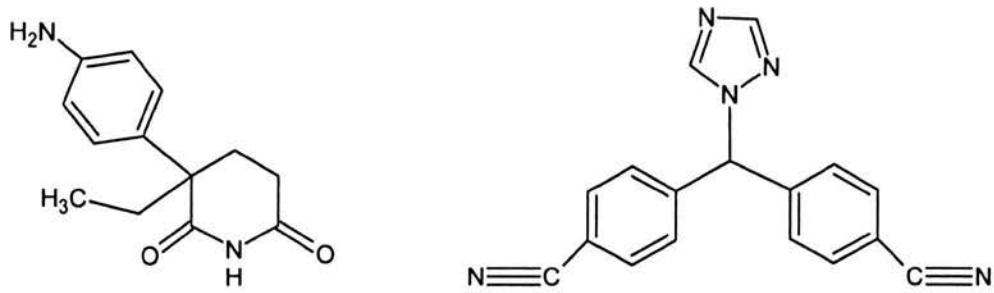

Aminoglutethimide letrozole

Figure 1.28: Examples of aromatase inhibitors

1.9.6. Clinical trials for breast cancer

Some early clinical trials have been conducted with the epidermal growth factor (EGFR) tyrosine kinase inhibitors (TKIs); gefitinib or erlotinib, either alone or in combination with other treatments. In one study, gefitinib was used alone or in combination with anastrozole for 4 to 6 weeks prior to surgery in women with oestrogen receptor (ER) and EGFR positive breast cancer. The results from the trial have reported that the combination of gefitinib and anastrozole (an aromatase inhibitor) reduces the tumour cell proliferation (Polychronis *et al.,* 2005). A phase II trial of tamoxifen alone and in combination with gefitinib was conducted in postmenopausal women with ER positive metastatic breast cancer and showed an increased progression-free survival (Osborne *et al.,* 2011). Recently, another clinical trial of anastrozole alone and in combination with gefitinib was conducted in women with ER positive advanced breast cancer. The results have reported progression-free survival (Christofanili *et al.,* 2010). Another aromatase inhibitor, letrozole, has been used along with a monoclonal antibody trastuzumab in patients with metastatic breast cancer and has been shown to be an acceptable, effective, and well-tolerated treatment for patients with metastatic oestrogen receptors breast cancer (Marcom *et al.,* 2007).

Tamoxifen is currently used in both pre and post-menopausal women (Pauhalla *et al.,* 2011). Different clinical trials have investigated the use of tamoxifen alone or in combination with other treatments and have showed an increase in recurrence free-survival (IBCSG, 2006; Morales *et al.,* 2007). In 2011, the Early Breast Cancer Trialists Collaborative Group (EBCTCG) overviewed 20 trials which evaluated tamoxifen. They have demonstrated that tamoxifen produces a significant reduction in recurrence during the initial 10 years following treatment (EBCTCG, 2011). Based on these results, tamoxifen is currently used as a standard treatment particularly in premenopausal women. Despite the great benefit of tamoxifen, approximately one-third of women treated with adjuvant hormonal therapy will have a recurrence of their cancer. (Puhalla *et al.,* 2011).

Aromatase inhibitors, such as anastrozole, letrozole and exemestane, inhibit the conversion of androgens and oestrogens. These aromatase inhibitors are currently used as adjuvant therapies for the treatment of breast cancer. The ATAC trial (Anastrozole, Tamoxifen, alone or in Combination), BIG 1–98 trial (letrozole-tamoxifen trial), IES trial (exemestane-tamoxifen), MA.17 trial (letrozole-tamoxifen) have confirmed significant improvements in disease-free survival (Cuzick *et al.,* 2010; Regan *et al.,* 2011; Coombes *et al.,* 2007).

1.10. Aims and objectives

The aims of the present study include the development of novel assays in the treatment of hormone-dependent cancers. As such, the project involves the development of an *in vitro* enzyme assay system for the biochemical evaluation of novel compounds designed and synthesised within laboratories at Kingston University. The study involves the initial screening of a range of compounds against CYP17 and 17β-HSD3 enzymes followed by the determination of IC_{50} and IC_{80} values.

The present study was also targeted towards the development of a cell culture based system for the further evaluation of the compounds as anti-metastatic agents against different cancer cell lines. This part of study focuses on the effect of the potential enzyme inhibitors on the viability of human cell lines.

The development of an *ex vivo* tumour and endothelial cell-adhesion model is also an aim in this project which can be used to determine the effect of CYP17 inhibitors on the adhesion of tumour cells on endothelium cell monolayers.

A further aim of the this study includes the determination of the expression of adhesion molecules and their effect on tumour cells in a tumour-endothelial cells co-culture following treatment with CYP17 inhibitors.

CHAPTER 2: MATERIALS AND METHODS

2.1. Radiometric enzyme assays

The assays involve the use of tritium (^3H) labelled substrates which are converted into ^3H-labelled products upon addition of enzyme. Rat testicular microsomes were used as the source of all three enzymes. The radiolabelled substrate and products were separated on a thin layer silica chromatogram. The samples were then added into a scintillation counter and the counts per minute (CPM) were recorded. The inhibitory activity of the compounds synthesised against these enzymes was also determined.

2.1.1. Materials and instrumentation

All non-radioactive steroids and laboratory reagents were Analar grade; ß-NADP (mono sodium salt), D-glucose-6-phosphate (mono sodium salt) and D-glucose-6-phosphate dehydrogenase (5mg/mL); grade II, from yeast (specific activity 140U/mg with glucose-6-phosphate), were obtained from Roche Diagnostics (Lewes, UK). Ketoconazole was obtained from Sigma-Aldrich (Dorset, UK). Radiolabelled [1, 2, 6, 7^{3}H] progesterone, [1, 2, 6, 7^{3}H] 17α-hydroxyprogesterone and [1, 2, 6, 7-^{3}H] androstenedione were obtained from GE Healthcare (Amersham, UK).

Radioactivity was measured using a Perkin-Elmer Tri-Carb 2900TR scintillation counter. Scintillation fluid was Optiscint Hisafe and was obtained from Perkin-Elmer Life and Analytical Sciences (Beaconsfield, UK).

Sprague-Dawley rats testes were obtained from Charles Rivers (Margate, Kent). Homogenisation of the rat testicular tissue was carried out using an Ultra-Turrax homogeniser (Janke and Kunkel, Germany). Excess tissue and the microsomal fraction were further homogenised with a Potter-Elvehjem homogeniser (Fisher Scientific, UK). Centrifugation was carried out using a Beckmann Coulter Ultracentrifugation machine. The optical density of solutions was measured using a UNICAM 8700 series UV/VIS spectrophotometer from Thermo Scientific (Loughborough, UK).

All assays for 17α-Hydroxylase and 17, 20 Lyase were based on the work of Owen *et al* (1999) while the 17 β-HSD3 assays were based on the work of Lain *et al*

(2001). Assays were carried out in triplicate and as such each value is the mean ± SEM of nine determinations.

2.1.2. Substrate, buffer and solution preparation

2.1.2.1. Substrate preparation of [1, 2, 6, 7-^{3}H] Progesterone

A stock solution was prepared by transferring 40 µL of radiolabelled [1, 2, 6, 7-^{3}H] progesterone (0.74 µM) in toluene to a glass vial. The toluene was removed under a stream of nitrogen. Unlabelled progesterone in propane-1-2-diol (199.26 µM, 1mL) was added to the radiolabelled residue and mixed thoroughly to give a final concentration of 200 µM.

2.1.2.2. Substrate preparation of [1, 2, 6, 7-^{3}H] 17α-hydroxyprogesterone

A stock solution was prepared by transferring 40 µL of radiolabelled [1, 2, 6, 7-^{3}H] 17α-hydroxyprogesterone (0.57 µM) in toluene to a glass vial. The toluene was removed under a stream of nitrogen. Unlabelled progesterone in propane-1-2-diol (199.43 µM, 1 mL) was added to the radiolabelled residue and mixed thoroughly to give a final concentration of 200 µM.

2.1.2.3. Substrate preparation of [1, 2, 6, 7-^{3}H] androstenedione

A stock solution was prepared by transferring 20 µL of radiolabelled [1, 2, 6, 7-^{3}H] androstenedione (0.22 µM) in toluene to a glass vial. The toluene: ethanol mixture was removed under a stream of nitrogen. Unlabelled progesterone in propane-1-2-diol (99.78 µM, 1 mL) was added to the radiolabelled residue and mixed thoroughly to give a final concentration of 100 µM

2.1.2.4. Sodium phosphate buffer pH 7.4

(A) 1.95 g of sodium dihydrogen orthophosphate ($NaH_2PO_4.2H_2O$) was dissolved in 250 mL of distilled water

(B) 2.23 g of disodium hydrogen orthophosphate ($Na_2HPO_4.2H_2O$) was dissolved in 250 mL of distilled water

Solution A was added to solution B until a pH of 7.4 was reached.

2.1.2.5. Potassium phosphate buffer pH 7.4

(A) 34.84 g of dipotassium hydrogen orthophosphate was dissolved in 1L of distilled water

(B) 13.61 g of potassium dihydrogen orthophosphate was dissolved in 500 mL of water.

Solution B was added to solution A until pH 7.4 was reached. The resulting buffer solution (250 mL) was further diluted to make a solution of 50 mM using water (750 mL). The pH of the diluted buffer was again checked and adjusted to pH 7.4 if required.

2.1.2.6. Sucrose phosphate buffer pH 7.4

21.39 g of sucrose was dissolved in 250 mL of 50 mM potassium phosphate buffer (pH 7.4).

2.1.2.7. NADPH-generating system

28.2 mg of D-glucose-6-phosphate, 8.6 mg of NADP-sodium salt and 15 µL D-glucose-6-phosphate dehydrogenase (140 U/mg) were added to 1 mL of sodium phosphate buffer (pH 7.4).

2.1.3. Preparation of testicular microsomes

Rat testes were de-capsulated and placed in sucrose phosphate buffer (pH 7.4). The tissue was then homogenised using an Ultra-Turrax homogeniser at short bursts while tissues were kept on ice to maintain the temperature below 4°C. Further homogenisation was carried out using a Potter homogeniser. The homogenised tissue was then centrifuged for 20 min at 4°C at 10,000*g*. The supernatant was retained while the pellet was discarded. The supernatant was again centrifuged for 1h at 4°C at 100,000*g*. The resulting pellet (microsomal fraction) was retained. The pellet was re-suspended in sodium phosphate buffer (pH 7.4) using a Potter homogeniser. Aliquots of 500 µL of suspension were pipetted and stored at -80°C.

2.1.4. Estimation of protein content of rat testicular microsomes

The protein content of the microsomal fraction was determined using the Folin-Lowry assay. This assay depends on the presence of aromatic amino acids in the protein (Lowry *et al*, 1951). A cupric/peptide bond complex (between the alkaline copper-phenol reagent used and the tyrosine and tryptophan residues of the protein) is formed and is enhanced by a phosphomolybdate complex with the aromatic amino acids. The protein content was determined colorimetrically with reference to a standard curve of bovine serum albumin (Gibson and Skett, 1994). The optimum absorbance was found to be λ_{max} 750 nm.

Bovine serum albumin (5 mg in 25 mL of distilled water) was used to make a stock protein solution (200 µg/mL). Standard solutions (0, 40, 80, 160 and 200 µg/mL, 1 mL) containing different amounts of bovine serum albumin protein stock were prepared. The microsomes were diluted by a factor of 100 (250 µL of micorosome in 25 mL of distilled water) and 1mL of these dilutions (in triplicate) tested alongside the standards.

Anhydrous sodium carbonate was dissolved in 0.1 M sodium hydroxide to make 2% of solution A. 200 mL of solution A was mixed with 2 mL of 1% copper sulphate and 2 mL of 2% sodium potassium tartrate to make solution B. 5 mL of solution B was added at 30 seconds interval to each test tube. After standing for 10min, a 50% diluted solution of Folin-Ciocalteu's phenol reagent (0.5 mL) was

added to each tube. The tubes were immediately vortexed and allowed to stand at room temperature (30 min). The optical density at λ_{max} 750 nm of each solution was measured against the blank.

2.1.5. Radiometric assays for 17α-OHase activity

The enzyme, 17α-OHase, catalyses the conversion of progesterone and pregnenolone into 17α-hydroxy-progesterone and 17α-hydroxy-pregnenolone respectively. The kinetic parameters of this enzyme have been determined as follows.

2.1.5.1. Validation of 17α-OHase activity

To validate the 17α-OHase assay, it was necessary to determine the dependency of the assay on a number of factors. The progesterone (final concentration 2 μM) was incubated for 30 min at 37°C in the following solutions.

- Sodium phosphate buffer (50 mM, pH7.4)
- Testicular microsomes (0.13 mg/mL, 10 μL) and sodium phosphate buffer, lacking the NADPH-generating system
- Testicular microsomes, denatured by addition of diethyl ether (2 mL), sodium phosphate buffer and an NADPH-generating system
- Testicular microsomes (0.13 mg/mL, 10 μL), sodium phosphate buffer and the NADPH-generating system

After incubation, the assay was quenched with diethyl ether (DEE) (2 mL). The solutions were vortexed, then left to stand on ice for 15 min. The organic phase was extracted into a separate clean tube. The assay mixture was further extracted with DEE (2x2 mL) and the organic layers were separated by freezing the bottom aqueous layer in liquid nitrogen. The assay tubes were left overnight in a fume cupboard and DEE was evaporated. 30 μL of ethanol was added to each tube and the solution spotted onto silica-based TLC plates along with carrier steroids (Progesterone (P), 17α-hydroxyprogesterone (17α-OHP), testosterone (T) and androstenedione (AD), 5mg/mL). The plates were developed using a mobile phase which consisted of 70 mL of dichloromethane and 30 mL of ethyl acetate. After

development, the separated spots were identified using a UV lamp, cut from the TLC plates and placed into a scintillation vial. 1 mL of acetone and 3 mL of scintillation fluid was then added. The samples were then vortexed and put in the scintillation counter to count ^{3}H for 3 mins. None of the samples showed detectable quantity of products. This indicated that both testicular microsomes and NADPH are essential for conversion of progesterone to its subsequent products. However, when both testicular microsome and NADPH system was added into reaction tube, the detectable quantity of products were found.

2.1.5.2. Protein determination for assay for 17α-OHase activity

This assay was carried out to ensure that the rate of appearance of product during the enzymatic reaction was proportional to the protein concentration.

The assay mixture contained protein at concentrations of 0.625, 1.25, 2.5, 3.75, 5 and 6.25 mg/mL (final concentration), radiolabelled progesterone (2 μM, 10 μL), an NADPH generating system (50 μL) and sodium phosphate buffer (pH 7.4, made up to 1 mL). The assay was initiated by adding protein (enzyme) and the mixture was incubated for 30 min at 37°C. The reaction was quenched by the addition of DEE (2 mL). The assay was completed as previously described (Section 2.1.5).

The percentage conversion of each sample was calculated as follows:

$$\%\ \text{conversion} \frac{\text{CPM (17}\alpha\text{-hydroxyprogesterone + Androstenedione + Testosterone)}}{\text{CPM (Progesterone 17}\alpha\text{-hydroxyprogesterone + Androstenedione + Testosterone)}} \times 100\%$$

2.1.5.3. Time dependent assay for 17α-OHase activity

A time dependent assay was carried out to determine the optimum time for the enzymatic reaction and to ensure that the assay was within the linear phase of the enzyme reaction. The radiolabelled progesterone (2 μM, 10 μL), NADPH generating system (50 μL) and sodium phosphate buffer (pH 7.4, 930 μL) were incubated in triplicate at 37°C in a shaking water bath for 5 min. The assay was initiated by the addition of testicular microsomes (final assay concentration 1.25 mg/mL, 10 μL). After 5, 10, 20, 30, 45, 60 and 90 min of incubation respectively, the assay tubes were quenched by the addition of 2 mL of DEE and placed on ice.

The assay was completed as previously described (Section 2.1.5.1) and percentage conversion was determined.

2.1.5.4. Determination of the Michaelis constant (K_m) for 17α-OHase activity

The assay was carried out in triplicate. The radiolabelled progesterone was serially diluted with propane-1,2-diol, to give a range of final incubation concentrations of 0.25, 0.5, 1, 2, 3, 4 and 5 μM. Assay mixtures (1 mL) contained the NADPH-generating system (50 μL), progesterone (10 μL) and phosphate buffer (930 μL, pH 7.4). The assay was initiated by the addition of the microsomes (10 μL, 1.25 mg/mL) and the mixture was incubated for 25 min. The reaction was quenched by the addition of 2 mL of DEE and placed on ice. The assay was completed as previously described (Section 2.1.5.1).

The velocity of the reaction (V: μM/min/mg) was calculated using following equation:

$$V = \frac{\text{CPM (AD + T + 17}\alpha\text{OHP) x Substrate concentration. [S] (}\mu\text{M)}}{\text{CPM (AD + T + 17}\alpha\text{OHP + P) x Protein Conc. (mg/ml) x time (min)}}$$

2.1.5.5. Preliminary screening of synthesised compounds for 17α-OHase inhibitory activity

Synthesised inhibitors and the reference drug KTZ were dissolved in dimethyl sulfoxide (DMSO) and diluted to give the required final incubation concentration of 5 μM and 100 μM. The total assay volume was 1 mL. Substrate (10 μL, 2 μM), inhibitors (20 μL), an NADPH generating system (50 μL) and sodium phosphate buffer (pH 7.6) (910μL) were added to each tube. The assay was initiated by the addition of microsomes (10μL, 1.25mg/mL). The tubes were incubated for 25 min at 37°C and were then quenched by the addition of 2 mL of DEE and placed on ice. Control samples with no inhibitor were also incubated. The assay was completed as previously described (Section 2.1.5.1).

The percentage inhibition for each sample was calculated as follows:

$$\%\,\text{Inhibition} = \frac{\text{Avg \% conversion of Blank} - \text{Avg \% conversion of compound}}{\text{Avg \% conversion of Blank}} \times 100\%$$

2.1.5.6. Determination of IC_{50} of compounds synthesised against 17α-OHase activity

IC_{50} is defined as the inhibitor concentration required for 50% inhibition of the enzyme activity. KTZ was used as a reference inhibitor to compare the inhibition exerted by the synthesised compounds against 17α-OHase activity. In the case of the IC_{50} assay, different concentrations of a single inhibitor (20 μL) were tested depending on their initial screening results. The assay was carried out in the same manner as described previously (Section 2.1.5.1). The % inhibition was calculated using the equation as described previously (Section 2.1.5.5). The IC_{50} of the compounds was calculated using a statistics package (GraphPad, Software, Inc. USA).

2.1.6. Radiometric assays for lyase activity

The bond between carbon (17) and carbon (20) of 17α- hydroxyl substrates is lysed by the enzyme 17, 20 lyase. The compounds were tested for 17, 20 lyase inhibitory activity, using the rat testicular microsome preparation. This enabled the measurements of the effect of the novel compounds on the rate of conversion of radiolabelled 17α-hydroxyprogesterone to androstenedione by the enzyme lyase. The assay was carried out in the same manner as described previously (Section 2.1.5.1-2.1.5.5).

The percentage conversion of 17α-hydroxyprogesterone to androstenedione and testosterone was then determined using the following equation

$$\%\ \text{conversion} = \frac{\text{CPM (Androstenedione + testosterone)}}{\text{CPM(Androstenedione+testosterone+17}\alpha\text{-hydroxyprogesterone)}} \times 100\%$$

2.1.6.1. Validation of the 17, 20 lyase activity of the conversion of 17α-hydroxyprogesterone to androstenedione

Radiolabelled 17α-hydroxyprogesterone (final concentration 2 μM) was incubated in the presence and absence of enzyme and an NADPH system to validate the lyase assay. The assay was completed as described previously (section 2.1.5.1). None of the samples showed detectable quantities of product. However, when both testicular microsome and NADPH system was added into reaction tube, the

detectable quantity of products were found indicating that testicular microsomes and NADPH are both essential requirements for the conversion of 17α-hydroxyprogesterone.

2.1.6.2. Protein determination for 17, 20 lyase activity

The assay was carried out in the same manner as described previously (Section 2.1.5.2) but in this assay, 17α-OHP was used as the substrate.

2.1.6.3. Time dependent assay for 17, 20 lyase activity

A time dependency assay was carried out in the same manner as described previously (Section 2.1.5.3) except that the assay was initiated by the addition of 40 μL (2.5 mg/mL) of testicular microsomes. The substrate used was 17α-OHP.

2.1.6.4. Determination of the Michaelis constant (K_m) for 17, 20 lyase activity

The testicular microsome (40 μL, 2.5 mg/mL) was thawed and added to the reaction mixture containing radiolabelled substrate, an NADPH system and phosphate buffer. The tubes were incubated for 15 mins and the assay was completed in the same manner as described previously (Section 2.1.5.4).

2.1.6.5. Preliminary screening of compounds synthesised against 17, 20 lyase inhibitory activity

The prepared substrate (10 μL, 2 μM), synthesised inhibitors (20 μL), an NADPH generating system (50 μL) and sodium phosphate buffer (pH 7.4) were added to each tube. The assay was initiated by the addition of microsomes (40 μL, 2.5 mg/mL). The tubes were incubated for 15 mins at 37°C and the assay was completed as previously described (Section 2.1.5.5).

2.1.6.6. Determination of IC_{50} of compounds synthesised against 17, 20 lyase activity

In the IC_{50} assay, different concentrations of a single inhibitor (20 μL) were tested depending on their initial screening results. The assay was carried out in the same manner as described previously (Section 2.1.5.6).

2.1.7. Radiometric assays for 17β-hydroxysteroid dehydrogenase type 3 (17β-HSD3) enzyme activity

Androstenedione is converted into testosterone by the enzyme 17β- HSD3. The kinetic parameters of 17β-HSD3 enzyme have been determined as follows.

2.1.7.1. Validation of the 17β-HSD3 activity for the conversion of androstenedione to testosterone

The substrate (androstenedione, final assay concentration 1 μM) was incubated in the presence and absence of enzyme and an NADPH system to validate the 17β-HSD3 assay. At the end of assay, the samples were read for radioactivity for 4 mins. None of the samples showed detectable quantities of testosterone. However, when both testicular microsome and NADPH system was added into reaction tube, the detectable qunatity of products were found indicating that testicular microsomes and NADPH are both essential requirements for the conversion of androstenedione to testosterone.

2.1.7.2. Protein determination for 17β-HSD3 activity

Radiolabelled androstenedione (10 μL, final assay concentration = 1 μM) was incubated with an NADPH-generating system (50 μL) and phosphate buffer (pH 7.4, 1 mL). The reaction was initiated by adding rat testicular microsomes (at protein concentrations of 0.097, 0.244, 0.487, 0.731 and 0.974 mg/mL). The solutions were then incubated for 30 mins at 37°C. After the incubation period, the reaction was quenched by adding 2 mL diethyl ether (DEE) and placed on ice. The assay was completed as previously described (section 2.1.5.1) and samples were read for radioactivity for 4 mins.

The percentage conversion was determined by using the following equation.

$$\%\ \text{conversion} = \frac{\text{CPM (Androstenedione)}}{\text{CPM (Androstenedione+testosterone)}} \times 100\%$$

2.1.7.3. Time dependent assay for 17β-HSD3 activity

Radiolabelled substrate (10 μL, final concentration 1 μM) along with an NADPH-generating system (50 μL) and sodium phosphate buffer (pH 7.4, 935 μL) was

added in reaction tubes at 37°C in a water bath. The reaction was then initiated by adding rat testicular microsomes (0.097 mg/mL, 5 µL) and incubated for different time periods (5, 10, 20, 30, 45, 60 and 90 mins). The reaction was then quenched by adding DEE (2 mL) and placed on ice. The assay was completed as described previously (section 2.1.5.1).

2.1.7.4 Determination of the Michaelis constant (K_m) for 17β-HSD3 activity

Radiolabelled androstenedione was serially diluted using propan-1, 2-diol, to give a range of final incubation concentrations of this substrate (0.25 to 6 µM). Reactions were carried out in triplicate. The total volume of each tube was 1 mL containing 10 µL of substrate, an NADPH-generating system (50 µL) and sodium phosphate buffer pH 7.4 (935 µL). This incubation mixture was kept in a water bath at a temperature of 37°C. The reaction was started by adding rat testicular microsomes (5 µL, protein concentration 0.007 µg/mL). The mixture was incubated for 35 mins at 37°C. After incubation the reaction was quenched by adding 2 mL of DEE. The assay was completed as previously described (Section 2.1.5.1).

The velocity of the enzyme reaction (V: µM/min/mg) was calculated using the following equation:

$$V = \frac{\text{CPM (AD) x Substrate concentration. [S] (µM)}}{\text{CPM (AD + T) x Protein Conc. (mg/ml) x time (min)}}$$

2.1.7.5. Preliminary screening of compounds synthesised against 17β-HSD3 activity

The prepared substrate (10 µL, 1 µM), synthesised inhibitors (20 µL), an NADPH generating system (50 µL) and sodium phosphate buffer (pH 7.4) were added to each tube. The assay was initiated by the addition of microsomes (5 µL, 0.097 mg/mL). The tubes were incubated for 35 mins at 37°C and the reaction was completed as previously described (Section 2.1.5.1).

2.1.7.6. Determination of IC_{50} of compounds synthesised against 17B-HSD3 activity

To determine IC_{50s}, different concentrations of a single inhibitor (20 µL) were tested depending on their initial screening results. The assay was carried out in the same manner as described previously (Section 2.1.5.6).

2.2. Cytotoxic and cell adhesion assays

2.2.1. Cell lines

Three kinds of cell lines have been used throughout this work.

a) Human vascular endothelial cells (HUVECs) were obtained from Promo Cell (Heidelberg, Germany). They were grown in 1:1 of MCDB131 with phenol red containing 20% of foetal bovine serum (FBS) (Gibco Invitrogen, UK) and L-Glutamine-Penicillin-Streptomycin (10,000U penicillin, 10 mg streptomycin/mL in 0.9%NaCl and 200 mM L-glutamine) (Sigma Aldrich, Poole, UK) and endothelial cell growth media (EBM-2) supplemented with growth factors (Lonza Biologics plc, Slough, UK).

   The cell density of a confluent monolayer of HUVECs was assumed to be 3.2 $x10^4$ cells/well of a 96-well plate (information from Corning Life Sciences, UK) and this number of cells was used to calculate the adherence ratio.

b) Human prostate cancer cell lines (DU-145 and PC-3) were a kind gift from Dr. Helmout Modjtahedi, Kingston University and were maintained in Dulbecco's modified essential media (DMEM) (Gibco Invitrogen, Paisley, UK) with 10% FBS and L-Glutamine-Penicillin-streptomycin.

c) Human breast cancer cell lines (MCF7) were obtained from the American Type Culture Collection. The media used for their growth was the same as for DU145 and PC3 cells.

DU145 and PC3 are hormone-independent prostate cancer cell lines whereas MCF7 is a hormone-dependent breast cancer cell line.

2.2.2. Materials and Instrumentation

Dulbecco's modified essential media (DMEM) without phenol red and phosphate buffer saline (DPBS) was purchased from Gibco Invitrogen, UK. Trypsin: EDTA (0.25:0.1%) was purchased from Thermo Scientific. Non-enzymatic cell dissociation solution (EDTA diluted to 0.1% in Phosphate Buffered Saline), bovine serum albumin (BSA), Thiazolyl Blue Tetrazolium Bromide (MTT) dye and DMSO were obtained from Sigma Aldrich (Poole, UK). Microvascular endothelial cell attachment factor was purchased from TCS Cell Works (Buckingham, UK). Phorbol-12-myristate-13-acetate (PMA) was purchased from Merck Chemicals Ltd, UK. TNF-alpha was obtained from R & D systems (Abingdon, UK). Cell tracker green™ was obtained from Invitrogen (Paisley, UK).

Hawksley improved Neubauer (BS.748) chambers were used to count the cells (Lancing, UK). A Labtech LT-4000 microplate reader was used to read the absorbance at 570nm (Ease Sussex, UK). A Fluostar Optima plate reader (BMG Labtech) was used to measure the intensity at an excitation wavelength set at 485 nm and emission at 520 nm (Bucks, UK). A fluorescent microscope (Leica DFC420C) was used for phase-contrast and fluorescent microscopy (Bucks, UK).

2.2.3. MTT assay

This assay was used to determine the cytotoxicity of the compounds which have been synthesised as potential CYP17 inhibitors. Based on the IC_{50} and IC_{80} values (Table 3.7), the compounds with the highest potency were short-listed.

MTT was first developed by Mosmann (1983). The yellow tetrazolium MTT (Thiazolyl Blue Tetrazolium Bromide) is reduced by mitochondrial dehydrogenases in living cells to a blue-magenta coloured formazan precipitate (Mosmann, 1983). The resulting intracellular purple formazan can be solubilised in DMSO and quantified by spectrophotometric means. The intensity of the purple coloured formazan crystals formed during the assay is directly proportional to the viability of cells which is measured at a wavelength of 570nm. (Tunney *et al.*, 2004; Rahman *et al.*, 2004).

The MTT reagent gives low background absorbance values in the absence of cells. For each cell type the linear relationship between cell number and signal produced (amount of formazan produced) is established, thus allowing an accurate quantification of changes in the rate of cell proliferation.

2.2.3.1. Preparation of MTT reagent

Stock solutions of MTT were prepared by dissolving 5mg of dye into 1 mL of phenol red free DMEM. The solution was mixed and further diluted by 1:10 to prepare working standard solutions (50 ng/mL).

2.2.3.2. Protocol for MTT assay

Human vascular endothelial cells (HUVECs), prostate cancer cells (PC3 and DU-145) and breast cancer cells (MCF7) were seeded at a density of $8x10^3$ per 100 µL of phenol red-free DMEM per well. The cells were incubated at 37°C in 5% CO_2 for 24 hrs. The media was then removed from each well and cells were washed with Dulbecco's phosphate buffer saline (DPBS). 100µL of compounds 31, 34, 38, 41, 48, 51 and KTZ (concentrations = IC_{80}) were dissolved in DMSO and media (DMEM) and were added to cells. DMSO in media was added to the wells as a vehicle control. Plates were incubated for another 24 hrs at 37°C in 5% CO_2. A stock solution of MTT dye (5 mg/mL) was diluted by 1:10 with media. 100 µL of MTT reagent was added into each well and then incubated for 2-4 hrs until a purple precipitate was visible. Media was then removed from the wells. 100 µL of DMSO was added to each well to dissolve the purple crystals that had formed. Plates were kept in the dark for 10-15 mins. Absorbance was measured at 570 nm using a Labtech LT-4000 microplate reader.

2.2.4. Adhesion assays

The assay to determine the adhesion of tumour cells on endothelial cells monolayer is based on that of Bild *et al.* (2004). The assay is further modified to develop an *in vitro* model to obtain an "adhered tumour cell-endothelial cell ratio" (TC: EC) in a co-culture. The TC: EC ratio has previously been determined using a fluorescent activated cell sorting (FACS) technique (Haddad *et al.*, 2010; Paprocka *et al.*, 2008).

2.2.4.1. Preparation of fluorescent media

Cell tracker green™ from Molecular Probes was used for the specific labelling of tumour cells. Before opening the dye vial, the lyophilised product was allowed to warm to room temperature. The dye was then dissolved in 10 µL of sterile DMSO to a concentration of 10 mM. The stock solution was then diluted to a final working concentration of 2.5 µM in serum-free DMEM. The working solution was warmed to 37°C before use.

2.2.4.2. Fluorescence labelling of tumour cells

Semi-confluent DU145, PC3 and MCF7 tumour cells were washed twice with DPBS and incubated with serum-free and phenol red-free DMEM containing 2.5µM cell tracker green™ for 30 min at 37°C in a CO_2 incubator (Bild *et al.*, 2004). Cells were then incubated with cell-tracker free and serum-free media for half an hour. Media was replaced with fresh media after every hour (2X). This enabled the complete conversion of the fluorescent label. The replacement of media after specific intervals also washed off the excess fluorescent dye.

2.2.5. *Effect of TNF-α on tumour cell adhesion*

A 100µL of the 0.1% gelatin solution was added into each well of the 96-well plates. The plates were then incubated at 37°C in 5% CO_2 for 30 mins. The gelatin was aspirated after half an hour. HUVEC cells were seeded in gelatin-coated plates and cultured in the 1:1 mixture of endothelial growth medium (EBM-2) with supplement mix and MCDB131 supplemented with L-Glutamine, Penicillin and Streptomycin and 20% FBS. Cells were incubated for 24-72 hrs until they formed a monolayer. HUVEC cells were checked for confluency before each set of experiments using phase-contrast microscopy. Monolayers were washed with DPBS. Confluent monolayers were subsequently incubated with 0-1 µg/mL TNF-alpha (TNF-α) in EGM-2 for 24 hours at 37°C to increase the adhesive potential of the endothelium (Haddad *et al.*, 2010). Endothelial monolayers were washed with media to remove TNF-α. The fluorescence labelled tumour cells (section 2.2.4.2) were harvested by adding non-enzymatic cell dissociation solution (0.1% EDTA) for 15 min at 37°C. Tumour cells ($8x10^4$ per well) in 100µL serum- free and phenol red free DMEM were added onto HUVEC monolayers. Endothelial cells were

incubated with tumour cells for 2 hours in 5% CO_2 at 37°C. Following this incubation, monolayers were washed 2X with DMEM to remove non-adherent cells. Tumour cell fluorescence, as an index of cell adherence, was detected using a Fluostar Optima plate reader (BMG Labtech) with the excitation wavelength set at 485 nm and emission at 520 nm. Phase contrast microscopy was performed to check the HUVEC monolayers for consistency and fluorescence microscopy was performed to ascertain tumour cell labelling. Images of tumour cells adhered onto endothelial monolayers were taken using both phase contrast and fluorescent microscopy simultaneously.

2.2.6. *Estimation of endothelial cell:tumour cell (EC:TC) ratio on TNF-α activated HUVEC monolayers*

HUVEC monolayers were activated with 10 ng/mL of TNF-α for 24 hours at 37°C in 5% CO_2. Different numbers of fluorescently-labelled tumour cells (10,000-160,000) were added to activated and non-activated HUVEC monolayers in 100μL serum-free DMEM for 2 hrs. Tumour cells alone (10,000 - 160,000) were also seeded in separate wells as a control which gave a measure of total fluorescence for that particular number of cells. Following two hours incubation, monolayers were washed twice with DMEM to remove non-adhered cells. The assay was completed as described previously (Section 2.2.5).

2.2.7. *Effect of CYP17 inhibitors on tumour cell adhesion to HUVEC monolayers*

Semi-confluent DU145, PC3 and MCF7 cells were treated with the synthesised CYP17 inhibitors at the concentrations equal to their IC_{80} values (Table 3.7) for 24 hrs. HUVEC monolayers were activated with 10ng/mL of TNF-α for 24 hrs. Tumour cells were fluorescently labelled with cell tracker green™ as described previously (section 2.2.4.2). Labelled tumour cells were added to both activated and non-activated HUVECs monolayers and the co-culture was incubated for 2 hrs. The assay was completed as described previously (section 2.2.5).

2.3. Immunostaining and flow cytometry

The expression of adhesion molecules was determined using fluorochrome-conjugated antibodies which bind to the adhesion molecules present on cell surfaces. The expression of adhesion molecules was viewed under a Leica DFC420C fluorescent microscope (Immunostaining) and quantification was carried out by flow cytometry (FACS) and Cell Quest pro software.

2.3.1. Materials and Instrumentation

Cells lines and media were used as described before (Section 2.2.1). Bovine serum albumin and paraformaldehyde powder 95% were purchased from Sigma Aldrich, UK. Eight chamber polystyrene tissue culture slides, BD perm/wash™ buffer, BD cytofix/cytoperm fixation and permeabilisation solution, BD Falcon polystyrene round bottom tubes (or FACS tubes) 12 x 75mm and FACS flow™ were purchased from BD Biosciences, UK.

Human FcR blocking reagent was purchased from MACS Miltenyi Bioteck, UK. FACS samples were centrifuged using a Heraeus FRESCO 17 centrifuge (Thermo Scientific), UK. FACS samples were read using FACS Calibur (BD Biosciences, UK).

2.3.2. Antibodies

Phycoerythrin or PE-Cy™ 5 Mouse IgG1 K Isotype control and PE-Cy™ 5 mouse anti-Human CD54 antibodies were obtained from BD Biosciences, UK. PE-conjugated mouse $IgG1_K$ (clone P3) and PE conjugated anti-human CD144 (VE-Cadherin) (clone 16B1) antibodies were purchased from eBiosciences, UK. ICAM-1 (15.2) (Cat no: Sc-107) mouse monoclonal IgG1 antibody was obtained from Santa Cruz Biotechnologies, USA. Donkey anti-mouse IgG conjugated antibody was purchased from R & D Systems, UK.

2.3.3. Determination of ICAM-1 protein expression by immunostaining

The immunostaining in the present study involves an indirect immunofluorescence technique which involves the use of two antibodies, a primary (1°Ab) and a secondary antibody (2 °Ab). The 1°Ab is specific to the antigen and is unlabelled. The fluorochrome is attached to the 2°Ab which binds to the 1°Ab. This technique is more sensitive than direct immunofluorescence since there is more amplification of the signal (Male *et al.,* 2010).

2.3.3.1. Anti-ICAM-1 (primary antibody) titration

Human endothelial (HUVEC) and tumour cells (PC3, DU145 and MCF7) were trypsinised and 60,000 cells were added to each chamber of the culture slide. Cells were incubated at 37°C in 5 % CO_2 until they formed monolayers. Media was then aspirated from each chamber and cells were washed with PBS. Cells were treated with 10ng/mL TNF-α for 24 hrs at 37°C in 5 % CO_2. After 24 hrs, media was again removed and cells were washed with PBS. Cells were fixed by adding 100µL of 3.7% paraformaldehyde for 10 mins. Cells were washed three times with PBS. 200µL of 1% BSA was added to cells for 30 mins at 37°C. Cells were washed three times with PBS. 200 µL of primary antibody (anti-ICAM) in 1%BSA was added at dilutions of 1:50, 1:100 1:200 and 1:500. Cells were incubated for an hour at room temperature. Cells were washed three times with PBS. 200µL of FITC-conjugated anti-mouse secondary antibody (2 °Ab) in 1% BSA was added to cells. Two types of control were prepared. In control 1, primary antibody (1°Ab) was not added whereas in control 2, secondary antibody (2 °Ab) was not added to cells. The staining of control cells determines the non-specific binding of antibody or high fluorochrome background signals. Cells were incubated for an hour at room temperature. After incubation, cells were washed three times with PBS. Chambers were then removed from the slide. One drop of VECTA SHIELD containing DAPI was added to each cell section. DAPI or 4, 6-diamidino-2-phenylindole is a fluorescent stain that binds strongly to A-T rich regions in DNA and is used to stain the nucleus of the cells. A cover slip was placed on top of the slide. Cells were viewed under a Leica DFC420C fluorescence microscope.

2.3.3.2 Anti-IgG1 (secondary antibody) titration

Monolayers of human vascular endothelial (HUVEC) and tumour cells (DU145, PC3 and MCF7) were washed with PBS. Cells were treated with 10 ng/mL TNF-α for 24hrs. After 24 hrs cells were washed with PBS. Cells were fixed by adding 100μL of 3.7% paraformaldehyde for 10 mins. Cells were again washed three times with PBS. 200μL of 1% BSA was added to cells for 30 mins at 37°C. Cells were washed three times with PBS. 200 μL of primary antibody (anti-ICAM) in 1%BSA (1:50) was added and cells were incubated for 1hr at room temperature. Cells were washed three times with PBS. 200μL of FITC-conjugated anti-mouse IgG1 antibody in 1% BSA was added to cells at dilutions of 1:50, 1:100 and 1:200. Controls with no primary antibody (1°Ab) and secondary antibody (2°Ab) were prepared. Immunofluorescence was completed as described previously (Section 2.3.3.1).

2.3.3.3. Effect of CYP17 inhibitors on ICAM-1 expression in endothelial and tumour cells

The effect of CYP17 inhibitors on adhesion of tumour cells on endothelial cell monolayers has been described previously (Section 2.2.7). The results (Figure 4.3.3.3) showed that compounds 38, 48 and 51 significantly decreased the adhesion of DU145, PC3 and MCF7 cells respectively on HUVEC monolayers. We have therefore specifically looked at the effect of these three compounds on the ICAM-1 expression on three tumour cell lines.

Semi-confluent tumour cells (DU145, PC3 and MCF7) in T25 flasks were washed with PBS. DU145, PC3 and MCF7 cells were activated by 10 ng/mL of TNF-α and also treated with compounds 38, 48 and 51 respectively. Another set of all three tumour cells were treated with ketoconazole.

No drug -TNF	No drug +TNF	KTZ -TNF	KTZ +TNF
No drug -TNF (No 1 Ab)	No drug -TNF (No 2 Ab)	38/48/51 -TNF	38/48/51 +TNF

Figure 2.1: Schematic diagram of 8-well tissue culture slides

Media was removed after 24 hrs and cells were counted using a haemocytometer. 60,000 cells were added per each chamber of the culture slide. Cells were incubated until they formed monolayers. Cells were then washed with PBS. Cells were stained as described previously. Anti-ICAM-1 and Anti-IgG1 antibodies were used at a dilution of 1:50 and 1:100 respectively.

2.3.4. Determination of ICAM-1 protein expression by flow cytometry

Fluorescent activated cell sorting (FACS) is a method which differentiates cells in a cell suspension according to their surface markers (antigens). It is a quick and reliable method. Different antibodies can be detected in the same run and cell clones can be classified according to their immunological properties (Urbanits *et al.*, 2002).

2.3.4.1. Principle of FACS

Cells are made immunofluorescent either directly or indirectly with specific monoclonal antibodies. The cell suspension is then forced to pass through a channel in the form of droplets containing single cells. An air-cooled argon gas laser emitting a monochromatic beam of light is fixed down the path of the channel. As cells pass through the laser beam, light is scattered in various directions. The monoclonal antibodies are associated with fluorochromes which cause an emission of light. This scattering and emission of light is detected by photomultiplier tubes which gives information about the relative size of the cell (forward light scatter-FSC), its shape or internal complexity (side light scatter-

SSC) as well as a diversity of cellular structures and antigens (fluorescence) (Nunez, 2001).

2.3.4.2. CD144 (VE-Cadherin) expression on TNF-α treated and un-treated HUVECS

Two T25 flasks of semi-confluent HUVECs were used. One flask was labelled as "treated" and the other one as "non-treated". Cells were washed with PBS. 10ng/mL of TNF-α in 10 mL of media was added in the "treated" flask while 10mL of media was added in the "non-treated" flask. Flasks were then incubated for 24 hrs after which media was removed from the flask and cells were trypsinised with trypsin: EDTA (0.25:0.1%). Twenty five thousand cells in 100μL were added into each eppendorf tube in duplicate. Cells were centrifuged at 1500 rpm for 5 mins. Pellets were re-suspended in BD perm/wash™ buffer. 1 μg of FcR block per 1 ml of cell suspension (2μL in 100 μL) was added to the cell suspensions for 10 mins at room temperature. Cells were centrifuged at 1500 rpm for 5 mins. PE-conjugated CD144 (VE-cadherin) at dilutions of 1:10, 1:50 and 1:100 in BD perm/wash™ buffer was added to the pellets and incubated for 1hr in a covered ice bucket. To duplicate tubes, equal concentrations of isotype controls were added. Cells were then centrifuged at 1500 rpm for 5 mins. Pellets were washed twice with BD perm/wash™ buffer to remove excess antibody. Pellets were re-suspended in 150μL of BD cytofix/cytoperm fixation and permeabilisation solution. 200 μL of FACS flow was added to cell suspension and samples were read using the FACS Calibur (BD Biosciences, UK).

2.3.4.3. CD144 (VE-Cadherin) expression on tumour cells

Semi-confluent DU145, PC3 and MCF7 were washed with PBS. Serum-free DMEM containing 2.5μM of cell tracker green™ was added and cells were incubated for 15 mins. Media was replaced after 15 mins and then after every 30 mins (2X) with cell tracker-free and serum-free media to wash-off excess fluorescent dye. Cells were then detached from the surface of the flasks by adding 5ml of non-enzymatic cell dissociation solution. Seventy five thousand cells in 100 μL of media were added into each eppendorf tube. Cells were centrifuged

at 1500 rpm for 5 mins. The experiments were completed as described previously (Section 2.3.4.2).

2.3.4.4. CD54 (ICAM-1) expression on TNF-α treated and un-treated HUVEC cells

The non-treated and TNF-α treated HUVECs (25, 000 per tube) in 100 µL of EBM-2 and MCB131 were added into eppendorf tubes. Samples were prepared as described previously (Section 2.3.4.2). PE-Cy5-conjugated CD54 and isotype control antibodies were added to cells at dilutions of 1:10, 1:50 and 1:100. Cells were incubated for 1 hour at 4°C. Pellets were washed twice with BD perm/wash™ buffer to remove excess antibody. Pellets were re-suspended in 150 µL of BD cytofix/cytoperm fixation and permeabilisation solution. 200 µL of FACS flow was added to the solution and samples were read using the FACS calibur machine.

2.3.4.5. CD54 (ICAM-1) expression on fluorescently labelled tumour cells

Tumour cells were labelled with cell tracker green as described before (Section 2.3.4.3). Seventy five thousand cells in 100 µL were added into each tube. Cells were centrifuged at 1500 rpm for 5 mins. Pellets were re-suspended in FACS wash. 1 µg of FcR block per 1 ml of cell suspension (2 µL in 100µL) was added to the cell suspension for 10 mins at room temperature. PE-Cy5-conjugated CD54 (ICAM-1) and isotype control antibody were added to cells at dilutions of 1:10, 1:50 and 1:100 and cells were incubated at 4°C. Cells were then centrifuged at 1500 rpm for 5 mins. The experiment was completed as described previously (Section 2.3.4.2).

2.3.4.6. Effect of CYP17 inhibitors on ICAM1 expression in a EC:TC co-culture

HUVEC cells were activated with 10 ng/mL of TNF-α for 24 hrs. DU145, PC3 and MCF7 cells were also treated with TNF-α and compounds 38, 48 and 51 respectively. Another set of all three tumour cells were treated with ketoconazole. Tumour cells were fluorescently labelled for 15 mins (Section 2.3.4.3). A non-enzymatic cell dissociation solution (5 mL) was added to the flasks. Tumour cells

(75, 000) were mixed with HUVECs (25,000). This co-culture was incubated for 2 hrs at 37°C. Cells were centrifuged at 1500 rpm for 5mins. Pellets were re-suspended in FACS wash. 1 µg of FcR block per 1 ml of cell suspension (2 µL in 100 µL) was added to cell suspensions for 10 mins at room temperature. Cells were centrifuged at 1500 rpm for 5 mins. PE-conjugated CD144 (1:50) and PE-Cy5-conjugated CD54 (1:50) antibodies were added to the pellet and incubated for 1hr in the dark. Respective isotype controls were also added into duplicate tubes. Cells were centrifuged at 1500 rpm for 5 mins. Excess antibody was washed off with FACS wash (3X). Pellets were re-suspended in 150 µL cell fix solution. 200µL of FACS flow was added into the cell suspension and samples were analysed by FACS Calibur.

2.4. Statistical analysis

Statistical analysis was done using a paired t-test (two-tail), one way ANOVA, Tukey's modified student's t-test (two-tail), two way ANOVA and Benferroni's t-test using a statistics package (GraphPad Prism 5.0, Software, Inc. USA) where appropriate.

CHAPTER 3: BIOCHEMICAL ESTIMATION OF THE INHIBITORY ACTIVITY OF COMPOUNDS SYNTHESISED AGAINST CYP17 AND 17β-HSD3

Androgens are important endocrine factors that are involved in the initiation and progression of androgen-dependent diseases such as benign prostate hyperplasia (BPH) and prostate cancer (Prins and Korach, 2008). Androgen ablation is considered as one of the treatments for hormone-dependant prostate cancer. Different therapies have been used to approach the ablation of androgens, such as surgical castration that includes; orchidectomy or prostactomy (Antonarakis *et al.,* 2010), blocking of androgen receptors (Wirth *et al.,* 2007) and use of luteininsing hormone releasing agonist (Tammela, 2004). Although this results in remissions lasting two to three years, nearly all patients will eventually progress to castration-resistant prostate cancer (CRPC), which is fatal in the majority of patients (Pienta and Bradley, 2006). This suggests that despite chemical and surgical castration, there is a continuous production of these hormones from the adrenal glands (Titus *et al.,* 2005; Maltais *et al.,* 2011). There is growing evidence that although castration blocks the generation of gonadal testosterone, androgens originating from other sources may continue to drive androgen receptor signalling, most notably the androgen glands, where 10-30% of the total serum androgens are produced (Bruno and Njar, 2007; Attard *et al.,* 2005). Studies also suggest that androgens may be synthesised *de novo* by castration-resistant tumours (Stanbrough *et al.,* 2006).

Anti-androgens may be weakly agonistic in prostate cancer cells with mutated or overexpressed androgen receptors (Chen *et al.,* 2004). Therefore therapies that inhibit the systemic biosynthesis of androgens through targeting CYP17 and 17β-HSD-Type III may thus represent a rational approach in the treatment of CRPC (Yap *et al.,* 2008; Day *et al.,* 2009; Marchais-Oberwinkler *et al.,* 2011). Both of these enzymes are P450 enzymes which catalyse the last step of androgen biosynthesis in both the testes and adrenal glands. Inhibition of these enzymes will therefore result in a complete block of androgen production (Hartmann, 2002; Vicker *et al.,* 2009).

The risk of getting side effects with enzyme inhibitors should also be minimal compared to different ablation therapies, as the enzyme has specific substrates and a unique expression profile (Day *et al.*, 2009; Maltais *et al.*, 2011).

The aim of the present study is therefore to investigate potential compounds designed and synthesised within the laboratories at Kingston University (Shah *et al.*, 2011; Ahmed *et al.*, 2009; Shahid *et al.*, 2008) that inhibit progression of prostate and breast cancer. The study involves initial screening of a range of compounds that inhibit the activity of CYP17; against both components of this enzyme and 17β-HSD3 enzyme.

3.1. Methods

The enzymes CYP17 and 17β-HSD 3 are present abundantly in testes of rats and humans (Scott *et al.,* 2009). Therefore, rat testicular microsomes were used as a source of these two enzymes. The enzymatic assays for enzyme CYP17 and 17β-HSD3 were based on that of Owen *et al.* (1999) and Lain *et al.* (2001) with few modifications described overleaf.

The concentration of total protein in the testicular homogenate was estimated by the Folin-Lowry method (Section 2.1.4). The radiolabelled substrates were mixed with non-radiolabelled substrates to obtain the required concentrations (Section 2.1.2). The cytochrome P450 enzymes used NADPH as the co-factor (Payne and Hales, 2004) so that the substrate was mixed with an NADPH generating system. The reaction was carried out at a physiological pH (7.6) and temperature (37°C).

The kinetic parameters of the enzymes CYP17 and 17β-HSD3 were determined prior to the evaluation of the inhibitory activity of the compounds, which have been synthesised as potential enzyme inhibitors. Therefore, the enzymatic reaction was carried out at different protein concentrations (protein-dependency assay) at varying time intervals (time-dependency assay) and different substrate concentrations (K_m determination) to find the optimum protein concentration, time and K_m values. The evaluation of the inhibitory activity of synthesised compounds was carried out along with control drugs; ketoconazole (KTZ), 7-hydroxyflavone and biacalein. The IC_{50} and IC_{80} were determined for the compounds using a statistics package (GraphPad Prism 5.0, Software, Inc. USA).

3.2. Results

3.2.1. Estimation of protein content of rat testicular microsome

The protein content of the microsomal homogenate fraction was determined using the Folin-Lowry assay. The mean absorbance of the protein was found to be 0.28 (O.D.) at 750 nm. The protein concentration in testicular microsomes was extrapolated from a graph plotted from the mean of three different experiments and calculated as 10.77 mg/mL (Figure 3.1).

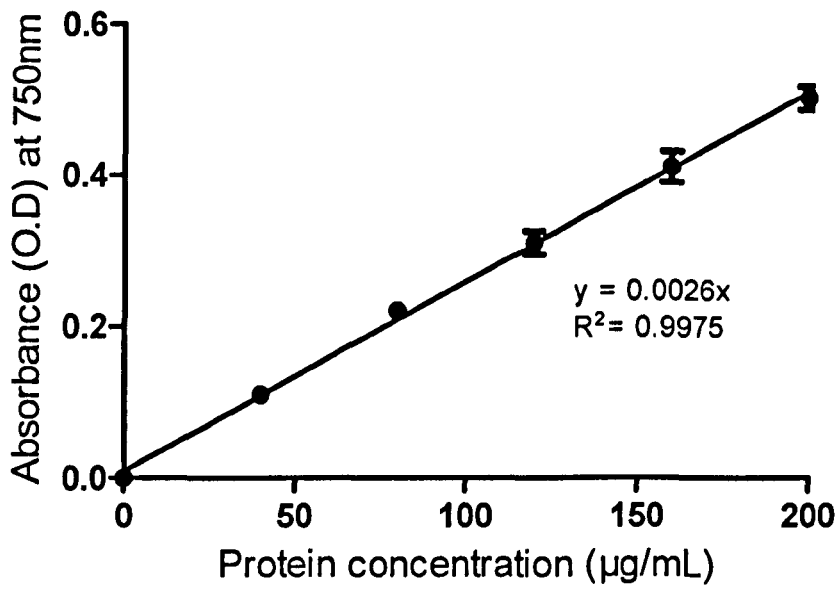

Figure 3.1: Standard curve for the estimation of total protein content of rat testicular microsomes by the Folin-Lowry method. *The concentration of protein was calculated using the graph equation. The data is the mean ± SEM of three different experiments (n = 3).*

3.2.2. Protein-dependency assay for the 17α-OHase enzyme

The testicular microsomes were added in different volumes to the reaction mixture to get various concentrations of enzymes. The % conversion was calculated using the equation previously mentioned (Section 2.1.5.2). The graph shows that the kinetics of the 17α-OHase reaction is linear for concentrations up to 0.11 mg/mL (Figure 3.2).

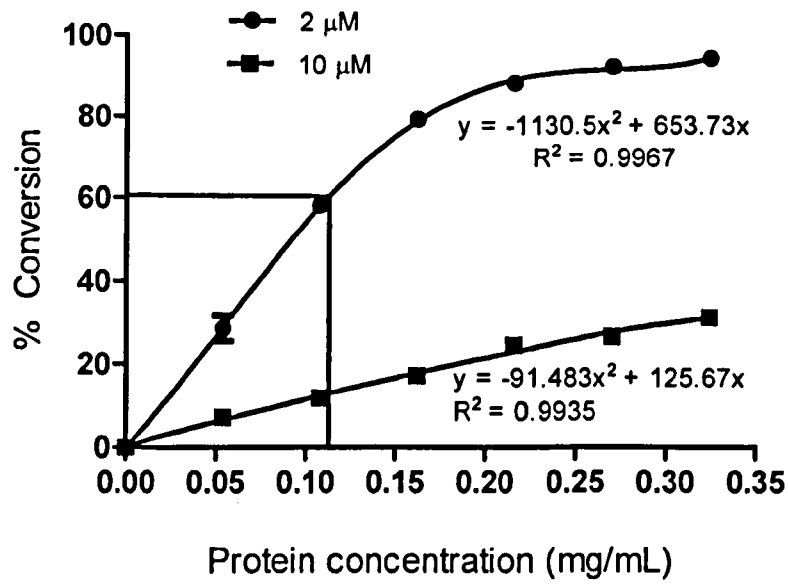

Figure 3.2: **The percentage conversion of progesterone to 17α-hydroxyprogesterone at varying protein concentrations.** *The data is the mean ± SEM of three different experiments (n = 3).*

3.2.3. Time-dependency assay for the 17α-OHase enzyme

The reaction mixture was incubated with 0.11 mg/mL protein at various time intervals. Two separate reactions were carried out with two different substrate concentrations. From figure 3.3, it can be concluded that the kinetics of the reaction are linear up to 25 mins from the start of the experiment.

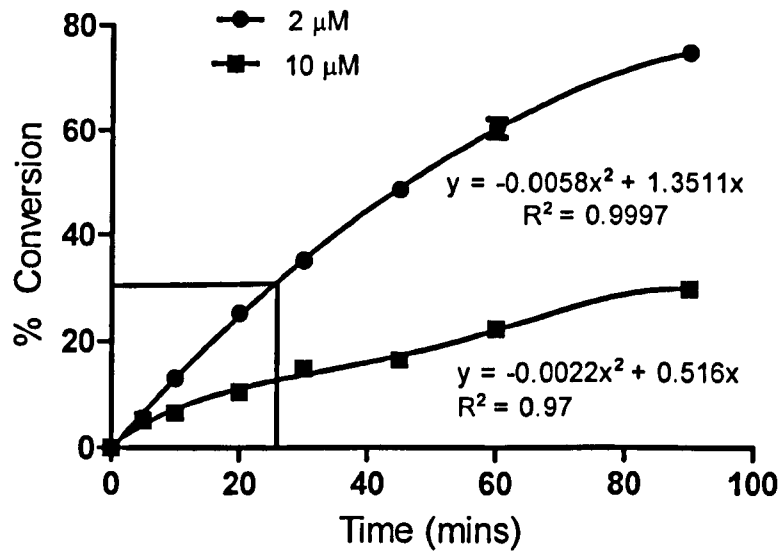

Figure 3.3: ***Graph to show percentage conversion of progesterone to 17α-*** **hydroxyprogesterone** ***at varying time intervals*** **with two different substrate concentrations.** *The data is the mean ± SEM of three different experiments (n =3).*

3.2.4. Determination of Michaelis constant (K_m) for the 17α-OHase enzyme

The Michaelis-Menten plot (Michaelis-Menten, 1913) is one of the earliest plots to determine the relationship between the substrate concentrations and enzyme activity. In Michaelis-Menten plots, V_{max} can only be achieved if the reaction is run at an infinite concentration of substrate. Therefore various methods for estimating the Km and V_{max} of the reaction (for example, Lineweaver & Burk, 1934; Eadie, 1942; Hofstee, 1952; Eisenthal & Cornish-Bowden, 1974) have been reported. However, different methods will give different estimates of K_m and V_{max} unless the data is error-free, because each method makes a different set of assumptions about the distribution of any error (Atkins and Nemmo, 1975).

Different concentrations of substrates were used in order to calculate the substrate concentration at half of the maximum velocity of the reaction or K_m. The reaction mixtures were then incubated with 0.11mg/mL of protein for 25 mins.

Each method of K_m determination is of value and lot of inherent variation between data is expected (Atkins and Nemmo, 1975). Thus the average K_m from five different methods was taken (Figure 3.4-3.8). The average K_m for the 17α-OHase enzyme was found to be 1.08 ± 0.061 μM (Table 3.1).

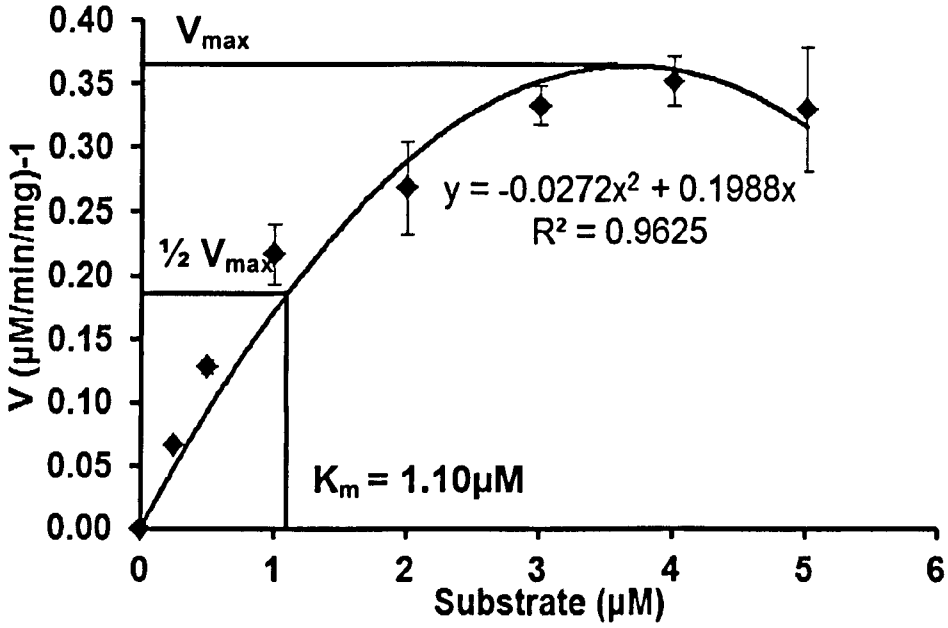

Figure 3.4: ***Michaelis-Menten plot for 17α-OHase enzyme. The V_{max} was found to be 0.36 (µM.min/mg)$^{-1}$.*** *The substrate concentration at ½ V_{max} = 0.18 (µM.min/mg)$^{-1}$ and was calculated as K_m = 1.10 µM. The data is the mean ± SEM of three different experiments (n = 3).*

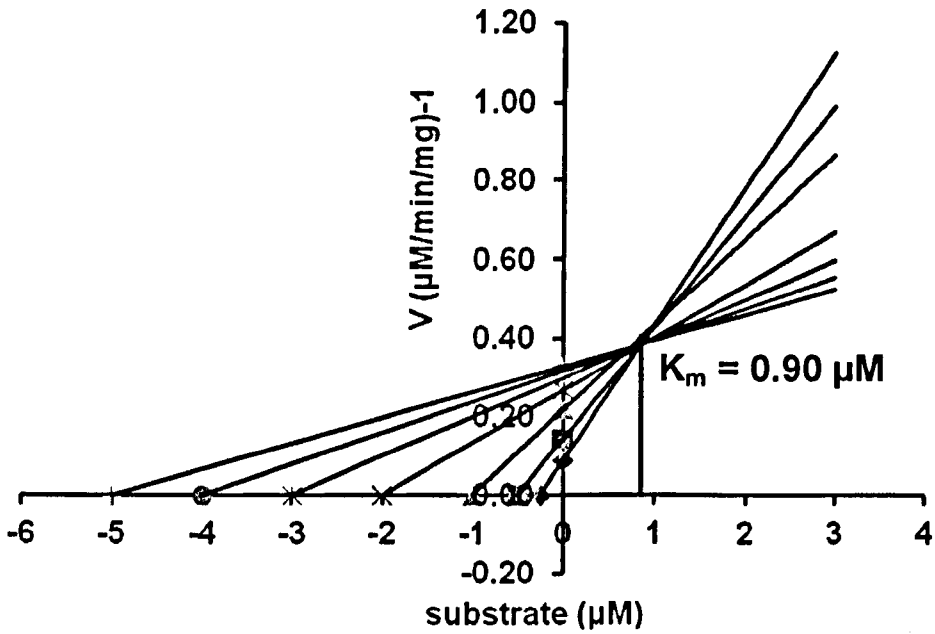

Figure 3.5: ***Direct linear plot for the 17α-OHase enzyme.*** *The point of intersection of all data sets is K_m. The data is the mean ± SEM of three different experiments (n = 3).*

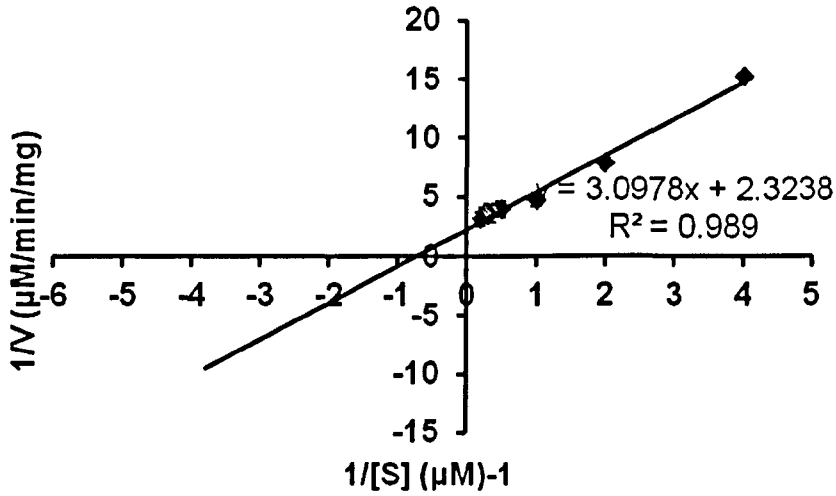

Figure 3.6: ***Lineweaver-Burk plot for the 17α-OHase enzyme.*** *The data is the mean ± SEM of three different experiments (n = 3).*

According to the Lineweaver-Burk equation:

$$\frac{1}{V} = \frac{Km}{Vmax} \times \frac{1}{S} + \frac{1}{Vmax}$$

From the graph (Figure 3.6); $y = 3.0978x + 2.3238$

So; $\frac{1}{Vmax} = 2.3238$ or $Vmax = \frac{1}{2.3238} = 0.4303$

Similarly; $\frac{Km}{Vmax} = 3.0978$

So; $K_m = 3.0978 \times 0.4303$

$\mathbf{K_m = 1.33\ \mu M}$

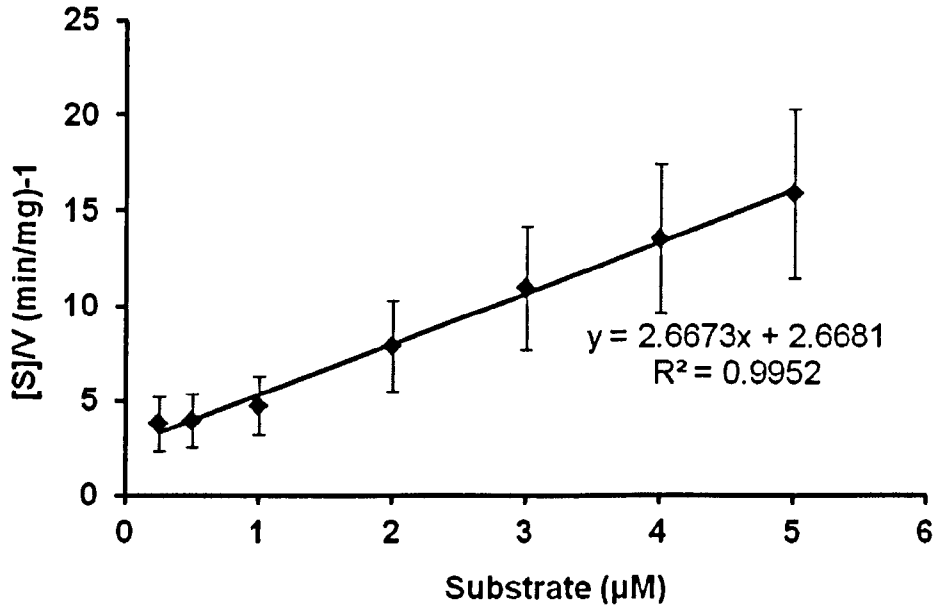

Figure 3.7: ***Hanes-Woolf plot for the 17α-OHase enzyme.*** *The data is the mean ± SEM of three different experiments (n = 3).*

According to the Hanes-Woolf equation:

$$\frac{S}{V} = \frac{Km}{Vmax} + \frac{1}{Vmax} \times S$$

From the graph (Figure 3.7); $y = 2.6673x + 2.6681$

Or $y = 2.6681 + 2.6673x$

So; $\frac{1}{Vmax} = 2.6673$ or $Vmax = \frac{1}{2.6673} = 0.3749$

Similarly; $\frac{Km}{Vmax} = 2.6681$

So; $K_m = 2.6681 \times 0.3749$

$\mathbf{K_m = 1.00\ \mu M}$

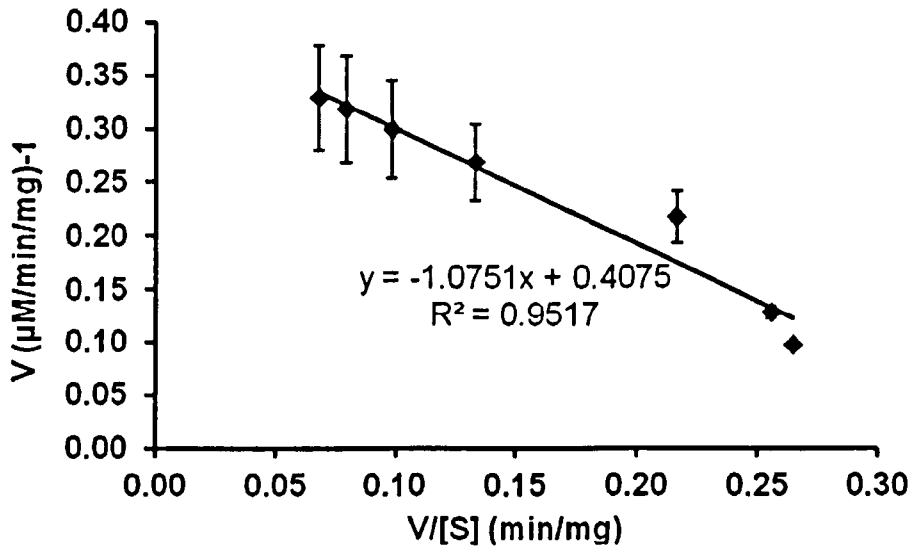

Figure 3.8: ***Eadie-Hofstee plot for the 17α-OHase enzyme.*** *The data is the mean ± SEM of three different experiments (n = 3).*

According to the Eadie-Hofstee equation:

$$V = -K_m \times \frac{v}{s} + V_{max}$$

From the graph (Figure 3.8); $y = -1.0751x + 0.4075$

Therefore; $\mathbf{K_m = 1.07\ \mu M}$

Plot	K_m (µM)
Michaelis-Menten	1.10
Lineweaver-Burk	1.33
Hanes-Woolf	1.00
Eadie-Hofstee	1.07
Direct Linear	0.90
Average ± SEM	**1.08 ± 0.061**

Table 3.1: ***Summary of K_m plots for the 17α-OHase enzyme.*** *The mean of K_m values from five different methods was calculated and reported as average K_m of 17α-OHase enzyme. The data is the mean ± SEM of three different experiments (n = 3).*

3.2.5. Preliminary screening of the compounds synthesised against the 17α-OHase enzyme

Three different series of the compounds were synthesised to inhibit the 17α-OHase and the 17, 20 lyase activity of the CYP17 enzyme. The compounds were tested alongside a known CYP17 inhibitor, ketoconazole (KTZ). The assay mixture contains radiolabelled substrate, inhibitors and NADPH in phosphate buffer. The assay was initiated by addition of 0.11 mg/mL of testicular microsomal homogenate and the reaction was incubated at 37°C for 25 mins. In order to saturate the enzyme active site, a concentration of substrate 3 times K_m was used. The % inhibition of the compounds was calculated using the equation previously mentioned (Section 2.1.5.5). The compounds were tested in four different series and results are shown overleaf (Table 3.2- 3.4). The results for the fourth series are shown in appendix 1.

The first series of compounds were synthesised as derivatives of benzyl-imidazole. The compounds in the first series, in general, are equipotent to the standard drug, ketoconazole (Table 3.2). The substitution of benzene rings at different positions varied the potency of the compounds. Compound 9 showed the highest inhibition of the 17α-OHase enzyme among all compounds (90.67 ± 0.76%; 84.70 ± 2.13%; mean ± SEM; in compound 9 and ketoconazole respectively). The compound 9 contains the CF3 group at the 4th position in the benzene ring.

Compounds	Structures	% Inhibition ± SEM ([I]= 5 μM)
KTZ	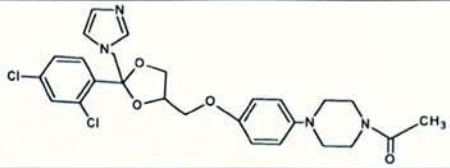	84.70 ± 2.13
1	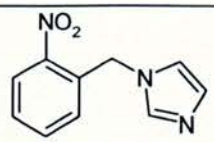	89.20 ± 0.16
2	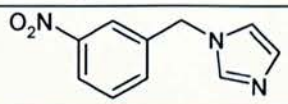	88.90 ± 0.16
3	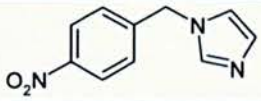	88.95 ± 0.43
4	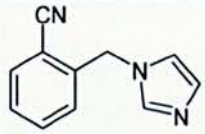	84.82 ± 0.09
5	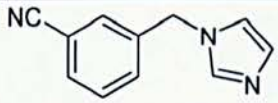	86.07 ± 1.04
6	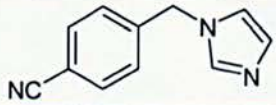	88.15 ± 1.70
7	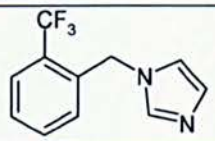	75.21± 14.82
8	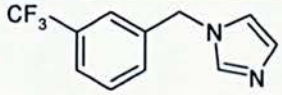	78.03 ± 9.17
9	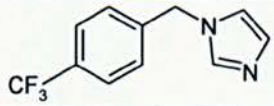	90.67 ± 0.76
10	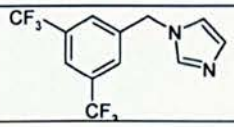	89.94 ± 1.45

Table 3.2: ***Summary of the initial screening of derivatives of benzyl-imidazole based compounds (series 1) against the enzyme 17α-OHase.*** *The compounds were tested alongside the reference drug ketoconazole (KTZ) at a concentration of 5 μM. The data is the mean ± SEM of three different experiments (n = 3).*

The % inhibition of the compounds 1-10 was not found to be significantly diffferent from the control drug KTZ (Figure 3.9)

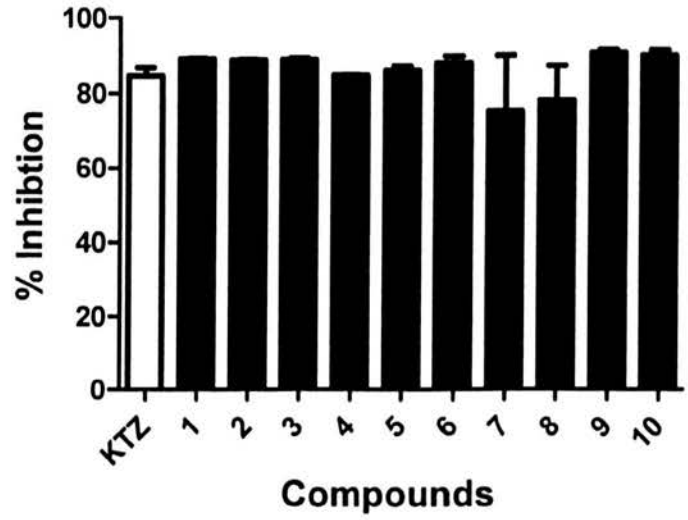

Figure 3.9: ***Effect of of derivatives of benzyl-imidazole based compounds (series 1) on the activity of the enzyme 17α-OHase.*** *The data is the mean ± SEM of three different experiments (n=3). The statistical analysis was done using Tukey's modified student's t-test where p = NS (Non-significant).*

The second series of compounds was based on sulfonate derivatives of 4-hydroxybenzyl imidazole compounds of different alkyl chain length (compounds 31- 37) and with different functional group substitutions (compound 38). In this series, most of the compounds showed greater inhibitory activity when compared to ketoconazole (Table 3.3). The initial increase in % inhibition was found to be associated with an increase in alkyl chain length which decreased later. Compound 38 and 35 showed the highest inhibition when compared to ketoconazole (75.77 ± 0.19, 65.80 ± 0.17%, 40.17 ± 0.01%; mean ± SEM; respectively, $p<0.05$). Compound 35 contains the eight carbons in the alkyl chain whereas compound 38 contains a CF3 group in the structure.

It has been noted that the % inhibition of ketoconazole decreased from 84.70 ± 2.13% (Table 3.2) to 40.17 ± 0.01% (Table 3.3) and 42.27 ± 0.01% (Table 3.4) when tested along three different series of synthesised compounds. The difference in % inhibition is subjected to change in lab conditions during each experiment and activity of testicular micorsome which changes over time. The percentage inhibtion was therefore calculated and based on negative control in each experiment.

Compounds	Structures	% Inhibition ± SEM ([I]= 5 μM)
KTZ	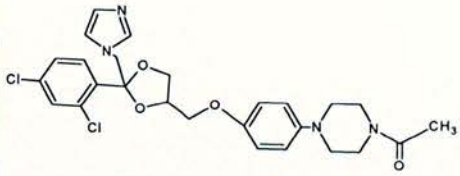	**40.17 ± 0.01**
31	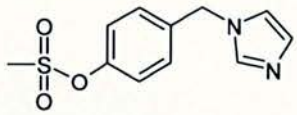	26.48 ± 1.38
32	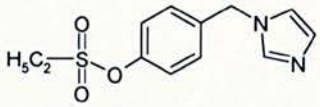	42.51 ± 0.84
33	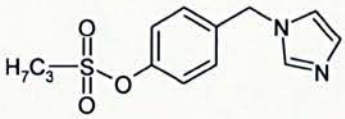	47.07 ± 0.56
34	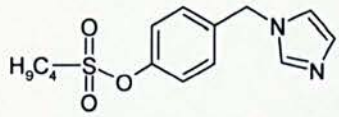	48.21 ±1.83
35	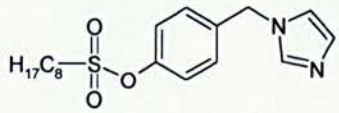	65.80 ± 0.17
36	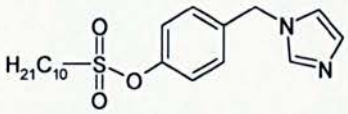	50.59 ± 2.56
37	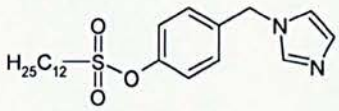	48.21 ± 3.18
38	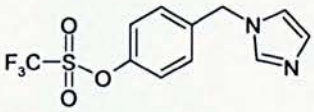	75.77 ± 0.19

Table 3.3: ***Summary of the initial screening of sulfonate derivatives of 4-hydroxybenzyl imidazole compounds of different alkyl length chains (series 2) against the enzyme 17α-OHase.*** *The compounds were tested alongside the reference drug ketoconazole (KTZ) at a concentration of 5 μM. The data is the mean ± SEM of three different experiments (n = 3).*

The sulfonate derivatives of 4-hydroxybenzyl imidazole compounds (compounds 31- 37) showed increased enzyme inhibition (Figure 3.10) when the alkyl chain length was increased to 10 carbons (compound 35). Compounds 35 and 36 showed a significantly higher % inhibition when compared to ketoconazole whereas compound 31 showed significantly less % inhibition when compared to ketoconazole. (65.80 ± 0.17%, 50.59 ± 2.56%, 40.17 ± 0.01%, 26.48 ± 1.37; mean ± SEM; respectively; $p<0.05$). The % inhibition of compound 35 was significantly higher than compounds 31, 32, 33, 34, 36 and 37. (26.48 ± 1.38%, 42.51 ± 0.84%, 47.07 ± 0.56%, 48.21 ± 1.83%, 50.59 ± 2.56% and 42.81 ± 3.18%; mean ± SEM; respectively, $p<0.05$).

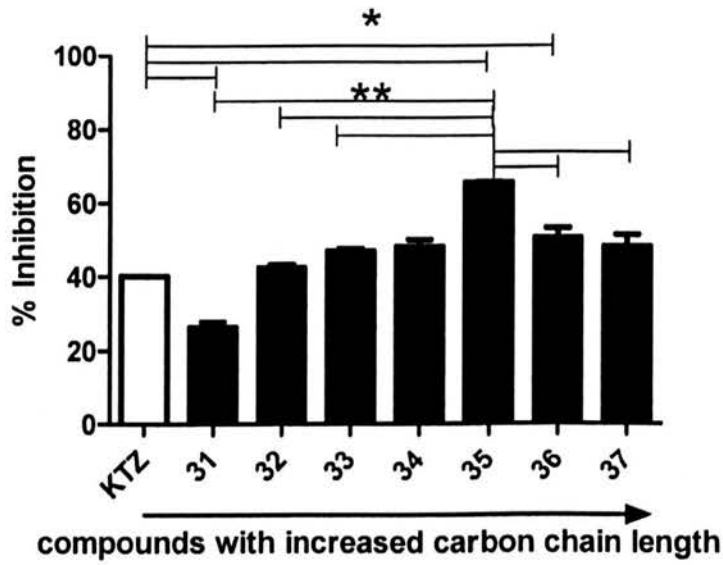

Figure 3.10: Effect of carbon chain length in series 2 (compounds 31-37) on percentage inhibition of compounds against the 17α-OHase. *Compound 31 has the methyl group (smallest alkyl chain) whereas compound 37 has an octyl group (bigger alkyl chain). The data is the mean ± SEM of three different experiments (n = 3). The statistical analysis was done using Tukey's modified student's t-test where *p < 0.05 vs. KTZ and ** p < 0.05 vs. Compound 35.*

Similar to the second series, compounds in the third series were sulfonate derivatives of 4-hydroxybenzyl imidazole compounds of different alkyl chain length (compounds 39- 46) and with different functional group substitutions (compounds 47-51). The compounds in this series showed highest potencies when compared to ketoconazole (Table 3.4). Compound 48 and 51 showed the highest percentage inhibition when compared to ketoconazole (76.50 ± 1.15%, 78.62 ± 1.54 %, 42.27 ± 0.01%; mean ± SEM; respectively; $p<0.05$).

Compounds	Structures	% Inhibition ± SEM ([I]= 5 μM)
KTZ	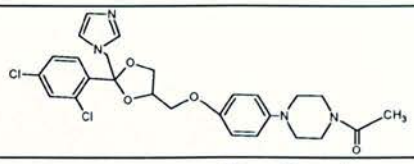	42.27 ± 0.01
39	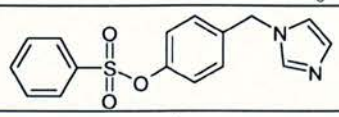	75.78 ± 0.13
40	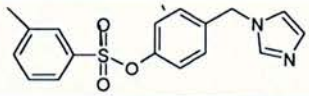	74.18 ± 0.89
41	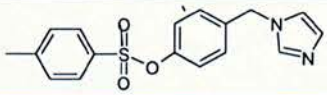	73.67 ± 0.16
42	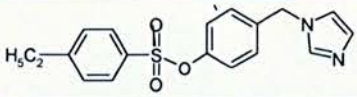	69.18 ± 2.49
43	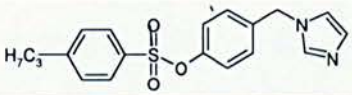	69.95 ± 0.19
44	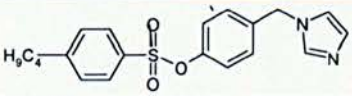	74.15 ± 0.12
45	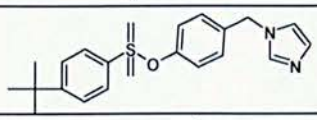	62.13 ± 3.22
46	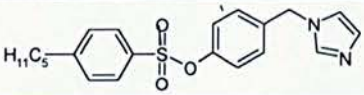	71.41 ± 0.06
47	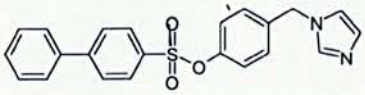	71.49 ± 3.86
48	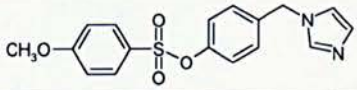	76.54 ± 1.11
49	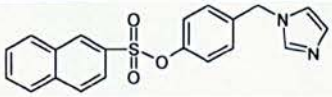	71.61 ± 0.01
50	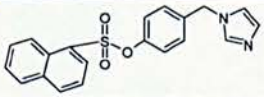	71.15 ± 0.79
51	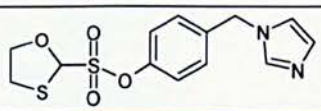	78.62 ± 1.54

Table 3.4: ***Summary of the initial screening of some sulfonate derivatives of 4-hydroxybenzyl imidazole compounds with different functional group substitution (series 3) against the enzyme 17α-OHase.*** *The compounds were tested alongside reference drug ketoconazole (KTZ) at a concentration of 5 μM. The data is the mean ± SEM of three different experiments (n = 3).*

Different alkyl chain lengths of derivatives of 4-hydroxybenzyl imidazole compounds (compounds 39-46) did not show any difference in inhibitory activity against the 17-αOHase (Figure 3.11). However, all compounds showed significantly higher inhibition of the enzyme 17α-OHase than ketoconazole (40.17 ± 0.01% (KTZ), 75.78 ± 0.13% (39), 74.18 ± 0.89% (40), 73.67 ± 0.16% (41), 69.18 ± 2.49% (42), 69.96 ± 0.19% (43), 74.15 ± 0.12% (44), 62.13 ± 3.22% (45) and 71.41 ± 0.06% (46); mean ± SEM; $p<0.05$).

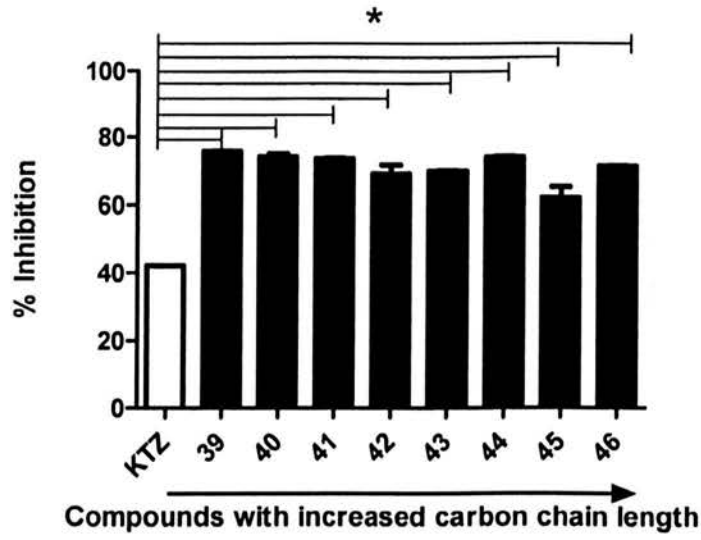

Figure 3.11: ***Effect of carbon chain length of sulfonate derivatives of 4-hydroxybenzyl imidazole compounds (compounds 39-46) on percentage inhibition of compounds against the 17α-OHase.*** *The data is the mean ± SEM of three different experiments (n = 3). The statistical analysis was done using Tukey's modified student's t-test where *p < 0.05 vs. KTZ.*

The presence of different functional groups on sulfonate derivatives of 4-hydroxybenzyl imidazole compounds (compounds 47-51) showed greater potencies of the compounds (Figure 3.12). The compounds 48 and 51 showed the highest inhibition when compared to ketoconazole (76.54 ± 1.11% and 78.62 ± 1.54%, 40.17 ± 0.01%; mean ± SEM; respectively; $p<0.05$).

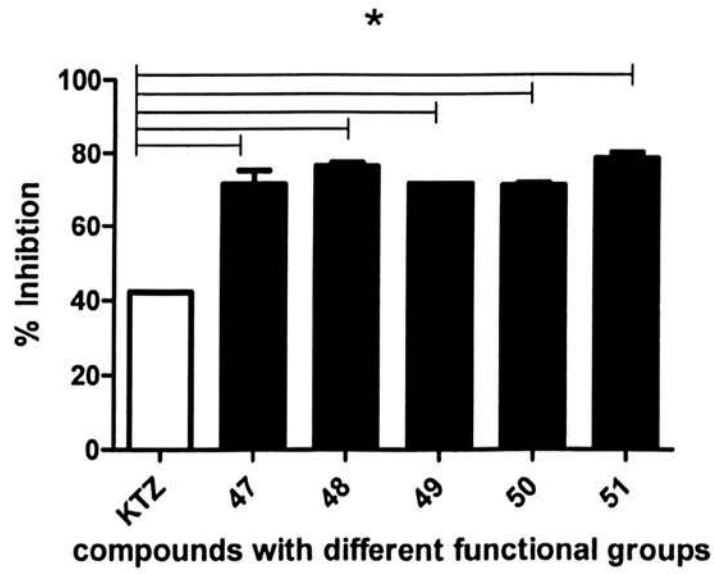

Figure 3.12: Effect of different functional groups on sulfonate derivatives of 4-hydroxybenzyl imidazole compounds (compounds 47-51) on percentage inhibition of the 17α-OHase. *The data is the mean ± SEM of three different experiments (n = 3). The statistical analysis was done using Tukey's modified student's t-test where *p < 0.05 vs. KTZ.*

IC_{50} is the concentration of an inhibitor required for 50% inhibition of the enzyme. Different dilutions of compounds in DMSO were made and added to the reaction mixture. The concentration of substrate that was used in the assays was three times K_m. The IC_{50} of the compounds (Figure 3.13) have been calculated using a statistics package (GraphPad Prism 5.0 Software, Inc. USA) and have been summarised overleaf (Table 3.5). The IC_{80} values were also calculated to find out the near maximal dose of these inhibitors. These concentrations were further used in *ex vivo* experiments.

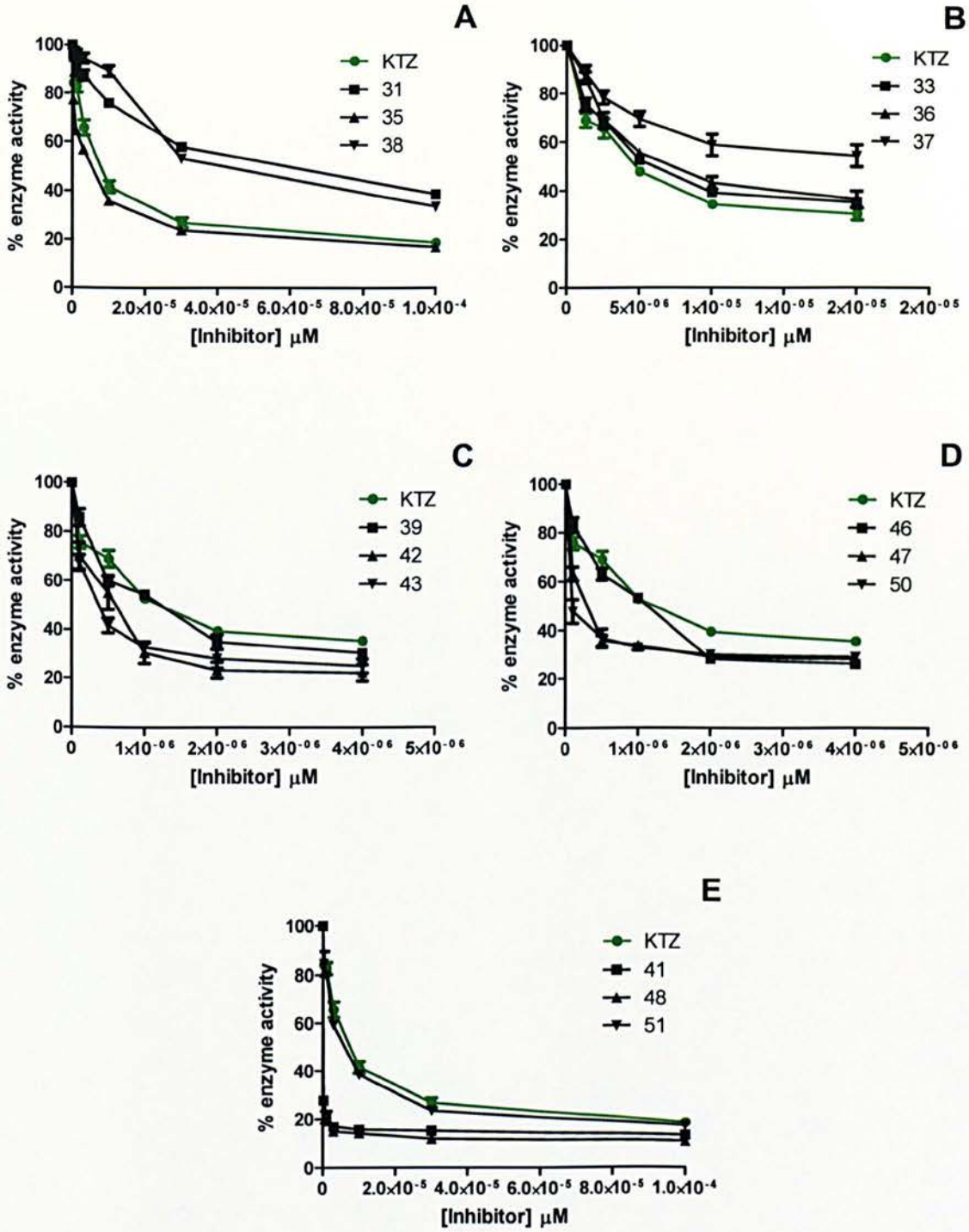

Figure 3.13: The % enzyme activity against different concentrations of compounds. *The enzyme activity was based on that of the control tube with no inhibitor (100% enzyme activity). The data is the mean ± SEM of three different experiments (n = 3). The green line shows the data for ketoconazole. (A) Dose response curves for compounds 31, 35, 38 and KTZ (B) Dose response curves for compounds 33, 36, 37 and KTZ (C) Dose response curves for compounds 39, 42, 43 and KTZ (D) Dose response curves for compounds 46, 47, 50 and KTZ (E) Dose response curves for compounds 41, 48, 51 and KTZ.*

The compounds which showed good inhibitory activity in the preliminary screening were short-listed to determine the IC_{50} values (Table 3.5). Compounds 31 and 41 were selected because they were the first compounds of the series. Compounds 38, 42, 43, 46, 47, and 51 showed the highest IC_{50} values (0.18 μM, 0.43μM, 0.32 μM, 0.48 μM, 0.24 μM and 0.14 μM respectively). The IC_{80} of the compounds which were selected to use in cell-based assays was calculated.

Compounds	IC_{50} (M)	IC_{80} (M)
KTZ	**5.25×10^{-06}**	**1.62×10^{-05}**
31	1.44×10^{-05}	4.71×10^{-05}
33	6.56×10^{-06}	NC
35	4.82×10^{-06}	$1.89 \times \times 10^{-05}$
36	7.89×10^{-06}	NC
37	2.19×10^{-05}	NC
38	1.82×10^{-07}	4.20×10^{-07}
39	1.06×10^{-06}	NC
41	1.35×10^{-06}	3.93×10^{-06}
42	4.28×10^{-07}	NC
43	3.22×10^{-07}	NC
46	4.83×10^{-07}	NC
47	2.39×10^{-07}	NC
48	1.21×10^{-06}	1.37×10^{-06}
50	1.11×10^{-05}	NC
51	1.40×10^{-07}	1.53×10^{-06}

Table 3.5: ***IC_{50} and IC_{80} values of azole- based compounds against the enzyme 17α-OHase.*** *(NC = not calculated). The data is the mean ± SEM of three different experiments (n = 3).*

3.2.6. Protein-dependency assay for the 17, 20 lyase

The 17, 20 lyase activity of CYP17 enzyme cleaves the bond between (C) 17 and (C) 20 of 17-α hydroxypregneolone and 17-α hydroxyprogesterone and converts them into dihydroepiandrostendione and androstenedione respectively. The synthesised compounds were also tested for inhibitory activity against the 17, 20 lyase enzyme.

The radiolabelled 17α-hydroxyprogesterone (2 μM) in a reaction mixture was incubated with various protein concentrations. The graph (Figure 3.14) shows that the kinetics of the reaction is linear for concentrations up to 0.20 mg/mL.

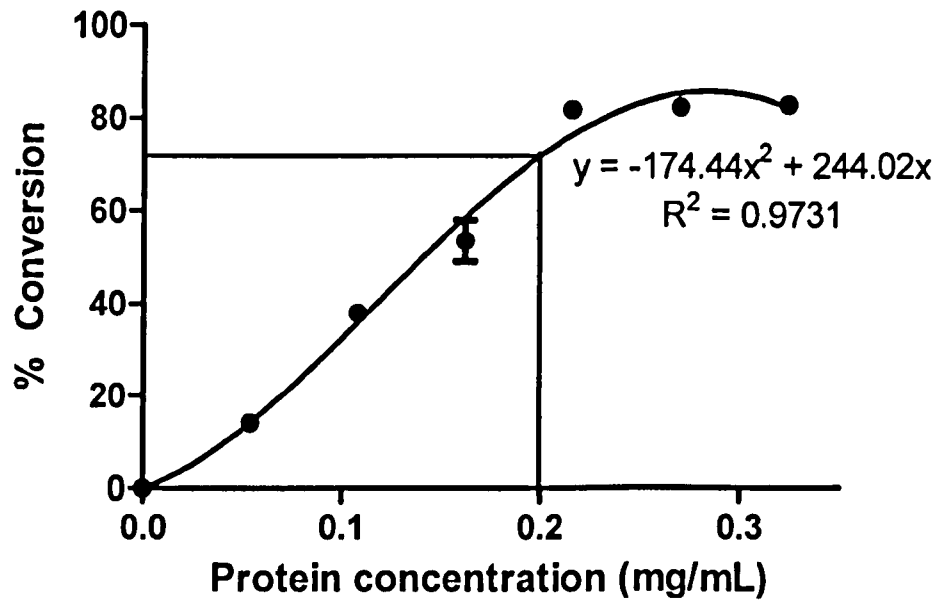

Figure 3.14: **Percentage conversion of 17α-hydroxyprogesterone to androstenedione at varying protein concentrations.** *The data is the mean ± SEM of three different experiments (n = 3).*

3.2.8. Time-dependency assay for the 17, 20 lyase

The substrate (2 μM) was incubated with 0.20 mg/mL protein concentration at different time intervals. We can conclude from the graph that the kinetics of the reaction is linear up to 30 mins (Figure 3.15).

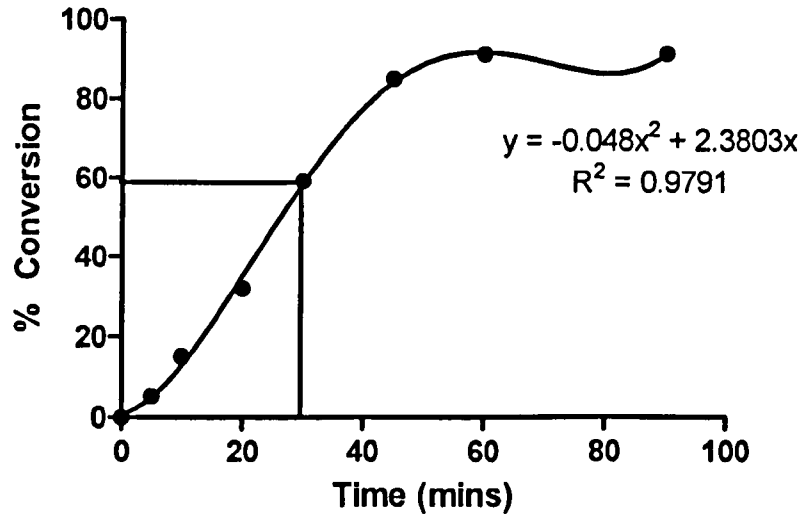

Figure 3.15: Graph to show percentage conversion of 17α-hydroxyprogesterone at varying time intervals. *The data is the mean ± SEM of three different experiments (n = 3).*

3.2.7. Determination of K_m for 17, 20 lyase

The K_m was determined from five different methods as described before (Section 3.2.4). The graphs for K_m of the 17, 20 lyase enzyme are shown in appendix 2.

Plot	K_m (μM)
Michaelis-Menten	1.20
Lineweaver-Burk	1.33
Hanes-Woolf	2.21
Eadie-Hofstee	2.64
Direct Linear	3.20
Average ± SEM	**2.11 ± 0.36**

Table 3.6: ***Summary of K_m plots for the 17, 20 lyase enzyme.*** *The mean of K_m values from five different methods was calculated and reported as average K_m of the 17, 20 lyase enzyme. The data is the mean ± SEM of three different experiments (n = 3).*

3.2.8. Preliminary screening of synthesised compounds against the 17, 20 lyase enzyme.

The same four series of the compounds were tested to determine their inhibitory activity against the enzyme,17, 20 lyase. Ketoconazole was used as a reference drug. The assay mixture contained radiolabelled substrate, inhibitors and NADPH in phosphate buffer. The assay was initiated by addition of 0.20 mg/mL of testicular microsomal homogenate and the reaction was incubated at 37°C for 30 mins. The concentration of substrate used was three times that of the K_m values.

The derivatives of benzyl-imidazole, in general, are equipotent to the standard drug, ketoconazole (Table 3.7) similar to their inhibition against the 17α-OHase enzyme (Table 3.2). Compounds 1 and 3 showed the highest inhibition of the 17α-OHase enzyme when compared to ketoconazole (87.17 ± 3.52%, 87.40 ± 4.25% and 75.58 ± 6.84; mean ± SEM; respectively).

Compounds	% Inhibition ± SEM ([I]= 5 μM)
KTZ	75.58 ± 6.84
1	87.17 ± 3.52
2	86.28 ± 4.52
3	87.40 ± 4.25
4	85.76 ± 4.15
5	85.76 ± 4.49
6	86.80 ± 4.25
7	86.81 ± 4.60
8	85.41 ± 5.20
9	86.66 ± 4.85
10	86.63 ± 4.44

Table 3.7: ***Summary of the initial screening of some imidazole-based compounds against the enzyme 17, 20 lyase.*** *The compounds were tested alongside reference drug ketoconazole (KTZ) at a concentration of 5 μM. The data is the mean ± SEM of three different experiments (n = 3).*

The % inhibition of the compounds 1-10 in series was not found to be significantly diffferent from the control drug KTZ (Figure 3.16)

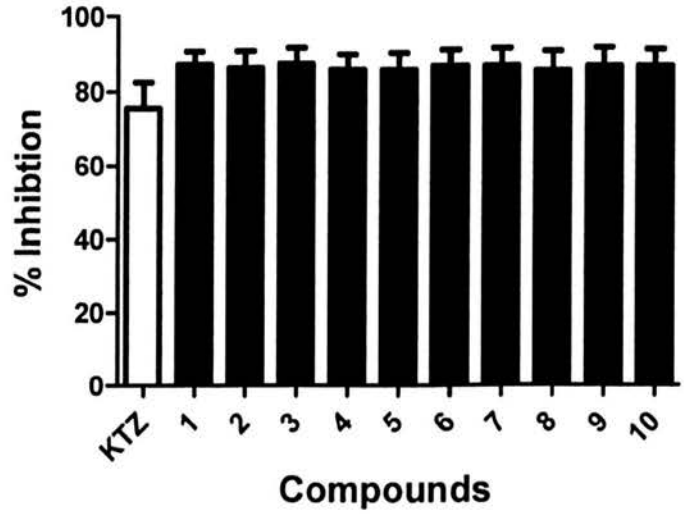

Figure 3.16: ***Effect of derivatives of benzyl-imidazole based compounds (series 1) against the enzyme 17, 20 lyase.*** *The data is the mean ± SEM of three different experiments (n=3). The statistical analysis was done using Tukey's modified student's t-test where p> 0.05.*

Compounds in series 2 and 3 are based on sulfonate derivatives of 4-hydroxybenzyl imidazole compounds of different alkyl chain length (compounds 31- 37) and with different functional group substitutions (compounds 38-46).

In the second series, compounds showed greater inhibitory activity when compared to ketoconazole (Table 3.3). The change in alkyl chain length did not produce any trend in the inhibitory activity as in the case of 17α-OHase inhibition. Compounds 35 and 38 showed the highest inhibition when compared to ketoconazole (75.80 ± 0.17%, 72.08 ± 1.82%, 47.67 ± 2.50%; mean ± SEM; respectively; $p<0.05$).

Similarly, compounds in the third series were sulfonate derivatives of 4-hydroxybenzyl imidazole compounds of different alkyl chain length (compounds 39- 46) and with different functional group substitutions (compounds 47-51). The compounds in this series showed highest potencies when compared to ketoconazole (Table 3.8). Compounds 48 and 39 showed the highest percentage inhibition when compared to ketoconazole (86.54 ± 1.11%, 75.78 ± 0.13 %, 51.77 ± 0.50%; mean ± SEM; respectively; $p<0.05$).

As described previously, the % inhibition of ketoconazole decreased from 75.58 ± 6.84% (Table 3.7) to 47.67 ± 2.50% and 51.77 ± 0.50% (Table 3.4) when tested along three different series of synthesised compounds. The difference in % inhibition is subjected to change in lab conditions during each experiment and activity of testicular micorsome which changes over time. The percentage inhibtion was therefore calculated and based on negative control in each experiment.

Compounds	% Inhibition ± SEM ([I]= 5 μM)	Compounds	% Inhibition ± SEM ([I]= 5 μM)
KTZ	**47.67 ± 2.50**	**KTZ**	**51.77 ± 0.50**
31	51.48 ± 3.62	39	75.78 ± 0.13
32	49.01 ± 0.34	40	74.18 ± 0.89
33	56.07 ± 0.44	41	58.67 ± 4.83
34	63.21 ± 3.16	42	64.18 ± 2.51
35	75.80 ± 0.17	43	64.95 ± 5.19
36	65.59 ± 2.40	44	74.15 ± 0.12
37	53.21 ± 1.82	45	62.13 ± 3.22
38	72.08 ± 1.80	46	71.41 ± 0.06
-	-	47	71.49 ± 3.86
-	-	48	86.54 ± 1.11
-	-	49	71.61 ± 0.01
-	-	51	71.15 ± 0.79

Table 3.8: ***Summary of the initial screening of sulfonate derivatives of 4-hydroxybenzyl imidazole compounds of different alkyl length chains (series 2) against the enzyme 17, 20 lyase.*** *The compounds were tested alongside the reference drug ketoconazole (KTZ) at a concentration of 100 μM. The data is the mean ± SEM of three different experiments (n = 3).*

The sulfonate derivatives of 4-hydroxybenzyl imidazole compounds (compounds 31- 51) showed increased enzyme inhibition (Figure 3.17).

In series 2, compound 35 (Figure 3.17A) showed significantly higher inhibition when compared to KTZ and compounds 31, 32, 33, and 37 (75.80 ± 0.17%, 47.67 ± 2.50%, 51.48 ± 3.62%, 49.01 ±0.34%, 56.07 ±0.44% and 53.21 ± 1.82%; mean

± SEM; respectively). Compounds 34 and 36 had significantly higher % inhibition when compared to KTZ.

All compounds in series 3 (Figure 3.17B), showed significantly higher inhibition when compared to ketoconazole. (51.77 ± 0.50% (31), 75.78 ± 0.13%(39), 74.18 ± 0.89% (40), 58.67 ± 4.83% (41), 64.18 ± 2.51% (42), 64.95 ± 5.19% (43), 74.15 ± 0.12% (44), 62.13 ± 3.22% (45), 71.41 ± 0.06% (46), 71.49 ± 3.86% (47), 86.54 ± 1.11% (48), 71.61 ± 0.01% (49) and 71.15 ± 0.79% (50); mean ± SEM; $p<0.05$).

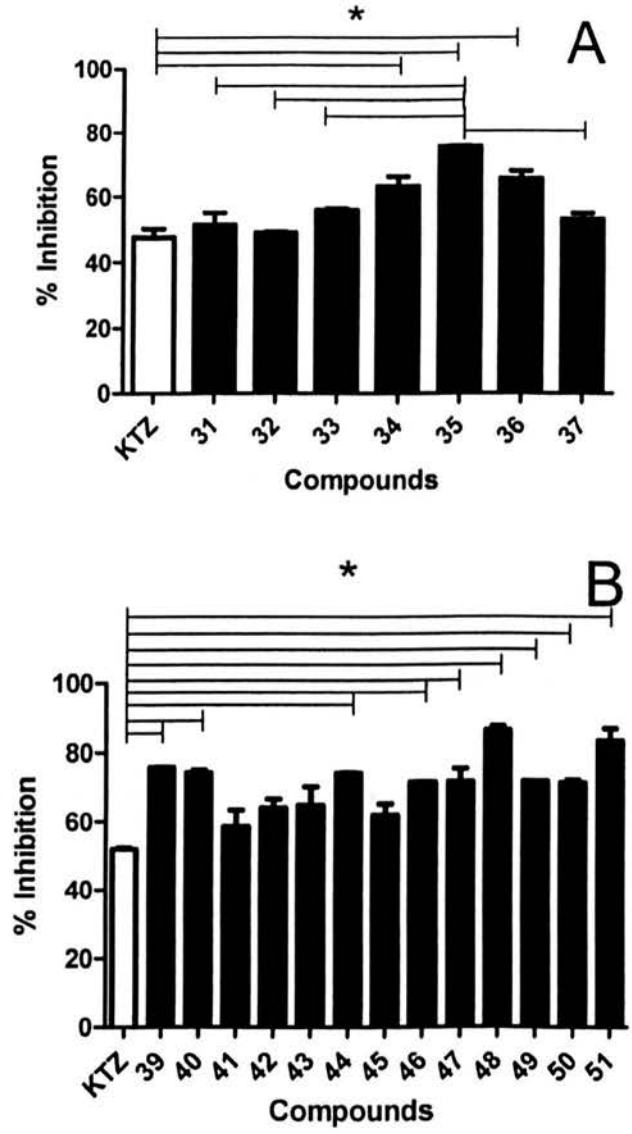

Figure 3.17: ***Effect of carbon chain length of sulfonate derivatives of 4-hydroxybenzyl imidazole compounds on % inhibition of compounds against the 17, 20 lyase.*** *The data is the mean ± SEM of three different experiments (n = 3). The statistical analysis was done using Tukey's modified student's t-test where *p < 0.05 vs. KTZ.(A) Compounds in series 2 (31- 37). (B) Compounds in series 3 (39 – 51).*

3.3. Results for the 17β-hydroxysteroid dehydrogenase 3

Androstenedione is converted into testosterone by the action of the enzyme 17β-hydroxysteroid dehydrogenase type 3. The conversion of substrate into product was estimated by radiometric assay (Section 2.1).

3.3.1. Estimation of protein content of rat testicular microsomes

The absorbance of the test sample was found to be 1.23 (O.D.) at a wavelength of 570 nm. By substituting this value in the graph equation, we have found that the concentration of testicular microsome is 41.16 mg/mL (Figure 3.18).

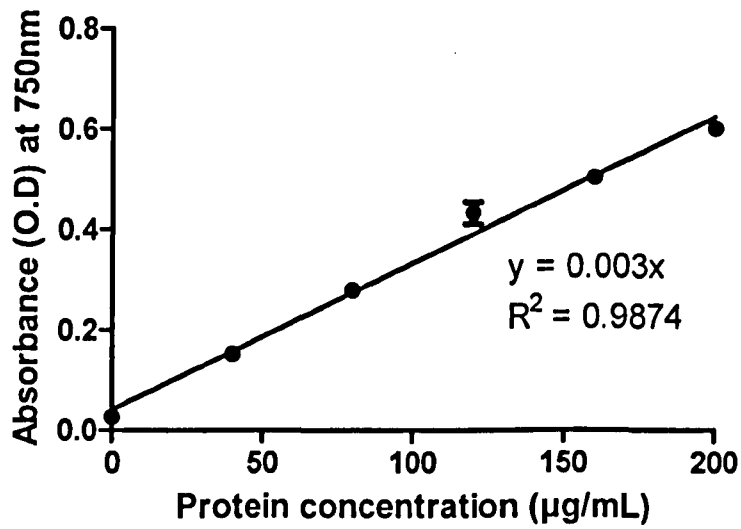

Figure 3.18: ***Standard curve for the estimation of total protein content of rat testicular microsomes by the Folin-Lowry method.*** *The concentration of protein was calculated using the graph equation. The data is the mean ± SEM of three different experiments (n =3).*

3.3.2. Protein dependency for the 17β-hydroxysteroid dehydrogenase 3

From the graph, it can be concluded that the kinetics of the reaction are linear for concentrations up to 0.20mg/mL at substrate concentrations of 1 μM and 5 μM (Figure 3.19).

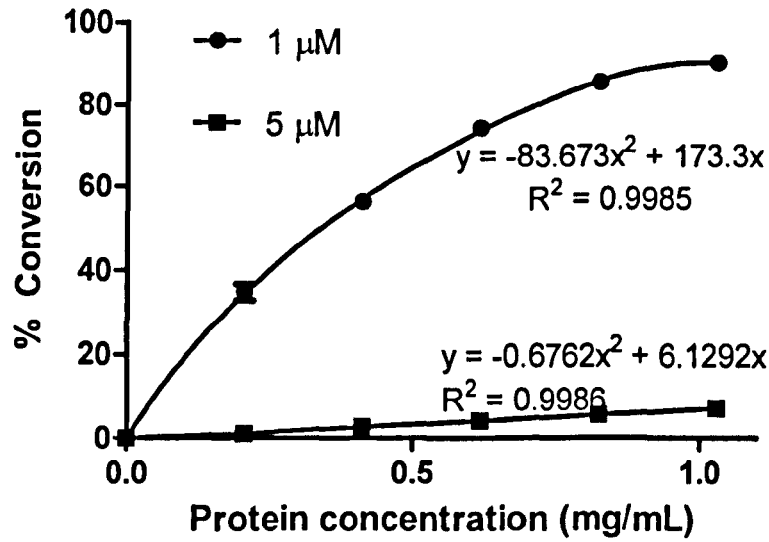

Figure 3.19: **The percentage conversion of progesterone to androstenedione to testosterone at varying protein concentrations.** *The data is the mean ± SEM of three different experiments (n = 3).*

3.3.3. Time dependency for the 17β-hydroxysteroid dehydrogenase 3

At 0.20 mg/mL protein concentration and substrate concentrations of 1 μM and 5 μM it can be concluded that the kinetics of the reactions are linear up to 35 mins (Figure 3.20).

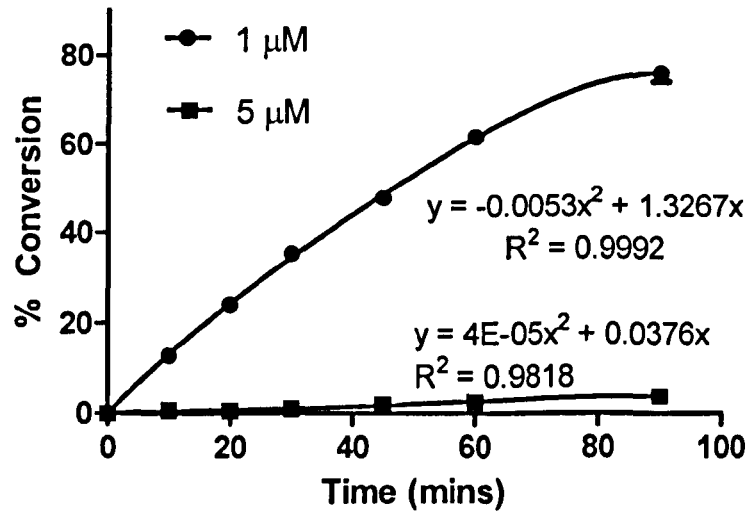

Figure 3.20: ***Graph to show percentage conversion of androstenedione to testosterone at varying time intervals*** **with two different substrate concentrations.** *The data is the mean ± SEM of three different experiments (n = 3).*

3.3.4. Determination of K_m for the 17β-hydroxysteroid dehydrogenase 3

The K_m was determined from five different methods as described before in section 3.2.4). The radiolabelled androstenedione was serially diluted to get various substrate concentrations. The assay was initiated by addition of 0.20 mg/mL of protein and incubated for 35 mins. The graphs are shown in appendix 3 whereas the results are summarised in Table 3.9.

Plot	K_m (μM)
Michaelis-Menten	1.40
Lineweaver-Burk	0.79
Hanes-Woolf	0.76
Eadie-Hofstee	1.04
Direct Linear	1.40
Average ± SEM	**1.08 ± 0.14**

Table 3.9: ***Summary of Km plots for the 17β-HSD3.*** *The mean K_m values from five different methods were calculated and reported as average K_m of 17β-HSD3. The data is the mean ± SEM of three different experiments (n = 3).*

3.3.5. Preliminary screening of compounds synthesised against the cytochrome P450 17β- hydroxysteroid dehydrogenase 3

Three different series of the compounds were tested to determine their inhibitory activity against the 17β-HSD3 enzyme. Series 5 consists of some acetic acid base derivatives of 4-hydroxy phenyl ketone-based compounds whereas series 6 and 7 consist of some transformed androstenedione-based compounds. Two known inhibitors of the 17β-HSD3; 7-hydroxy flavone (FLV) and baicalein (B), were also tested along with the synthesised compounds.

The assay mixture contained radiolabelled substrate, inhibitors and NADPH in phosphate buffer. The assay was initiated by addition of 0.20 mg/mL of testicular microsomal homogenate and the reaction was incubated at 37°C for 35 mins. The concentration of substrate used was three times that of K_m values.

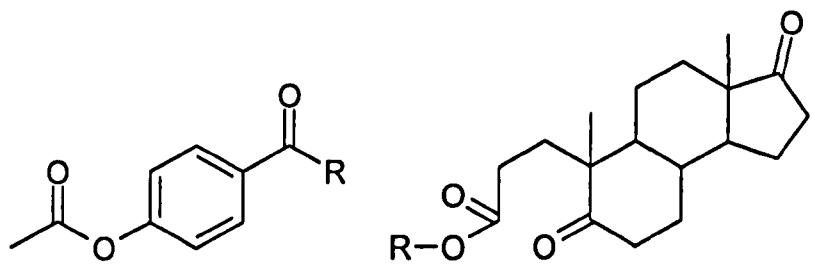

Series 5 series 6 and 7

Figure 3.21: General structures of some acetic acid based derivatives of 4-hydroxy phenyl ketones (series 5) and some transformed androstenedione compounds (series 6 and 7) where R is various functional groups.

The initial screening of some acetic acid based derivatives of 4-hydroxy phenyl ketones, in series 5, showed that compounds had better inhibitory activity against 17β-HSD3 when compared to control drugs; FLV and Baicalein (Table 3.10). The inhibition of enzyme increased when the alkyl chain length was increased from one carbon to seven carbon atoms. However the inhibitory activity decreased further when the alkyl chain length was further increased to nine carbons. Compound 132 showed the highest % inhibition (40.51 ± 0.14%). against 17β-HSD3.

Compounds	R=	% Inhibition ± SEM ([I]= 100 μM)
FLV	**N/A**	**12.90 ± 0.18**
Baicalein	**N/A**	**13.66 ± 0.09**
125	H	14.31 ± 0.27
126	CH_3	13.38 ± 0.01
127	C_2H_5	13.00 ± 0.26
128	C_3H_7	17.83 ± 0.11
130	C_5H_{11}	36.49 ± 0.77
131	C_6H_{13}	40.25 ± 1.35
132	C_7H_{15}	40.51 ± 1.93
133	C_8H_{17}	37.05 ± 2.50
134	C_9H_{19}	16.45 ± 3.08
135	$CycloC_3H_5$	31.60 ± 3.66
136	$CycloC_4H_7$	23.12 ± 4.24
137	$CycloC_5H_9$	32.87 ± 4.81
138	$CycloC_6H_{11}$	38.22 ± 5.39
139	Benzene	32.85 ± 5.97

Table 3.10: ***Summary of the initial screening of some acetic acid based derivatives of 4-hydroxy phenyl ketones (series 5) against the enzyme 17β-HSD3.*** *The compounds were tested alongside control drugs; 7-hydroxyflavone and baicalein, at a concentration of 100 μM. The data is the mean ± SEM of three different experiments (n = 3).*

The results showed (Figure 3.22) that synthesised compounds had significantly higher inhibition when compared to 7-hydroxyflavone and baicalein (14.31 ± 0.01% (126), 36.49 ± 0.77% (130), 40.25 ± 1.35% (131), 40.51 ± 1.93% (132), 37.05 ± 2.50% (133), 31.60 ± 3.66% (135), 32.87 ± 4.81% (137), 38.22 ± 5.39% (138), 32.85 ± 5.97% (139), 12.90 ± 0.18% (FLV), 13.66 ± 0.09% (Baicalein); mean ± SEM, %; $p<0.05$). Compound 132 showed the highest % inhibition among all compounds.

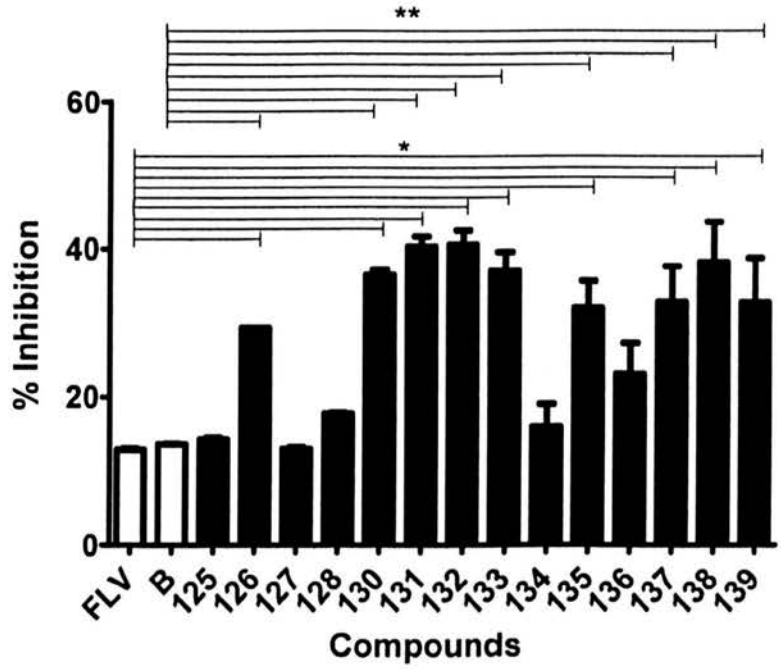

Figure 3.22: Effect of some acetic acid based derivatives of 4-hydroxy phenyl ketones (series 5) when compared to control drugs. *The data is the mean ± SEM of three different experiments (n= 3). The statistical analysis was done using Tukey's modified student's t-test where *p < 0.05 vs.FLV and **p < 0.05 vs. Baicalein.*

In series 6 (compounds 172 – 184), half of the compounds showed better inhibitory activity when compared to 7-hydroxyflavone. However, when compared to baicalein, only a few compounds showed higher % inhibition (Table 3.11). Compound 176 showed the highest potency (43.18 ± 0.19%) when compared to both control drugs. The compounds of series 7 (compounds 185-196), in general, were equipotent to 7-hydroxyflavone and baicalein. The highest % inhibition was given by compound 189 (39.76 ± 0.20%) when compared to control drugs.

Compounds	R=	% Inhibition ± SEM ([I]= 100 μM)	Compounds	R=	% Inhibition ± SEM ([I]= 100 μM)
FLV	N/A	25.01 ± 0.11	FLV	N/A	28.89 ± 0.11
Baicalein	N/A	30.73 ± 0.16	Baicalein	N/A	35.18 ± 0.16
172	CH_3	16.82 ± 0.21	185	C_4H_7	33.79 ± 0.21
173	C_2H_5	15.40 ± 0.16	186	C_5H_9	38.85 ± 0.16
174	C_3H_7	31.68 ± 0.14	187	C_6H_{11}	38.09 ± 0.14
175	C_4H_9	38.96 ± 0.05	188	C_7H_{13}	32.70 ± 0.05
176	C_5H_{11}	43.18 ± 0.19	189	C_8H_{15}	39.76 ± 0.20
177	C_6H_{13}	38.00 ± 0.77	190	C_4H_7	35.28 ± 0.77
178	C_7H_{15}	34.66 ± 1.35	191	C_5H_9	36.88 ± 1.35
179	C_8H_{17}	28.88 ± 1.93	192	C_6H_{11}	36.64 ± 0.30
180	C_9H_{19}	16.16 ± 2.50	193	C_7H_{13}	36.52 ± 2.51
183	$C_{12}H_{25}$	21.94 ± 4.24	194	C_8H_{15}	36.36 ± 0.33
184	$C_{13}H_{27}$	25.87±4.18	195	C_9H_{17}	35.18 ± 3.66
-	-	-	196	$C_{10}H_{15}$	38.18 ± 4.24

Table 3.11: ***Summary of the initial screening of some transformed androstenedione compounds (series 6 and 7) against the enzyme 17β-HSD3.*** *The compounds were tested alongside control drugs; 7-hydroxyflavone and baicalein, at a concentration of 100 μM. The data is the mean ± SEM of three different experiments (n = 3).*

The results for the compounds in series 6 showed (Figure 3.23) that compounds 175, 176 and 177 had significantly higher inhibititon when compared to 7-hydroxyflavone and baicalein (38.96 ± 0.05%, 43.18 ± 0.19%, 38.00 ± 0.77%, 25.01 ± 0.11%, 30.73 ± 0.16%; mean ± SEM; respectively; $p<0.05$).

Similarly, compounds 186, 187 and 189 and 196 of series 7, showed significantly higher inhibititon when compared to 7-hydroxyflavone (38.85 ± 0.16%, 38.09 ± 0.14%, 39.76 ± 0.20%, 38.18 ± 4.25%, 28.89 ± 0.11%; mean ± SEM; respectively; $p<0.05$).

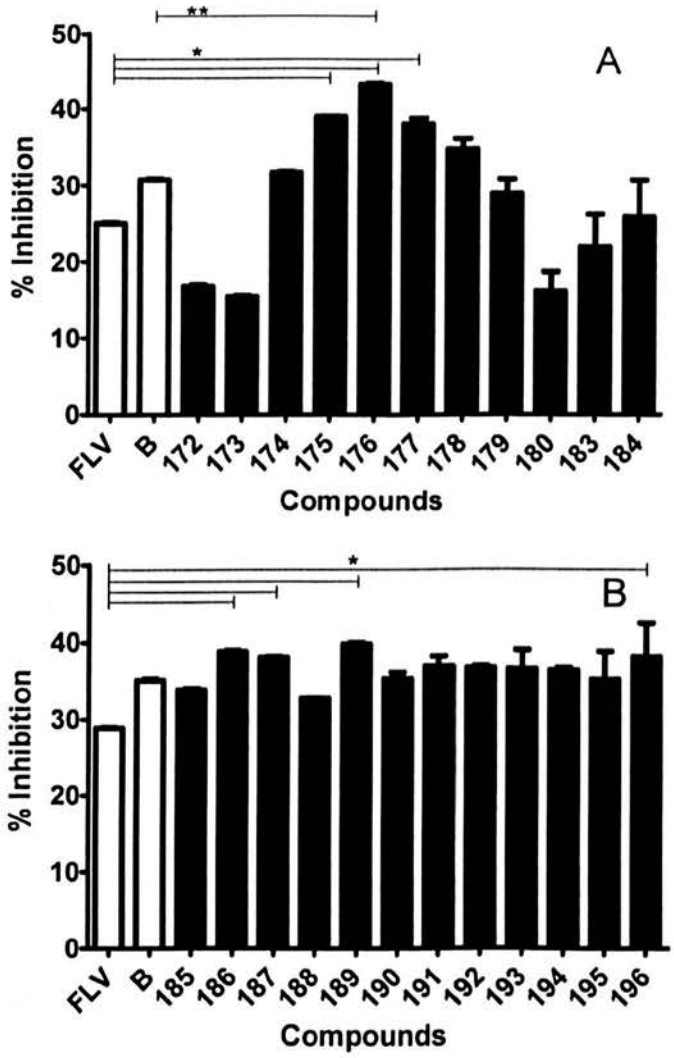

Figure 3.23: ***Effect of carbon chain length (compound 126 – 134) on the inhibition of the 17β-HSD3.*** *The data is the mean ± SEM of three different experiments (n=3). The statistical analysis was done using Tukey's modified student's t-test where *p < 0.05 vs.FLV and **p < 0.05 vs. Baicalein. (A) Compounds in series 6 (B) Compounds in series 7.*

3.4. Discussion

3.4.1. Development of the CYP17 and 17β-HSD3 assays

The enzymes CYP17 and 17 β–HSD3 are the two main enzymes that catalyse the synthesis of the potent androgens; testosterone and dihydrotestosterone, which are involved in the progression of hormone-dependent diseases (Yap *et al.*, 2008; Day *et al.*, 2009).

All assays for the 17α-hydroxylase and 17, 20 lyase were based on that of Owen *et al* (1999) while the 17 β-HSD3 assays were based on that of Lain *et al.* (2001) although there were few modifications made to the reported assays. The changes in the previous methods are described below.

These assays determined the rate of conversion of radiolabelled progesterone to 17α-hydroxyprogesterone (17α-hydroxylase), then to androstenedione (lyase) and finally to testosterone (17β-HSD3). The rat testicular microsome was used as a source of these enzymes. The radiolabelled substrate and the synthesised inhibitors were incubated with the enzyme along with NADPH generating systems at a pH of 7.4 and at 37°C. After the incubation, the reaction was quenched with diethyl ether.

A novel approach was adopted for the extraction of organic compounds from the reaction mixture after the reaction was quenched. The steroids in the diethyl ether layer were separated from the bottom aqueous layer by freezing the aqueous layer in liquid nitrogen for 5 mins. This caused the freezing of the aqueous layer and the organic layer was extracted with a pasteur pipette. This results in the absolute recovery of all the steroids (both substrates and products) as compared to previous methods (Owen *et al.*, 1999; Lain *et al.*, 2001) which cause variable loss of the organic phase while separating from the liquid phase.

The reaction products along with the substrate were then separated using thin layer chromatography (TLC). The acetone in the assay (Owen *et al.*, 1999) was replaced with ethanol to dissolve the radiolabelled products and substrate as ethanol evaporates more quickly than acetone. The samples were spotted on TLC plates.

For the hydroxylase assay, a similar ratio (7:3) of dichloromethane (DCM) and ethyl acetate (EA) was used to develop TLC plates as reported previously (Owen *et al.,* 1995; Lain *et al.,* 2001). However in the case of lyase and 17β-HSD 3 assays a 9:1 ratio of DCM: EA was used.

The results of the study show that the development of the assays has been successful and has allowed the evaluation of inhibitory activity against both components of the enzymes CYP17 and 17β-HSD3.

3.4.2. Inhibitory activity of compounds synthesised as 17-α OHase and 17, 20 lyase inhibitors.

Azole-based compounds have been investigated as inhibitors of a number of cytochrome P450 enzymes such as 14α- demethylase (Suryadevara *et al.,* 2009), aromatase (Gobbi *et al.,* 2007) and CYP17 (Reid *et al.,* 2008). The last two were used as targets for the treatment of hormone-dependent breast and prostate cancer respectively.

Ketoconazole, an anti-fungal agent was the first compound discovered with CYP17 inhibitory activity. However, it is not a very potent inhibitor of CYP17 and non-selective as it inhibits other cytochrome P450 enzymes. Besides it shows a number of notable side effects including liver damage (Bruno and Njar, 2007; Moreira *et al.,* 2007). This leads to the search for more active and selective CYP17 inhibitors.

A number of imidazole-based compounds have been synthesised as potential CYP17 inhibitors. The designing of these molecules was mainly based on an iron-nitrogen (Fe-N) bond that forms between the haem iron of the enzyme active site and the nitrogen atom of the inhibitor via a co-ordinate bond formation (Shahid *et al.,* 2008).

In the this study, three different series of imidazole-based compounds were evaluated as CYP17 inhibitors; (i) substituted benzyl imidazole (compounds 1-10), (ii) substituted sulfonate derivatives of 4-hydroxybenzyl imidazole (compounds 31-52) and (iii) substituted phenyl ethanone compounds (compounds 370-410) (Figure 3.24).

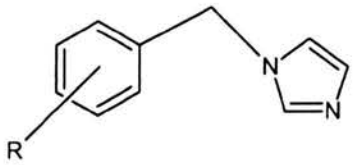

Series 1

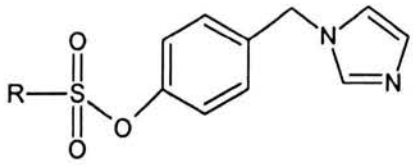

Series 2

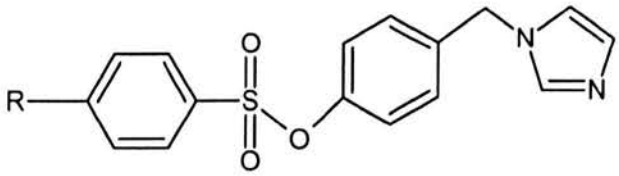

Series 3

Figure 3.24: General structures of the series of the CYP17 inhibitors used in the this study

The synthesis of a series of derivatives of benzyl imidazole inhibitors has been reported previously (Owen *et al.*, 2006; Shahid *et al.*, 2008 and Owen *et al.*, 2008). The compounds are synthesised by substituting the phenyl moiety. The phenyl moieties potentially interact with the hydrogen moieties at the active site of the enzyme CYP17 which interact with the initial substrate as well as the 17α-hydroxylated steroids (such as 17α-hydroxypregnenolone and 17α-hydroxyprogesterone). These hydrogen bonding groups bind to C (3) of the substrate and hence stabilise the enzyme-substrate complex (Ahmed *et al,* 2009). We have previously shown that derivatives of imidazole-based substituted phenyl ethanone inhibits the enzyme 17α- hydroxylase/17, 20-lyase (known as CYP17 or P-45017α) through the use of the C=O moiety in binding to one of the two hydrogen bonding groups whilst an appropriate functionality on the phenyl ring system may allow additional interactions to take place, thereby resulting in potent inhibitory activity (Shah *et al.,* 2011). These results showed that most of the compounds in the series were weak inhibitors of 17α-OHase as compared to the standard inhibitor ketoconazole (KTZ). Almost all compounds were found to possess higher percentage inhibition of the lyase part of the enzyme as compared to KTZ. The weak inhibitory activity of compounds against 17α-OHase as compared to lyase has been suggested in reducing side-effects as the compounds would not be expected to interfere with corticosteroid synthesis (Ahmed *et al.,* 2009).

Series 1:

The preliminary data of the benzyl imidazole based compounds showed that the inhibitory activity of the compounds, against 17-α OHase and 17, 20 lyase, are more or less similar to the control drug ketoconazole. Compound 9 showed the best potency (86.66 ± 4.85% inhibition) against hydroxylase among all compounds (Table 3.7). The compounds in the series contain a basic general structure (Figure 3.30) but a different R group. Compound 9 contains a CF3 group at the fourth position of the benzene ring. Owen *et al.* (2006) have previously shown that the enzyme CYP17 has the greatest selectivity for the compound containing CF3 as R groups and hence are the good lead compounds in the design and synthesis of more potent inhibitors of CYP17. Moreover, the substitution of the benzene ring at the fourth position gave the highest potency of designed compounds (Owen *et al.*, 2006). Our data showed similar results as compounds with a substitution at the fourth position of the benzene ring showed the highest inhibition of the enzyme. This suggests that substitution of the CF3 group at the fourth position increases the potency of these inhibitors.

Series 2 :

In the case of sulfonate derivatives of 4-hydroxybenzyl imidazole-based compounds, the preliminary data shows that the compounds 35 and 38 have better inhibitory activity against hydroxylase then KTZ. The results showed that the inhibitory activity of the compounds against 17-αOHase increased when alkyl chain length was increased from one carbon to eight carbons and then decreased further when the alkyl chain was increased to twelve carbons. Shahid *et al.* (2008) and Owen *et al.* (2008) have shown using the substrate haem complex approach that the length of a compound plays a key role in determining the overall inhibitory activity.

All compounds in series 2 showed the better inhibitory activity against the 17, 20 lyase part of the CYP17 enzyme. However, the difference in alkyl chain length of the compounds did not show any trend in % inhibition as in the case of the 17α-OHase enzyme.

In series 2, Compound 38 showed the highest % inhibition of both 17α-OHase and 17, 20 lyase activity as compared to ketoconazole and other compounds. The chemical structure of the compounds showed the presence of CF3 as the R group. This is similar to series 1 and another reported study which showed the compounds containing a CF3 group in the structure showed the highest potency (Owen *et al.,* 2006).The concentration of the inhibitor needed to inhibit the activity of an enzyme by half (IC_{50}) for the compound 35 and 38 was found to be 4.82 μM and 0.18 μM respectively.

Series 3:

In the this study, the sulfonate derivatives of 4-hydroxybenzyl imidazole compounds with different substitution groups in series 3 are the most potent inhibitors of 17α-OHase and 17, 20 lyase as compared to the other two series.

Ahmed *et al.,* (2009) have proposed that sulfonate derivatives of 4-hydroxybenzyl imidazole compounds have additional binding activity with the enzyme to increase their potency; (i) the 4-substituent on the phenyl ring undergoes polar–polar interaction with one of the hydrogen bonding groups at the active site, (ii) the second interaction involves the sulfonate moiety where S=O groups interact with the active site. Both interactions increase the stability of the inhibitor–enzyme complex which leads to an increase in the potency of the inhibitor in comparison to compounds which are only able to interact with a single hydrogen bonding group.

The substitution of the methoxy group in compound 48 increased the potency of the compounds. Compound 48 was found to be the most potent inhibitor of the 17α-OHase and the 17, 20 lyase activity of the CYP17 enzyme. The IC_{50} values of the two most potent compounds 48 and 51 were found to be 1.21 μM and 0.14 μM respectively.

The inhibitors used in the this study have shown good potency when compared to those reported by Ahmed *et al.* (2009) who have designed similar kinds of sulfonate derivatives of imidazole-based compounds.

3.4.3. Inhibitory activity of compounds synthesised as 17β-HSD3 inhibitors

The enzyme 17β-HSD3 reduces the C19 steroid Δ4-androstene-3, 17-dione to testosterone in the presence of NADPH (Laplante and Poirier, 2008) which further converts into dihydrotestosterone (DHT) by the action of a reductase enzyme. DHT stimulates the growth of hormone-dependent prostate tumours (Day *et al.*, 2008). Several inhibitors of 17β-HSD have been reported to date. A non-aromatic A-ring and C (17) carbonyl moiety have been reported to be very important features of any potential inhibitor of 17β-HSD (Owen *et al.*, 2004; Day *et al.*, 2008)

The natural substrate androsterone is considered to be a suitable lead compound for the development of 17β-HSD3 inhibitors (Maltais *et al.*, 2002). The androsterone has been modified at different positions to synthesise a series of steroidal inhibitors. The substitution at position 16 of androsterone produces weak inhibitors of type 3 of the 17β-HSD enzyme (Tchedam-Ngatcha *et al.*, 2000). However, when the natural substrate was modified at the 3β position, this led to the discovery of potent inhibitors of this enzyme (Maltais *et al.*, 2011; Tchedam-Ngatcha *et al.*, 2006; Maltais *et al.*, 2002; Tchedam-Ngatcha *et al.*, 2000) The non-steroidal compounds e.g. 7-hydroxyflavone and baicalein (IC_{50} = 9.0 and 9.3 mM respectively) were also reported to inhibit 17β-HSD3 (Le Lain *et al.*, 2001).

The series of potential steroidal as well as non-steroidal inhibitors of 17β-HSD 3 were tested along with two known inhibitors: 7-hydroxy flavone and baicalein. Series 5 (compounds 125 – 139) are acetic acid-based derivatives of 4-hydroxy phenyl ketones while series 6 (compounds 172 – 184) and 7 (compounds 185 – 197) are the transformed androstenedione compounds (Figure 3.25).

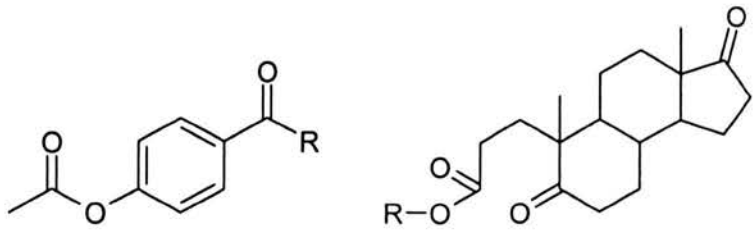

Series 5 Series 6 and 7

Figure 3.25: General structures of the series of the 17β-HSD3 inhibitors used in the this study

Series 5:

A structure-activity relationship study, by Lota *et al.* (2006), suggests that the 4-hydroxy moiety of phenyl ketone inhibitors interacts with the enzyme active site through a potential hydrogen bonding with groups at the 17β-HSD active site. We have evaluated a series of similar compounds. Our results show that for the straight alkyl chain derivatives of hydroxyl phenyl, the enzyme inhibition increases as the number of carbon atoms have increased from a one carbon to a seven carbon alkyl group. The potency of these compounds was decreased as the number of carbons increased to nine carbons. This decrease in inhibitory activity has been suggested as a steric interaction between the alkyl chain and the enzyme active site (Lota *et al.,* 2008). Compound 132 appeared to be the most potent compound (% inhibition = 40.51 ± 1.93%) as compared to standard 7-hydroxy flavone and baicalein. The data for cyclo-derivatives shows that all compounds possess similar levels of inhibition. These results are similar to those shown by Lota *et al.* (2008) who reported the synthesis and biological evaluation of a series of similar kinds of hydroxyl phenyl ketones as 17β-HSD3 inhibitors.

Series 6 and 7:

The natural substrate has previously been used to generate a series of 17β-HSD 3 inhibitors (Maltais *et al,* 2011; Tchedam-Ngatcha *et al,* 2006; Maltais *et al,* 2002; Tchedam Ngatcha *et al,* 2000). Based on that, we have also evaluated the series of compounds which were synthesised by transforming the natural substrate, androstenedione at the 3rd carbon position. The data of the first series of the

compounds shows that compound 176 has the highest percentage inhibition of enzyme activity as compared to 7-hydroxy flavone and baicalein. However the compounds of this series are not shown to be very potent inhibitors. In the second series, compound 189 was shown to be the most potent (39.76 ± 0.20%) as compared to 7-hydroxy flavone and baicalein. The compounds in the second series are shown to be poor inhibitors of 17β-HSD3. Most of the compounds have potency equal to baicalein.

3.5. Conclusion

In conclusion, the development of the three different assays (against 17α-OHase, 17, 20 lyase and 17β-HSD3) has been undertaken involving the initial partial purification of the microsomal enzyme followed by the determination of kinetic parameters. Using the assay, a number of synthesised compounds have been evaluated and their initial screening data and the IC_{50} values, for a number of the more potent inhibitors of the two components of CYP17 have also been determined.

The inhibitors of CYP17 were found to be more potent than the 17β-HSD3 inhibitors. Furthermore, the CYP17 inhibitors were reported to have an anti-adhesion effect on tumour cells whereas no work has been done on the effect of 17β-HSD3 inhibitors. Therefore the potent inhibitors of the enzyme CYP17 were used in further cell-based studies.

CHAPTER 4: CYTOTOXICITY OF CYP17 INHIBITORS AND THEIR EFFECT ON THE ADHESION OF TUMOUR CELLS TO ENDOTHELIAL CELL MONOLAYERS

The CYP17 inhibitors were tested to determine their effect on adhesion of prostate and breast cancer cell lines on human vascular endothelial cell monolayers. DU145 and PC3 cells were the two human prostate cancer cell lines used whereas MCF7 cells was the human breast cancer cell lines used in the this study. Human vascular endothelial cells or HUVECs was the non-cancerous cell line used. DU145 cells were derived from the brain metastasis whereas the PC3 cells were derived from bone metastasis of prostate cancer. MCF7 cells were derived from the pleural effusion of the breast cancer patient.

4.1. MTT assay to determine the cytotoxicity of CYP17 inhibitors

Prior to the testing in *ex vivo* models, the compounds were checked for any cytotoxic effects on both tumour and normal endothelial cell lines. There are a number of tests to assess the anti-growth effects of chemotherapeutic agents *in vitro* (Ulukaya *et al.*, 2008). The reduction of tetrazolium salts in the MTT assay is now widely accepted as a reliable way to examine cell proliferation (Wilson *et al.*, 1990). It was first developed by Mosmann (1983). The MTT assay is comparatively cheaper and is the most frequently used assay for assessing cell proliferation and viability (Ulukaya *et al.*, 2008).

Inhibitors of CYP17 have been tested previously for their cytotoxicity on human prostate cancer cell lines and have been shown to be cytotoxic (Moreira *et al.*, 2007: Moreira *et al.*, 2008). Ketoconazole, a well-known CYP17 inhibitor, has been used in high doses (800-1200 mg/dl) for prostate cancer treatment. The high dose causes many significant side effects, one of which is hepatotoxicity (or cytotoxicity of liver cells) and has been withdrawn for cancer treatment (Vasaitis *et al.*, 2011; Nussbaumer *et al.*, 2011). Cytotoxic drugs kill not only cancer cells but also normal and healthy tissue so there is a demand for effective and safer anti-cancer therapies that decrease the frequency of adverse effects (Ismael *et al.*, 2008).

4.2. Effect of CYP17 inhibitors on tumour cell adhesion

The interaction of malignant cells from the primary tumour with endothelial cells in the blood vessels is one of the most important preliminary events that cause metastasis (Geng 2003; Haddad *et al.*, 2010). Altered adhesion is one of the pathological factors involved in metastasis and progression of tumour proliferation (Kilsdonk *et al.*, 2010). One of the most important factors in the development of prostate cancer is the dysfunction in the adhesion of epithelial cells from the prostate and prostate cancer cells that possess abnormalities in the intercellular and cell-matrix adhesion molecules (Mason *et al.*, 2002). A previous study has suggested that prostate cancer metastasis to the bones is a result of preferential adhesion to human bone marrow endothelial (HBME) cells (Lehr and Pienta, 1998). Bone metastasis of breast cancer cells depends on the adhesion of the extracellular matrix of the bones that is mediated by integrins and other adhesion receptors (Habermann, 2003). McCrohon and colleagues (1999) have shown that a 24 hr exposure to androgens (testosterone and dihydrotestosterone) significantly increases monocyte adhesion to interleukin 1β- stimulated endothelial cell monolayers. When an androgen receptor antagonist was used, the adhesion was abolished (McCrohon *et al.*, 1999). It has been proposed that tumour cell interaction with the endothelium is similar to that of leukocytes interacting with the endothelial cells of blood capillaries (Hashimoto *et al.*, 2004; Sheikh *et al.*, 2005; Cinamon *et al.*, 2004; Al-Mehdi *et al.*, 2000).

Various studies have reported the involvement of androgens in the expression of adhesion molecules. Dihydrotestosterone (DHT) increases the expression of vascular adhesion molecule (VCAM1) on tumour necrosis factor (TNF-α) pre-treated HUVECs (McCrohon *et al.*, 1999). The effect of DHT on prostate cancer cell adhesion to human bone marrow endothelial cells (HBME) monolayers has been investigated. DHT has been shown to increase the expression of adhesion molecules (Cooper *et al.*, 2002).

Melanoma cell adhesion molecule (MCAM) is a glycoprotein that regulates cell-cell and cell-matrix adhesion. The enzyme CYP17 regulates the gene that encodes for MCAM and matrix metalloproteinases (MMPs) and it has been observed that the knockdown of CYP17 in endometrial cancer cells reduces the invasive properties

of these cancer cells. These facts have suggested that CYP17 can affect the metastatic potential of endometrial carcinomas by regulation of cell–cell interaction. Although the mechanisms underlying CYP17-mediated regulation of these components are not known, it suggests that inhibition of CYP17 expression could be a promising therapeutic approach for the treatment of carcinomas (Chen *et al.*, 2011).

Inhibitors of the enzyme CYP17, responsible for androgen production, have previously been tested to determine their effect on the adhesion of MCF7 cell lines to human endothelial cells. Although many novel synthesised compounds did not show any significant effect, letrozole, a known CYP17 inhibitor, was shown to decrease tumour cell attachment to the endothelium (Build *et al.*, 2004). In another study, ketoconazole (KTZ), which has been used as a reference drug in this project, was also shown to decrease expression of adhesion molecules (Sasaki *et al.*, 2003). Consequently, the compounds used in this project are azole-based compounds and their synthesis is based on the interaction of ketoconazole with the enzyme active site where the imidazole ring of ketoconazole forms the covalent bond with the haem iron of the active site (Section 1.6.6).

The aim of this chapter therefore includes the determination of anti-adhesion effects of these synthesised CYP17 inhibitors. The adhesive capacity of different tumour cell lines in the presence and absence of CYP17 inhibitors was also monitored. The effect of tumour necrosis factor alpha (TNF-α) on the adhesive potential of the endothelium was also monitored. One of the main aims of the present study was to develop an *ex vivo* "tumour-endothelial cells adhesion model". This model was used to determine the ratio of adherent tumour cells to endothelial cells.

4.3. Results for the cytotoxicity of CYP17 inhibitors against human endothelial and cancer cell lines

In the radiometric enzymatic assays in the previous chapter, compounds 31, 35, 38, 41, 48 and 51 showed greater potencies than the control drug, ketoconazole. These compounds were therefore tested along with ketoconazole to determine their cytotoxic and anti-adhesion effects. To obtain the maximal response in cell-based assays, the IC_{80} of the compounds were calculated using a statistical package (GraphPad, Software, Inc. USA) (Section 3.2.6.). The compounds were tested on four different cell lines. DU145 and PC3 were the two prostate cancer cell lines used and MCF7 was the human breast cancer cell line used in these cell-based assays. Human vascular endothelial cells (HUVECs) are non-cancerous endothelial cell lines to which tumour cells adhere and were also tested.

All compounds were dissolved in dimethyl sulfoxide (DMSO) and added to cells for 24 hours. The control cells were treated with 0.1 % DMSO only. The viable cells converted the yellow MTT dye into purple formazan crystals. The absorbance of the samples was measured at 570 nm. The cell viability was calculated as % of absorbance of control (DMSO) cells. The results are shown overleaf (Figure 4.1-4.4).

The results showed that the viability of DU145 cells (Figure 4.1) was not affected by ketoconazole when compared to the control. Similarly, the synthesised CYP17 inhibitors did not have any cytotoxic effect on DU145 cells when compared to either control or KTZ.

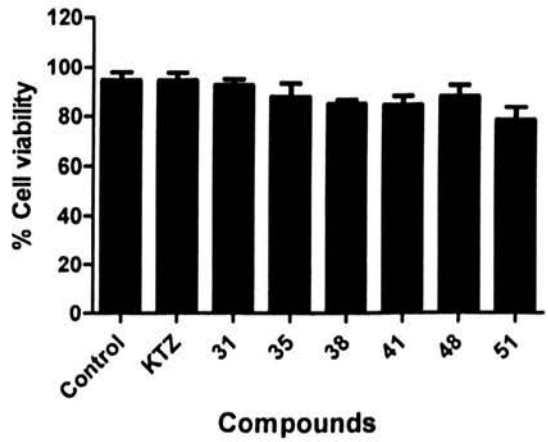

Figure 4.1: ***Effect of CYP17 inhibitors on the viability of DU145 cells.*** *The concentrations of compounds used, were equal to IC_{80}. The data is shown as mean ± SEM of three different experiments (n=3). The statistical analysis was done using Tukey's modified student's t-test (two-tail) where p>0.05*

In PC3 cells, ketoconazole did not cause any cytotoxic effects (Figure 4.2). However, compound 51 significantly decreased the viability of PC3 cells when compared to control (75.60 ± 3.38% and 93.21 ± 1.98%; mean ± SEM; respectively; p<0.05). None of the other compounds were seen to have an effect.

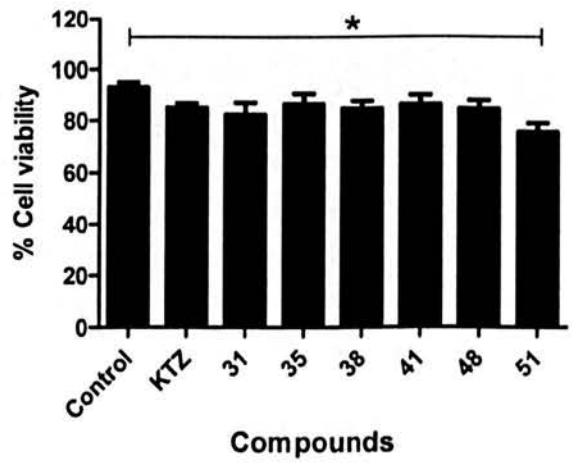

Figure 4.2: ***Effect of CYP17 inhibitors on the viability of PC3 cells.*** *The concentrations of compounds used, were equal to IC_{80}. The data is shown as mean ± SEM of three different experiments (n=3). The statistical analysis was done using Tukey's modified student's t-test (two-tail) where *p < 0.05 vs. control.*

Despite cell viability of 84.50 ± 6.45% in controls, no significant effect on MCF7 cell growth was observed when cells were incubated with any of the compounds when compared to either control or ketoconazole (Figure 4.3). Ketoconazole also did not have any effect on the viability of MCF7 cells.

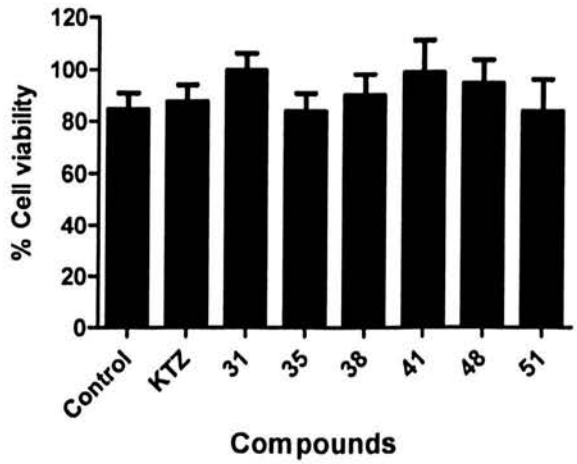

Figure 4.3: Effect of CYP17 inhibitors on the viability of MCF7 cells. *The concentrations of compounds used, were equal to IC_{80}. The data is shown as mean ± SEM of three different experiments (n=3). The statistical analysis was done using Tukey's modified student's t-test (two-tail) where p>0.05.*

Similar to all cancer cell lines, ketoconazole did not affect the viability of HUVECs. Moreover, treatment with the synthesised compounds did not produce any cytotoxic effects on HUVECs (Figure 4.4).

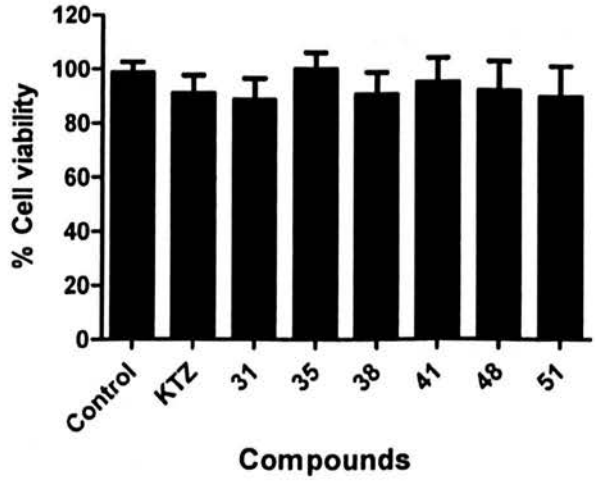

Figure 4.4: Effect of CYP17 inhibitors on the viability of HUVEC cells. *The concentrations of compounds used, were equal to IC_{80}. The statistical analysis was done using Tukey's modified student's t-test (two-tail) where p>0.05. The data is shown as mean ± SEM of three different experiments (n=3).*

4.4. Results for adhesion assays

The adhesion of tumour cells to endothelial cells is one of the important steps in the development of cancer metastasis (Laubli and Borsig, 2010). The compounds which have been synthesised to inhibit the enzyme CYP17 and to inhibit androgen production, have been tested to determine their effects on tumour cell adhesion to human vascular endothelial cells.

4.4.1. Dose- dependent curve of TNF-α

The pre-treatment of HUVEC with TNF-α has been shown to enhance the cell adhesion in a dose dependent manner (Kate *et al.,* 2004; Rainger and Nash, 2001; Ikuta *et al.,* 1991). HUVECs were therefore incubated with varying concentrations of TNF-α (0-1000 ng/mL) for 24 hrs. All three tumour cell lines; DU145, PC3 and MCF7 cells, were labelled with cell tracker green™ dye (Section 2.2.4.2.). Fluorescently labelled tumour cells (40,000 and 80,000 per well in two different experiments) were added to HUVEC monolayers and any non-adherent cells were washed off after two hours. Tumour cell fluorescence was measured as an index of tumour cell adherence and fluoresence was presented in arbitrary unit (A.U.).

The results showed that 10 ng/mL of TNF-α gave the maximal response with all three cell lines at concentrations of 40,000 and 80,000 tumour cells/ well (Figure 4.5). A two-way ANOVA was done to find any significant difference between the two different experiments which were carried out with different numbers of tumour cells per well.

In DU145 cells, with 10 ng/mL of TNF-α, the adherence of 80,000 DU145 cells was significantly higher when compared with 40,000 DU145 cells (3671 ± 91.82 fluorescence and 3443 ± 104.48 fluorescence; mean ± SEM; respectively; $p<0.05$). The other concentrations of TNF-α did not produce any difference in the cell adhesion of 80,000 and 40,000 DU145 cells per well (Figure 4.5A).

The adhesion of 80,000 PC3 cells per well was significantly increased by 0.1 ng/mL TNF-α when compared to 40,000 cells per well (2973 ± 127.94 fluorescence and 2292 ± 70.44 fluorescence; mean ± SEM; respectively; $p<0.05$),

1ng/mL TNF-α (3227.67 ± 87.09 fluorescence and 2556.33 ± 230.93 fluorescence; mean ± SEM respectively; $p<0.05$), 10 ng/mL TNF-α (3635.33 ± 50.14 fluorescence and 3067.33 ± 147.02 fluorescence; mean ± SEM; respectively; $p<0.05$), 100 ng/mL TNF-α (3366 ± 249.33 fluorescence and 2789 ± 193.59 fluorescence; mean ± SEM; respectively; $p<0.05$) and 1000 ng/mL TNF-α (31533 ± 242.78 fluorescence and 2485.33 ± 191.94 fluorescence; mean ± SEM; respectively; $p<0.05$) (Figure 4.5B).

For MCF7 cells, the adhesion of 80,000 cells per well was significantly increased by 0.1 ng/mL TNF-α when compared to 40,000 cells per well (34166.33 ± 73.79 fluorescence and 1649 ± 342.87 fluorescence; mean ± SEM; respectively; $p<0.05$), 1 ng/mL TNF-α (3450 ± 229.34 fluorescence and 1842.33 ± 253.60 fluorescence; mean ± SEM; respectively; $p<0.05$), 10 ng/mL TNF-α (3600.33 ± 132.14 fluorescence and 2058.33 ± 125.92 fluorescence; mean ± SEM; respectively; $p<0.05$), 100 ng/mL TNF-α (2891.67 ± 118.75 fluorescence and 1928.67 ± 221.50 fluorescence; mean ± SEM; respectively ; $p<0.05$) and 1000 ng/mL TNF-α (2966.33 ± 261.39 fluorescence and 1932 ± 97.02 fluorescence; mean ± SEM; 80,000 and 40,000 MCF7 cells respectively) (Figure 4.5C).

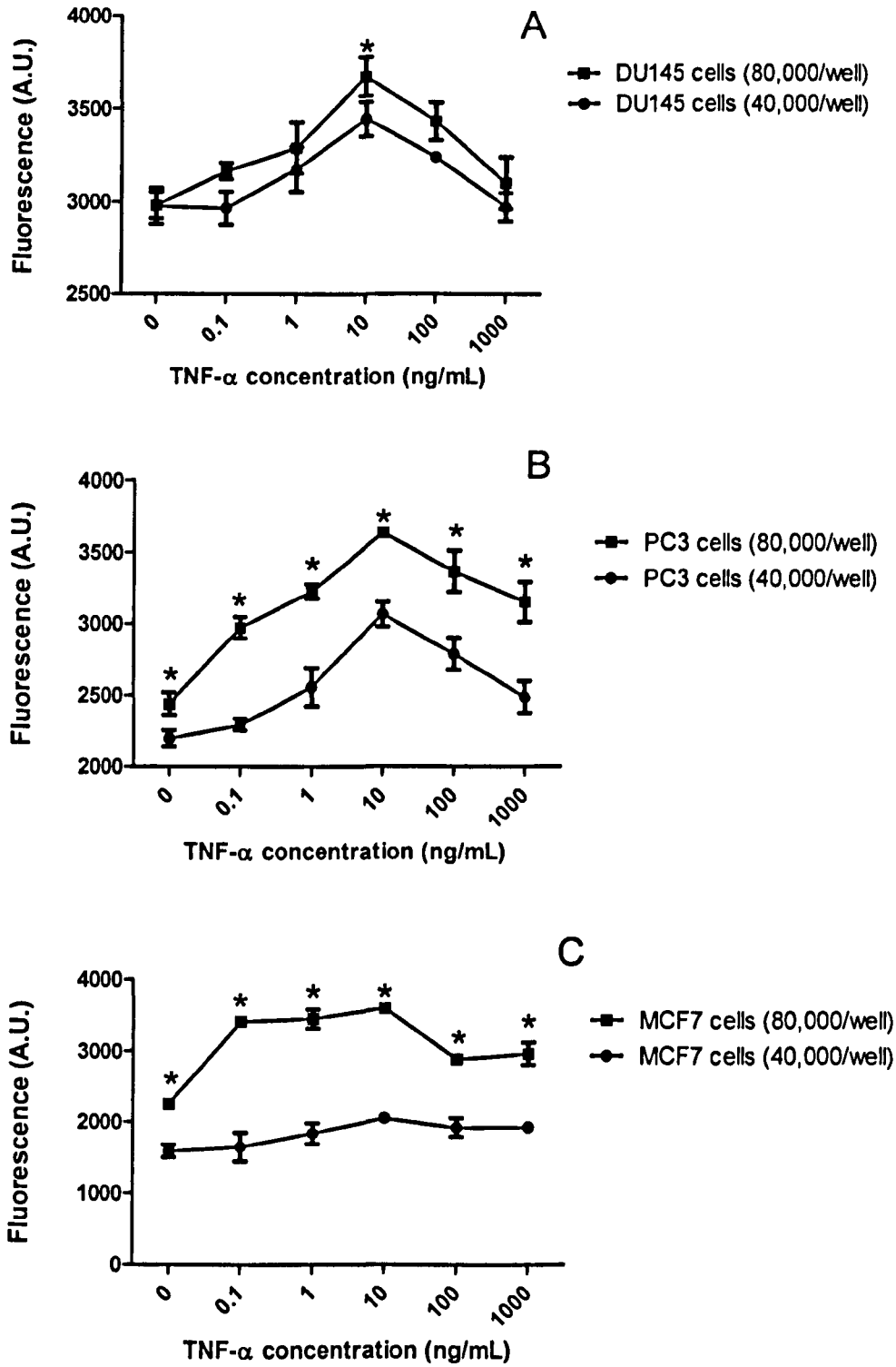

Figure 4.5: ***Effect of different concentrations of TNF-α on the adhesion of tumour cells on HUVEC monolayers treated with TNF-α for 24 hours.*** *Fluorescently labelled tumour cells (40,000 and 80,000 cells/well) were added to HUVEC monolayers for two hours. The data is shown as mean ± SEM of three different experiments (n=3). Statistical analysis was done using a Two-way ANOVA and a post Bonferroni test where * $p < 0.05$ vs. 40,000 cells. (A) DU145 cells (B) PC3 cells (C) MCF7 cells.*

4.4.2. Effect of number of tumour cells on cell adhesion

HUVEC monolayers were stimulated with TNF-α (10 ng/mL) for 24 hours. Different numbers of fluorescently labelled tumour cells (10,000 – 160,000) were added to HUVEC monolayers and non-adherent cells were washed off after two hours.

The cells in the control wells were not washed-off and total fluorescence of each cell line was calculated. Tumour cell fluorescence was measured as an index of cell adherence.

The results showed that the total fluorescence was decreased after washing off non-adherent cells (Figure 4.6). The results showed that adhesion of DU145 cells to TNF-α stimulated HUVECs was significantly higher than non-stimulated HUVECs when the DU145 cells were added in a concentration of 80,000 per well (25967 ± 1637 fluorescence and 20477 ± 510.5 fluorescence; mean ± SEM; respectively; $p<0.05$) and 160,000 per well (56152 ± 1722 fluorescence and 48303 ± 1472 fluorescence; mean ± SEM; respectively; $p<0.05$).

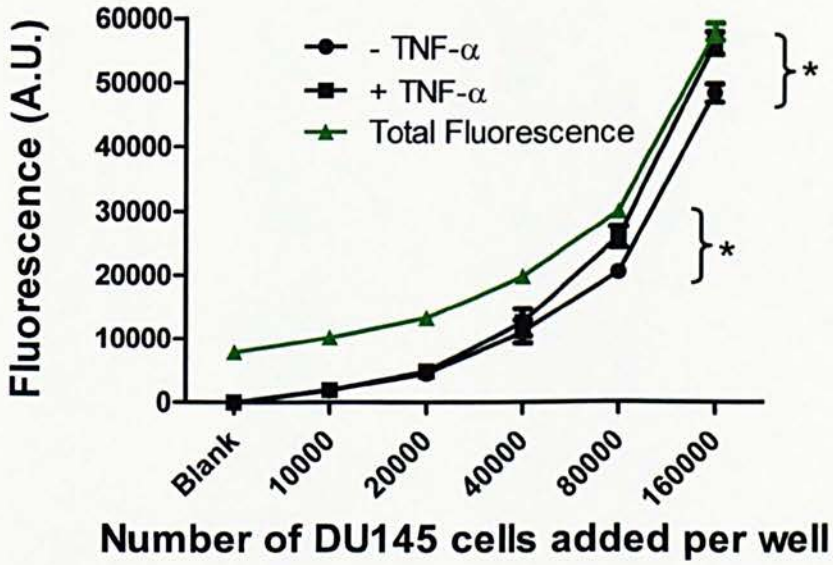

Figure 4.6: ***Adhesion of DU145 cells on HUVEC monolayers in the presence and absence of TNF-α (10ng/mL).*** *DU145 cells were added in different concentrations(10,000 – 160,000) to HUVEC monolayers for two hours. The data is shown as mean ±SEM of three different experiments (n=3). Statistical analysis was done using a Two-way ANOVA and a post Bonferroni test where * $p < 0.05$ vs. –TNF-α.*

In PC3 cells, the total fluorescence was decreased after washing off non-adherent cells (Figure 4.7). In the presence of TNF-α, the adhesion of PC3 cells to HUVECs was significantly higher than non-treated HUVECs when the PC3 cells were added at a concentration of 80,000 per well (24353 ± 123.5 fluorescence and 20620 ± 306.8 fluorescence; mean ± SEM; respectively; $p<0.05$) and 160,000 per well (51938 ± 528.5 fluorescence and 44039 ± 1725 fluorescence; mean ± SEM; respectively; $p<0.05$).

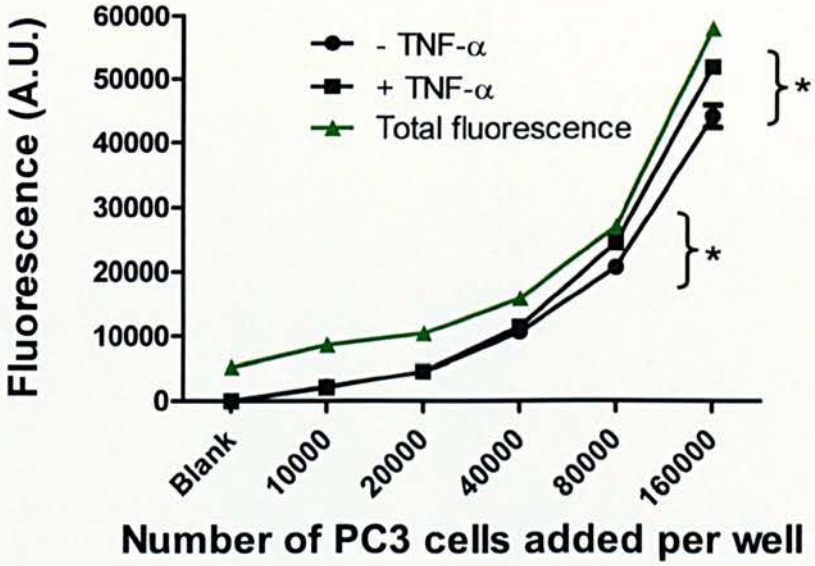

Figure 4.7: ***Adhesion of PC3 cells on HUVEC monolayers in the presence and absence of TNF-α (10ng/mL).*** *PC3 cells were added in different concentrations (10,000 – 160,000) to HUVEC monolayers for two hours. The data is shown as mean ± SEM of three different experiments (n=3). Statistical analysis was done using a Two-way ANOVA and a post Bonferroni test where * $p < 0.05$ vs. –TNF-α.*

Similar to the other two cell lines, the total fluorescence for MCF7cells was decreased after washing off non-adherent cells (Figure 4.8). The adhesion of MCF7 cells to TNF-α stimulated HUVECs was significantly higher than non-stimulated HUVECs when the MCF7 cells were added at a concentration of 80,000 per well (29021 ± 1351 fluorescence and 23447 ± 1854 fluorescence; mean ± SEM; respectively; $p<0.05$) and 160,000 per well (53519 ± 1890 fluorescence and 46653 ± 2964 fluorescence; mean ± SEM; respectively; $p<0.05$).

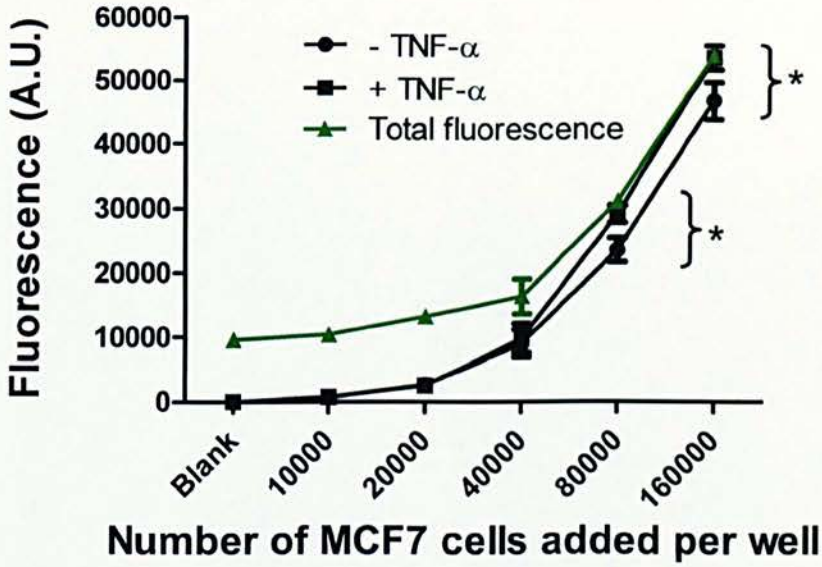

Figure 4.8: ***Adhesion of MCF7 cells on HUVEC monolayers in the presence and absence of TNF-α (10ng/mL).*** *MCF7 cells were added in different concentrations (10,000 – 160,000) to HUVEC monolayers for two hours. The data is shown as mean ± SEM of three different experiments (n=3). Statistical analysis was done using a Two-way ANOVA and a Post Bonferroni test where * $p < 0.05$ vs. –TNF-α.*

4.4.3. Determination of tumour:endothelial cell ratio (TC:EC)

The tumour cells were added in different concentrations (10,000 – 160,000 cells/well) to non-stimulated and 10 ng/mL TNF-α stimulated HUVEC monolayers. The cell density of a confluent monolayer of HUVECs was assumed to be 3.2 x 10^4 cells/well of a 96-well plate (Corning Life Sciences, UK). The fluorescence given by the total number of tumour cells added into a well was measured as "total fluorescence" whereas fluorescence given by adherent tumour cells was measured as "obtained fluorescence". The total and obtained fluorescence was used to calculate the number of tumor cells adherent to HUVECs. The ratio of adherent tumour cells (TC) to each HUVEC (EC) was calculated. The TC: EC were compared before and after washing off non-adherent cells.

The DU145: HUVEC ratio was increased proportionally to the number of DU145 cells added to the well. This increase was also observed with TNF-α (Figure 4.9). When comparing the effect of TNF-α on the ratio of adherent DU145 cells, it was found that TNF-α significantly increased the proportion of cells adherent when DU145 cells were added to HUVEC monolayers, at a concentration of 80,000 cells per well (2.89 ± 0.18 and 2.29 ± 0.10; mean ± SEM; respectively; $p<0.05$) and 160,000 cells per well (5.54 ± 0.17 and 4.99 ± 0.12; mean ± SEM; respectively ; $p<0.05$).

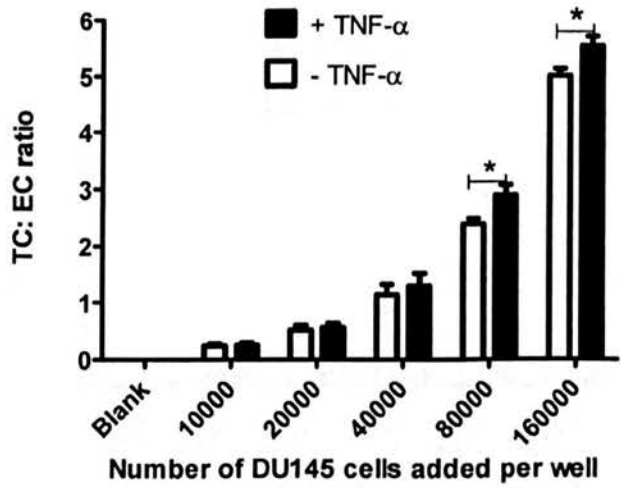

Figure 4.9: ***The ratio of DU145 cells bound to each HUVEC in the presence and absence of TNF-α (10ng/mL).*** *The data is shown as mean ± SEM of three different experiments (n=3). Statistical analysis was done using a Two-way ANOVA and a Post Bonferroni test where * $p < 0.05$ vs. –TNF-α.*

The data (Table 4.1) shows that the DU145: HUVEC ratio decreased near to half after washing off non-adherent tumor cells.

DU145:HUVEC ratio (before washing)	DU145:HUVEC ratio (after washing) -TNF	DU145:HUVEC ratio (after washing) +TNF
0.5	0.24 ± 0.04	0.26 ± 0.04
1.0	0.53 ± 0.08	0.57 ± 0.08
2.0	1.15 ± 0.18	1.31± 0.22
4.0	2.42 ± 0.10	2.93 ± 0.18
8.0	5.06 ± 0.13	5.61 ± 0.17

Table 4.1: ***The DU145: HUVEC ratio before and after washing off non-adherent tumour cells.*** *The mean of the fluorescence arbitrary unit from three different experiments (n=3) were used to calculated the number of tumour cells which were adhered to HUVEC monlayers after washing. The DU145: HUVEC ratio was calculated by dividing the number of tumour cells to the number of HUVECs in a 96-well plate.*

In the absence of TNF-α, the PC3: HUVEC ratio was increased proportionally to the number of PC3 cells added to the well (Figure 4.10). The results were similar when HUVECs were pre-incubated with TNF-α. When comparing the effect of TNF-α, the ratio of PC3 cells adhered to each HUVEC was significantly increased by TNF-α when PC3 cells were added at a concentration of 80,000 cells per well (2.78 ± 0.01 and 2.56 ± 0.03; mean ± SEM; respectively; $p<0.05$) and 160,000 cells per well (4.87 ± 0.05 and 4.13 ± 0.16; mean ± SEM; respectively; $p<0.05$).

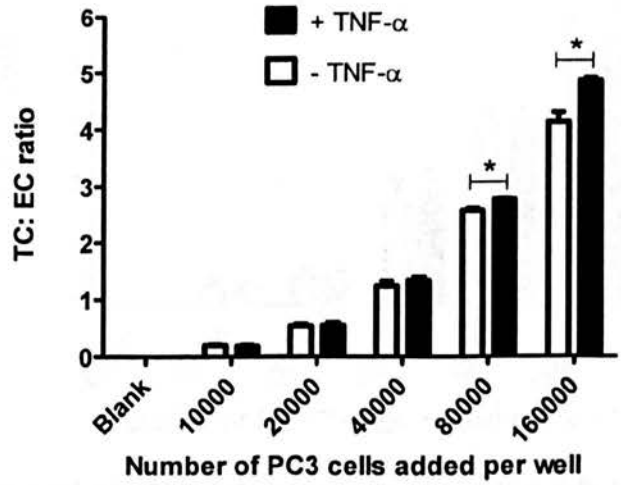

Figure 4.10: ***The ratio of PC3 cells bound to each HUVEC in the presence and absence of TNF-α (10ng/mL).*** *The data is shown as mean ± SEM of three different experiments (n=3). Statistical analysis was done using a Two-way ANOVA and a post Bonferroni test where * $p < 0.05$ vs. –TNF-α.*

Similar to DU145 cells, the ratio of adherent PC3 to each HUVEC was decreased as a result of washing (Table 4.2).

PC3:HUVEC ratio (before washing)	PC3:HUVEC ratio (after washing) -TNF	PC3:HUVEC ratio (after washing) +TNF
0.5	0.20 ± 0.01	0.19 ± 0.02
1.0	0.55 ± 0.03	0.55 ± 0.05
2.0	1.25 ± 0.08	1.35 ± 0.07
4.0	2.61 ± 0.03	2.81 ± 0.01
8.0	4.18 ± 0.16	4.93 ± 0.05

Table 4.2: ***The PC3: HUVEC ratio before and after washing off non-adherent tumour cells.*** *The mean of the fluorescence arbitrary unit from three different experiments (n=3) were used to calculated the number of tumour cells which were adhered to HUVEC monlayers after washing. The PC3: HUVEC ratio was calculated by dividing the number of tumour cells to the number of HUVECs in a 96-well plate.*

Similar to the two prostate cancer cell lines, the MCF7: HUVEC ratio was increased proportionally to the number of MCF7 cells added to the well in the presence and absence of TNF-α (Figure 4.11). However, when comparing the effect of TNF-α, the ratio of adherent MCF7 cells to each HUVEC was not affected by TNF-α.

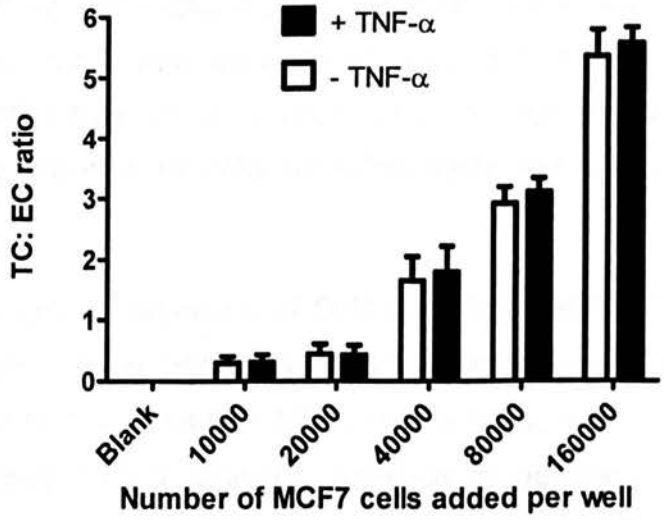

Figure 4.11: ***The ratio of MCF7 cells bound to each HUVEC in the presence and absence of TNF-α (10ng/mL).*** *The data is shown as mean ± SEM of three different experiments (n=3). Statistical analysis was done using a Two-way ANOVA and a post Bonferroni test where p>0.05*

The MCF7: HUVEC ratio was decreased near to half after washing non-adherent tumour cells as in the case of DU145 and PC3 cells (Table 4.3).

MCF7:HUVEC ratio (before washing)	MCF7:HUVEC ratio (after washing) -TNF	MCF7:HUVEC ratio (after washing) +TNF
0.5	0.29 ± 0.12	0.31 ± 0.12
1.0	0.45 ± 0.17	0.43 ± 0.16
2.0	1.67 ± 0.40	1.82 ± 0.42
4.0	2.96 ± 0.27	3.14 ± 0.23
8.0	5.43 ± 0.44	5.64 ± 0.01

Table 4.3: ***The MCF7: HUVEC ratio before and after washing off non-adherent tumour cells.*** *The mean of the fluorescence arbitrary unit from three different experiments (n=3) were used to calculated the number of tumour cells which were adhered to HUVEC monlayers after washing. The MCF7: HUVEC ratio was calculated by dividing the number of tumour cells to the number of HUVECs in a 96-well plate.*

4.4.4. Effect of CYP17 inhibitors on DU145 cells adhesion to HUVEC monolayers

The tumour cells were treated with different CYP17 inhibitors for 24 hours and labelled with cell tracker green dye. The tumour cells were added to non-stimulated and TNF-α stimulated HUVEC monolayers for two hours. The tumour cells in the control tube were treated with DMSO (0.1%) in media only. The percentage of cell adhesion of tumour cells to HUVEC was calculated by comparing the absorbance of cells following treatment with cells in untreated control.

In the absence of TNF-α, adhesion of DU145 cells on HUVEC monolayers was significantly decreased by ketoconazole (KTZ) when compared to control (88.25 ± 3.96% and 100 ± 0.01%; mean ± SEM; respectively; $p<0.05$) (Figure 4.12A). Similarly, synthesised CYP17 inhibitors significantly decreased the adhesion of DU145 cells when compared to control and ketoconazole (60.93 ± 3.35%, 69.30 ± 3.82%, 66.56 ± 2.23% and 62.06 ± 5.32% and 88.25 ± 3.96%; mean ± SEM; in the presence of compounds 38, 41, 48 and 51 and KTZ respectively; $p<0.05$).

The adhesion of DU145 cells on HUVEC monolayers, pre-stimulated with TNF-α (10ng/mL), was not decreased by ketoconazole (Figure 4.12B). However the synthesised CYP17 inhibitors significantly decreased the adhesion of DU145 cells when compared to control and ketoconazole. (69.85 ± 4.08%, 76.14 ± 3.77%, 70.45 ± 1.71% and 66.61 ± 7.18%, 100 ± 0.01% and 98.15 ± 2.92%; mean ± SEM; in the presence of compounds 38, 41, 48 and 51 and KTZ and control respectively; $p<0.05$).

When the adhesion of DU145 cells on non-stimulated and stimulated HUVEC monolayers was compared no significant difference in the DU145 cell adhesion was found.

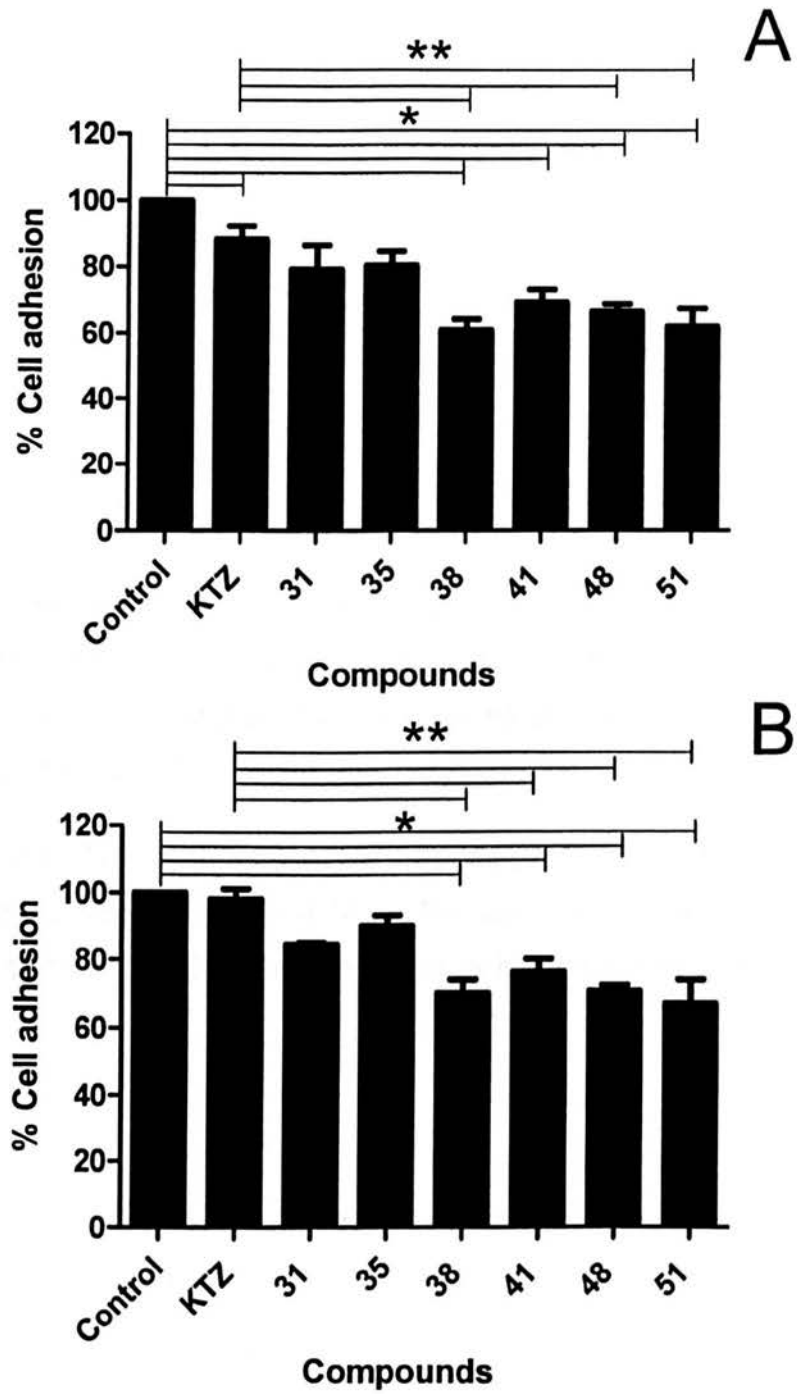

Figure 4.12: Effect of CYP17 inhibitors on DU145 cell adhesion to non-stimulated and TNF-α stimulated HUVEC monolayers. *The data is shown as mean ± SEM of three different experiments (n=3). (A) In the absence of TNF-α (B) In the presence of TNF-α. The statistical analysis was done using Tukey's modified student's t-test (two-tail) where *p<0.05 vs. control and **p<0.05 vs. KTZ. A two-way ANOVA was done where p>0.05.*

4.4.5. Fluorescence and phase-contrast microscopy of DU145 cells adhesion on HUVEC monolayers in the presence of CYP17 inhibitors

The adhesion of tumour cells to HUVEC monolayers was viewed under a fluorescent and phase-contrast microscope. The fluorescently labelled (green) tumour cells adhered to HUVEC monolayers (shown in the righthand-side panel of the figures overleaf). Compound 38 was found to be more potent in decreasing the adhesion of DU145 cells to HUVEC monolayers. Therefore representative figures of cell adhesion using compound 38 were used. See appendices 4 and 5 for other compounds.

In the absence of TNF-α, the adhesion of DU145 cells (Figure 4.13) to HUVEC monolayers was decreased by ketoconazole when compared to control (Figure 4.13C). Compound 38 reduced the cell adhesion to a greater degree than ketoconazole and control (Figure 4.13E).

In the presence of TNF-α, ketoconazole decreased the adhesion of DU145 cells when compared to control (Figure 4.14C). The adhesion of DU145 cells was also decreased by compound 38 when compared to ketoconazole and control (Figure 4.14E).

Adhesion of DU145 cells in the absence of TNF-α

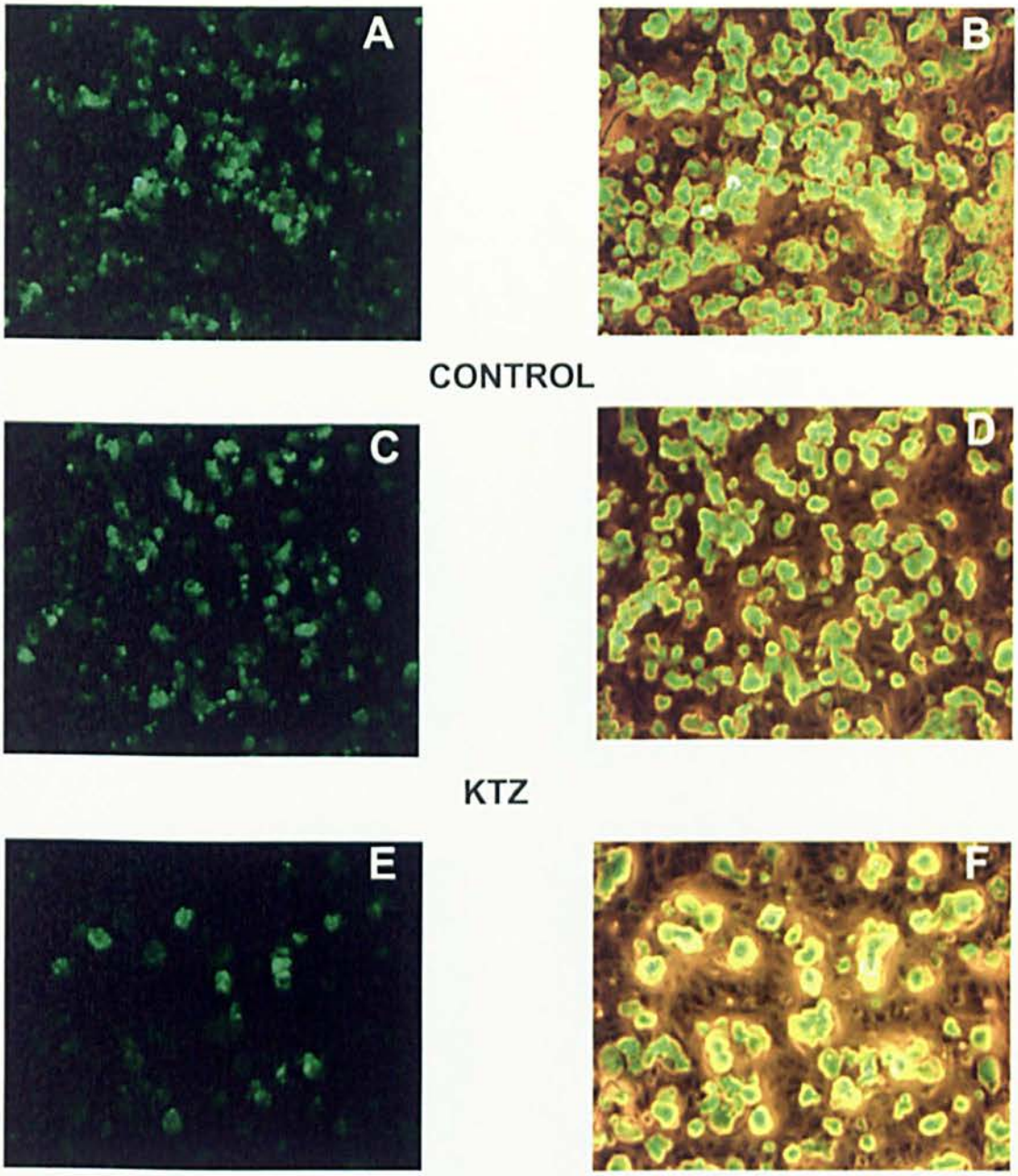

Figure 4.13: ***Fluorescence and phase-contrast microscopy of DU145 cells attached to non-stimulated HUVEC monolayers.*** *DU145 cells were treated with CYP17 inhibitors for 24 hours. Fluorescently labelled DU145 cells (green) are attached to the HUVEC monolayer. (A-B) Untreated DU145 cells (C-D) DU145 cells treated with KTZ (E-F) DU145 cells treated with compound 38. Images were acquired using a fluorescent microscope at X100 magnification. The images are qualitatively representative of three different experiments (n=3).*

Adhesion of DU145 cells in the presence of TNF-α (10ng/mL)

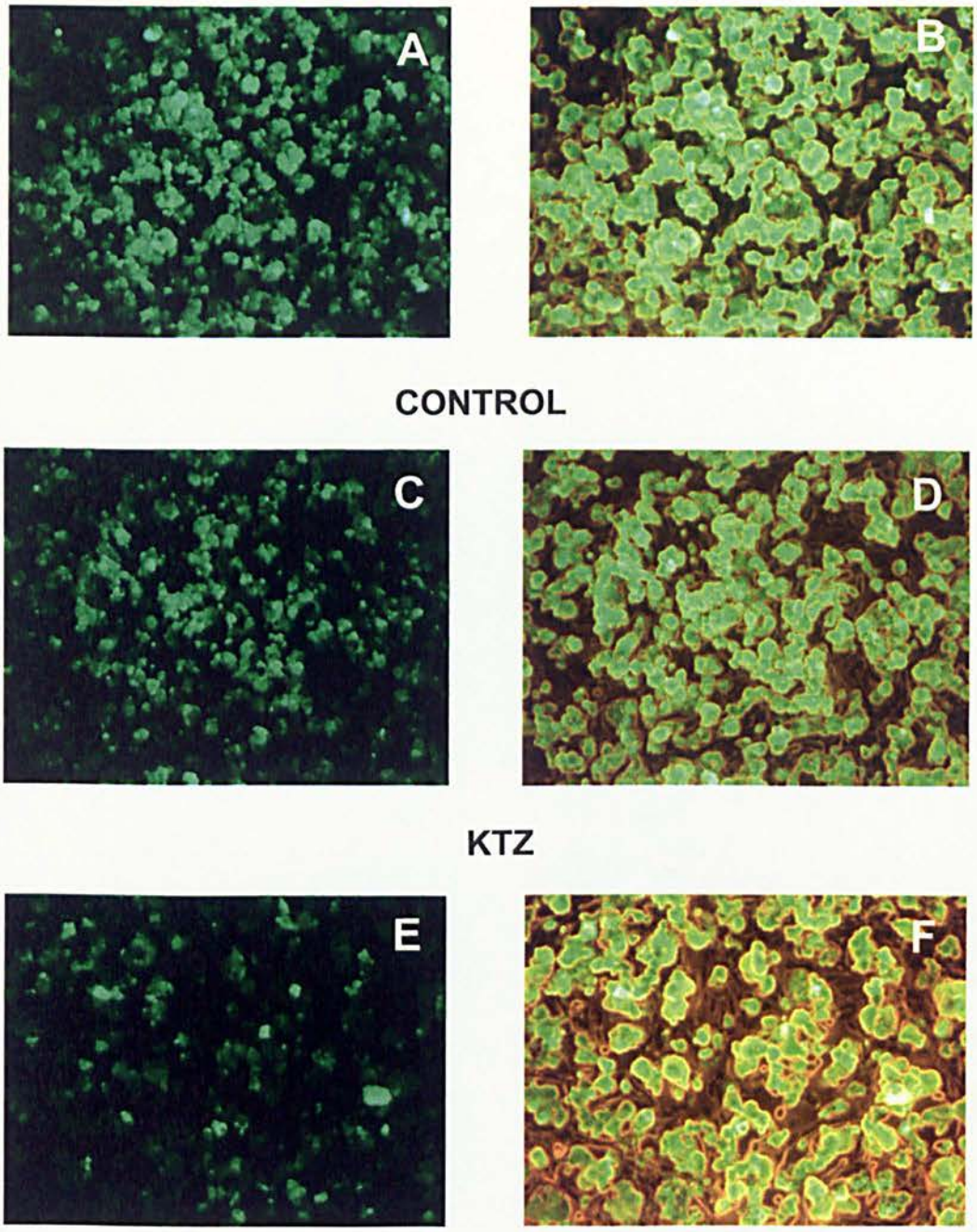

Figure 4.14: ***Fluorescence and phase-contrast microscopy of DU145 cells attached to TNF-α stimulated HUVEC monolayers.*** *DU145 cells were treated with CYP17 inhibitors for 24 hours. Fluorescently labelled Du145 cells (green) are attached to the HUVEC monolayer. (A-B) Untreated DU145 cells (C-D) DU145 cells treated with KTZ (E-F) DU145 cells treated with compound 38. Images were acquired using a fluorescent microscope at X100 magnification. The images are qualitatively representative of three different experiments (n=3).*

4.4.6. Effect of CYP17 inhibitors on PC3 cells adhesion to HUVEC monolayers

In the absence of TNF-α, adhesion of PC3 cells to HUVEC monolayers was significantly decreased by ketoconazole (KTZ) when compared to control (73.05 ± 9.74% and 100 ± 0.01%; mean ± SEM; respectively; $p<0.05$) (Figure 4.15A). However, the synthesised CYP17 inhibitors; 48 and 51, decreased the adhesion of PC3 cells when compared to control (65.79 ± 9.39% and 64.56 ± 5.04% and 100 ± 0.01%; mean ± SEM; in compounds 48, 51 and control respectively; $p<0.05$)

The adhesion of PC3 cells to HUVEC monolayers, pre-stimulated with TNF-α (10ng/mL), was not decreased by ketoconazole (Figure 4.15B). However compounds 48 and 51 significantly decreased the adhesion of PC3 cells when compared to control (74.26 ± 5.42% and 71.52 ± 4.45% and 100 ± 0.01%; mean ± SEM; in compounds 48, 51 and control respectively).

When compared the adhesion of PC3 cells to non-stimulated and stimulated HUVEC monolayers, was found to be not significantly different.

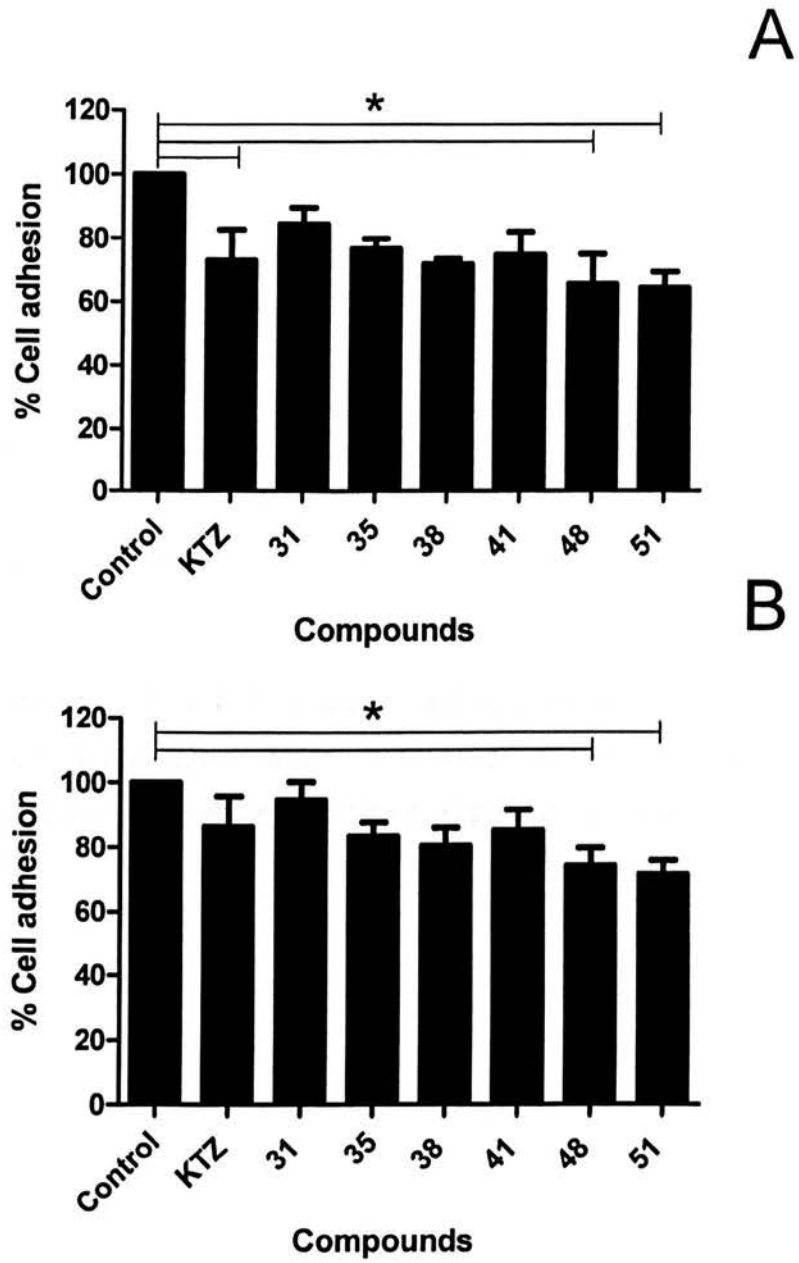

Figure 4.15: ***Effect of CYP17 inhibitors on PC3 cell adhesion to non-stimulated and TNF-α stimulated HUVEC monolayers.*** *The data is shown as mean ± SEM of three different experiments (n=3). (A) In the absence of TNF-α (B) In the presence of TNF-α. The statistical analysis was done using Tukey's modified student's t-test (two-tail) where *p<0.05 vs. Control. A two-way ANOVA was done where p>0.05.*

4.4.7. Fluorescence and phase-contrast microscopy of PC3 cells adhesion to HUVEC monolayers in the presence of CYP17 inhibitors

In PC3 cells, compound 48 was more potent in decreasing the adhesion of PC3 cells to HUVEC monolayers as described previously. Therefore representative figures of cell adhesion using compound 48 were used. See appendices 6 and 7 for compound 51.

In the absence of TNF-α, the adhesion of PC3 cells to HUVEC monolayers was decreased by ketoconazole when compared to control (Figure 4.16C). Compound 48 reduced the cell adhesion when compared to control and ketoconazole (Figure 4.16E).

In the presence of TNF-α, ketoconazole did not decrease the adhesion of PC3 cells to HUVEC monolayers when compared to control (Figure 4.17C). The adhesion of PC3 cells was decreased by compound 48 when compared to control (Figure 4.17E).

Adhesion of PC3 cells in the absence of TNF-α

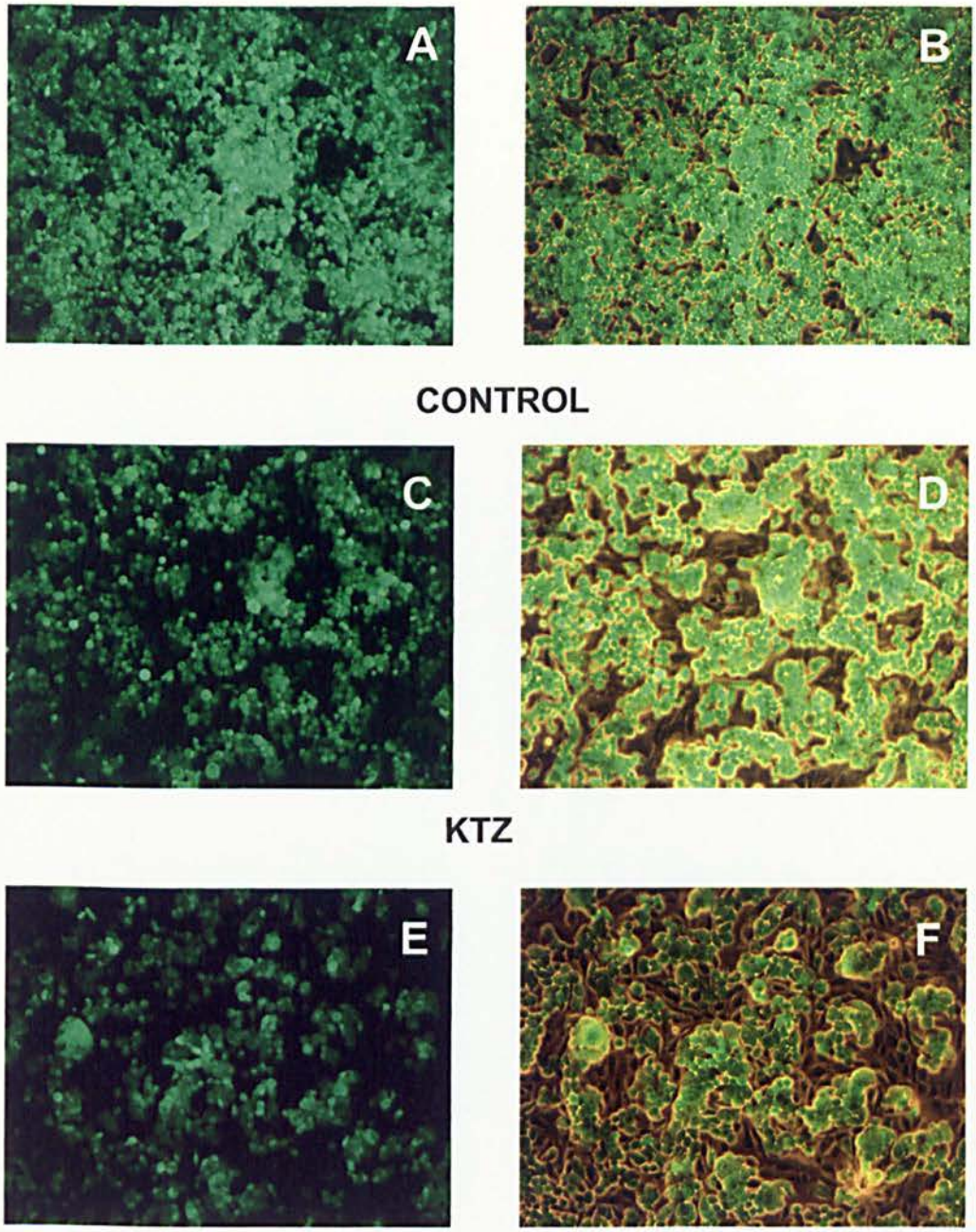

Figure 4.16: ***Fluorescence and phase-contrast microscopy of PC3 cells attached to non-stimulated HUVEC monolayers.*** *PC3 cells were treated with CYP17 inhibitors for 24 hours. Fluorescently labelled PC3 cells (green) are attached to the HUVEC monolayer. (A-B) Untreated PC3 cells (C-D) PC3 cells treated with KTZ (E-F) PC3 cells treated with compound 48. Images were acquired using a fluorescent microscope at X100 magnification. The images are qualitatively representative of three different experiments (n=3).*

Adhesion of PC3 cells in the presence of TNF-α (10ng/mL)

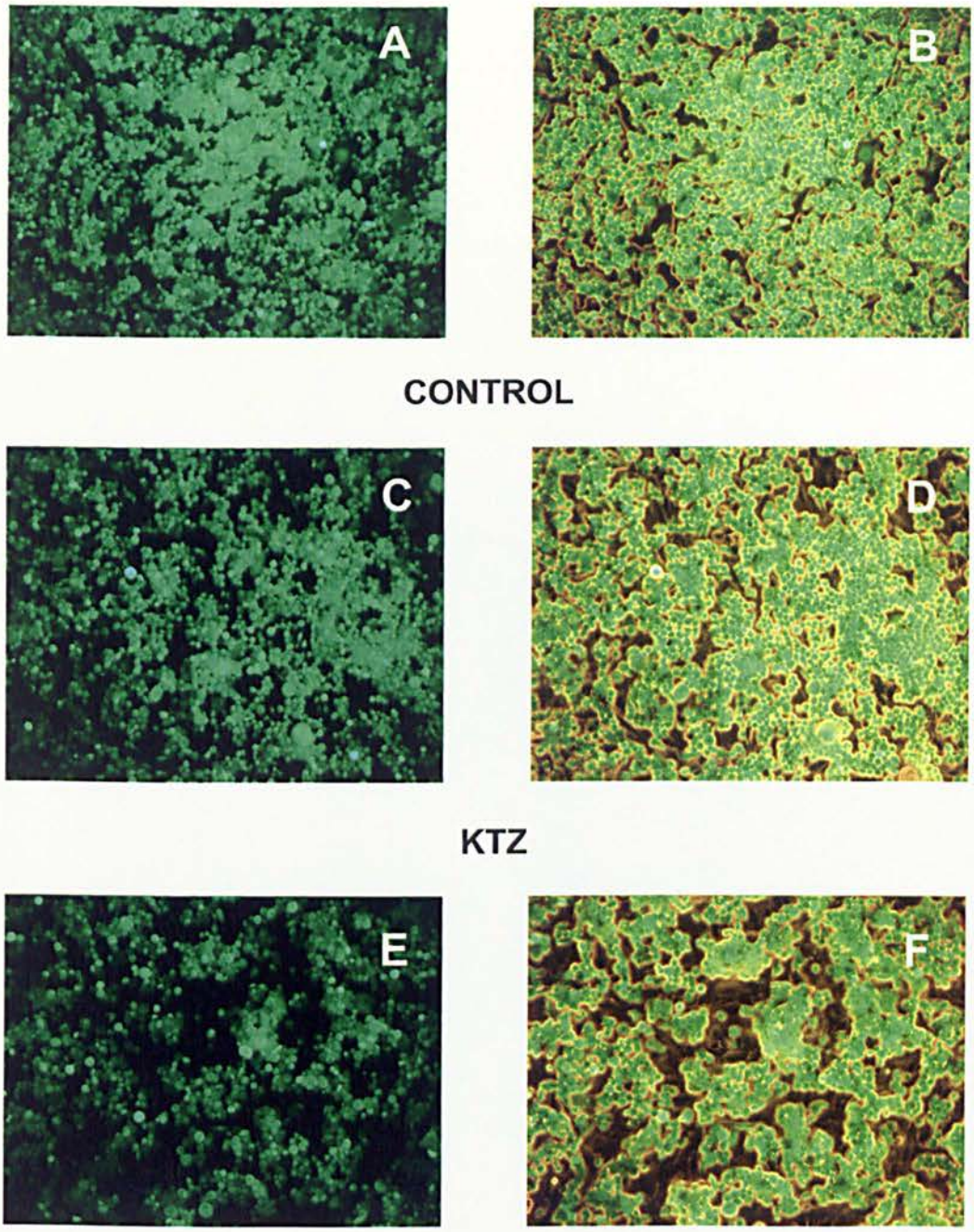

Figure 4.17: ***Fluorescence and phase-contrast microscopy of PC3 cells attached to TNF-α stimulated HUVEC monolayers.*** *PC3 cells were treated with CYP17 inhibitors for 24 hours. Fluorescently labelled PC3 cells (green) are attached to the HUVEC monolayer. (A-B) Untreated PC3 cells (C-D) PC3 cells treated with KTZ (E-F) PC3 cells treated with compound 48. Images were acquired using a fluorescent microscope at X100 magnification. The images are qualitatively representative of three different experiments (n=3).*

4.4.8. Effect of CYP17 inhibitors on MCF7 cells adhesion to HUVEC monolayers

In the absence of TNF-α, adhesion of MCF7 cells to HUVEC monolayers was significantly decreased by ketoconazole (KTZ) when compared to control (68.81 ± 5.15% and 100 ± 0.01%; mean ± SEM; respectively; $p<0.05$) (Figure 4.18A). Compounds 41, 48 and 51 significantly decreased the adhesion of MCF7 cells when compared to control and ketoconazole (74.83 ± 3.53%, 73.41 ± 2.79% and 65.12 ± 4.04%, 100 ± 0.01% and 68.81 ± 5.15%; mean ± SEM; compounds 41, 48, 51, control and ketoconazole respectively; $p<0.05$).

The adhesion of MCF7 cells on HUVEC monolayers, pre-treated with TNF-α (10ng/mL), was significantly decreased by ketoconazole when compared to control (72.29 ± 5.48% and 100 ± 0.01%; mean ± SEM; respectively; $p<0.05$) (Figure 4.18B). Similarly, compounds 48 and 51 significantly decreased the adhesion of MCF7 cells when compared to control (77.92 ± 3.31%, 68.98 ± 2.51% and 100 ± 0.01%; mean ± SEM; in compounds 48, 51 and control respectively; $p<0.05$)

When compared, the adhesion of MCF7 cells on un-stimulated and stimulated HUVEC monolayers, was not siginificantly different.

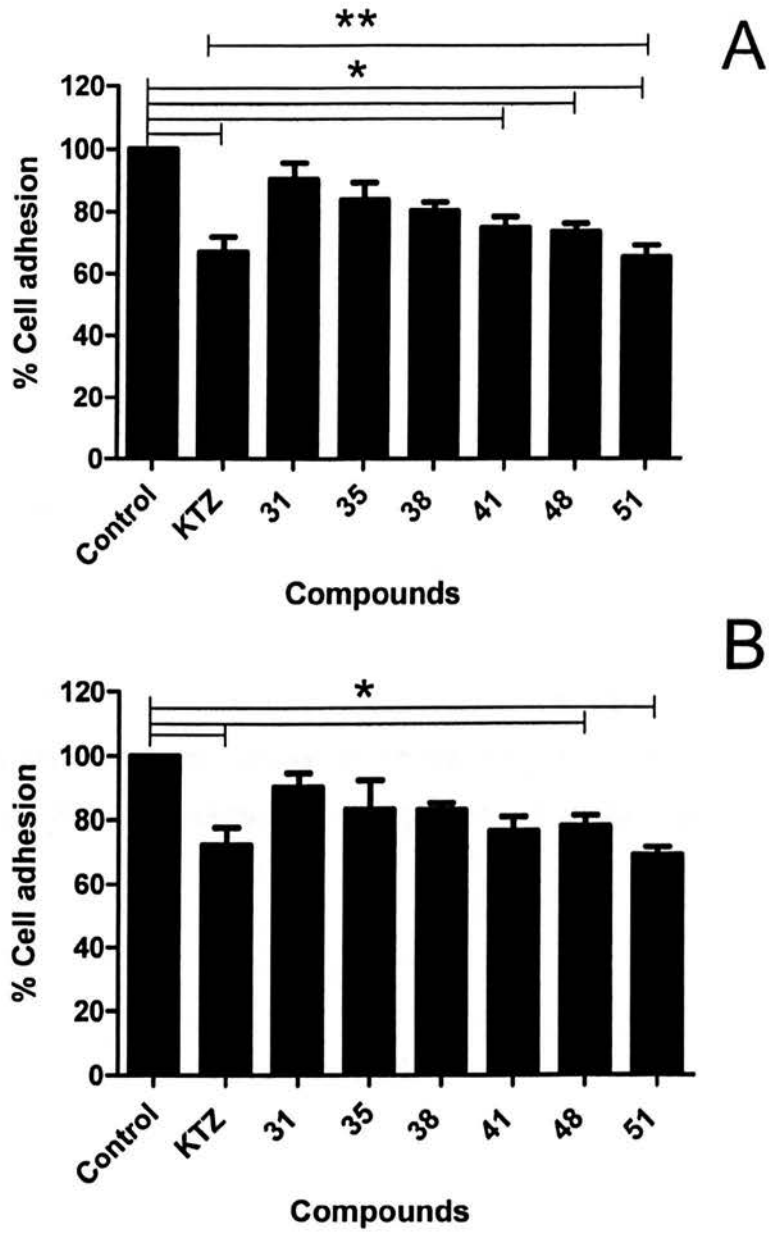

Figure 4.18: Effect of CYP17 inhibitors on MCF7 cell adhesion to non-stimulated and TNF-α stimulated HUVEC monolayers. *The data is shown as mean ± SEM of three different experiments (n=3). (A) In the absence of TNF-α (B) In the presence of TNF-α. The statistical analysis was done using Tukey's modified student's t-test (two-tail) where *p<0.05 vs. control and *p < 0.05 vs. KTZ. A two-way ANOVA was done where p>0.05.*

4.4.9. Fluorescence and phase-contrast microscopy of MCF7 cells adhesion to HUVEC monolayers in the presence of CYP17 inhibitors

In MCF7 cells, compound 48 was presumed to be more potent in decreasing the adhesion of MCF7 cells to HUVEC monolayers. Therefore representative figures of cell adhesion using compound 51 were used. See appendices 8 and 9 for compound 48.

In the absence of TNF-α, the adhesion of MCF7 cells to the HUVEC monolayer was decreased by ketoconazole when compared to control (Figure 4.19C). Compound 51 reduced the cell adhesion when compared to control and ketoconazole (Figure 4.19E).

In the presence of TNF-α, ketoconazole decreased the adhesion of MCF7 cells to HUVEC monolayers when compared to control (Figure 4.20C). The adhesion of MCF7 cells was also decreased by compound 51 when compared to control (Figure 4.20E).

Adhesion of MCF7 cells in the absence of TNF-α

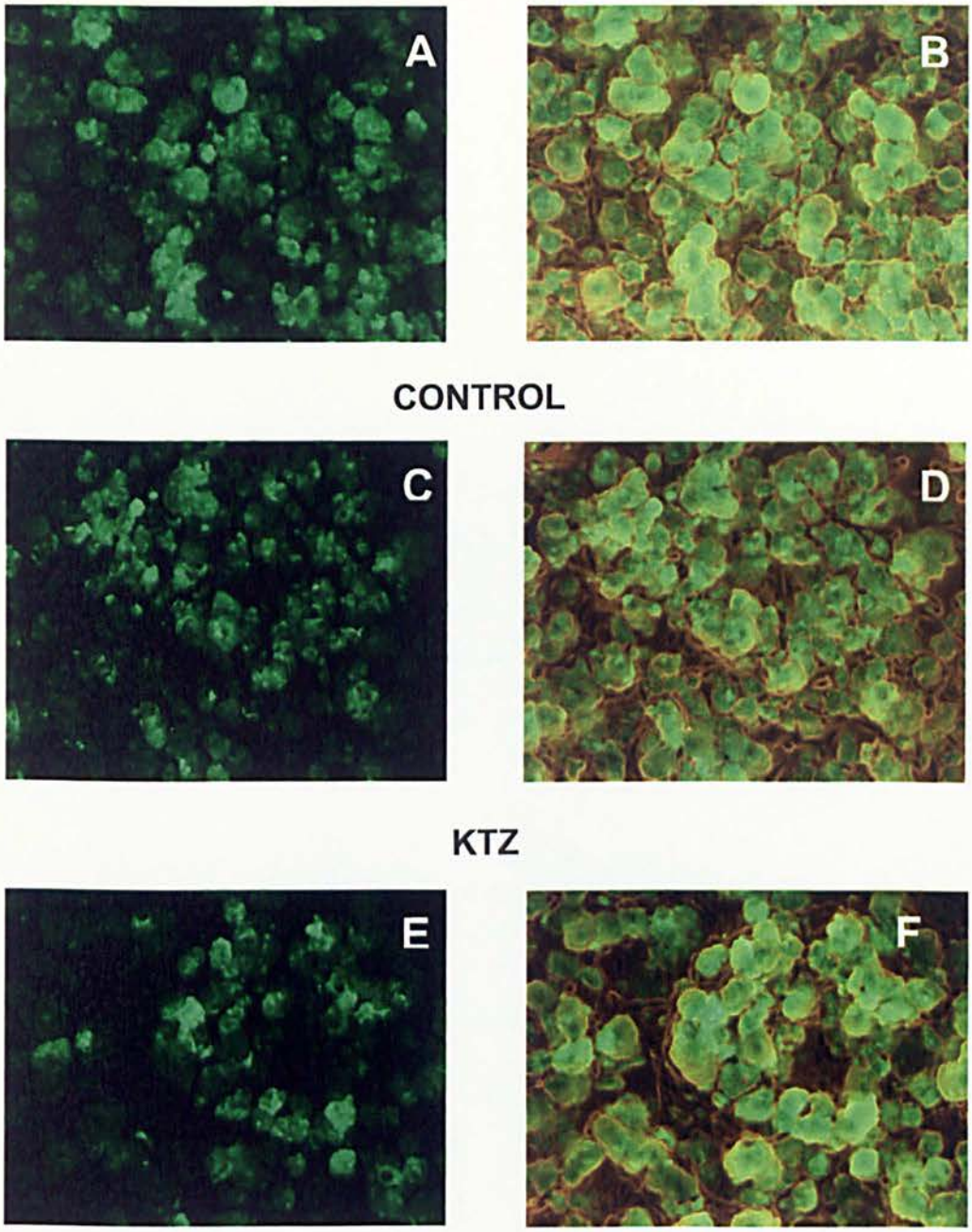

COMPOUND 51

Figure 4.19: ***Fluorescence and phase-contrast microscopy of MCF7 cells attached to non-stimulated HUVEC monolayers.*** *MCF7 cells were treated with CYP17 inhibitors for 24 hours. Fluorescently labelled MCF7 cells (green) are attached to the HUVEC monolayer. (A-B) Untreated MCF7 cells (C-D) MCF7 cells treated with KTZ (E-F) MCF7 cells treated with compound 51. Images were acquired using a fluorescent microscope at X100 magnification. The images are qualitatively representative of three different experiments (n=3).*

Adhesion of MCF7 cells in the presence of TNF-α (10ng/mL)

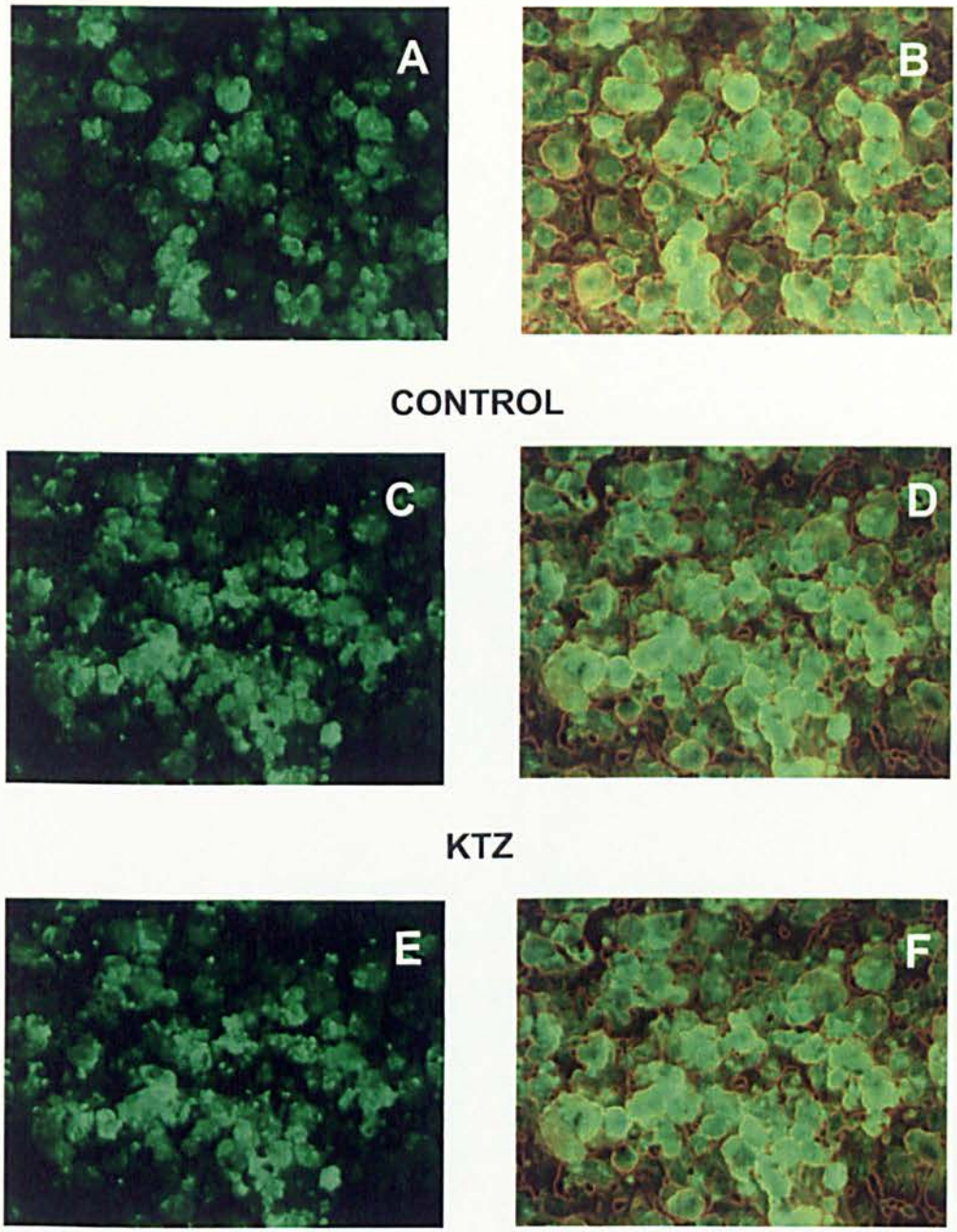

Figure 4.20: ***Fluorescence and phase-contrast microscopy of MCF7 cells attached to TNF-α stimulated HUVEC monolayers****. MCF7 cells were treated with CYP17 inhibitors for 24 hours. Fluorescently labelled MCF7 cells (green) are attached to the HUVEC monolayer. (A-B) Untreated MCF7 cells (C-D) MCF7 cells treated with KTZ (E-F) MCF7 cells treated with compound 51. Images were acquired using a fluorescent microscope at X100 magnification. The images are qualitatively representative of three different experiments (n=3).*

4.5. Discussion

4.5.1. Cytotoxicity of the compounds

The cytotoxic drugs which are normally used to eliminate cancer cells not only kill cancer cells but also healthy tissues and hence cause many side effects. There is therefore a need for safer anticancer therapies. (Ismael *et al.*, 2008).

The inhibitors of CYP17 used in the this study were tested for their cytotoxicity against normal and cancer cells prior to use in *ex vivo* model studies. Another main reason for checking the cytotoxicity of these compounds was to confirm if the loss of cell adhesion is purely due to the effect caused by the synthesised compounds and not because of unhealthy and dead cells. The cytotoxicity of all the compounds were checked at a concentration which gave near maximal response i.e. IC_{80} (Table 3.5) as these concentrations were further used in *ex vivo* models.

We have used two different kinds of prostate cancer cell lines: DU145 are derived from brain metastasis whereas PC3 cells are derived from bone metastasis. The results showed that these compounds did not have any cytotoxic effect on DU145 cells, however when tested on PC3 cells, compound 51 significantly decreased the percentage cell viability. The results can be compared to those of Moreira *et al.* (2007) and Moreira *et al.* (2008) who reported that inhibitors of CYP17 are cytotoxic on human prostate cancer cell lines. The compounds were also tested on breast cancer cells (MCF7) and human vascular endothelial cells (HUVECs). The data showed that none of these compounds have any cytotoxic effect on MCF7 cells or HUVECs.

In our study, Ketoconazole (KTZ) did not show any cytotoxicity or decrease in cell viability on any cell lines. However, KTZ has been reported to cause cytotoxicity of liver cells when used in high doses (800-1200 mg/dl) for the treatment of prostate cancer (Vasaitis *et al.*, 2011; Nussbaumer *et al.*, 2011). We can justify our results on the basis of the fact that the concentration of KTZ used in these experiments was far less than those used for prostate cancer treatment (Vasaitis *et al.*, 2011; Nussbaumer *et al.*, 2011). This also applies to other CYP17 inhibitors tested in our study. Therefore, all these compounds need to be tested at our conentrations to confirm their non-cytotoxicity.

4.5.2. Cell adhesion

4.5.2.1. Effect of TNF-alpha on tumour cell adhesion

Cytokines increase the expression of adhesion molecules in a wide variety of cell types (Hanlon *et al.*, 2002) and therefore enhance the adhesion of tumour cells. Tumour necrosis factor alpha (TNF-α) is among one of those cytokines and has been used to activate endothelial cells to evaluate adhesion interactions of leukocytes and tumour cells with endothelial cells (Yoon *et al.*, 2010; Haddad *et al.*, 2010; Paprocka *et al.*, 2008; Sasaki *et al.*, 2003; Sheski, *et al*, 1998).

The pre-treatment of HUVEC with TNF-α, enhanced the cell adhesion in a dose dependent manner (Kate *et al.*, 2004; Rainger and Nash, 2001; Ikuta *et al.*, 1991). We incubated the HUVECs with varying concentrations of TNF-α (0-1000 ng/mL) for 24 hours. Tumour cells were used at 40,000 and 80,000 cells per well in two different experiments. Following incubation, non-adherent cells were washed off and tumour cell fluorescence was measured as an index of cell adherence. The results show that maximal DU145 cell adhesion was achieved after pre-incubation with 10 ng/mL TNF-α. The pre-incubation with the higher concentrations of TNF-α did not enhance the adhesion any further. Similar results were found with another prostate cancer cell line, PC3, and breast cancer cell line MCF7.

The adhesion of tumour cells to HUVECs activated with TNF-α have shown comparable results as reported. Setty *et al.*, (2008) exposed the endothelial cell monolayers with TNF-α (10 ng/mL) for 6 hours whereas Kate *et al.* (2004) pre-incubated the endothelial cell monolayers with 0-100 ng/mL of TNF-α for one hour. Hu *et al.* (2011) stimulated the endothelial monolayers for 4 hrs with 10 ng/mL TNF-α. In the this study, we have found that a 24 hour treatment of 10 ng/mL of TNF-α increases the adhesive potential of the endothelium maximally as shown by others (Hu *et al.*, 2011; Setty *et al.*, 2008; Kate *et al.*, 2004).

The results showed that the adhesion of tumour cells is significantly increased by TNF-α with higher numbers of tumour cells added to the HUVEC monolayer. This suggests that the higher number of tumour cells is associated with an increased risk of tumour cell interaction with the endothelium and hence the extravasation of tumour cells to secondary sites.

4.5.2.2. Adhesion of tumour cells to non-stimulated and TNF-α stimulated HUVEC monolayers

To confirm the effect of activation of endothelial cells on tumour cell adhesion, we used two systems of endothelial cell monolayers. One of them was exposed to TNF-α (10 ng/mL) for 24 hrs while the other was left non-stimulated. After 24 hrs, five different, fluorescently labelled, tumour cell suspensions (10,000-160, 000 cells/ well) were added to both monolayers.

The results showed that initially there was no significant difference in adhesion of DU145, PC3 and MCF7 cells in the presence or absence of TNF-α. However when the numbers of tumour cells were increased above 40,000 cells per well, the cell adhesion was increased significantly. We can therefore, conclude that as the number of tumour cells increase, more tumour cells attached to activated HUVEC monolayers. This gives an indication that higher numbers of tumour cells in the circulation are an increased risk for cancer progression.

The results also showed that the total fluorescence of tumour cells was decreased after washing. The washing of non-adherent tumour cells can be compared to the tumour cells in the blood circulation subjected to haemodynamic forces. Therefore, not all of them adhered to the endothelium of blood vessels (Chotard-Ghodsina *et al.*, 2007). The adhesive properties of different tumour cells determine the different metastatic potential of any cancer. The tumour cells with high adhesive potential would still adhere under high pressure (Schluter *et al.,* 2006). We have seen in the present study that when tumour cells are added in higher numbers, the adhesion of tumour cells to non-stimulated and stimulated endothelium is comparatively higher. This suggests that during the growth of tumours, there are more chances of tumour cell interaction to the endothelium which might lead to metastasis.

4.5.2.3. Development of a novel method to determine the TC:EC ratio in a co-culture

Determination of tumour cell numbers bound to each endothelial cell is useful to compare the adhesive capacities of endothelial cell lines towards different adhering cancer cells (Paprocka *et al.*, 2008).

To determine the number of tumour cells bound to each HUVEC, a fluorescent activated cell sorting (FACS) technique has been used previously (Haddad *et al.*, 2010; Paprocka *et al.*, 2008). In the this study, we have developed a simple assay to quantify the tumour - endothelial cell (TC: EC) ratio. The technique used here is simpler and cheaper to perform than FACS analysis and gives a reliable method for quantifying tumour cell adhesion.

Monolayers of endothelial cells were grown after adding 20,000 HUVECs in each well of gelatin- coated 96-well plates. The plates were incubated for 24-48 hours until they formed a monolayer. Unterluggauer *et al.* (2007) have reported that HUVEC cells on a gelatine coated plate show a doubling time between 20-40 hours when grown from 0-5 days. We can therefore conclude that the number of HUVECs originally plated at 0 day would not remain the same after they had formed a monolayer. The cell density of a confluent monolayer of HUVECs was assumed to be 3.2×10^4 cells/well of a 96-well plate (Corning Life Sciences, UK) and this was used to calculate the TC: EC ratio in the this study.

Five co-culture models for each cell line were developed. Each model had a similar number of HUVECs but different number of tumour cells (i.e. 10,000-160,000) per well. The ratio of TCs: ECs used in each system was calculated as 0.5:1, 1:1, 2:1, 4:1 and 8:1. Following the incubation of two cell types for 2 hrs, the non-adherent cells were washed off. The ratio of the number of tumour cells adhered to each HUVEC was again calculated (Section 4.3.2.3).

Our results show that DU145 and PC3 have a significantly greater TC: EC ratio with TNF-α treated HUVECs as compared to non-treated endothelial cells. The DU145: EC ratio was found to be 2.93 for 80,000 cells/ well and 5.94 for 160,000 cells/ well (Table 4.1) as compared to the non-treated counterparts. Similarly, for PC3 cells these ratios were found to be 2.81 and 4.93 (Table 4.2) respectively as

compared to non-treated cells. However, for MCF7 cells the ratio was not significantly different in non-stimulated and TNF-α stimulated HUVECs (Figure 3.13).

We can report that washing reduces the ratio of DU145, PC3 and MCF7 added to HUVECs by approximately half. These results are comparable with those shown by Haddad *et al.* (2010) who have reported that after washing about 50% of the total added TCs remained adhered to the EC monolayer.

The ratio of tumour cells adhering per one endothelial cell (reported as R) was calculated in another study (Paprocka *et al.,* 2008). The monolayers of five endothelial cells of different origins were incubated with tumour cells for 20 mins. Their results show that approximately two colon carcinoma cells adhered to one intestinal endothelial cell, whereas in the case of the remaining four endothelial cell lines examined, the R did not exceed one colon carcinoma cell per one endothelial cell.

Haddad *et al.,* (2010) and Paprocka *et al.,* (2008) have used only a fixed number of tumour cells. In contrast, we have chosen five doubling dilutions of a tumour cell suspension and have got consistency throughout the results. Therefore, we can conclude that our findings are more reliable as compare to previous studies.

4.5.2.4. Effect of CYP17 inhibitors on tumour cell adhesion to HUVEC monolayers

The enzyme CYP17 is a cytochrome P450 enzyme that is also known as a mixed function oxidase or monooxygenase (Mason, 1957). It has been reported that TNF-α-induced endothelial cell adhesion molecule expression is cytochrome *P*450 monooxygenase dependent and inhibitors of CYP450 monooxygenases such as ketoconazole attenuate this expression (Sasaki *et al.,* 2003).

Several compounds have been designed to produce an anti-cell adhesion effect. The inhibitors of enzyme CYP17 have also been studied although not much work has been reported and not much data is available to date. One of the main works on the effect of CYP17 on cell adhesion was reported by Bild *et al.,* 2004. They hypothesized that as the products of several P450 enzymes contribute to the

progression of certain kinds of cancer, inhibitors of these enzymes e.g. CYP17 can have the potential to reduce cancer cell adhesion. According to their results, compounds BW40 and BW39 reduced MCF7 cell adhesion to 29% and 53%. Liarozole which is a known CYP17 inhibitor has been shown to significantly decrease the tumour cell adhesion. (Bild *et al.*, 2004).

Inhibitors of CYP17 are used for the treatment of hormone-dependent prostate cancer (Yap *et al.,* 2008). Previously, Bild *et al.* (2004) has tested these inhibitors to determine their effect on breast cancer cell adhesion only. Therefore, in the present study, the adhesion of prostate as well as breast cancer cells in the presence of CYP17 inhibitors was observed. Also, we have used both hormone-dependent, MCF7 breast cancer cell lines, and hormone-independent, DU145 and PC3 prostate cancer cell lines. The compounds exert a similar effect on both hormone-dependent and hormone-independent cancer cells.

On the basis of IC_{80} data, we selected several CYP17 inhibitors (section 4.3) and the reference drug KTZ to check their potency in reducing tumour cell adhesion. The data show that both in the presence and absence of TNF-α, compounds 38, 41, 48 and 51 significantly decreased the adhesion of DU145 cells to HUVEC monolayers as compared to control and KTZ. The compound 38, however, has shown the maximum reduction in cell adhesion. The phase contrast and fluorescence microscopy has shown that fluorescently labelled (green) DU145 cells are attached to a HUVEC monolayer. The fluorescence (as an index of adherence) was decreased when tumour cells were treated with synthesised inhibitors as compared to control and KTZ. Similarly, compounds 48 and 51 significantly decreased the PC3 and MCF7 cells adhesion to non-activated and activated endothelial cells monolayer. The images showed that the compounds have decreased the adhesion of PC3 cells and MCF7 cells as compared to control and KTZ.

The adhesion of all three tumour cell lines, pre-treated with ketoconazole and other drugs, on TNF-α stimulated HUVEC monolayers was similar to adhesion on non-stimulated monolayers. This can be because the addition of tumour cells causes inflammation of HUVEC monolayers and endothelial cells get activated in the absence of TNF-α. As a result, the adhesive potential of HUVEC monolayers

has been found to be increased as a result of inflammation (McDonald *et al.*, 2009).

4.6. Conclusion

In conclusion, a tumour-endothelial cell adhesion model was developed and the ratio of tumour cells to each HUVEC was determined. The interaction of tumour cells to the endothelium is proportional to the number of tumour cells added and are associated with an increased risk of cancer progression. We can also conclude that a 24 hour treatment with 10 ng/mL TNF-α increases the adhesive potential of the endothelium. However, the addition of tumour cells on HUVEC monolayers stimulates the HUVEC monolayers in the absence of any cytokine. The synthesised non-cytotoxic inhibitors of CYP17 compounds reduced the adhesion of prostate and breast cancer cells to activated and un-activated HUVEC monolayers. The anti-adhesion effect of the synthesised compounds was better than known CYP17 inhibitor, ketoconazole. We can also summarise that the CYP17 inhibitors exert similar effect on hormone-dependent and hormone-independent cancer cell lines.

CHAPTER 5: EXPRESSION OF ICAM-1 IN ENDOTHELIAL AND TUMOUR CELLS AND EFFECT OF CYP17 INHIBITORS ON ICAM-1 EXPRESSION ON TUMOUR CELL'S SURFACE.

Adhesion molecules are important in cell-cell interactions. Various adhesive molecules, including intracellular adhesion molecule-1 (ICAM-1), vascular cell adhesion molecule-1 (VCAM-1), and E-selectin are responsible for the endothelial adhesion of cancer cells (Park *et al.,* 2009; Hanlon *et al.,* 2002). Many cancer cells express similar adhesion molecules that are also expressed on the leukocytes therefore the interaction of tumour cells to endothelial cells is similar to that of leukocytes (Iiizumi *et al.*, 2007).

ICAM-1 was originally shown to mediate homotypic lymphocyte aggregation and mediate adhesion to endothelial cells (Giavazzi *et al.,* 1992). However, ICAM-1 is expressed on various types of cancer cells (Takizawa *et al.,* 1999). The expression of ICAM-1 has been reported to have an important role in potential metastasis (Francavilla *et al.,* 2009). It has been reported that blocking ICAM1 with a monoclonal antibody inhibits growth of melanoma in an *in-vivo* model (Wang *et al.,* 2006). It has been hypothesised that the mucin-1 (MUC-1) protein on the surface of the tumour cells binds to ICAM-1 on endothelial cells. This binding induces intracellular calcium signalling, resulting in different chemokines being released. These chemokines increase the expression of ICAM-1 on tumour cells themselves and also attract macrophages to the site of endothelial-tumour cell binding. These macrophages, after binding to tumour cells, release more chemokines that attract polymorphonuclear leukocytes (PMNs). This binding of PMNs to tumour cells activates PMNs and they release elastases which digest the endothelial membrane. This is followed by trans-endothelial migration of tumour cells which initiates metastasis to other organs. Different studies have shown that expression of ICAM-1 relates to the extent of disease (Roland *et al.,* 2007). The interaction between tumour and endothelial cells (TC-EC co-culture) up-regulates the expression of different adhesion molecules that include ICAM-1, VCAM-1 and E-selectin (Haddad *et al.,* 2010).

The inhibitors of CYP17 have also been reported to decrease the adhesion of tumour cells on endothelial cell monolayers (Bild *et al.,* 2004). Furthermore, the expression of ICAM-1 was also reported to be decreased by the inhibitors of cytochrome P450 enzymes, such as ketoconazole (Sasaki *et al.,* 2003). Therefore, in the this study, we have investigated if the novel compounds which have been synthesised to inhibit CYP17 enzymes affect ICAM-1 expression in three different tumour cells lines when co-cultured with endothelial cells.

5.1. Methods

A fluorescence activated cell sorting (FACS) technique was used to determine the ICAM-1 levels on HUVEC and tumour cell's surfaces. HUVECs and tumour cells were treated with TNF-α (10ng/mL) for 24 hours as described previously (Section 4.3.2). The un-treated and treated tumour cells were further treated with ketoconazole and other synthesised inhibitors of CYP17 for 24 hours. The fluorochrome-conjugated antibodies were titrated at different concentrations to determine the optimum concentrations of the antibodies used in the FACS experiments. Cells alone and in co-culture were then treated with PE-conjugated CD144 (VE-Cadherin) and PE-Cy5 conjugated CD54 (ICAM-1) antibodies for an hour.

The expression of ICAM-1 on the surface of tumour and endothelial cell surfaces was viewed by immuno-staining (immunofluorescence). The cells were fixed using paraformaldehyde. The FITC and TRITC-labelled anti- ICAM-1 antibodies were added to fixed cells for an hour. The nuclei of the cells were stained with DAPI in VECTA SHIELD.

5.2. Results

5.2.1. Titration of PE- conjugated CD144 (VE-Cadherin) antibody using flow cytometry

CD144 is an endothelial cell marker. PE-conjugated isotype control and CD144 antibody were titrated. Dilutions of 1:15, 1:50 and 1:100 were added to the HUVECs for an hour. The cell population was gated and 10,000 events were counted. The results were represented as a percentage of 10,000 gated events and are shown in appendix 10. By looking at the titration results, a concentration of 1:100 of isotype control and CD144 was used in the following FACS analysis.

5.2.2. Titration of PE-Cy5-conjugated CD54 (ICAM-1) antibody using flow cytometry

As for the CD144 antibody, PE-Cy5-conjugated isotype control and CD54 antibody were diluted in the ratio of 1:10, 1:50 and 1:100 and added to three different types of tumour cells for an hour. The antibody titrations for PC3 cells are shown in appendix 11. Similar results were obtained with DU145 and MCF7 cells. A concentration of 1:100 of isotype control and CD54 was used in the following FACS analysis.

5.2.3. Expression of ICAM-1 on HUVECs by flow cytometry

Human vascular endothelial cells (HUVECs) were stimulated by treating them with TNF-α (10 ng/mL) for 24 hours (Defazio *et al.,* 1998; Balwani *et al.,* 2011). The non-stimulated and TNF-α stimulated HUVEC cells were incubated with PE-Cy5-conjugated ICAM-1 (CD54) antibody (1:100) for one hour. 10,000 events were counted and the cells were gated (Figure 5.1A). The results (Figure 5.1) showed that TNF-α increased the expression of ICAM-1 and can be seen as a mean of three experiments in Figure 5.2.

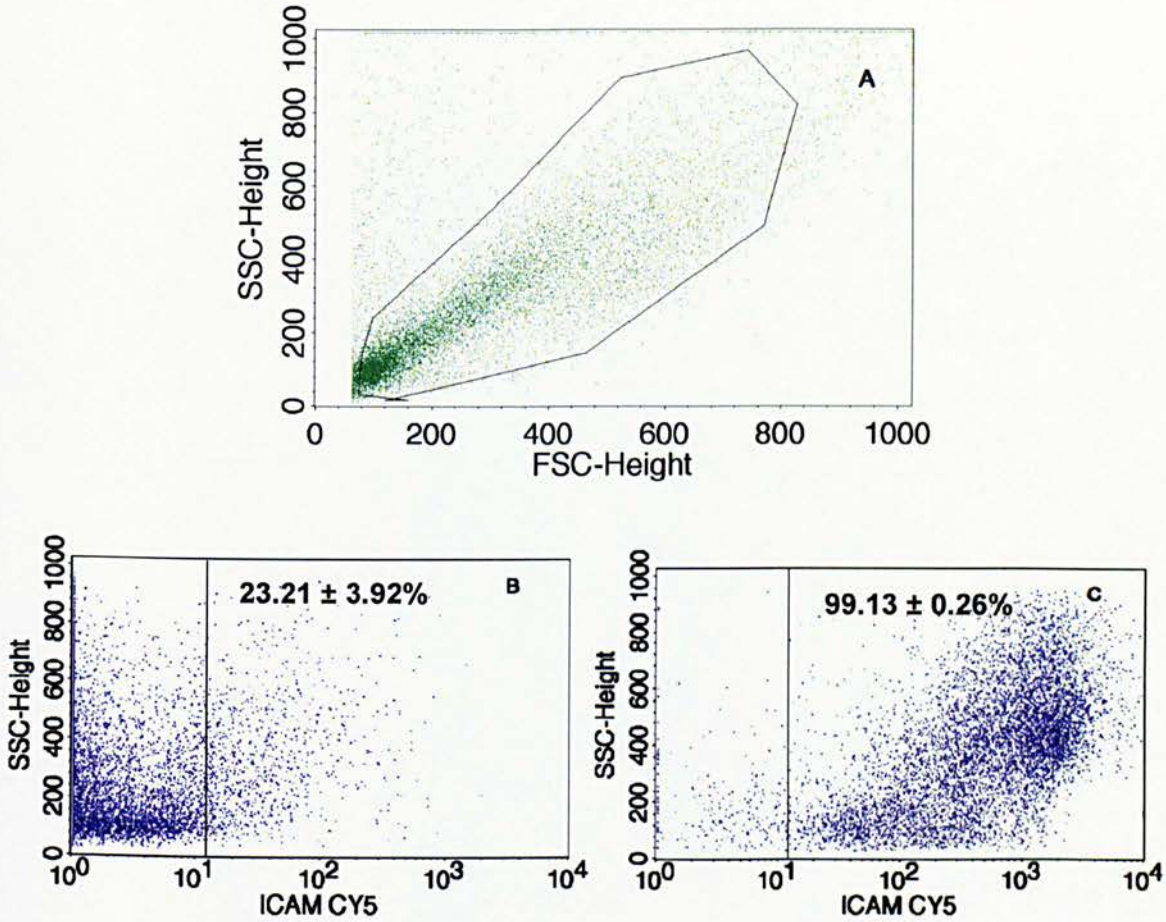

Figure 5.1: ***ICAM-1 (CD54) expression on HUVECs following incubation with TNF-α (10ng/mL) for 24 hours.*** *(A) Forward scatter (FSC) and side scatter (SSC) plot showing the gated cells. (B) ICAM-1 expression on non-stimulated HUVECs (C) ICAM-1 expression on TNF-α stimulated HUVEC. ICAM-1 expression a % of 10,000 gated events. The FACS plots are representative of three different experiments.*

When analysed using a paired student's t-test, TNF- α (10 ng/mL) significantly increased the expression of ICAM-1 (Figure 5.2) on HUVECs as compared to control cells which were treated with media only (99.13 ± 0.54% and 23.21 ± 0.01% mean ± SEM; respectively; $p<0.05$).

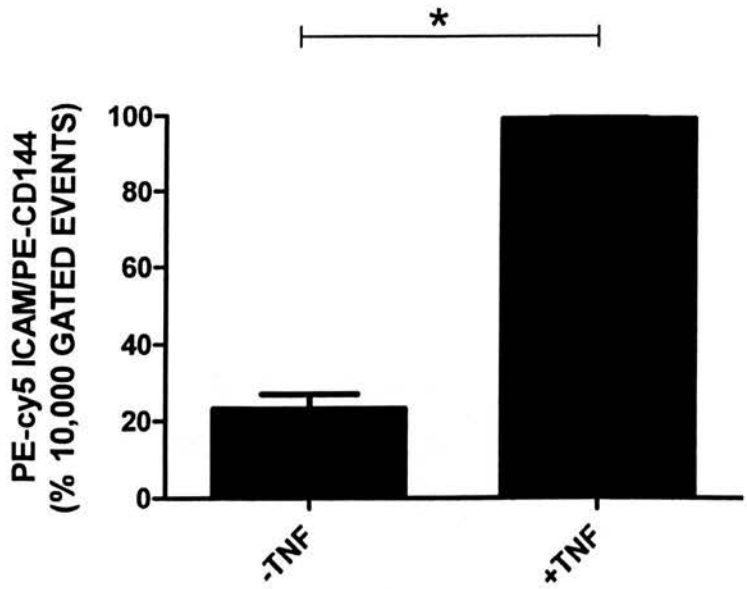

Figure 5.2: ***Histogram showing the effect of 24 hours incubation of TNF-α (10 ng/mL) on ICAM-1 expression in HUVECs.*** *ICAM-1 was determined as % of 10,000 gated events. The data is the mean of ten different experiments (n=10) where *p<0.05 using an unpaired Student's t-test.*

5.2.4. Expression of ICAM-1 on HUVECs by immunofluorescence

The increased expression of ICAM1 was confirmed using immunofluorescence. Cells were stimulated with TNF-α (10 ng/mL) for 24 hours to induce activation of ICAM-1. The cells were then incubated with FITC labelled secondary antibody and the nuclei were stained with DAPI. The images (Figure 5.3) showed that when stimulated with TNF-α, the FITC-labelled ICAM-1 expression increased (Figure 5.3D) when compared with un-treated cells (Figure 5.3B).

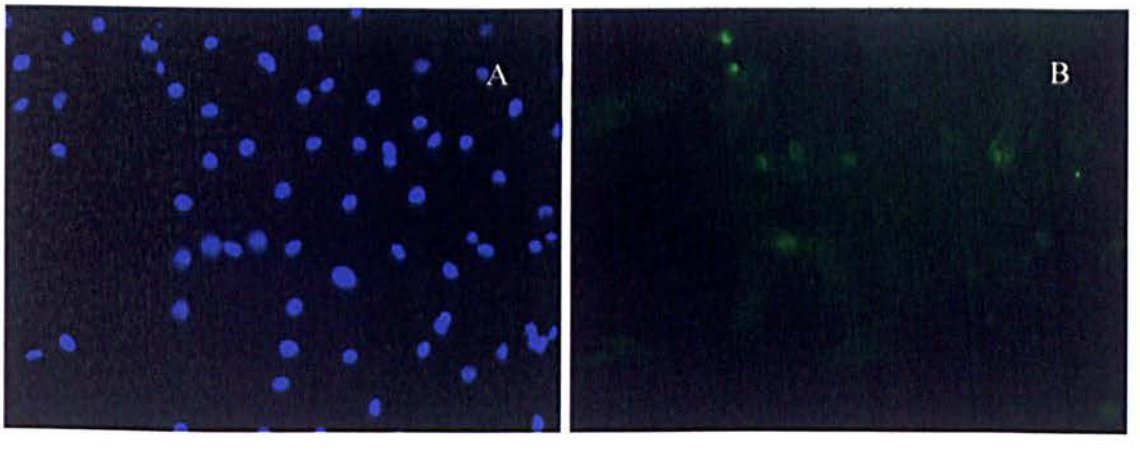

Untreated HUVECs (No TNF-α)

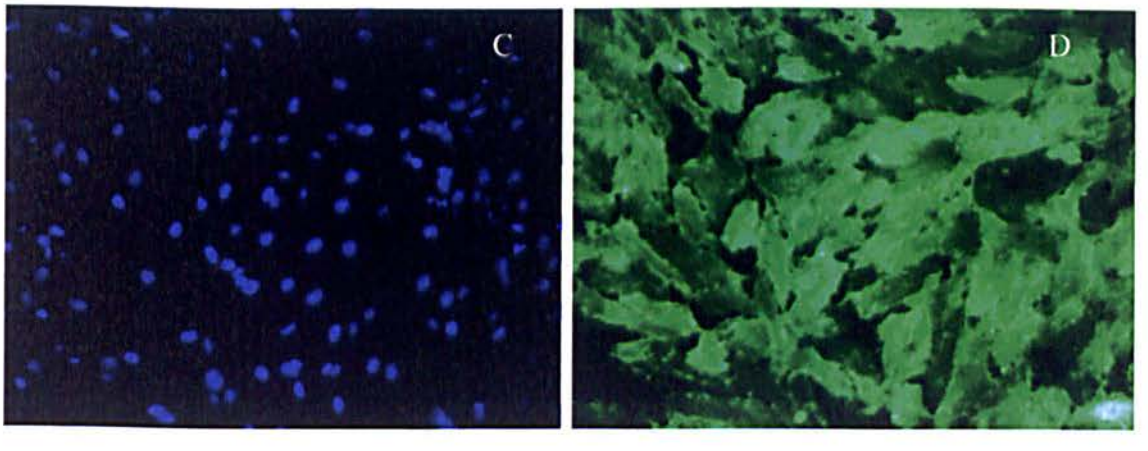

Activated HUVECs (TNF-α 10ng/mL)

Figure 5.3: ***Expression of ICAM1 by HUVECs.*** *(A) The nuclei of the non-stimulated HUVECs are stained with DAPI (B) ICAM-1 expression by non-stimulated HUVECs (C) DAPI-stained nuclei of HUVECs stimulated with 10 ng/mL of TNF-α for 24 hours. (D) ICAM-1 expression in stimulated HUVECs. Images were acquired using a fluorescent microscope at X100 magnification. The images are qualitatively representative of three different experiments (n=3).*

5.2.5. *Basal expression of ICAM-1 on tumour cells using flow cytometry*

Three tumour cell lines (DU145, PC3 and MCF7) were treated with both TNF-α (10 ng/mL) and media for 24 hrs. The non-stimulated (-TNF) and stimulated (+TNF) tumour cells were then treated with a series of synthesised CYP17 inhibitors for an additional 24 hours. Ketoconazole (KTZ) was used as a reference drug.

The six different treatments on tumour cells were as shown in the table below:

-TNF	+ TNF
Control	Control
+ KTZ	+ KTZ
+ compounds (+38/48/51)	+ compounds (+38/48/51)

Table 5.1: Different treatments on tumour cells

10, 000 events were gated. The percentage of gated events showed that the greatest basal levels of ICAM-1 expression was in DU145 cells and the least basal expression of ICAM-1 was in MCF7 cells (99.16 ± 0.61%; 76.62 ± 0.01% and 6.74 ± 0.69%; mean ± SEM; in DU145 cells, PC3 cells and MCF7 cells respectively) (Figures 5.4 - 5.6).

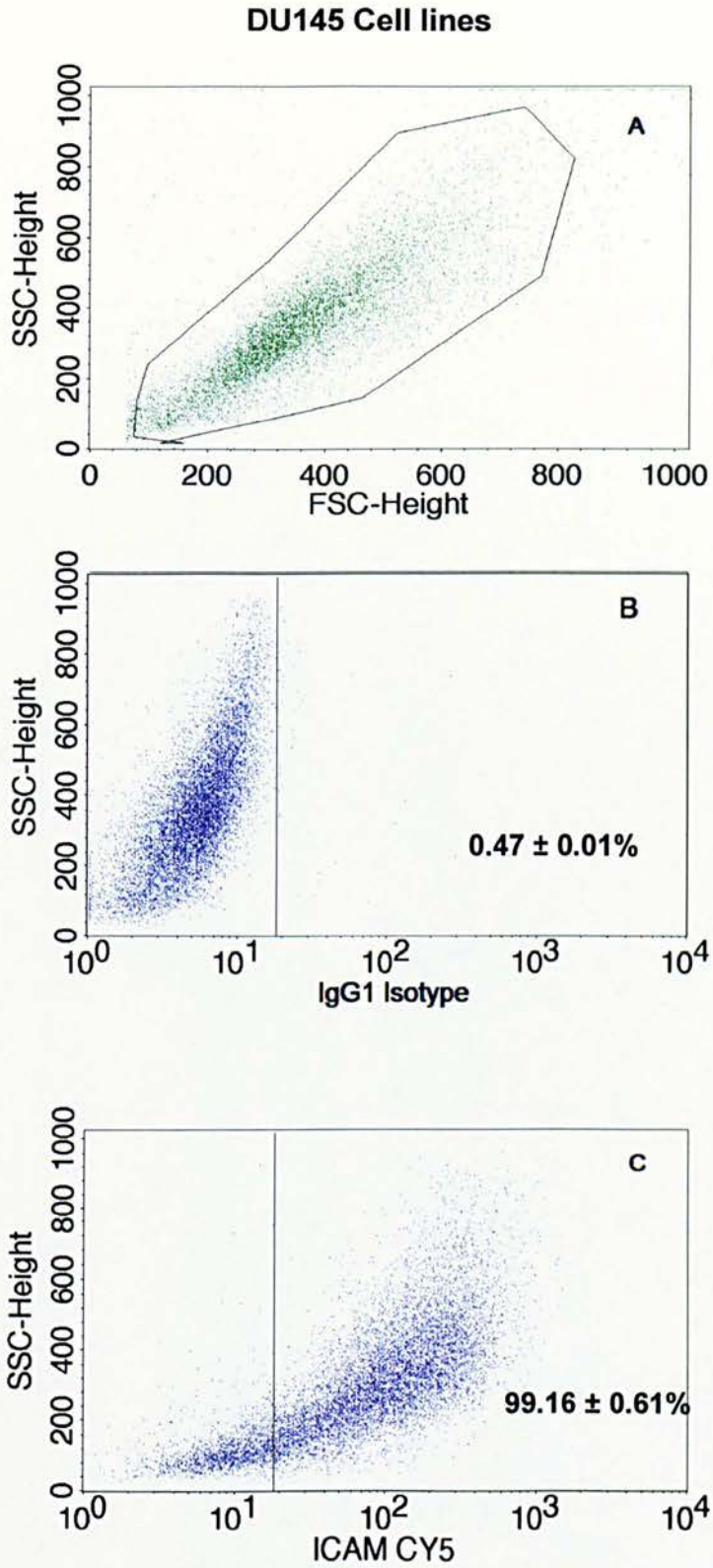

Figure 5.4: ***The expression of ICAM-1 on DU145 cells.*** *(A) FSC-SSC plot showing the gated cells. A total of 10,000 cells were gated (B) DU145 cells treated with Isotype control (1:100) (C) DU145 cells treated with PE-Cy5 conjugated ICAM-1 (1:100). A percentage of 10,000 gated events were shown. The FACS plots are representative of three different experiments.*

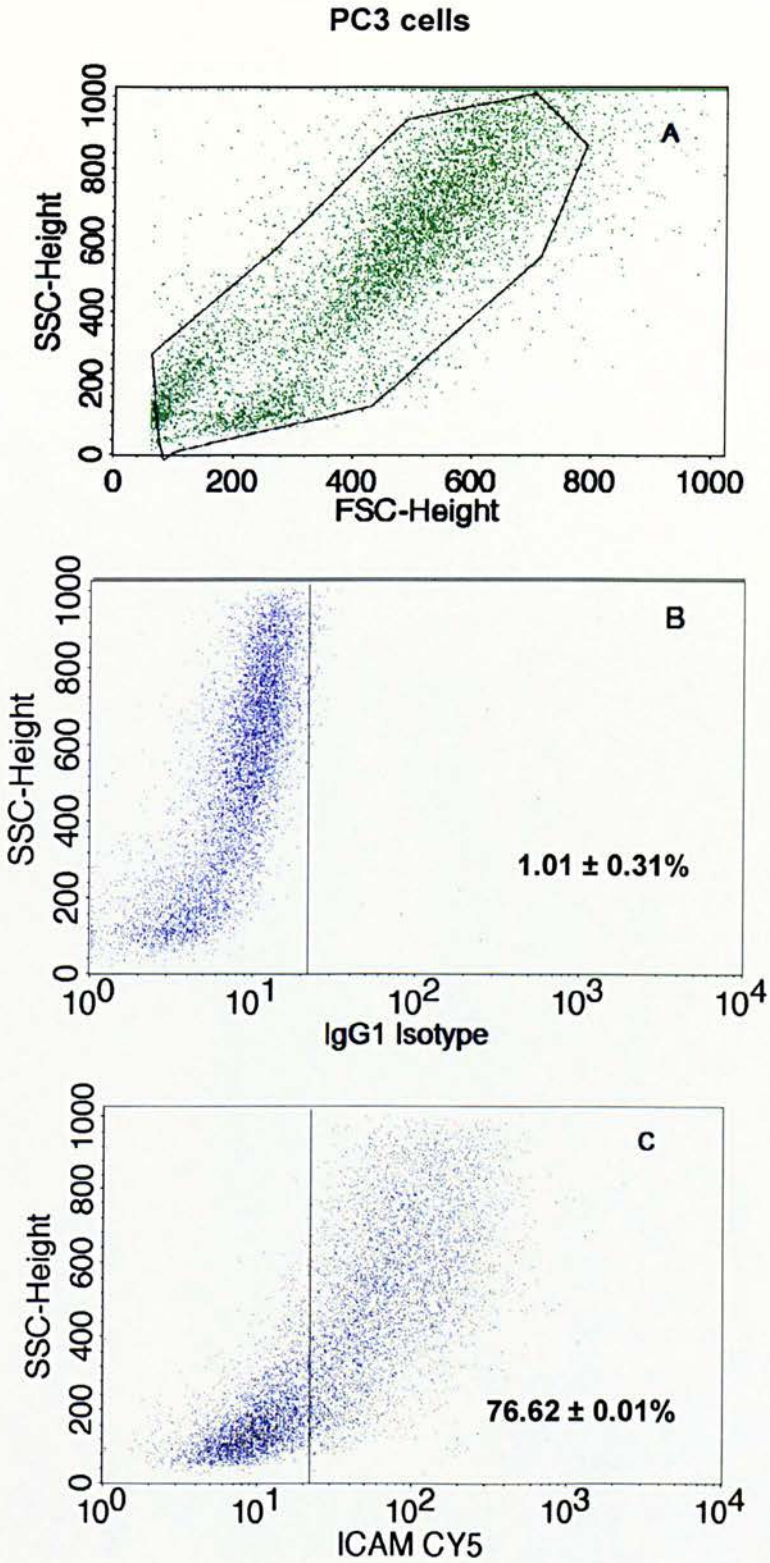

Figure 5.5: ***The expression of ICAM-1 on PC3 cells.*** *(A) FSC-SSC plot showing the gated cells. A total of 10,000 cells were gated (B) PC3 cells treated with Isotype control (1:100) (C) PC3 cells treated with PE-Cy5 conjugated ICAM-1 (1:100). A percentage of 10,000 gated events were shown. The FACS plots are representative of three different experiments.*

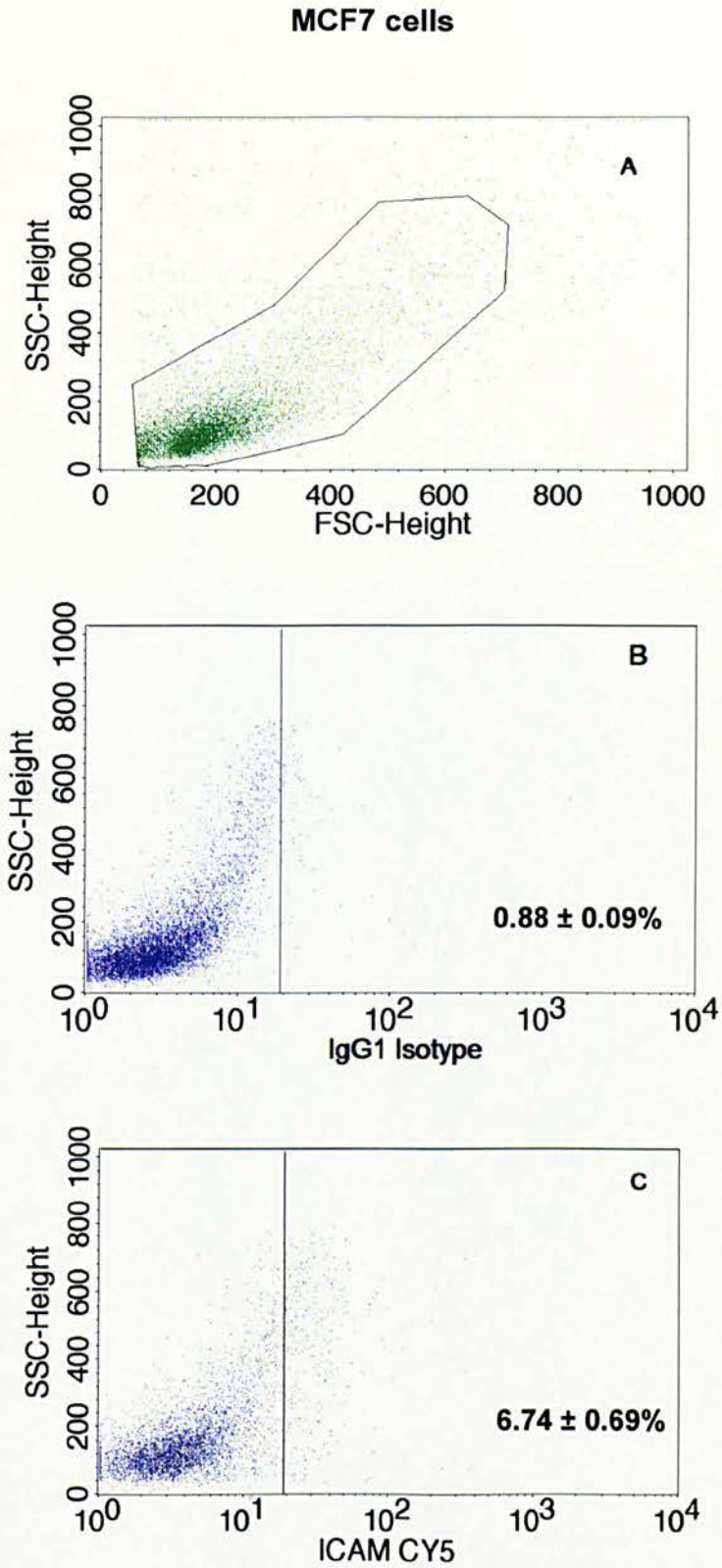

Figure 5.6: ***The expression of ICAM-1 on MCF7 cells.*** *(A) FSC-SSC plot showing the gated cells. A total of 10,000 cells were gated (B) MCF7 cells treated with Isotype control (1:100) (C) MCF7 cells treated with PE-Cy5 conjugated ICAM-1 (1:100). A percentage of 10,000 gated events were shown. The FACS plots are representative of three different experiments.*

5.2.6. Effect of CYP17 inhibitors on ICAM-1 expression using flow cytometry

Upon stimulation with TNF-α, no alteration in ICAM-1 expression was observed in DU145 cells with no drug. This was also observed with ketoconazole and other synthesised CYP17 inhibitor; compound 38 (Figure 5.7). Basal levels of ICAM-1 were at 99.16 ± 0.16%, therefore it was difficult to see any increase.

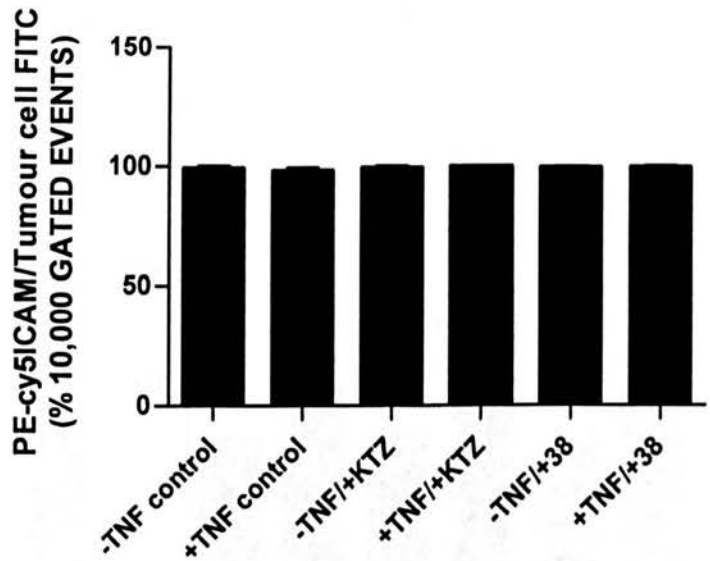

Figure 5.7: ***Histograms showing the expression of ICAM-1 as % of 10, 000 gated events in DU145 cells.*** *DU145 cells were treated with ketoconazole and compound 38 for 24 hours prior to incubation with PE-Cy5 ICAM-1 antibody for an hour. The statistical analysis was done using one way ANOVA and a post Tukey's modified t-test where p>0.05. The results are the mean of three experiments (n=3).*

In PC3 cells, TNF-α significantly increased the expression of ICAM-1 in un-treated (76.62 ± 0.01% and 98.34 ± 1.22%; mean ± SEM; ICAM-1 in the presence and absence of TNF-α respectively; $p<0.05$), ketoconazole-treated (78.02 ± 1.11% and 94.09 ± 4.55%; mean ± SEM; ICAM-1 in the presence and absence of TNF-α respectively; $p<0.05$) and compound 48-treated (79.05 ± 1.56% and 98.80 ± 0.71%; mean ± SEM; ICAM-1 in the presence and absence of TNF-α respectively; $p<0.05$) PC3 cells (Figure 5.8). Ketoconazole did not have any significant effect on ICAM-1 expression in non-stimulated PC3 cells and cells stimulated with TNF-α. Similarly, when non-stimulated and TNF-α stimulated PC3 cells were treated with compound 48, the ICAM-1 expression did not change significantly when compared to control.

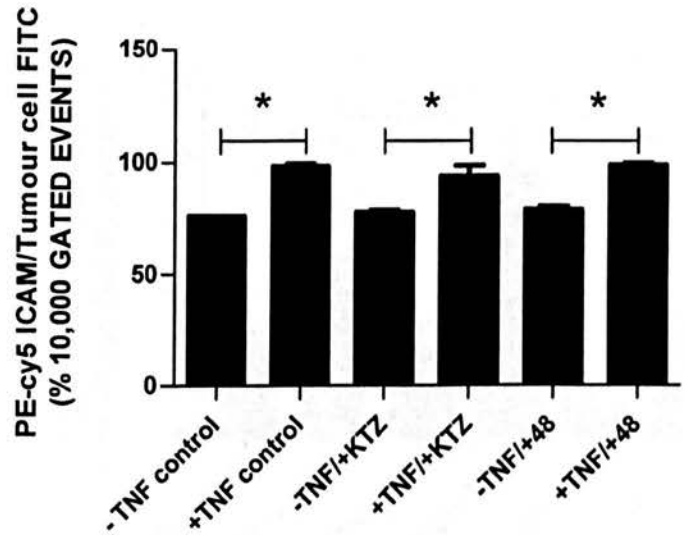

Figure 5.8: ***Histograms showing the expression of ICAM-1 as % of 10, 000 gated events in PC3 cells.*** *PC3 cells were treated with ketoconazole and compound 48 for 24 hours prior to incubation with PE-Cy5 ICAM-1 antibody for an hour. The statistical analysis was done using one way ANOVA and a post Tukey's modified t-test where *p<0.05 as compared to their activated counterparts. The results are the mean of three experiments (n=3).*

The expression of ICAM-1 level in MCF7 cells (Figure 5.9) was significantly increased by TNF-α when compared to non-stimulated and non-treated cells (6.74 ± 0.69%, 12.10 ± 0.68%; mean ± SEM; ICAM-1 in the presence and absence of TNF-α respectively; $p<0.05$), ketoconazole-treated (6.35 ± 1.79%, 18.94 ± 0.90%; mean ± SEM; ICAM-1 in the presence and absence of TNF-α respectively; $p<0.05$) and compound 51-treated (2.63 ± 0.44%, 7.69 ± 1.21%; mean ± SEM; ICAM-1 in the presence and absence of TNF-α respectively; $p<0.05$) MCF7 cells (Figure 5.9). Similar to DU145 and PC3 cells, ketoconazole did not change the expression of ICAM-1 in non-stimulated and TNF-α stimulated MCF7 cells when compared to control. However, compound 51 significantly decreased the ICAM-1 levels in non-stimulated MCF7 cells and cells which were pre-incubated with TNF-α.

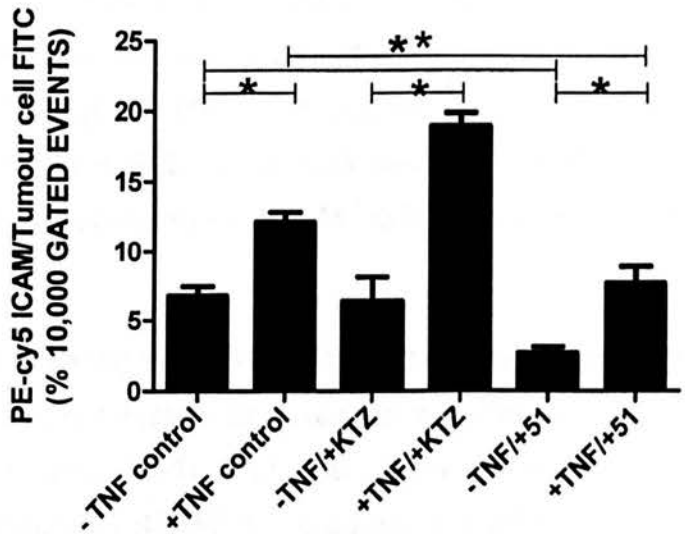

Figure 5.9: ***Histograms showing the expression of ICAM-1 as % of 10, 000 gated events in MCF7 cells.*** *MCF7 cells were treated with ketoconazole and compound 51 for 24 hours prior to incubation with PE-Cy5 ICAM-1 antibody for an hour. The statistical analysis was done using one way ANOVA and a post Tukey's modified t-test where *p<0.05 as compared to their activated counterparts and **p<0.05 as compared to control. The results are the mean of three experiments (n=3).*

5.2.7. *Immunostaining for ICAM1 expression on tumour cells surface*

The effect of CYP17 inhibitors on the expression of ICAM-1 was visualised by immunostaining of the tumour cells. The tumour cells were stimulated with TNF-α for 24 hours and then treated with CYP17 inhibitors for an additional 24 hours. The tumour cells were fluorescently stained for an hour with a TRITC-labelled anti-ICAM-1 antibody following treatments (Table 5.1). The nuclei of the cells were stained with DAPI in VECTA SHIELD. The ICAM-1 expression and the nuclei were viewed under different fluorescent wavelengths and the two images were overlayed (Figures 5.10- 5.12).

In DU145 cells, TNF-α did not cause any alteration in ICAM-1 fluorescence (Figure 5.10). Pre-incubation with TNF-α did not affect the expression of ICAM-1 in control DU145 cells, and cells treated with either ketoconazole or compound 38. Both in the presence and absence of TNF-α, ketoconazole and compound 38 did not change the expression of ICAM-1 in DU145 cells when compared to control. In summary, the ICAM-1 expression in DU145 cells did not change in response to any treatment.

In PC3 cells, prior incubation with TNF-α increased the expression of ICAM-1 in control PC3 cells and cells treated with ketoconazole and compound 48 compared to un-treated cells (Figure 5.11). However, when compared to control cells, ketoconazole and compound 48 did not produce any effect on the expression of ICAM-1 in PC3 cells, with or without prior incubation with TNFα, when compared to control cells.

Similar to PC3 cells, the basal levels of ICAM-1 expression in MCF7 cells increased upon addition of TNF-α in control MCF7 cells and cells treated with compound 51 (Figure 5.12). In MCF7 cells, when compared to control both non-stimulated cells and cells pre-treated with TNF-α, ketoconazole and compound 51 decreased the ICAM-1 expression as compared to control.

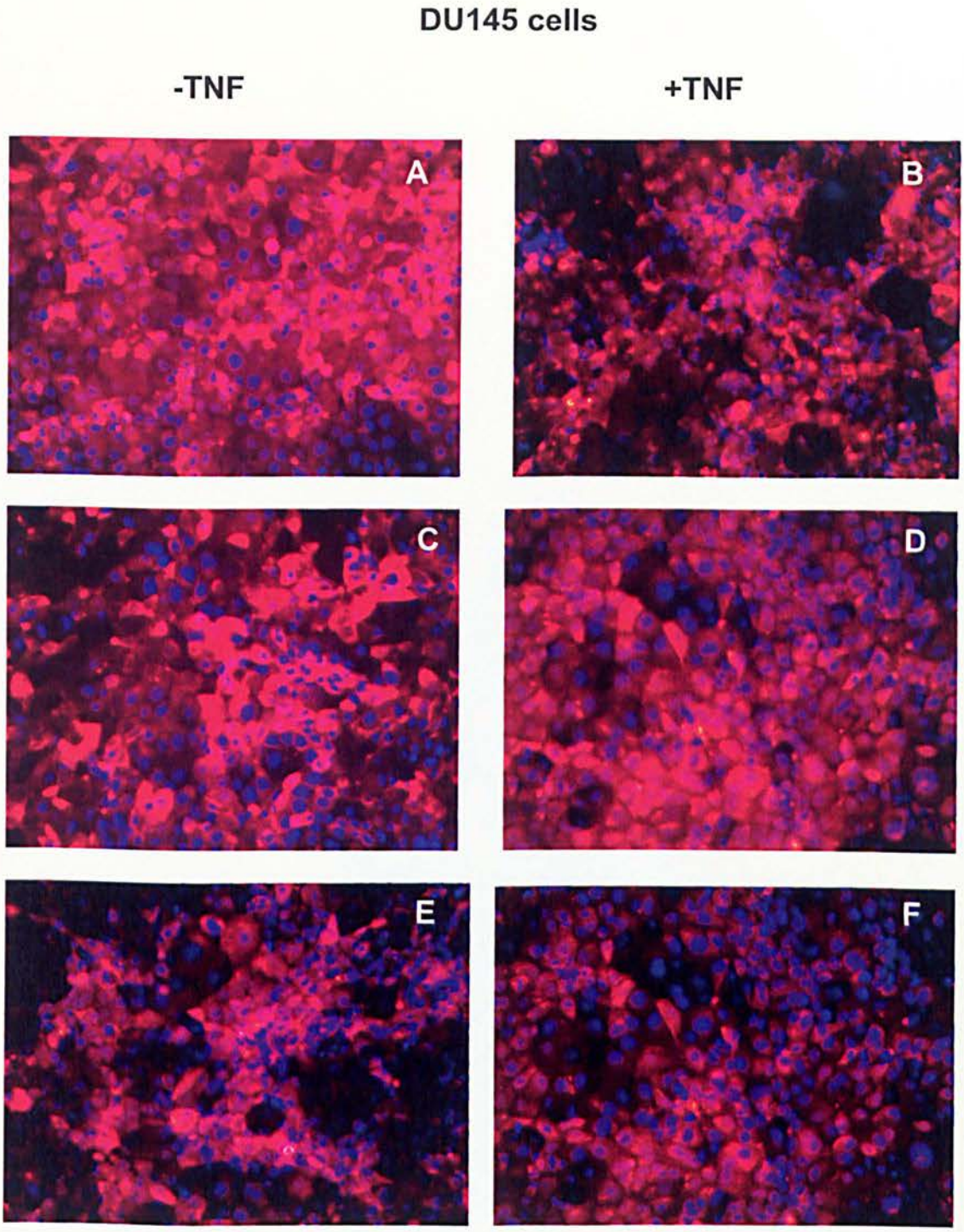

Figure 5.10: ***Immunofluorescence of non-stimulated (left) and stimulated (right) DU145 cells.*** *Cells were incubated with TRITC-labelled anti-ICAM1 antibody for an hour. (A) DU145 cells treated with media only (B) DU145 cells treated with 10ng/mL of TNF-α (C) DU145 cells treated with KTZ (D) DU145 cells treated with TNF-α and KTZ. (E) DU145 cells treated with compound 38 (F) DU145 cells treated with TNF-α and compound 38. The images showed the ICAM-1 expression (red) and the nuclei (blue). Images were acquired using a fluorescent microscope at X100 magnification. The images are qualitatively representative of three different experiments.*

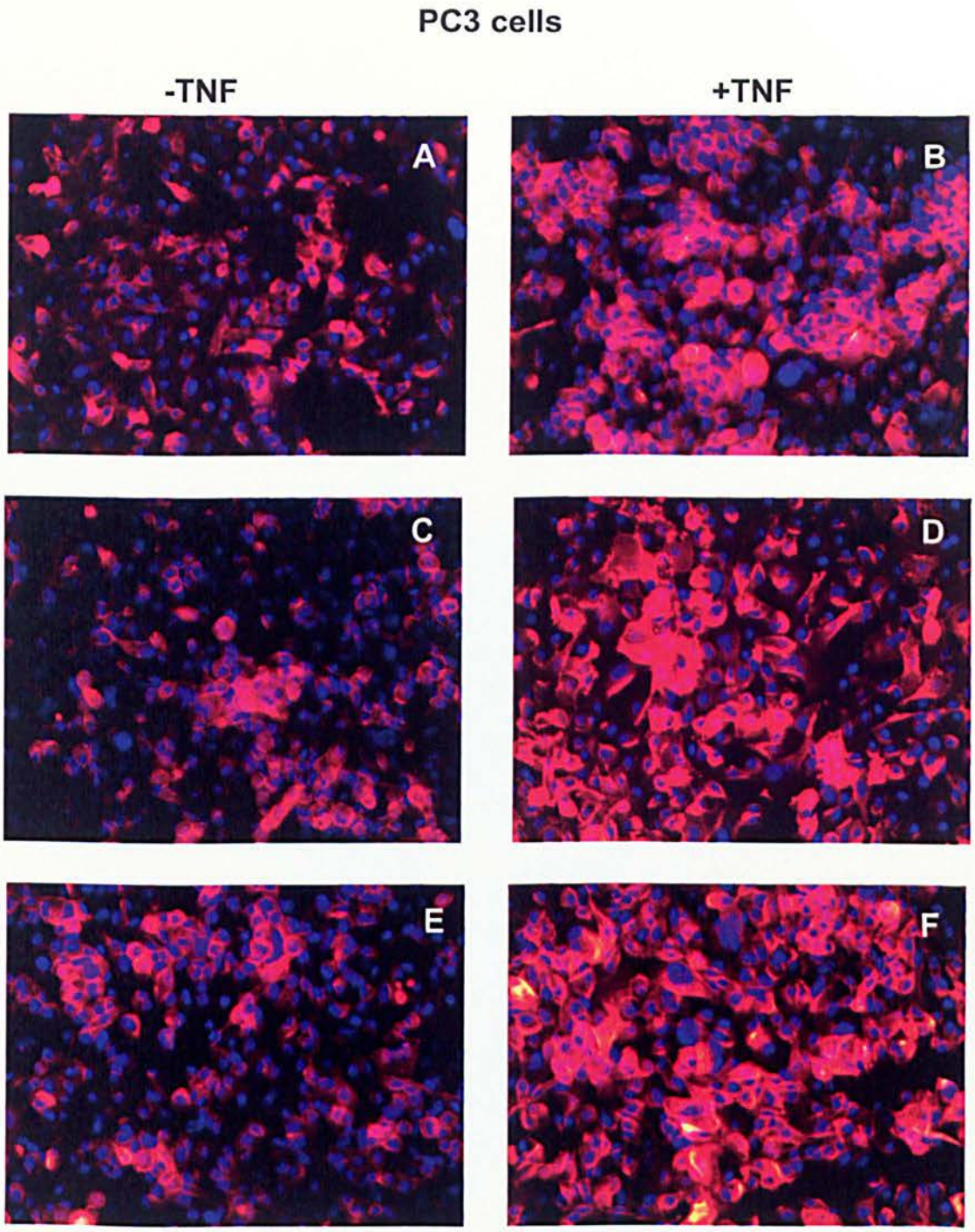

Figure 5.11: ***Immunofluorescence of non-stimulated (left) and stimulated (right) PC3 cells.*** *Cells were incubated with TRITC-labelled anti-ICAM1 antibody for an hour. (A) PC3 cells treated with media only (B) PC3 cells treated with 10ng/mL of TNF-α (C) PC3 cells treated with KTZ (D) PC3 cells treated with TNF-α and KTZ. (E) PC3 cells treated with compound 48 (F) PC3 cells treated with TNF-α and compound 48. The images showed the ICAM-1 expression (red) and the nuclei (blue). Images were acquired using a fluorescent microscope at X100 magnification. The images are qualitatively representative of three different experiments.*

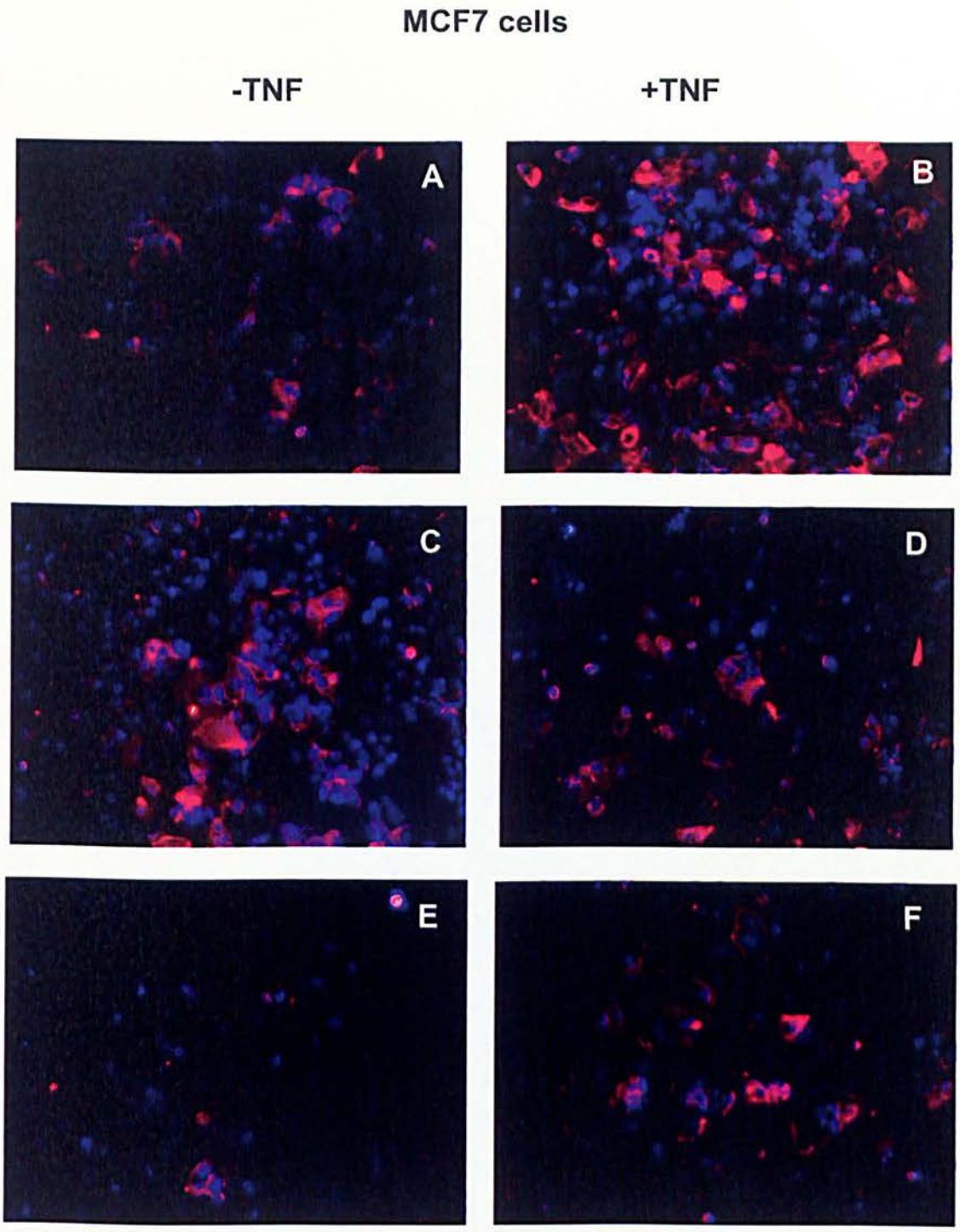

Figure 5.12: ***Immunofluorescence of non-stimulated (left) and stimulated (right) MCF7 cells.*** *Cells were incubated with TRITC-labelled anti-ICAM1 antibody for an hour. (A) MCF7 cells treated with media only (B) MCF7 cells treated with 10ng/mL of TNF-α (C) MCF7 cells treated with KTZ (D) MCF7 cells treated with TNF-α and KTZ. (E) MCF7 cells treated with compound 51 (F) MCF7 cells treated with TNF-α and compound 51. The images showed the ICAM-1 expression (red) and the nuclei (blue). Images were acquired using a fluorescent microscope at X100 magnification. The images are qualitatively representative of three different experiments.*

5.2.8. Gating strategy in a co-culture using flow cytometry

Having demonstrated that cells could be activated to different degrees by TNF-α, we were interested to see what would happen when the cells are cultured together. Upon acquisition of data using a flow cytometer, two different cell populations based on size (FSC) and granularity (SSC) plot appeared (Figure 5.13A). Two regions R1 and R2 were therefore selected on the plot for analysis. As the tumour cells were fluorescently labelled with cell tracker green (FITC), the two cell populations could be easily distinguished. The cells that fluoresced and therefore deduced to be tumour cells were back-gated on a FITC/SSC plot to determine their position in the FSC, SSC plot. The tumour cell FITC vs. SSC showed that all FITC positive tumour cells were contained within both gates in the sample (Figure 5.13B). The cells were gated. To determine if the size and granularity of the EC- TC complexes contributed to the two discrete populations, we then back-gated the cells co-stained with both CD144 PE + cell tracker FITC. We found once more that the complexes were equally distributed between R1 + R2.

Due to the nature of the FITC-labelled tumour cells showing two discrete populations of cells following culture the data for both R1 and R2 was acquired for all FACS analysis.

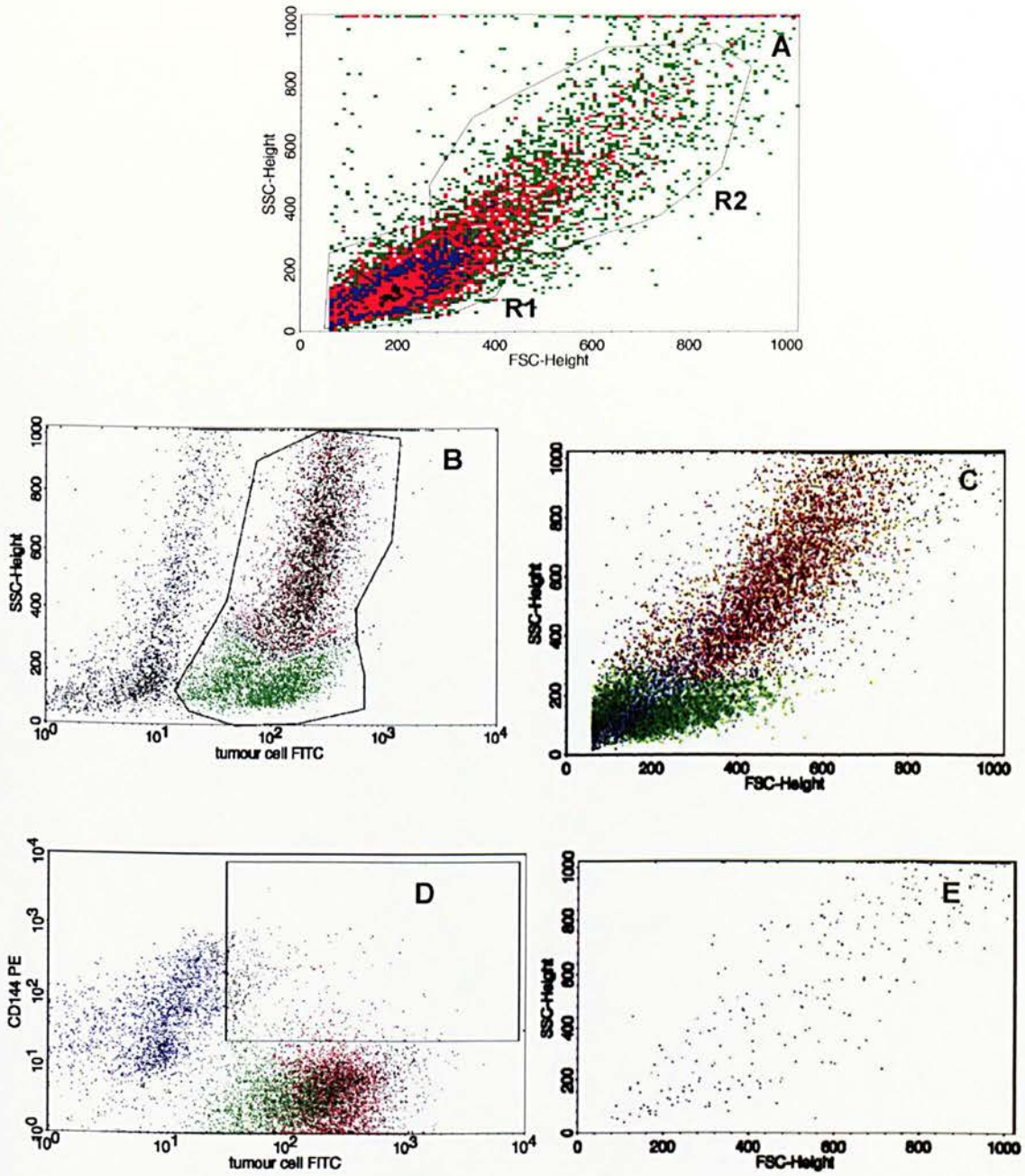

Figure 5.13: ***FACS plots for tumour and endothelial cells co-culture for two hours. A total of 10,000 events were counted.*** *(A)The FSC-SSC plot showing R1 and R2 regions. (B) FITC- positive tumour cells were gated. The FITC-negative cell population is shown in blue. (C) The FITC- positive tumour cells were back-gated in the FSC-SSC plot to show the localisation of tumour cells (red and green). (D) The FACS plot shows the cells co-stained; FITC positive tumour cells (red and green) and PE-conjugated CD144 labelled HUVECs. The cell population, positive for both FITC and PE were gated as tumour-HUVEC complexes. (E) The tumour- HUVEC complexes were shown in the FSC-SSC plot. The results were expressed as % of 10,000 gated events.*

5.2.9. Basal levels of ICAM-1 expression in co-culture using flow cytometry

To determine the effect of tumour cell-endothelial cell (TC: EC) interactions on ICAM1 expression, tumour cells were added to HUVEC monolayers for 2 hours. Cells were washed and a PE-Cy5 conjugated CD54 (ICAM-1) was added to the co-culture. Samples were then analysed by flow cytometry to determine the expression of ICAM-1. A total of 10,000 events were counted and results were reported as % of 10,000 gated events.

The FACS plots (Figure 5.14- 5.16) showed the expression of CD144 (VE-Cadherin) and CD54 (ICAM-1) on both endothelial (HUVECs) and tumour cell lines (DU145, PC3 and MCF7) during two hours of co-culture in the absence of any drug treatment or TNF-α stimulation. Following co-culture, both tumour and endothelial cells expressed ICAM-1 on their surfaces. The data for the expression of ICAM-1 was acquired for both R1 and R2 regions. The results for both regions, R1 and R2 were analysed and found to be equivalent. A t-test was carried out to determine the significant difference between results of R1 and R2 regions and no significant difference was found, therefore FACS plots for R1 were shown as representative data. Tumour cells were labelled with cell tracker green to distinguish them from the HUVECs. Cells labelled with PE- conjugated CD144 were considered to be HUVEC.

<u>DU145 cells</u>

In a DU145: HUVEC co-culture, 28.72 ± 0.01% of the total gated events were CD144-PE positive HUVECs whereas 65.12 ± 0.51% of the total gated events were FITC positive DU145 cells (Figure 5.14D). 5 ± 0.11% of events showed DU145: HUVECs complex (Figure 5.14D). Gating on the FITC positive DU145 cells, we found that 68.55± 1.01% expressed ICAM-1, compared to only 26.05 ± 2.01% of PE-positive CD144 HUVEC cells (Figure 5.14E).

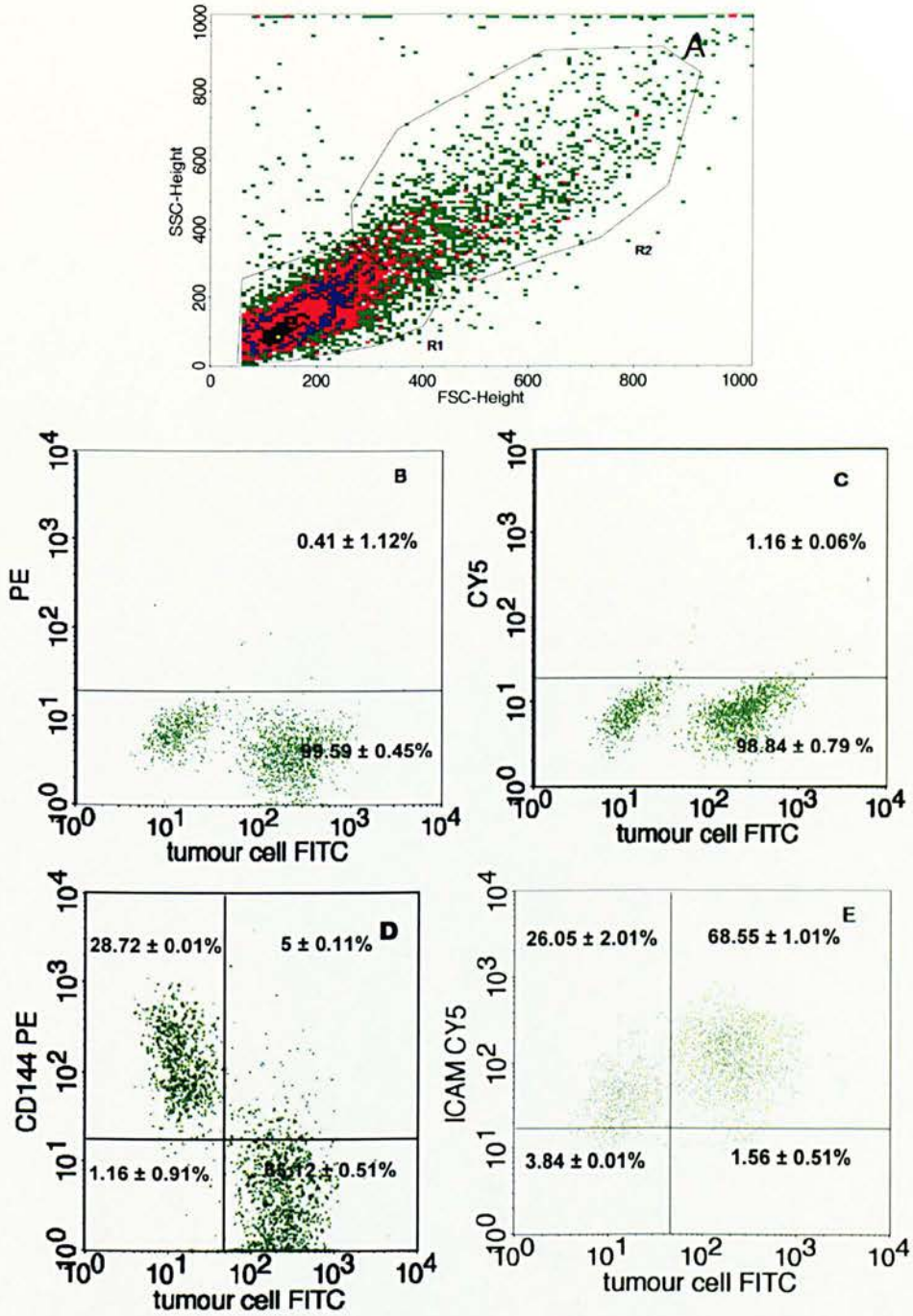

Figure 5.14: ***Flow cytometry of two hours co-culture of DU145 cells and HUVECs.*** *A total of 10,000 events were counted and results were expressed as % of gated events. (A) FSC and SSC plot showing R1 and R2 and the distribution of the cell populations according to cell size and cell shape. Analysis of R1 and R2 found results to be equivalent. All data are therefore represented as R1. (B) Isotype control for PE (C) Isotype control for PE-Cy5 (D) The HUVECs were stained with PE labelled CD144 (upper left of the quadrant) and FITC labelled DU145 cells (lower right of the quadrant). (E) Both HUVECs (upper left) and DU145 cells (upper right) expressed PEcy5 labelled ICAM1. The graphs are representative of three different experiments and shows the data in the absence of any drug or cytokine (TNF-α) treatments.*

PC3 cells:

In a PC3: HUVECs co-culture, 17.04 ± 3.14% of the total gated events were CD144-PE positive HUVECs whereas 79.86 ± 0.21% of the total gated events were FITC-positive PC3 cells (Figure 5.15D). 2.28 ± 1.91% of events showed a PC3: HUVECs complex (Figure 5.15D). Gating on the FITC positive PC3 cells, we found that 78.74 ± 2.01% expressed ICAM-1 compared to only 14.05 ± 0.11% of PE-positive CD144 cells (Figure 5.15E).

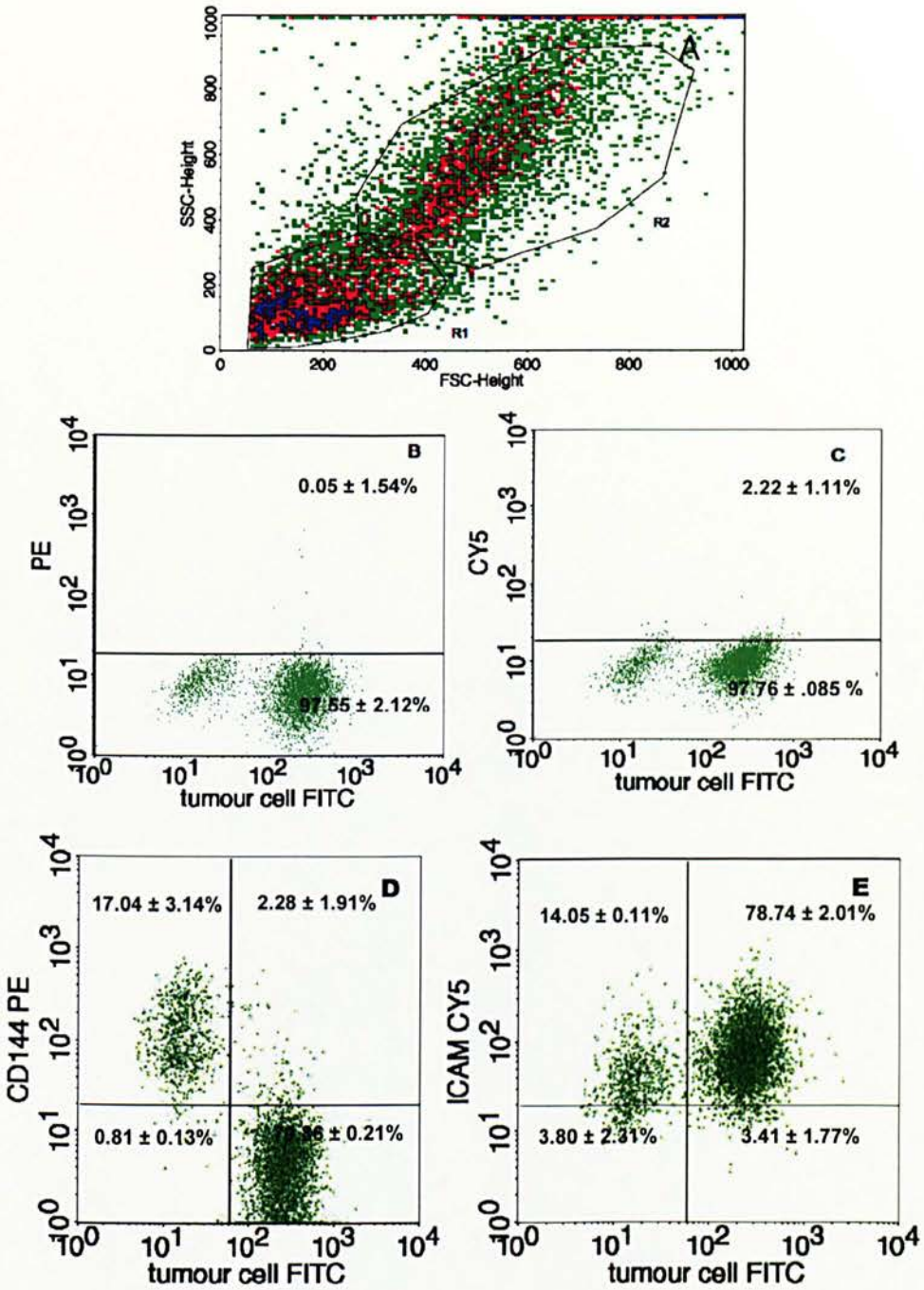

Figure 5.15: ***Flow cytometry of two hours co-culture of PC3 cells and HUVECs.*** *A total of 10,000 events were counted and results were expressed as % of gated events. (A) FSC and SSC plot showing R1 and R2 and the distribution of the cell populations according to cell size and cell shape. Analysis of R1 and R2 found results to be equivalent. All data are therefore represented as R1.(B) Isotype control for PE (C) Isotype control for PE-Cy5 (D) The HUVECs were stained with PE labelled CD144 (upper left of the quadrant) and FITC labelled PC3 cells (lower right of the quadrant). (E) Both HUVECs (upper left) and PC3 cells (upper right) expressed PEcy5 labelled ICAM1. The graphs are representative of three different experiments and shows the data in the absence of any drug or cytokine (TNF-α) treatments.*

MCF7 cells:

In a MCF7: HUVECs co-culture, 42.48 ± 3.11% of the total gated events were CD-144 PE positive HUVECs whereas 48.50 ± 0.01% of the total gated events were FITC-positive MCF7 cells (Figure 5.16D). 6.27 ± 1.16% of events showed MCF7: HUVECs complexes (Figure 5.16D). Gating on the FITC positive MCF7 cells, we found that 15.67 ± 2.11% expressed ICAM-1, compared to only 5.74 ± 0.12% of PE-positive CD144 cells (Figure 5.16E).

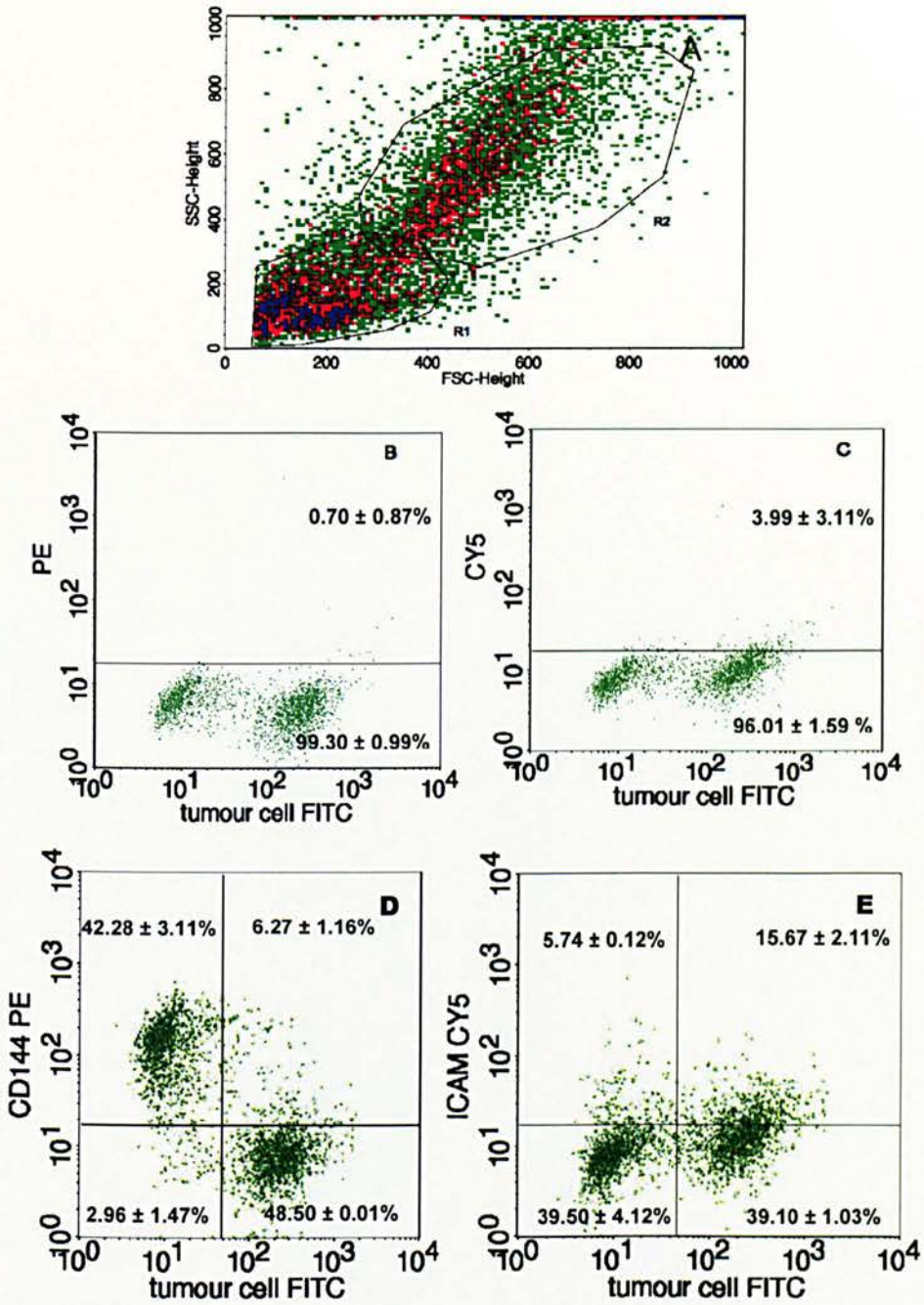

Figure 5.16: ***Flow cytometry of two hours co-culture of MCF7 cells and HUVECs.*** *A total of 10,000 events were counted and results were expressed as % of gated events. (A) FSC and SSC plot showing R1 and R2 and the distribution of the cell populations according to cell size and cell shape. Analysis of R1 and R2 found results to be equivalent. All data are therefore represented as R1.(B) Isotype control for PE (C) Isotype control for PE-Cy5 (D) The HUVECs were stained with PE labelled CD144 (upper left of the quadrant) and FITC labelled MCF7 cells (lower right of the quadrant). (E) Both HUVECs (upper left) and MCF7 cells (upper right) expressed PEcy5 labelled ICAM1. The graphs are representative of three different experiments and shows the data in the absence of any drug or cytokine (TNF-α) treatments.*

5.2.10. *Effect of CYP17 inhibitors on the expression of ICAM-1 in tumour cells compared with HUVECs in a co-culture using flow cytometry*

The HUVECs were stimulated with TNF-α (10ng/mL) for 24 hours whereas all three tumour cell lines; DU145, PC3 and MCF7 were treated with CYP17 inhibitors for 24 hours. HUVEC and tumour cells were then co-cultured for two hours. Following co-culture, PE-Cy5 conjugated ICAM-1 antibody was added for an hour. The FSC- SSC plot showed two discrete populations of cells following culture (Figure 5.13A). The data for both R1 and R2 was acquired and compared using a student's paired t-test (two-tail). No significant difference was found, therefore the results for R1 has been explained overleaf as representative data.

DU145 cells:

The basal expression of ICAM-1 in DU145 cells (Figure 5.17) was higher than non-stimulated and TNF-α stimulated HUVECs in the co-culture (72.40 ± 2.76%, 65.68 ± 3.04%, 23.27 ± 2.47% and 30.15 ± 3.95%; mean ± SEM; ICAM-1 in DU145 cells co-cultured with non-stimulated HUVECs, DU145 cells co-cultured with stimulated HUVECs, non-stimulated HUVECs and stimulated HUVECs respectively; $p<0.05$).When treated with ketoconazole, the increased expression of ICAM-1 was maintained in DU145 cells and was significantly higher as compared to HUVECs. The HUVECs stimulated with TNF-α also showed lower levels of ICAM-1 as compared to DU145 cells (74.11 ± 1.09%, 73.21± 1.13%, 20.33 ± 2.93% and 22.10 ± 3.21 %; mean ± SEM; ICAM-1 in DU145 cells co-cultured with non-stimulated HUVECs, DU145 cells co-cultured with stimulated HUVECs, non-stimulated HUVECs and stimulated HUVECs respectively; $p<0.05$).When treated with compound 38, similar results were observed as with ketoconazole (83.90 ± 2.12%, 74.59 ± 2.56%, 13.77 ± 1.30% and 23.19 ± 2.90%; mean ± SEM; ICAM-1 in DU145 cells co-cultured with non-stimulated HUVECs, DU145 cells co-cultured with stimulated HUVECs, non-stimulated HUVECs and stimulated HUVECs respectively; $p<0.05$). These effects were the same in both regions (R1 and R2) gated. The ICAM-1 expression in non- stimulated and stimulated HUVECs was not significantly different.

HUVECs vs. DU145 CELLS

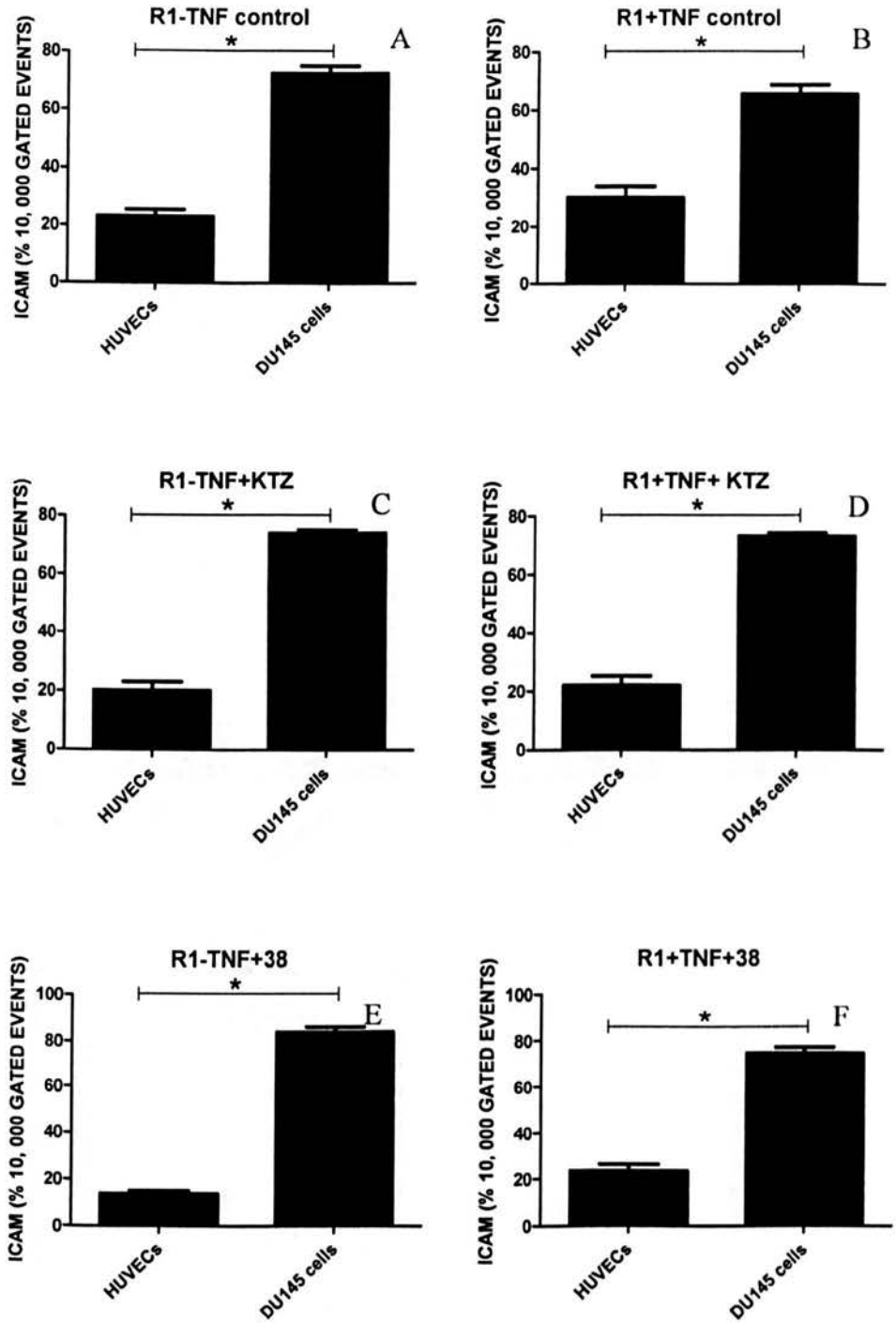

Figure 5.17: The expression of ICAM1 in HUVECs and DU145 cells (co-cultured for two hours) in R1. *ICAM-1 expression was the % of 10,000 gated events. (A) Cells were co-cultured in media only (B) HUVECs were treated with TNF-α before co-culture with DU145 cells (C) Non-treated HUVECs co-cultured with DU145 cells pre-treated with KTZ (D) HUVECs treated with TNF-α were co-cultured with DU145 cells pre-treated with KTZ (E) Non-treated HUVECs co-cultured with DU145 cells pre-treated with compound 38 (D) HUVECs treated with TNF-α were co-cultured with DU145 cells pre-treated with compound 38. The data is the mean of three different experiments (n = 3). Statistical analysis was done using un-paired student's t test (two-tailed) where *p<0.001 as compared to HUVECs.*

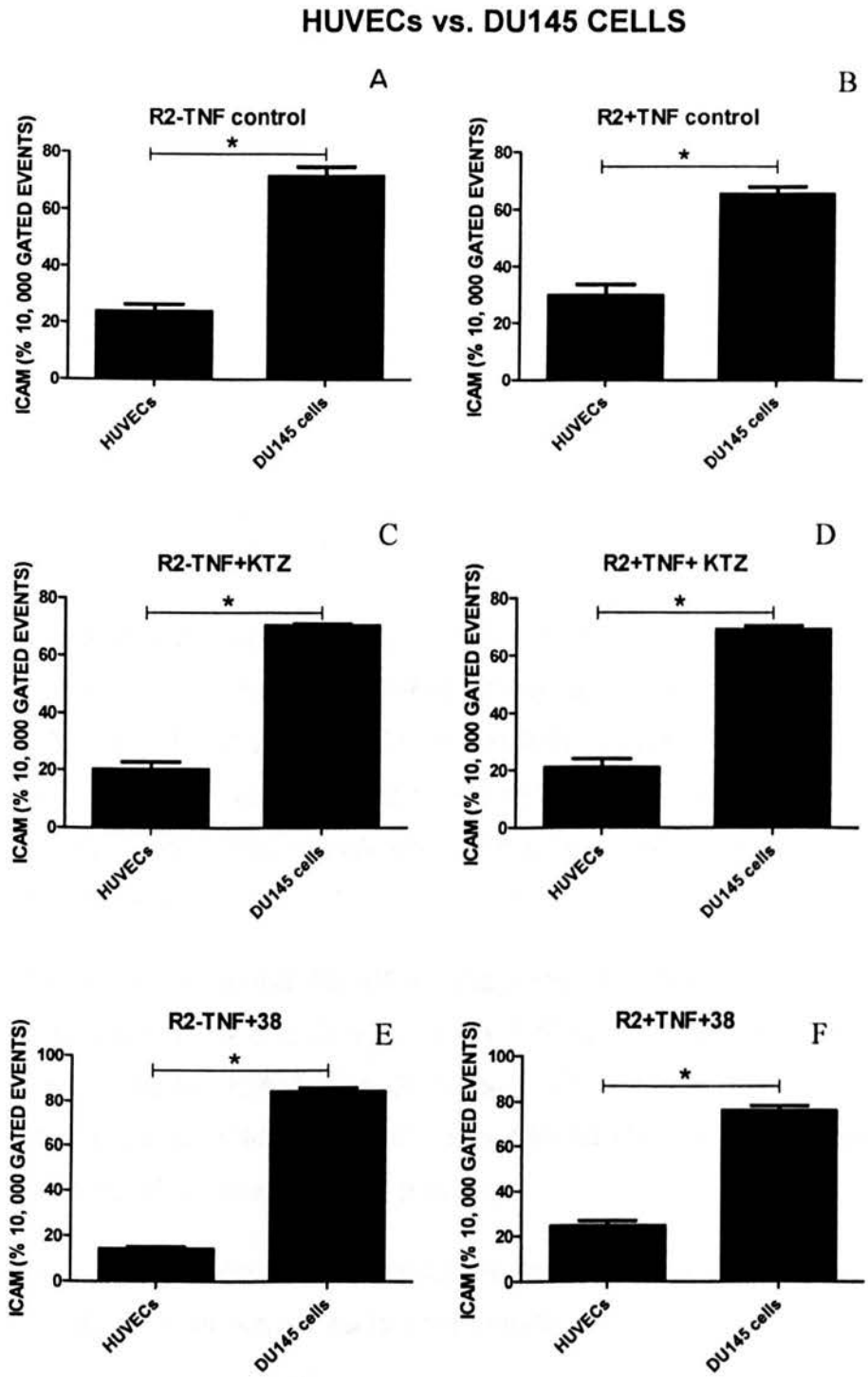

Figure 5.18: ***The expression of ICAM1 in HUVECs and DU145 cells (co-cultured for two hours) in R2.*** *ICAM-1 expression was the % of 10,000 gated events. (A) Cells were co-cultured in media only (B) HUVECs were treated with TNF-α before co-culture with DU145 cells (C) Non-treated HUVECs co-cultured with DU145 cells pre-treated with KTZ (D) HUVECs treated with TNF-α were co-cultured with DU145 cells pre-treated with KTZ (E) Non-treated HUVECs co-cultured with DU145 cells pre-treated with compound 38 (D) HUVECs treated with TNF-α were co-cultured with DU145 cells pre-treated with compound 38. The data is the mean of three different experiments (n = 3). Statistical analysis was done using un-paired student's t test (two-tailed) where *p<0.001 as compared to HUVECs.*

PC3 cells:

The FSC- SSC plot showed two discrete populations of cells following culture (Figure 5.13A). The data for both R1 and R2 was acquired and compared using a student's paired t-test (two-tail). No significant difference was found, therefore the results for R1 has been explained overleaf as representative data.

The expression of ICAM-1 in control PC3 cells (Figure 5.19) was significantly higher than non-stimulated and TNF-α stimulated HUVECs (57.07 ± 6.50%, 56.99 ± 4.02%, 11.13 ± 2.32% and 33.69 ± 2.92%; mean ± SEM; ICAM-1 in PC3 cells co-cultured with non-stimulated HUVECs, PC3 cells co-cultured with stimulated HUVECs, non-stimulated HUVECs and stimulated HUVECs respectively; $p<0.05$).

PC3 cells treated with ketoconazole showed higher expression of ICAM-1 as compared to non-stimulated and TNF-α stimulated HUVECs (62.02 ± 2.62%, 55.89 ± 0.84%, 11.54 ± 2.54% and 41.90 ± 0.40%; mean ± SEM; ICAM-1 in PC3 cells co-cultured with non-stimulated HUVECs, PC3 cells co-cultured with stimulated HUVECs, non-stimulated HUVECs and stimulated HUVECs respectively; $p<0.05$).

When treated with compound 48, PC3 cells showed similar results as observed with ketoconazole (52.13 ± 2.53%, 60.73 ± 2.57%, 8.31 ± 1.20% and 32.31 ± 1.76%; mean ± SEM; ICAM-1 in PC3 cells co-cultured with non-stimulated HUVECs, PC3 cells co-cultured with stimulated HUVECs, non-stimulated HUVECs and stimulated HUVECs respectively; $p<0.05$).

The treatment of PC3 cells with ketoconazole and compound 48 did not alter the expression of ICAM-1 as compared to control cells.

However the HUVECs which were treated with TNF-α had significantly increased expression of ICAM-1 when compared to non-treated HUVECs (33.69 ± 2.92% and 11.13 ± 2.37%; 41.90 ± 0.40% and 11.54 ± 2.54%; 32.31 ±1.76% and 8.31± 1.20%;mean ± SEM; ICAM-1 in HUVECs co-cultured with non-treated PC3 cells, KTZ-treated PC3 cells and compound 48-treated PC3 cells respectively; $p<0.05$). These effects were same in both regions (R1 and R2) gated.

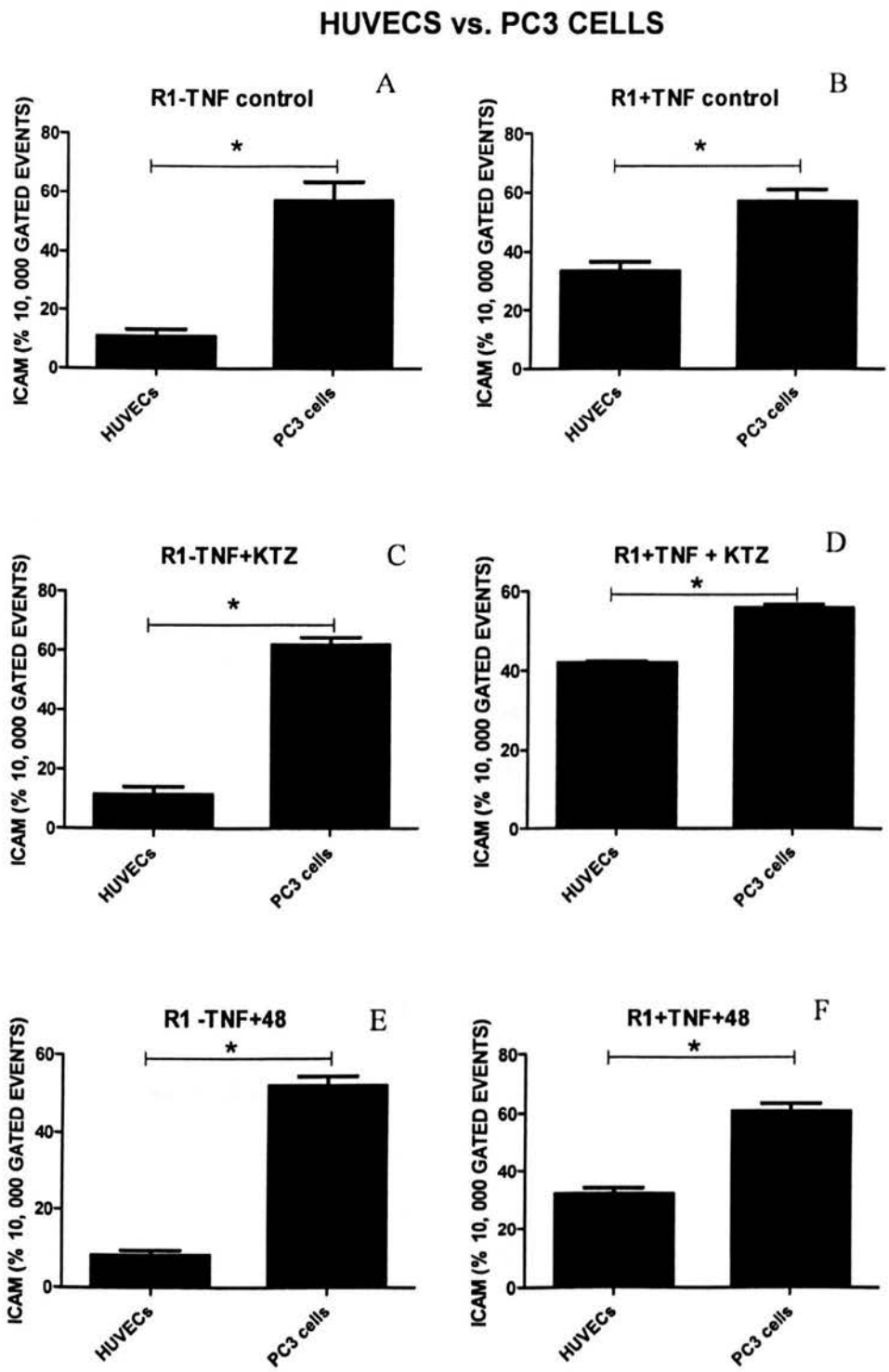

Figure 5.19: ***The expression of ICAM1 in HUVECs and PC3 cells (co-cultured for two hours) in R1.*** *ICAM-1 expression was the % of 10,000 gated events. (A) Cells were co-cultured in media only (B) HUVECs were treated with TNF-α before co-culture with PC3 cells (C) Non-treated HUVECs co-cultured with PC3 cells pre-treated with KTZ (D) HUVECs treated with TNF-α were co-cultured with PC3 cells pre-treated with KTZ (E) Non-treated HUVECs co-cultured with PC3 cells pre-treated with compound 48 (D) HUVECs treated with TNF-α were co-cultured with PC3 cells pre-treated with compound 48. The data is the mean of three different experiments (n = 3). Statistical analysis was done using un-paired student's t test (two-tailed) where *p<0.01 as compared to HUVECs.*

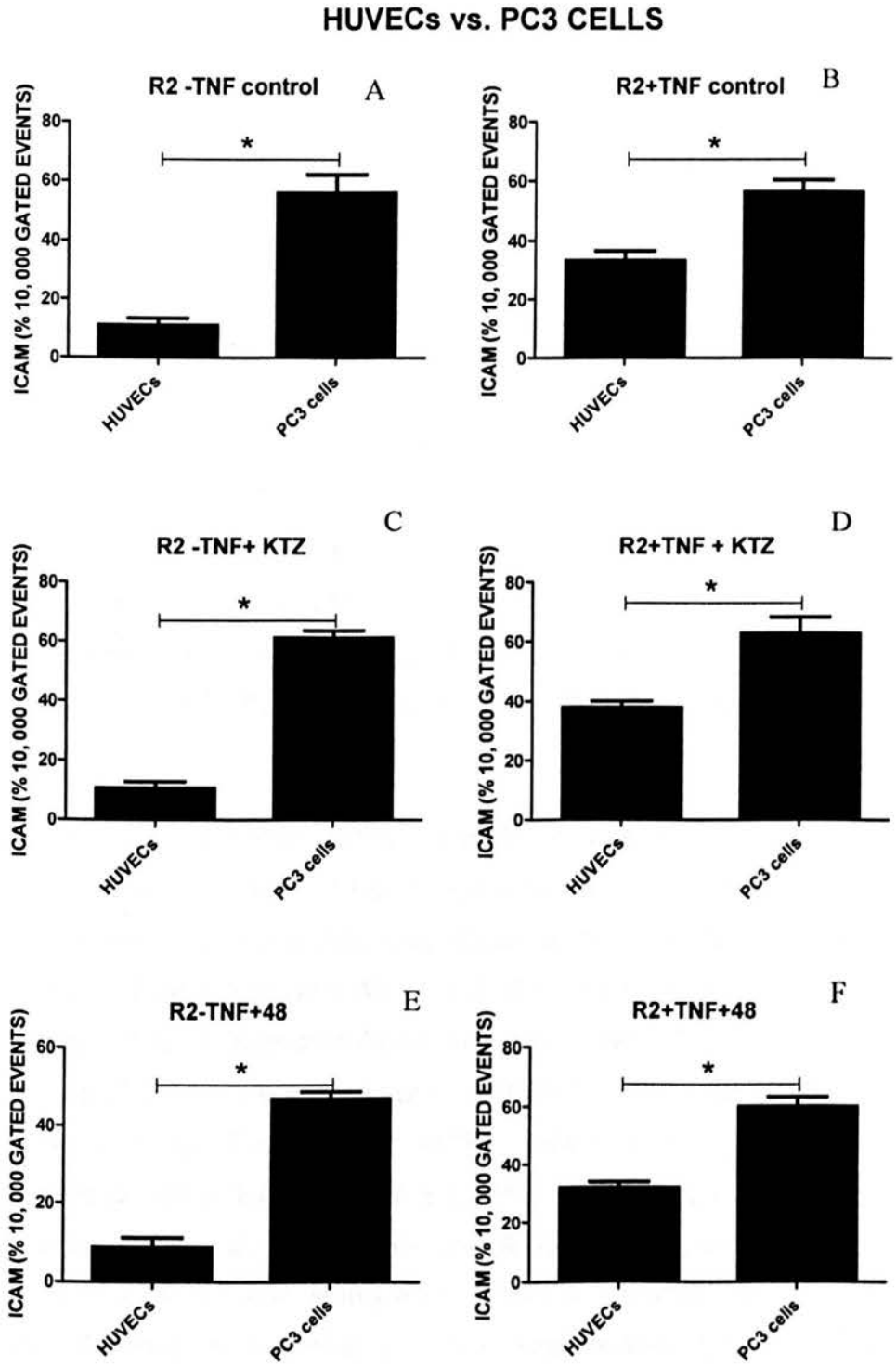

Figure 5.20: ***The expression of ICAM1 in HUVECs and PC3 cells (co-cultured for two hours) in R2.*** *ICAM-1 expression was the % of 10,000 gated events. (A) Cells were co-cultured in media only (B) HUVECs were treated with TNF-α before co-culture with PC3 cells (C) Non-treated HUVECs co-cultured with PC3 cells pre-treated with KTZ (D) HUVECs treated with TNF-α were co-cultured with PC3 cells pre-treated with KTZ (E) Non-treated HUVECs co-cultured with PC3 cells pre-treated with compound 48 (D) HUVECs treated with TNF-α were co-cultured with PC3 cells pre-treated with compound 48. The data is the mean of three different experiments (n = 3). Statistical analysis was done using un-paired student's t test (two-tailed) where *p<0.05 as compared to HUVECs.*

MCF7 cells:

The data for both R1 and R2 was acquired and compared using a student's paired t-test (two-tail). No significant difference was found, therefore the results for R1 has been explained overleaf as representative data.

MCF7 cells demonstrated significant differences in their expression of ICAM-1 between R1 and R2 regions (Figure 5.21 and 5.22).

In R1, basal levels of ICAM1 were elevated in MCF7 cells compared to non-stimulated HUVECs (23.57 ± 1.68%, and 12.95 ± 2.97%; mean ± SEM; ICAM-1 in MCF7 and non-stimulated HUVECs respectively; $p<0.05$). However, upon TNF-α-stimulation, ICAM-1 levels increased in HUVECs significantly, so that this difference in expression was no longer maintained. (44.37 ± 1.18%, and 43.52 ± 3.53%; mean ± SEM; ICAM-1 in MCF7 and stimulated HUVECs respectively; p=NS).

A similar trend was observed following addition of KTZ, whereupon stimulation with ICAM-1 caused a difference between the expression of MCF7 and endothelial cells, so that they both expressed equivalent results of ICAM-1 (40.41 ± 5.90%, 50.22 ± 2.16%, 7.66 ± 1.56 and 46.31 ± 2.35%; mean ± SEM; ICAM-1 in MCF7 cells co-cultured with non-stimulated HUVECs, MCF7 cells co-cultured with stimulated HUVECs, non-stimulated HUVECs and stimulated HUVECs respectively; $p<0.05$). Treatment of MCF7 cells with compound 51 produces similar results (25.09 ± 0.45%, 44.47 ± 0.55%, 13.50 ± 1.35 and 42.70 ± 2.55%; mean ± SEM; ICAM-1 in MCF7 cells co-cultured with non-stimulated HUVECs, MCF7 cells co-cultured with stimulated HUVECs, non-stimulated HUVECs and stimulated HUVECs respectively; $p<0.05$). The treatment of MCF7 cells with ketoconazole and compound 51 did not alter the expression of ICAM1 as compared to control cells.

The results also showed that TNF-α significantly increased the ICAM-1 expression in HUVECs then non-treated HUVECs (43.52 ± 3.53% and 12.95 ± 2.97%; 46.31 ± 2.35% and 7.66 ± 1.56%; 42.70 ± 2.55% and 13.50 ± 1.35%; mean ± SEM; ICAM-1 in HUVECs co-cultured with non-treated MCF7 cells, KTZ-treated MCF7 cells and compound 51-treated MCF7 cells respectively; $p<0.05$).

R2 demonstrated a diverse expression of ICAM-1. Unlike R1, HUVECs and MCF7 cells expressed equivalent amounts of ICAM-1 when quiescent. MCF7 cells co-cultured with activated HUVECs showed significantly increased expression (70 ± 1.34% and 14.11 ± 1.14%; mean ±SEM; in the presence and absence of TNF-α, $p<0.05$).

When treated with ketoconazole, MCF7 cells were found to consistently express increased levels of ICAM-1 compared to non-treated and TNF-α treated HUVECs (47.04 ± 0.30% and 31.99 ± 2.18%; mean ±SEM; in the presence and absence of TNF-α, $p<0.05$).

However upon addition of compound 51, MCF7 cells expression was once more equivalent to that of un-activated and activated HUVECs (46.83 ± 1.31% and 16.10 ± 1.60%; mean ±SEM; in the presence and absence of TNF-α; $p<0.05$).

We found in general that tumour cells had increased ICAM1 expression compared to HUVECs when quiescent, this was true of DU145, PC3 and MCF7. Furthermore, these levels of ICAM-1 expression remained significantly higher than even TNF-α stimulated HUVECS in every tumour cell line except for MCF7 cells. This was also true following treatments with either the synthesised drugs or control, ketoconazole.

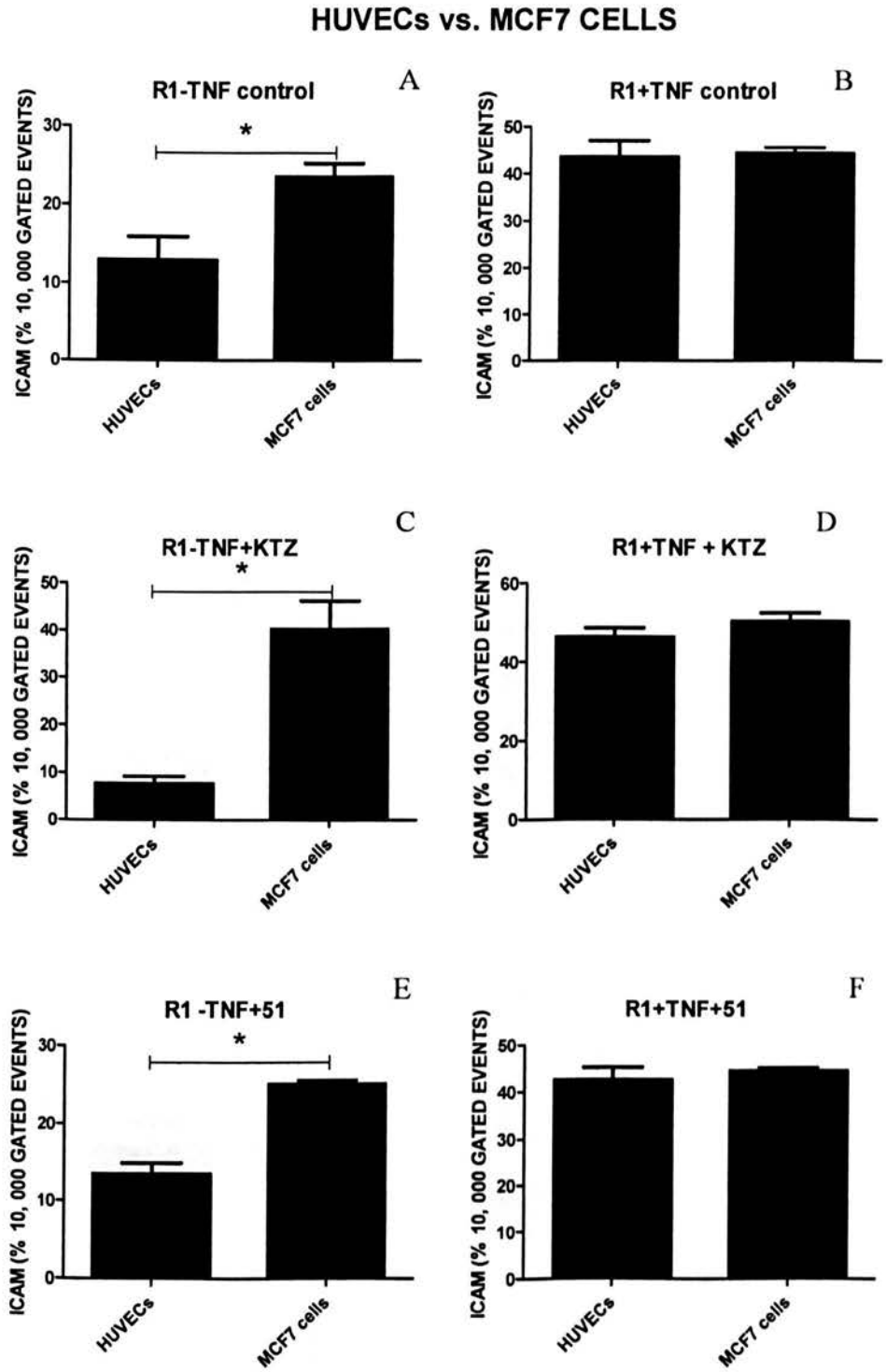

Figure 5.21: ***The expression of ICAM1 in HUVECs and MCF7 cells (co-cultured for two hours) in R1.*** *ICAM-1 expression was the % of 10,000 gated events. (A) Cells were co-cultured in media only (B) HUVECs were treated with TNF-α before co-culture with MCF7 cells (C) Non-treated HUVECs co-cultured with MCF7 cells pre-treated with KTZ (D) HUVECs treated with TNF-α were co-cultured with MCF7 cells pre-treated with KTZ (E) Non-treated HUVECs co-cultured with MCF7 cells pre-treated with 51 (D) HUVECs treated with TNF-α were co-cultured with MCF7 cells pre-treated with 51. The data is the mean of three different experiments (n = 3). Statistical analysis was done using un-paired student's t test (two-tailed) where *p<0.05 as compared to HUVECs.*

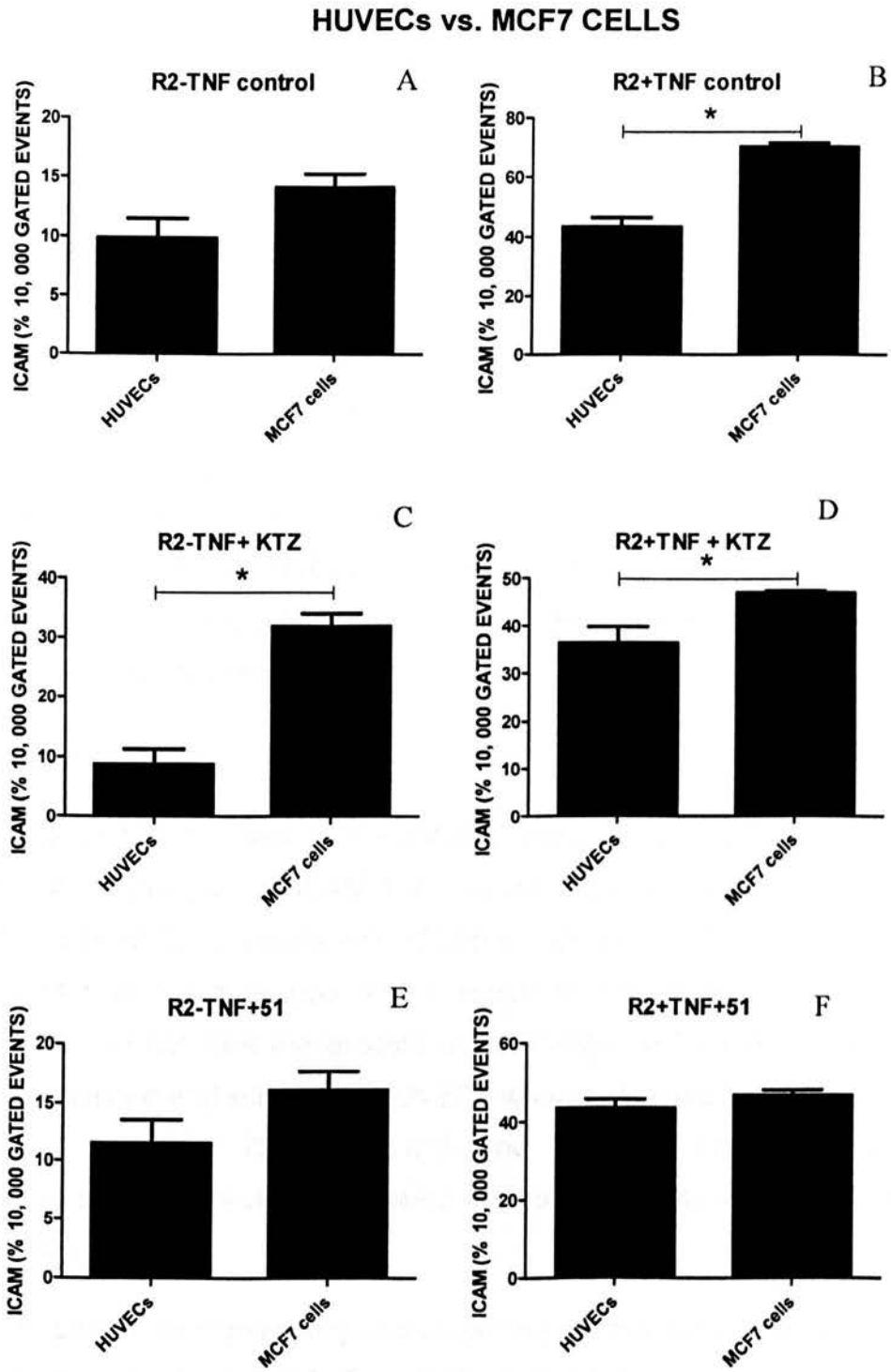

Figure 5.22: ***The expression of ICAM1 in HUVECs and MCF7 cells (co-cultured for two hours) in R2.*** *ICAM-1 expression was the % of 10,000 gated events. (A) Cells were co-cultured in media only (B) HUVECs were treated with TNF-α before co-culture with MCF7 cells (C) Non-treated HUVECs co-cultured with MCF7 cells pre-treated with KTZ (D) HUVECs treated with TNF-α were co-cultured with MCF7 cells pre-treated with KTZ (E) Non-treated HUVECs co-cultured with MCF7 cells pre-treated with 51 (D) HUVECs treated with TNF-α were co-cultured with MCF7 cells pre-treated with 51. The data is the mean of three different experiments (n = 3). Statistical analysis was done using un-paired student's t test (two-tailed) where *p<0.05 as compared to HUVECs.*

5.2.11. *Effect of CYP17 inhibitors on ICAM-1 expression in tumour cells following co-culture with HUVECs using flow cytometry*

The effect of CYP17 inhibitors on the expression of ICAM-1 on the tumour cell's surfaces was determined (Figure 5.23- 5.25) by treating the tumour cells with the CYP17 inhibitors for 24 hours prior to co-culturing with non-treated and TNF-α treated endothelial cells. The co-culture was further incubated with ICAM-1 antibody (1: 100) for an hour. 10,000 events were counted as percentage of gated (R1 and R2) events. A student's t-test was carried out to determine the significant difference between results of R1 and R2 regions and no significant difference was found between the two regions, therefore the results for R1 has been explained overleaf as representative data.

DU145 cells:

Co-culturing of DU145 cells with HUVECs, pre-incubated with TNF-α, did not increase the expression of ICAM-1 in DU145 cells as compared to cells co-cultured with HUVECs in media only (65.68 ± 3.04% and 72.40 ± 2.76%; mean ± SEM; ICAM-1 in the presence and absence of TNF-α respectively, $p<0.05$). Ketoconazole did not alter the expression of ICAM-1 in DU145 cells co-cultured with non-stimulated and stimulated HUVECs when compared to un-treated DU145 cells (74.11 ± 1.09%, 73.21 ± 1.13% and 72.40 ± 2.76%; mean ± SEM respectively; $p<0.05$).These effects were the same in both regions (R1 and R2) gated (Figure 5.23).

In R1, Compound 38 significantly increased the expression of ICAM-1 in DU145 cells compared to control (83.90 ± 2.1% and 72.40 ± 2.76%; mean ± SEM respectively). Following co-culturing of DU145 cells with TNF-α treated HUVECs, this pattern was also seen with increased ICAM-1 expression related to control cells incubated with TNF-alone (74.59 ± 65.68%; 72.40 ± 2.76%; mean ± SEM; respectively; $p<0.05$). Similar results were observed in R2.

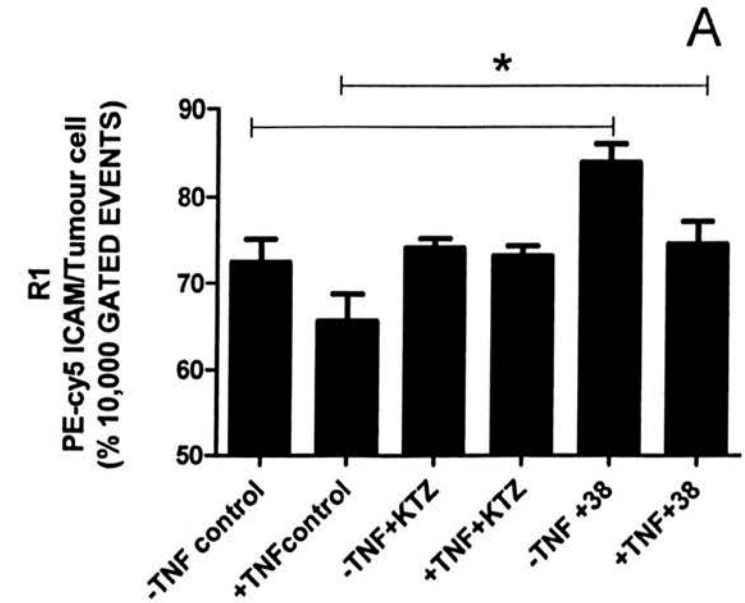

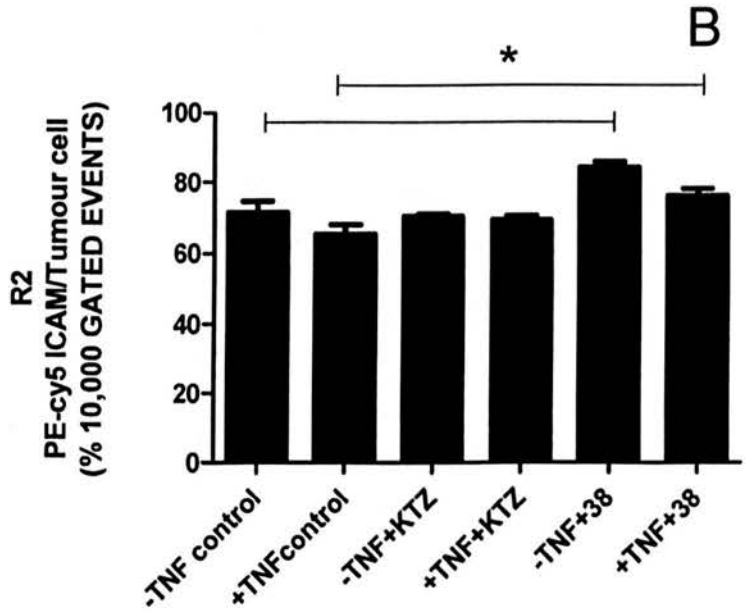

Figure 5.23: Effect of compound 38 on ICAM-1 expression in DU145 cells when incubated with HUVECs for two hours. *ICAM-1 expression as % of 10,000 gated events (A) ICAM-1 expressed on DU145 cells in R1 (B) ICAM-1 expressed in DU145 cells in R2. The data is the mean of three different experiments (n = 3) where *p<0.05 using Tukey's modified student's t-test.*

PC3 cells:

In PC3 cells (Figure 5.24), co-culturing with HUVECs that had been pre-incubated with TNF-α, did not increase the expression of ICAM-1 when compared with co-cultured non-stimulated HUVECs (56.99 ± 2% and 57.07 ± 2.55%, mean ± SEM respectively; $p<0.05$). Ketoconazole did not alter the expression of ICAM-1 in DU145 cells co-cultured with non-stimulated and stimulated HUVECs when compared to control (62.02 ± 2.62% and 55.89 ± 0.84% and 57.07 ± 2.55%; mean ± SEM respectively; $p<0.05$). Compound 48 did not change the expression of ICAM-1 in PC3 cells with non-stimulated and TNF-α stimulated HUVECs when compared to control (52.13 ± 2.53% and 60.73 ± 2.57% and 57.07 ± 2.55%; mean ± SEM; respectively; $p<0.05$).

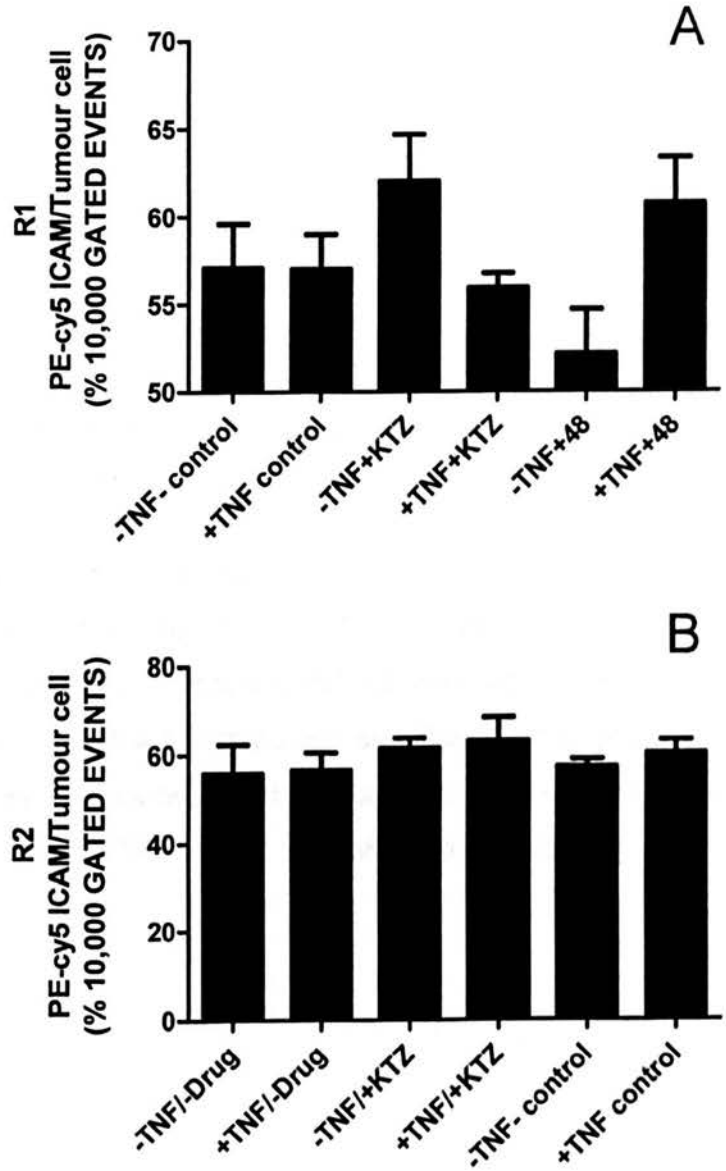

Figure 5.24: ***Effect of compound 48 on ICAM-1 expression in PC3 cells when incubated with HUVECs for two hours.*** *ICAM-1 expression as % of 10,000 gated events (A) ICAM-1 expressed on PC3 cells in R1 (B) ICAM-1 expressed in PC3 cells in R2. The data is the mean of three different experiments (n = 3) where p>0.05 using Tukey's modified student's t-test.*

MCF7 cells:

In MCF7 cells (Figure 5.25) of R1, the basal expression of ICAM-1 increased following co-culturing with HUVECs, stimulated by TNF-α when compared to non-stimulated HUVECs (54.37 ± 1.18% and 41.97 ± 2.99%; mean ± SEM; respectively; $p<0.05$). TNF-α activation of HUVECs increased the expression of ICAM-1 in MCF7 cells treated with compound 51 as compared to non-treated MCF7 cells (4.47 ± 4.56% and 25.42 ± 3.75%; mean ± SEM; respectively; $p<0.05$). Moreover, basal levels of ICAM-1 were significantly decreased following incubation with compound 51 as compared to control (25.43 ± 3.75% and 41.97 ± 2.99%, mean ± SEM; respectively; $p<0.05$).

In R2 also, the basal expression of ICAM-1 increased following stimulation by TNF-α (61.60 ± 4.50%; 40.11 ± 1.97%; mean ± SEM; respectively; $p<0.05$), although no decrease with compound 51 was observed from baseline. In the presence of TNF-α, ICAM-1 expression significantly decreased in the presence of ketoconazole and compound 51 when compared to control (47.04 ± 0.30%, 43.50 ± 3.05% and 41.97 ± 2.99%; mean ± SEM; respectively; $p<0.05$).

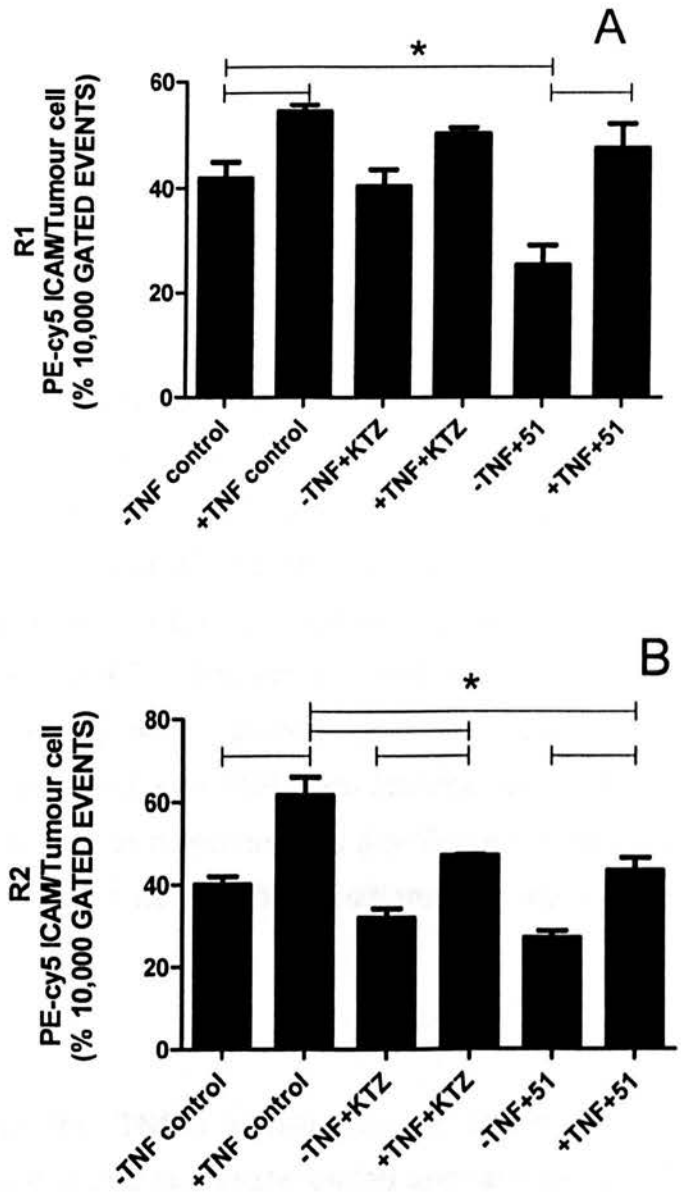

Figure 5.25: Effect of compound 51 on ICAM-1 expression in MCF7 cells when incubated with HUVECs for two hours. *ICAM-1 expression as % of 10,000 gated events (A) ICAM-1 expressed on MCF7 cells in R1 (B) ICAM-1 expressed in MCF7 cells in R2. The data is the mean of three different experiments (n = 3) where *p<0.05 using Tukey's modified student's t-test.*

5.2.12. *Tumour cell/ HUVEC complexes in co-culture using flow cytometry*

During co-culture, tumour cells bind to HUVECs and form complexes. The effect of CYP17 inhibitors on tumour: endothelial cell complexes were determined (Figure 5.26- 5.28) both in R1 and R2 regions. The tumour cells were treated with CYP17 inhibitors for 24 hours before co-culturing with non-stimulated and TNF-α stimulated HUVECs for two hours as described previously. Both tumour and endothelial cells were labelled with different fluorochromes. Tumour cells were labelled with cell tracker green and were FITC-positive in flow cytometry whereas HUVECs were labelled with a PE-labelled CD144 endothelial cell marker. The tumour: endothelial cell complexes were determined as % double staining (i.e. %CD144/FITC). A total of 10, 000 gated events were counted. The results were reported for both R1 and R2. The tumour: endothelial cell complexes which were treated with media only were labelled as -TNFα control while those in which HUVECs were pre-treated with TNFα are labelled as +TNFα control. A two-way ANOVA was carried out to determine the significant difference between results of R1 and R2 regions and no significant difference was found between the two regions.

<u>DU145 cells:</u>

In DU145 cells in R1, TNF-α significantly increased the number of TC: EC complexes when compared to non-stimulated and un-treated cells (control) (9.12 ± 0.75 and 3.94 ± 0.67; mean ± SEM; respectively; $p<0.05$). With no prior activation by TNF-α, only compound 38 decreased the percentage of TC: EC complexes when compared to control (media alone) (1.21 ± 0.18 and 3.94 ± 0.67; mean ± SEM; respectively; $p<0.05$) but not ketoconazole. However, when studying activated (TNF-α) HUVECs, ketoconazole and compound 38 (4.3 ± 0.35 and 1.04 ± 0.06; mean ± SEM; respectively; $p<0.05$) both decreased the number of EC: TC complexes as compared to control (9.12 ± 0.75).

In R2, with no prior activation by TNF-α, compound 38 decreased the percentage of TC: EC complexes when compared to control (1.30 ± 0.23 and 4.18 ± 0.61; mean ± SEM; respectively; $p<0.05$). However, when studying activated (TNF-α)

HUVECs, ketoconazole and compound 38 both decreased the number of EC: TC complexes as compared to control (3.50 ± 0.49, 1.41 ± 0.17 and 5.70 ± 0.55; mean ± SEM; respectively; $p<0.05$).

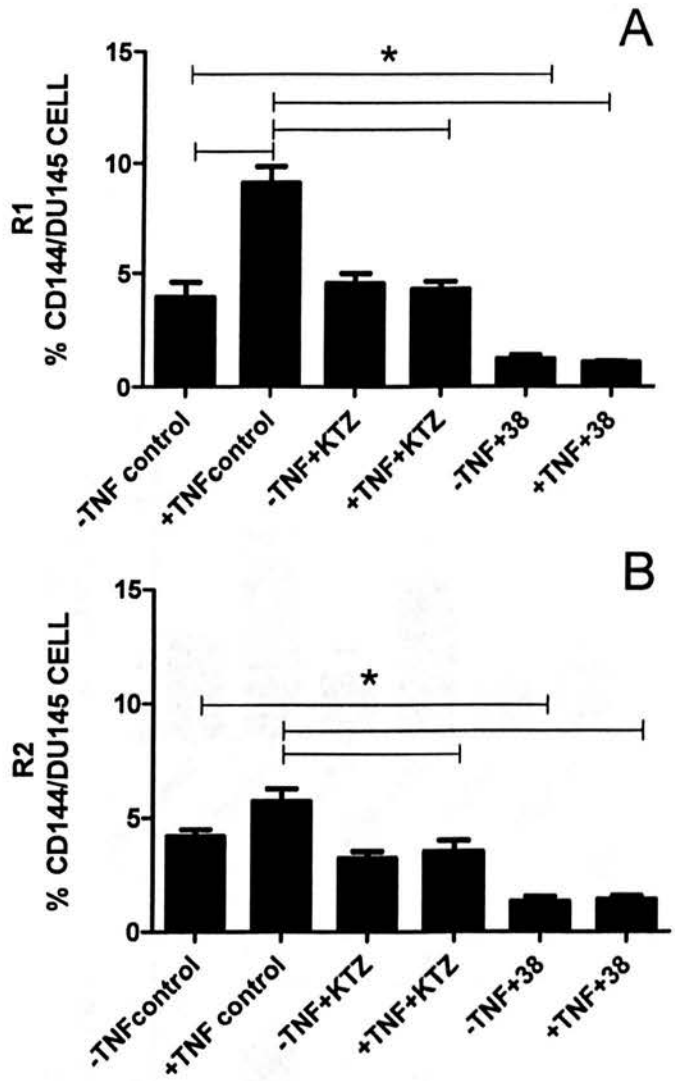

Figure 5.26: ***Effect of CYP17 inhibitors on DU145 and HUVECs complexes of 10,000 gated events.****(A) % CD144/DU145 cells of 10, 000 gated events in R1 ((B) % CD144/DU145 cells of 10,000 gated events in R2. The data is the mean of three different experiments (n =3) where *p<0.05 using Tukey's modified student's t-test.*

PC3 cells:

For PC3 cells, in R1, TNF-α significantly increased the number of TC: EC complexes when compared to un-treated and non-stimulated cells (5.32 ± 0.65 and 2.55 ± 0.12; mean ± SEM; respectively; $p<0.05$). With prior activation by TNF-α, compound 48 decreased the percentage of TC: EC complexes when compared to control (1.92 ± 0.52 and 5.32 ± 0.65; mean ± SEM; respectively; $p<0.05$). Similarly, in R2, the percentage of TC: EC complexes was decreased by compound 48 when compared to control (1.96 ± 0.77 and 5.05 ± 0.65; mean ± SEM; respectively; $p<0.05$). In both R1 and R2, ketoconazole did not affect the TC: EC complexes.

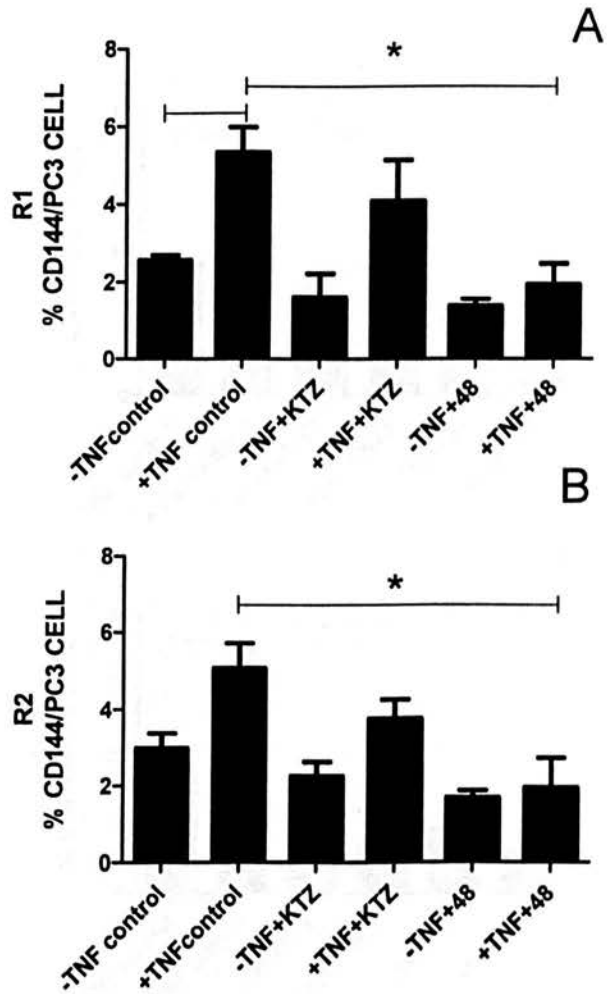

Figure 5.27: ***Effect of CYP17 inhibitors on PC3 and HUVECs complexes of 10,000 gated events.*** *(A) % CD144/PC3 cells of 10, 000 gated events in R1 ((B) % CD144/PC3 cells of 10,000 gated events in R2. The data is the mean of three different experiments (n =3) where *p<0.05 using Tukey's modified student's t-test.*

MCF7 cells:

In MCF7 cells, pre-treatment of HUVECs with TNF-α increased the TC: EC complexes in both R1 and R2. In R1, with no prior activation by TNF-α, compound 51 decreased the percentage of TC: EC complexes when compared to control (media alone) (6.13 ± 0.18 and 9.37 ± 0.21; mean ± SEM; respectively; $p<0.05$). However, when studying stimulated HUVECs, ketoconazole and compound 48 both decreased the number of EC: TC complexes when compared to control (12.40 ± 0.66, 4.52 ± 0.28 and 9.37 ± 0.21; mean ± SEM; respectively; $p<0.05$). The trend in results in R2 was similar. In the presence of TNF- α, ketoconazole and compound 48 both decreased the number of EC: TC complexes (3.73 ± 1.20 and 2.97 ± 0.81 and 9.37 ± 0.21; mean ± SEM; respectively; $p<0.05$).

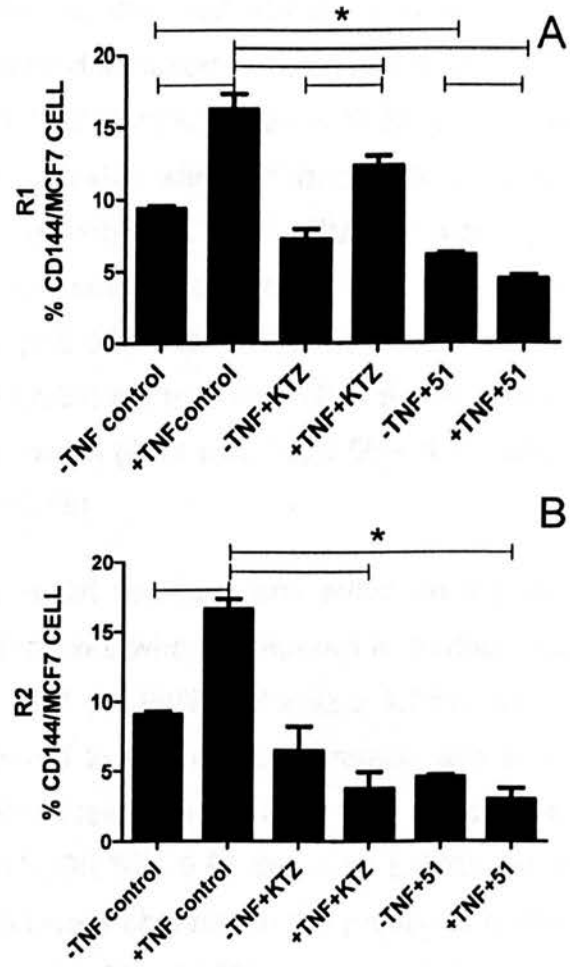

Figure 5.28: ***Effect of CYP17 inhibitors on MCF7 and HUVECs complexes of 10,000 gated events.*** *(A) % CD144/MCF7 cells of 10, 000 gated events in R1 ((B) % CD144/MCF7 cells of 10,000 gated events in R2. The data is the mean of three different experiments (n =3) where *p<0.05 using Tukey's modified student's t-test.*

5.2.13. *Total ICAM-1 in DU145/HUVEC complexes (Triple stain) in co-culture using flow cytometry*

The tumour cells and HUVECS were labelled with cell tracker green (FITC) and PE-labelled CD144 respectively. After co-culturing for two hours, PE-Cy5 labelled ICAM-1 (1: 100) was added for one hour. A total of 10,000 events were calculated as % of gated events and expression of PE-Cy5, PE and FITC reported. A two-way ANOVA was carried out to determine the significant difference between results of R1 and R2 regions and no significant difference was found between the two regions.

DU145 cells:

In the absence of TNF-α, the total ICAM-1 expression in DU145: HUVEC co-culture was significantly decreased by compound 38 when compared to control (3.36 ± 0.67% and 1.12 ± 0.13%; mean ± SEM; respectively; $p<0.05$). Similarly when HUVECs were activated with TNF-α, prior to co-culturing with DU145 cells, the total ICAM-1 expression on DU145: HUVEC was significantly decreased by compound 38 when compared to control (1.00 ± 0.04% and 5.20 ± 1.11%; mean ± SEM; respectively; $p<0.05$). Ketoconazole did not decrease the expression of ICAM-1 on DU145: HUVEC complexes both in the absence and presence of TNF-α when compared to control (4.43 ± 0.285, 3.56 ± 0.6% and 1.12 ± 0.13%; mean ± SEM; respectively; $p<0.05$).

However in R2, TNF-α did not have any effect on the expression of ICAM-1 in DU145: HUVECs complexes when compared to tumour cell complexes with non-stimulated HUVECs (4.04 ± 1.98% and 2.92 ± 1.36%; mean ± SEM; respectively; $p<0.05$). When compared to control, ketoconazole and compound 38 also did not alter the ICAM-1 expression in tumour cell complexes with non-stimulated HUVECs (2.92 ± 1.36%, 30.30 ± 0.86 and 1.24 ± 0.20; mean ± SEM; respectively; $p<0.05$). Similar results were obtained in the presence of stimulated TNF-α (4.04 ± 1.98%, 2.54 ± 0.86% and 1.35 ± 0.16%; mean ± SEM; respectively; $p<0.05$).

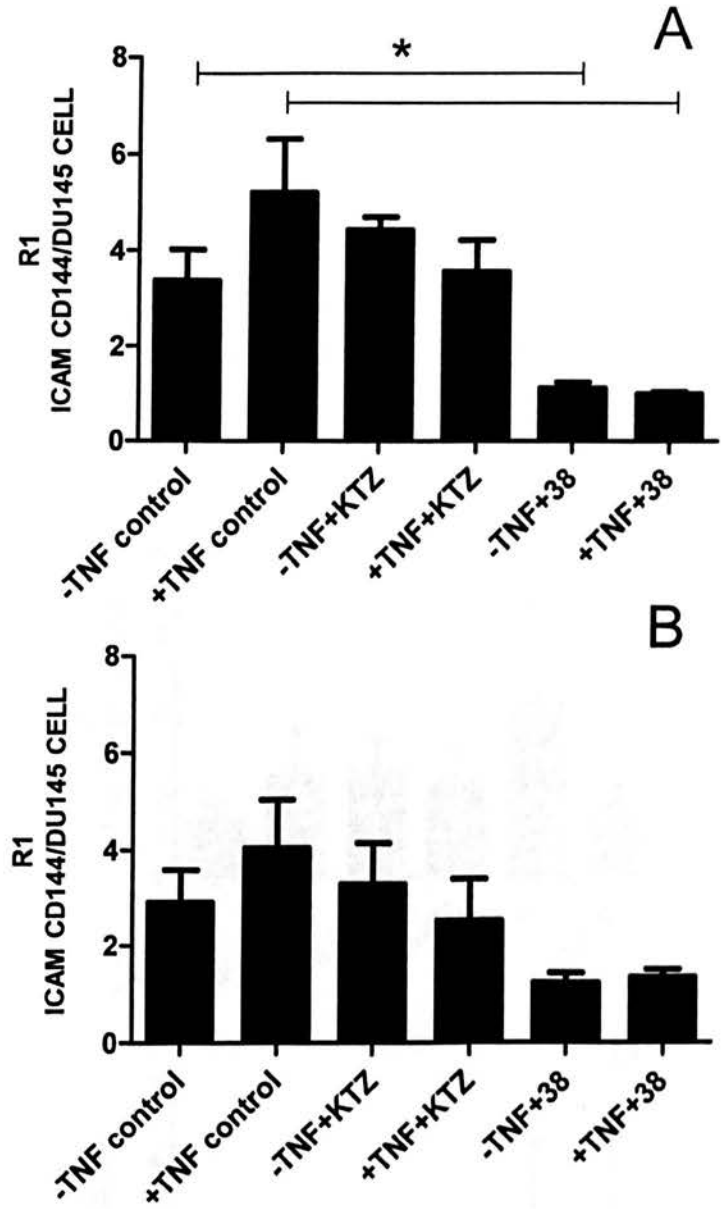

Figure 5.29: ***The total ICAM-1 expression in DU145: HUVECs. A total of 10,000 events were counted.*** *(A) ICAM/CD144/DU145 cells as % of 10,000 gated events for R1 (B) ICAM/CD144/DU145 cells as % of 10,000 gated events for R2. The data is the mean of three different experiments (n =3) where *p<0.05 using Tukey's modified student's t-test.*

PC3 cells:

In PC3: HUVEC complexes, with no prior activation of TNF-α, the total ICAM-1 expression were not significantly changed by ketoconazole or compound 48 when compared to control (2.70 ± 0.72%, 4.50 ± 2.17% and 1.48 ± 0.32%; mean ± SEM; respectively; $p<0.05$). Similarly, when HUVECs were treated with TNF-α, neither ketoconazole nor compound 48 significantly changed the ICAM-1 expression on PC3: HUVEC complexes when compared to control (2.30 ± 0.79%, 1.80 ± 0.47% and 2.51 ± 1.17%; mean ± SEM; respectively; $p<0.05$). The trend in results in R2 was similar to R1.

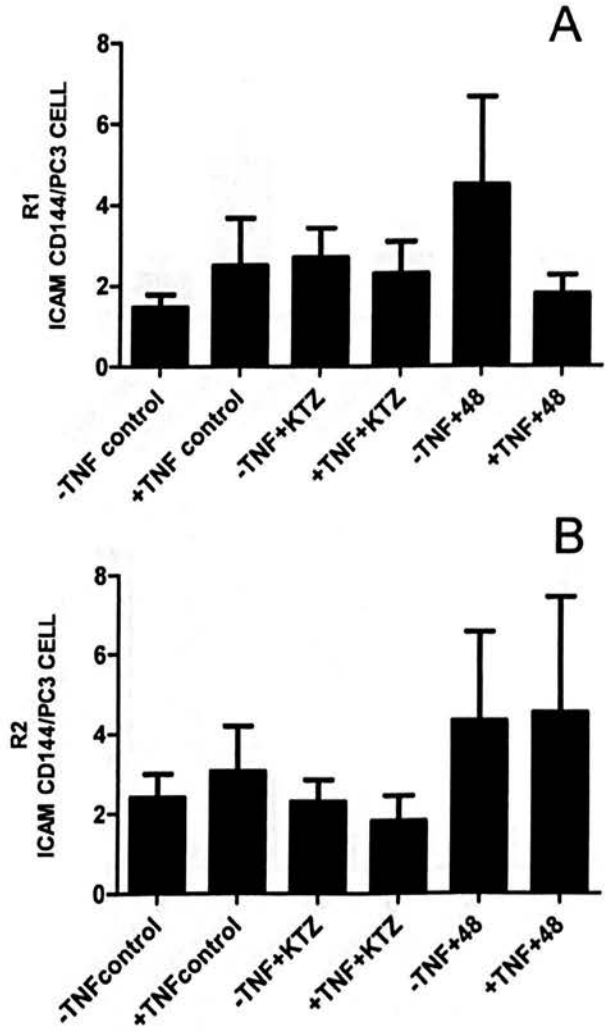

Figure 5.30: ***The total ICAM-1 expression in PC3: HUVECs. A total of 10,000 events were counted.*** *(A) ICAM/CD144/PC3 cells as % of 10,000 gated events for R1 (B) ICAM/CD144/PC3 cells as % of 10,000 gated events for R2. The data is the mean of three different experiments (n =3) where p>0.05 using Tukey's modified student's t-test.*

MCF7 cells:

In MCF7: HUVEC complexes, with no prior activation of TNF-α, the total ICAM-1 expression was not significantly changed by ketoconazole or compound 51 when compared to control (1.87 ± 1.00%, 3.00 ± 0.94% and 2.07 ± 0.74%; mean ± SEM; respectively; $p<0.05$). Similarly, when HUVECs were treated with TNF-α, neither ketoconazole nor compound 51 significantly changed the ICAM-1 expression on MCF7: HUVEC complexes (2.92 ± 1.34%, 2.60 ± 0.26% and 7.35 ± 3.70%; mean ± SEM; respectively; $p<0.05$). The trend in results in R1 and R2 was similar.

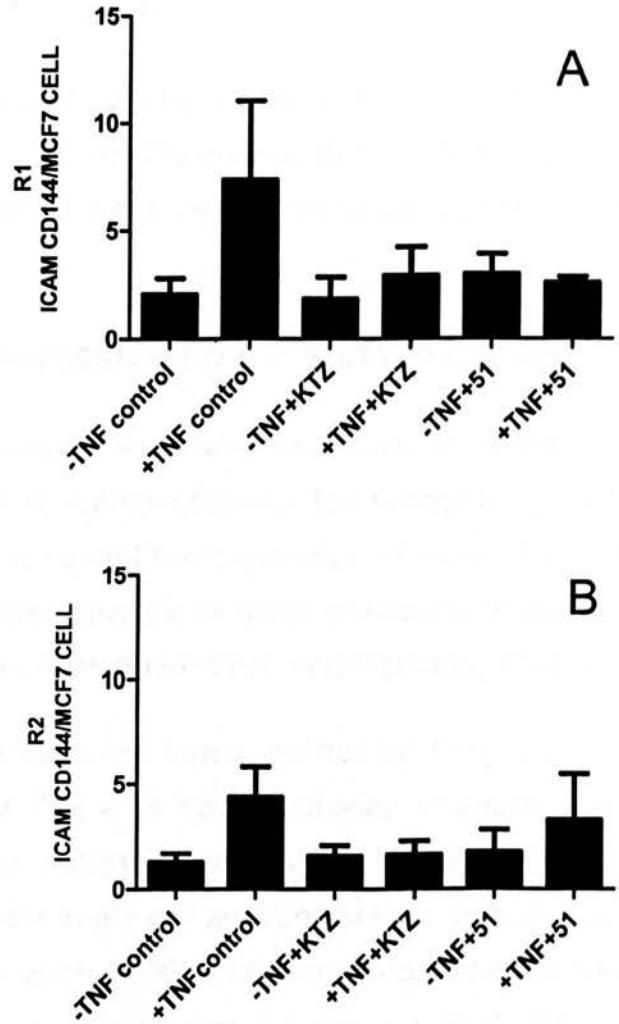

Figure 5.31: ***The total ICAM-1 expression in MCF7: HUVECs. A total of 10,000 events were counted.*** *(A) ICAM/CD144/MCF7 cells as % of 10,000 gated events for R1 (B) ICAM/CD144/MCF7 cells as % of 10,000 gated events for R2. The data is the mean of three different experiments (n =3) where p>0.05 using Tukey's modified student's t-test.*

5.3. Discussion

The homotypic and heterotypic interactions of tumour cells is regulated by cell adhesion molecules (CAMs) (Feng *et al.*, 2011). The intracellular adhesion molecule 1 (ICAM-1) is one of the adhesion molecules that facilitates cell interactions (Boggenrieder and Herlyn, 2003; Haass *et al.*, 2005 Park, 2009). The increased levels of ICAM-1 correlate with the progression of tumour in cancer patients (Galicchio, *et al.*, 2008; Hanlon *et al.*, 2002; Buitrago *et al.*, 2011; Hayes and Siegel, 2009; Georgolios *et al.*, 2006; Kammerer *et al.*, 2004) Therefore ICAM-1 can be used as a biomarker to assess the progression and prognosis of tumours (Buitrago *et al.*, 2011).

The adhesion molecules are up regulated by cytokines in a wide variety of cell types (Hanlon *et al.*, 2002). We investigated the capacity of TNF-α (10ng/mL) to up-regulate the ICAM-1 on a population of cells known to respond to ICAM-1 expression.

5.3.1. ICAM-1 expression on the surface of HUVEC

The vascular endothelium expresses low levels of ICAM-1 in a quiescent state, and different pro-inflammatory cytokines, like tumour necrosis factor alpha (TNF-α) or interleukin-1 (IL-1) control the expression of most of the endothelial adhesion molecules that involve activation of major transcription factors such as NF-kB and AP-1 (Dustin and Springer, 1988; Chen and Manning, 1995; Ahmad *et al.*, 1998).

Our results are consistent with those reported by Yang *et al.* (2005) and Balwani *et al.* (2011) and show that a 24 hour incubation of endothelial cells with 10ng/mL TNF-α increases the expression of ICAM-1. ICAM-1 present on the endothelium plays an important role in the cell arresting step of the adhesion process (Scalia *et al.*, 1998; Bourdillon *et al.*, 2000) and is involved in the trans-endothelial migration of leukocytes to sites of inflammation (Lawson and Wolf, 2009).

5.3.2. Effect of CYP17 inhibitors on the basal ICAM-1 expression on tumour cell surface

The expression of ICAM-1 in tumours has been shown to be important for the immunogenicity of cancer cells (Webb *et al.*, 1991). The three cancer cell lines used in the this study; DU145, PC3 and MCF7, express basal levels of ICAM-1 that increase following exposure to a cytokine such as TNF-α or IFN-γ (Lee *et al.*, 2010; Chen *et al.*, 2011; Lassila and Komi, 2000). However, the levels of ICAM-1 expression on the cell surface can be variable when compared to the concentration of soluble ICAM-1 after treatment with cytokines such as IFN-γ and TGF-βI (Rokhlin and Cohena, 1996).

We have therefore incubated cancer cells with and without 10ng/mL of TNF-α for 24 hours and measured ICAM-1 levels basally and following stimulation. The flow cytometry quantitatively determined ICAM-1 expression with immunofluorescence qualitatively supporting these findings. The effect of the CYP17 inhibitors was then investigated along with TNF-α, to determine their effect on the expression of ICAM-1. The tumour cells were fluorescently labelled with cell tracker green. The expression of ICAM-1 was reported as PE-Cy5 ICAM/tumour cell FITC and determined as a percentage of 10,000 events gated.

<u>DU145 cells</u>

The expression of ICAM-1 on DU145 cells did not change significantly in response to TNF-α. In fact, the basal expression remained elevated and did not increase further following addition of 10ng/mL TNF-α. This has also been demonstrated following immunofluorescence. These results are in contrast to Lee *et al.* (2010), who have shown that the expression of ICAM-1 in DU145 cells can be induced by 10ng/mL TNF-α. Furthermore, treatments with compound 38 which is the compound shown to have the greatest inhibitory effect on adhesion of DU145 cells did not show significant alteration in ICAM-1 expression, either increasing or decreasing.

Liu (2000) has reported the adhesion molecule profiles of three prostate cancer cell lines; LNCaP, PC3, and DU145. The CD molecules were grouped into four ranks, based on the percentage of positive events (i.e. >50%, 40 –50%, 20 – 40%,

and 10 –20%). For DU145 cell lines, CD54 (ICAM-1) has the highest score (>50%) among other adhesion molecules. Considering that basal ICAM-1 expression was never altered, either with TNFα or following addition of the inhibitory compound, it would be interesting to look at the expression of other adhesion molecules in case of DU145 cell lines as it is difficult to interpret these data.

PC3 cells:

The PC3 cells stimulated with TNF-α had significantly increased levels of ICAM-1 when compared with non-stimulated cells. Immunofluorescence also demonstrated an increased expression of ICAM-1. These results are consistent with previous studies on PC3 cells that have reported that 10 ng/mL and 100ng/mL of TNF-α increase the expression of ICAM-1 (Lee *et al.,* 2010; Chen *et al.,* 2011). Following incubation with KTZ or compound 48, no changes in ICAM-1 levels on PC3 cells were observed either with or without TNF-α. Therefore we can conclude that CYP17 inhibitors did not decrease the ICAM-1 levels in PC3 cells.

MCF7 cells:

ICAM-1 expression levels have been shown to positively correlate with the metastatic potential of breast cancer cell lines. Due to its association with malignant progression, ICAM-1 might represent a new target in the treatment of breast cancer patients (Rosette *et al.*, 2005; Schroder *et al.,* 2011).

When investigating ICAM-1 expression on the breast cancer cell line MCF7, the flow cytometry showed that the basal levels of ICAM-1 were very low in these cells. Indeed, immunohistochemical analysis of breast cancer tissues indicate low expression levels of ICAM1 (Ogawa *et al.,* 1998) with weak staining of MCF7 cells with ICAM-1 antibodies (Constantinou *et al.*, 1998).

It has been reported that TNF-α can increase the expression of ICAM-1 on MCF7 and other breast cancer cell lines (Alexandra *et al.,* 1997). In concordance with this study, our results have shown that TNF-α has significantly increased the ICAM-1 levels of MCF7 cells.

Unlike the other inhibitors specific for the cell lines DU145 and PC3, the CYP17 inhibitor; compound 51 significantly decreased the ICAM-1 levels of stimulated and

non-stimulated MCF7 cells when compared to control with immunofluorescence demonstrating similar results. These results confirm previous studies that decreased the expression of cell adhesion molecules following treatment with cytochrome P450 enzyme inhibitors (Sasaki *et al.*, 2003). This is further complimented by the knowledge that in breast cancer tissue the expression of ICAM-1 has been associated with a good overall prognosis (Ogawa *et al.*, 1998).

5.3.3. Gating the tumour cell and HUVEC population

The interaction between tumour and endothelial cells (TC-EC co-culture) up-regulates the expression of different adhesion molecules that include ICAM-1, VCAM-1 and E-selectin (Haddad *et al.*, 2010). Therefore the expression of ICAM-1 in all tumour cells when co-cultured with HUVECs was also studied.

Both tumour and endothelial cells were labelled with different fluorochromes; the tumour cells were labelled with a cytoplasmic cell tracker green dye while the endothelial cells were labelled with a PE-conjugated CD144 (VE-Cadherin) antibody which is an endothelial cell exclusive marker. ICAM-1 expression was seen on both cell types in the resting and activated state.

In the absence of any treatment, the FACS plots for DU145: HUVEC co-culture and PC3: HUVEC co-culture showed that when tumour and endothelial cells were co-cultured together, both cell types expressed higher levels of ICAM-1 cells. These results are consistent with other studies that have reported the upregulation of adhesion molecule expression, that include ICAM-1, VCAM-1 and E-selectin, following co-culture between tumour and endothelial cells (Takahashi *et al.*, 1996; Haddad *et al.*, 2010).

However, the co-culturing of the breast cancer cell line MCF7 with HUVEC did not cause a noticeable increase in the expression of ICAM-1 in MCF7 as in the case of the other two cancer cell lines. One reason for this could be that the basal expression of ICAM-1 in MCF7 cells is very low and has been found in other studies (Rosette *et al.*, 2005; Alexandra *et al.*, 1997). ICAM-1 is also not the only cell adhesion molecule which is over-expressed as a result of co-culture, therefore there might be needed to investigate other adhesion molecules.

5.3.4. ICAM-1 expression in tumour cells vs. HUVECs in co-culture

In this study, both tumour and endothelial cells in co-culture had an increased expression of adhesion molecules on their surfaces and endothelial expression of ICAM was compared as a standard (Haddad *et al.*, 2010).

DU145 cells

Following co-culture of un-treated DU145 cells with non-stimulated and stimulated HUVECs, the expression of ICAM-1 was higher on DU145 cells than compared with non-stimulated and stimulated HUVECs. No decrease in this ICAM expression was observed following treatment with ketoconazole, when compared to un-stimulated and stimulated HUVECs. This was also demonstrated when DU145 cells were pre-treated compound. Thus the expression of ICAM-1 in DU145 cells was consistently greater than that expressed on HUVEC following either treatment. Haddad *et al.*, (2010) have shown that the incubation of tumour cells with HUVECs results in increased expression of ICAM-1 on T24-GFP bladder carcinoma cell lines compared to the HUVECs. The HUVECs themselves are constantly in a state of inflammation following co-culture with DU145 cells as endothelial ICAM-1 expression was similar both in the presence and absence of TNF-α. We and others have shown that DU145 cells have a huge basal expression of ICAM-1 (Liu, 2000) with high levels of ICAM-1 associated with an increased malignant potential of cancer cells (Francavilla *et al.*, 2009) that can cause increased inflammation of HUVECs.

We can conclude that DU145 cells express ICAM-1 to a high level, basally and following stimulation. Moreover their co-culture with HUVEC results in HUVECs activation demonstrated by an increased expression of ICAM-1. This would create an increased adhesive capability of the HUVEC allowing potential further adhesion of cells that include cancerous and pro-inflammatory cells to the endothelium.

None of the compounds affected these adhesive properties and so treatment would have to focus on some other aspect of adhesion.

PC3 cells

In a similar fashion to DU145 cells, the expression of ICAM-1 in the un-treated prostate cancer cell line, PC3 cells remained higher when compared to non-stimulated and stimulated HUVECs. Furthermore, these levels of ICAM-1 expression remained significantly higher when PC3 cells were treated with ketoconazole and compound 48. The co-culturing with PC3 cells caused an activation of HUVECs which resulted in comparatively higher expression of ICAM-1 in HUVECs.

MCF7 cells

Following incubation with HUVEC, the MCF7 cells showed differential expression of ICAM-1 in the two regions. The cells in the first region (R1) were smaller in size and granularity and might be considered more immature cells. In contrast, the second region gated (R2) contain mature cells that were bigger in size and granularity. The MCF7 cells in R1 when un-treated or treated with ketoconazole and compound 51, showed higher expression of ICAM-1 when compared to quiescent, non-stimulated HUVECS. Whereas in R2, the ICAM-1 expression in MCF7 cells was equal to that shown in HUVECs, demonstrating that the expression of ICAM-1 in potentially more immature MCF7 cells is greater than the matured MCF7 cells and have similar levels of ICAM-1 as non-stimulated HUVECs.

However, mature MCF-7 cells in R2 had lower ICAM expression than HUVECs incubated in TNF-α which was not observed in the immature R1 region. This was also true following treatments with either the synthesised drugs or the control, ketoconazole.

The differences in the two discrete cell populations are not only due to their morphology but also basal expression of ICAM and also the ability to react to stimuli. These cells could be at different levels of maturity based on their morphology, but further assessments would have to be undertaken, before reaching a definitive conclusion. If we assume R1 was the immature region and R2 the mature region, we can say that immature MCF7 cells increase ICAM-1

expression in quiescent HUVECS, while HUVECs pre-treated with TNF-α, have increased ICAM-1 expression as a result of co-culturing with mature MCF7 cells.

In summary, all tumour cells studied had increased ICAM-1 expression compared to HUVECs when quiescent, furthermore, these levels of ICAM-1 expression remained significantly higher than even TNF-α stimulated HUVECS in every tumour cell line except for MCF7 cells. This pattern remained in the presence of either the synthesised drugs or control Ketoconazole.

5.3.5. Inhibitory effect of CYP17 inhibitors on ICAM-1 expression in tumour cells in co-culture

Cellular adhesion molecules are involved in tumour progression and metastasis (Banks *et al.,* 1993). ICAM-1 is associated with a number of inflammatory and immune responses, as well as with epithelial tumourigenesis (Pantel *et al.,* 1995). ICAM-1 is a cell adhesion molecule, but it also elicits a signalling response which may potentially enhance a metastatic phenotype (Hubbard and Rothelin, 2000). Increased expression of ICAM-1 correlates with an increased metastatic potential of prostate cancer (Gho *et al.,* 2001) and breast cancer cells (Rosette *et al.*, 2005).

Exposure to cytokines such as TNF-α or IFN-γ can increase the expression of ICAM-1 on tumour cells (Lee *et al.,* 2010; Chen *et al.,* 2011; Lassila and Komi, 2000). In this study we showed that TNF-α (10ng/mL) increased the expression of ICAM-1 in all tumour cell lines except DU145.

Ketoconazole and other inhibitors of CYP17 and other CYP1450 have been reported to decrease the cell adhesion and expression of cell adhesion molecules (Bild *et al,* 2004; Sasaki *et al.,* 2003). Ketoconazole, in this study, decreased the ICAM-1 expression in MCF7 cells which were co-cultured with activated HUVECs. However in DU145 and PC3 cells, ketoconazole did not change the expression of ICAM-1.

Looking at the synthesised CYP17 inhibitors, which had greater IC_{50s}, compound 38 decreased cell adhesions between HUVEC and DU145 cells but increased the ICAM-1 expression suggesting adhesion was via another molecule. However, augmented levels of ICAM-1 are important in the progression of other cancers

such as colon cancer, breast cancer, prostate cancer and others (Gallicchio, *et al.*, 2008; Hanlon *et al.,* 2002; Buitrago *et al.*, 2011; Hayes and Siegel, 2009; Georgolios *et al.,* 2006; Kammerer *et al.,* 2004), although the importance of ICAM in prostate cancer has not been comprehensively reported. As compound 38 was one of the most potent inhibitors of CYP17, decreasing adhesion between cancer and HUVECs, it is a useful tool for further investigation into the mechanism by which it can affect the adhesion process. Conversely, in the prostate cancer PC3 cells lines; the inhibitory compound 48 did not have any effect on either adhesion or the expression of ICAM-1.

In MCF7 cells, the adhesion between HUVECS and cancer cells was decreased following incubation with compound 51 alongside a decreased expression of ICAM-1 in MCF7 cells. This confirmed previous findings that inhibitors of cytochrome P450 enzyme decreased the expression of cell adhesion molecules (Sasaki *et al.,* 2003) and also adhesion between tumour cells and endothelial cell monolayer using CYP17 inhibitors (Bild *et al.,* 2004).

5.3.6. Inhibitory effect of CYP17 inhibitors on tumour cell:HUVEC complexes

As mentioned in the previous section, the inhibitors did affect both expression of ICAM and subsequent adhesion between HUVEC and tumour cells in culture following two hour co-culture. In general the CYP17 inhibitors reduced the adhesion of tumour cells on endothelial cells that was further confirmed by a decrease in the number of tumour-endothelial cell complexes upon washing the plate.

<u>DU145 cells:</u>

In the absence of stimulation by TNF-α, the number of DU145: HUVEC complexes were significantly decreased by compound 38 but not ketoconazole. However, with activation of HUVECs with TNF-α, the number of DU145: HUVEC complexes were decreased by both ketoconazole and compound 38. This shows that the treatment of DU145 cells with KTZ and compound 38 has reduced the adhesion ability of DU145 cells to HUVECs which results in decrease DU145: HUVEC complexes.

In contrast the ability of the other prostate cell line PC3 to form complexes with endothelial cells was not affected by KTZ, when the HUVEC were either stimulated with TNF, or quiescent. Similarly the inhibitory compound 48 did not decrease the number of PC3 and stimulated HUVECs complexes. Compound 48 was found to decrease complex number formation only when the HUVEC were non-stimulated. We can therefore conclude that the adhesive property of PC3 cells was not affected by KTZ and compound 48 to a great extent.

In the breast cancer cell lines, Ketoconazole and compound 51 decreased the number of MCF7: HUVEC complexes with un-stimulated and TNF-α stimulated HUVECs, demonstrating the effectiveness of these inhibitors etc.

In summary, the synthesised inhibitors of CYP17; compounds 38 and 51 decreased the number of complexes between tumour and non-stimulated HUVECs and between tumour and stimulated HUVECs. Compound 48 also reduced the number of PC3: HUVEC complexes in the absence of TNF-α. Ketoconazole was best at reducing the number of MCF7: HUVEC complexes.

A decrease in the number of tumour: endothelial complexes suggest a poor adhesion of tumour cells to endothelial cells. This confirmed the preliminary results of tumour cell adhesion in *ex vivo* models (chapter 4) that CYP17 inhibitors; compounds 38, 48 and 51 are better than the control drug ketoconazole in decreasing the adhesion of tumour cells to endothelial cell monolayers.

5.3.7. Total ICAM-1 levels in tumour cell: HUVEC complexes

To confirm the effect of CYP17 inhibitors on ICAM-1 expression within the tumour endothelial cell complex, we calculated the total ICAM-1 levels in a tumour: HUVECs complex by multiplying the PE-Cy5 ICAM-1 to PE-CD144/tumour cell FITC (triple staining). This would examine the ability of the inhibitors to alter ICAM-1 levels.

In the prostate cancer cell line, DU145 cells endothelial cell complexes, compound 38 significantly decreased the ICAM-1 levels with non-stimulated and stimulated HUVECs as compared to –TNF and +TNF controls respectively. There is therefore an association in the formation of the tumour cell-endothelial cell complex with a decrease in ICAM-1 surface expression on DU145 cells. Previous studies have

shown that inhibitors of cytochrome 450 enzymes decrease expression of adhesion molecules (Sasaki *et al.*, 2003).

The compounds 48 and 51 did not have any effect on expression of ICAM-1 on the other prostate cell line (PC3) or the breast cancer cell line (MCF7) respectively when they were co-cultured with non-stimulated and stimulated HUVECs.

We can summarise the adhesion of DU145 cells to HUVEC was decreased by compound 38. However the expression of ICAM-1 in DU145 cells was not affected as a result of treatment with compound 38. We can therefore conclude that compound 38 did not decrease the adhesion of DU145 cells by decreasing the expression of adhesion molecule, ICAM-1. Therefore there is a need to investigate other adhesion molecules and other adhesion mechanisms which can be targeted by CYP17 inhibitors.

5.4. Conclusion

The ICAM-1 expression in individual endothelial and tumour cells was significantly increased by TNF-α, unsurprisingly. Ketoconazole and synthesised inhibitors did not have any significant effect on ICAM-1 expression in tumour cells except compound 51 which decreased the expression of ICAM-1 in non-stimulated and stimulated breast cancer cell line, MCF7 cells.

For cells in co-culture, the prostate cancer cell lines, expressed more basal ICAM-1 when compared to non-stimulated and stimulated HUVECs, indeed the basal levels of ICAM-1 on DU145 cells were too elevated to analyse.

The tumour: endothelial cells complexes were significantly decreased by KTZ and synthesised CYP17 inhibitors in these cells, and although the levels of ICAM-1 on these cells were not decreased by the CYP17 inhibitors; compound 38, 41. We can therefore conclude that ketoconazole and synthesised CYP17 inhibitors decreased the adhesion of tumour cells but they did not affect the ICAM-1 levels in tumour cells. Therefore, investigation for other adhesion molecules e.g. Integrin, selectin or VCAM-1 can be carried out.

The effect of CYP17 inhibitors was different between prostate and breast cancer cell lines. The effect of inhibitors on breast cancer MCF7 cells was more

distinguishable as compared to DU145 and PC3 and could be perhaps due to initial low levels of ICAM-1 in these cells that could be stimulated and altered.

These results have highlighted differences between adhesion molecule expressions with cell lines of the same cancer type. This can be because these cancer lines are different metastasis of prostate cancer; PC3 cells are the bone metastasised prostate cancer cell lines whereas DU145 are the brain metastasised prostate cancer lines. The results also showed difference in adhesion molecule expression between different cancer type and that tumour adhesion cannot be assumed to have the same mechanisms in these cases.

6. SUMMARY AND CONCLUSION

In the this study, the development of radiometric enzyme assays (against 17α-OHase, lyase and 17β-HSD 3) has been undertaken involving the initial partial purification of the microsomal enzyme followed by the determination of kinetic parameters. Using the assay, a number of synthesised compounds have been evaluated and their initial screening data and IC_{50} values, for a number of the more potent inhibitors of CYP17 (hydroxylase and lyase) and 17β-HSD3 have also been determined.

A number of synthesised imidazole-based compounds have been tested for inhibitory activity against CYP17. The substituted benzyl imidazole, substituted sulfonate derivatives of 4-hydroxybenzyl imidazole and substituted phenyl ethanones have been shown as potent inhibitors of CYP17. The androsterone has been modified at different positions to synthesise a series of steroidal inhibitors of 17β-HSD 3. The series of transformed androstenedione and acetic acid-based derivatives of 4-hydroxy phenyl ketones have been shown as potent steroidal and non-steroidal inhibitors of 17β-HSD 3. However when compared, the inhibitors of CYP17 were found to be more potent than 17β-HSD3 inhibitors in inhibiting the enzymes activity. Therefore inhibitors of CYP17 were used in cell-based assays.

An MTT assay was performed in order to investigate the cytotoxicity of the synthesised CYP17 inhibitors which showed no effect of these inhibitors on the viability of non-cancerous and cancerous cell lines in most cases.

In this study, a tumour-endothelial cell adhesion model was developed. HUVECs were grown in monolayers on which tumour cells adhered. The present work showed that the inhibitors of enzyme CYP17, responsible for androgen production, decreased the adhesion of prostate and breast cancer cells on a non-stimulated and TNF-α- stimulated HUVEC monolayer. The anti-adhesion effect of the synthesised compounds was better than ketoconazole.

We can conclude the the novel synthesised CYP17 inhibitors exert similar effect on hormone-dependent and hormone-independent cancer cell lines.

We can also conclude that the basal expression of ICAM-1 on tumour cells is varied in different cancer cell types. An alteration in the ICAM-1 expression in response to different drug treatments depends on the basal levels of ICAM-1. TNF-α increases the basal expression of ICAM-1 in both endothelial and tumour cell lines.

We have also shown that co-culturing of tumour cells with endothelial cells causes an activation of endothelial cell monolayers that resulted in an increased endothelial cell expression of ICAM-1. The expression of ICAM-1 in tumour cells is higher than endothelial cells in a co-culture.

The CYP17 inhibitors did not decrease the expression of ICAM-1 in prostate cancer cell lines. However in the breast cancer cell line, compound 51 decreased the ICAM-1 expression.

The mechanism by which these compounds decreased cell adhesion and the expression of other adhesion molecules needs further investigation. As such, the CYP17 inhibitors used in this study, can also be investigated further for their effect on expression of other adhesion molecules such as integrin, selectins, cadherins and VCAM-1 etc. Different cell signalling cascades, for example growth factor receptor pathways and expression of various genes responsible for different proteins invovled in tumuor cell adhesion can also be targeted in future. It would also be interesting to study the effect of inhibitors of CYP17 inhibitors on a broad range of cancer cell lines and cell lines of similar origin.

7. PUBLICATIONS

- Shah, K., Jandu, B., **Abdullah, A.** and Ahmed, S. (2011). Synthesis, biochemical evaluation and rationalisation of the inhibitory activity of a range of derivatives of 2-imidazol-1-yl-1-phenyl-ethanone as potential novel inhibitors of 17α-hydroxylase/17, 20-lyase (p-$450_{17\alpha}$). Letters in Drug Design and Discovery, **8 (6):** 516-522.

- Le Gresley, A, **Abdullah, A.,** Chawla, D., Desai, P., Ghosh, U., Gollapalli, U., Kiran, M., Lafon, S. (2011). Diacrylamides as selective G-quadruplex ligands in *in vitro* and *in vivo* assays. MedChemComm, **2 (6):** 466-470.

- **Abdullah, A.,** Arrigoni, F., Snabaitis, A. and Freestone, N.S. (2010). Tumour cell adhesion on endothelial cell monolayers. Journal of Pharmacy and Pharmacology, **62(10):** 1496.

- Jandu, B., **Abdullah, A.,** Owen, C.P. and Ahmed, S. (2008). Novel inhibitors of the enzyme complex 17α-hydroxylase (17α-OHase) and 17,20-lyase in the fight against androgen-dependent prostate cancer. Journal of Pharmacy and Pharmacology, **60:** A-52.

8. CONFERENCE ABSTRACTS

- "Inhibitors of CYP17 and role of its inhibitors on tumour cell adhesion". Ammara Abdullah, Imran Shahid, Francesca I.F. Arrigoni, Andrew K. Snabaitis, Nicholas S. Freestone. UK-Pharmsci 2011, East Midlands conference centre, Nottingham, September 2011.

- "Quantification of tumour cell adhesion on endothelial cell monolayers". Ammara Abdullah, Francesca I.F. Arrigoni, Andrew K. Snabaitis, Nicholas S. Freestone. (2011). Physiology 2011, University of Oxford, July 2011.

- "Tumour cell adhesion on endothelial cell monolayers". Ammara Abdullah, Imran Shahid, Francesca I.F. Arrigoni, Andrew K. Snabaitis, Nicholas S. Freestone. UK-Pharmsci 2010, East Midlands conference centre, Nottingham, September 2010.

- "Continued search for potent inhibitors of 17α-hydroxylase/17, 20-lyase in the treatment of androgen-dependent prostate cancer". Priya K. Acharya, Ammara Abdullah, Imran Shahid, Caroline, P. Owen, Sabbir Ahmed. 42nd IUPAC Congress Chemistry Solution 2009, Glasgow, August 2009.

- "Novel inhibitors of the enzyme complex 17α-hydroxylase/17, 20-lyase". Ammara Abdullah, Baljeet Jandu, Caroline, P. Owen, Sabbir Ahmed. RSC South East Regional Organic Meeting, Department of Chemistry, University College London, December 2008.

- "Novel inhibitors of the enzyme complex 17α-hydroxylase (17α-OHase) and 17, 20-lyase in the fight against androgen-dependent prostate cancer". Ammara Abdullah, Baljeet Jandu, Caroline, P. Owen, Sabbir Ahmed. British Pharmaceutical Conference, Manchester, September 2008.

9. REFERENCES

- Abate-Shen, C. and Shen, M. M. (2000). Molecular genetics of prostate cancer. Genes and Development, **14:** 2410-2434.

- Abate-Shen, C., Shen, M. M. and Gelmann, E. (2008). Integrating differentiation and cancer: The Nkx3.1 homeobox gene in prostate organogenesis and carcinogenesis. Differentiation, **76:** 717–727.

- Abraham, J. and Staffurth, J. (2011). Hormonal therapy for cancer. Medicine, **39 (12):** 723-727.

- Aggarwal, S., Thareja, S., Verma, A., Bhardwaj, T. R. and Kumar, M. (2010). An overview on 5α-reductase inhibitors. Steroids, **75:** 109–153.

- Ahmed, S. (1995). Molecular modelling of inhibitors of 17α-hydroxylase- a novel approach. Biorganic Medicinal Chemistry, **5:** 2795-2800.

- Ahmad, M., Theofanidis, P. and Medford, R.M. (1998). Role of activating protein-1 in the regulation of the vascular cell adhesion molecule-1 gene expression by tumor necrosis factor-alpha. Journal of Biological Chemistry, **273:** 4616–4621.

- Ahmed, S. (1999). A novel molecular modelling study of inhibitors of the 17α-hydroxylase component of the enzyme system 17α-hydroxylase/17,20-lyase(P-45017α). Biorganic Medicinal Chemistry, **7**: 1487-1496.

- Ahmed, S. (2004). The use of the novel substrate–heme complex approach in the derivation of a representation of the active site of the enzyme complex 17α-hydroxylase and 17, 20-lyase. Biochemical and Biophysical Research Communications, **316:** 595–598.

- Ahmed, S., Shahid, I., Dhanani, S. and Owen, C.P. (2009). Synthesis and biochemical evaluation of a range of sulfonated derivatives of 4-hydroxybenzyl imidazole as highly potent inhibitors of rat testicular 17α-hydroxylase/17, 20-lyase (P-45017α). Bioorganic and Medicinal Chemistry Letters, **19:** 4698–4701.

- Akhtar, M., Calder, M. R., Corina, D. L. and Wright, J. N. (1982). Mechanistic studies on C-19 demethylation in oestrogen biosynthesis. Biochemical Journal, **201:** 569–580.

- Akhtar, M., Corina, D., Miller, S., Shyadehi, A. Z. and Wright, J. N. (1994a). Mechanism of the acyl-carbon cleavage and related reactions catalysed by multifunctional P-450s: Studies on cytochrome P-$450_{17\alpha}$. Biochemistry, **33:** 4410-4418.

- Akhtar, M., Corina, D., Miller, S., Shyadehi, A. Z. and Wright, J. N. (1994b). Incorporation of label from $^{18}O_2$ into acetate during side-chain cleavage catalysed by cytochrome P-$450_{17\alpha}$ (17α-hydroxylase-17, 20-lyase). Journal of the Chemical Society, Perkin Transactions, **1:** 263-267.

- Akhtar, M., Lee-Robichaud, Akhtar, M. E. and Wright, J. N. (1997). The impact of aromatase mechanism on other P450s. Journal of Steroid Biochemistry and Molecular biology, **61 (3-6):** 127-132.

- Akhtar, M., Wright, J. N. and Lee-Robichaud, P. (2011). A review of mechanistic studies on aromatase (CYP19) and 17α-hydroxylase-17, 20-lyase (CYP17). Journal of Steroid Biochemistry and Molecular Biology, **125:** 2-12.

- Al-Mehdi, A. B., Tozawa, K., Fisher, A. B., shientag, L., Lee, A. and Muschel, R. J. (2000). Intravascular origin of metastasis from the proliferation of endothelium-attached tumor cells: A new model for metastasis. Nature Medicine, **6 (1):** 100-102.

- Angst, B. D., Marcozzi, C. and Magee, A. I. (2001). The cadherin superfamily: diversity in form and function. Journal of Cell Science, **114:** 629-641.

- Antonarakis, E. S., Carducci, M. A. and Eisenberger, M. A. (2010). Novel targeted therapeutics for metastatic castration-resistant prostate cancer. Cancer letters, **291:** 1-13.

- Armutlu, P., Ozdemir, M. E., Ozdas, S., Kavakli, I. H. and Turkay, M. (2009). Discovery of novel CYP17 inhibitors for the treatment of prostate cancer with structure-based drug design. Letters in Drug Design and Discovery, **6:** 337-344.

- Arya, M., Bott, S. R., Shergill, I. S., Ahmed, H. U., Williamson, M., Patel, H. R. (2006).The metastatic cascade in prostate cancer. Surgical Oncology, **15:** 117–128

- Atkins, G. L. and Nimmo, I. A. (1975). A comparison of seven methods for fitting the michaelis-menten equation. Biochemical Journal, **149:** 775-777.

- Attard, G., Belldegrun, A. S. and Bono, J. S. D. (2005). Selective blockade of androgenic steroid synthesis by novel lyase inhibitors as a therapeutic strategy for treating metastatic prostate cancer. British Journal of Urology International, **96:** 1241–1246.

- Attard, G., Reid, A. H. M., Hern, R. A., Parker, C., Oommen, N. B., Folkerd, E., Messiou, C., Molife, L. R., Maier, G., Thompson, E., Olmos, D., Sinha, R., Lee, G., Dowsett, M., Kaye, S. B., Dearnaley, D., Kheoh, T., Molina, A. and Bono, J. S. D. (2009). Selective inhibition of CYP17 With abiraterone acetate is highly active in the treatment of castration-resistant prostate cancer. Journal of Clinical Oncology, **27:** 3742-3748.

- Auchus, R. J. and Miller, W. L. (1999). Molecular modelling of human P45017α (17α-hydroxylase/17,20-lyase): Insights into reaction mechanisms and effects of mutations. Molecular Endocrinology, **13**: 1169-1182.

- Aylon, Y. and Oren, M. (2011). New plays in the p53 theater. Current Opinion in Genetics & Development, **21:** 86–92.

- Ayub, M. and Levell, M. J. (1987). Inhibition of testicular 17α-hydroxylase and 17, 20-lyase but not 3β-hydroxysteroid dehydrogenase-isomerase or 17β-hydroxysteroid oxidoreductase by ketoconazole and other imidazole drugs. Journal of Steroid Biochemistry, **28:** 521-531.

- Balwani, S., Nandi, D., Jaisankar, P. and Ghosh, B. (2011). 2-Methyl-pyran-4-one-3-O-β-D-glucopyranoside isolated from leaves of Punica granatum inhibits the TNFa-induced cell adhesion molecules expression by blocking nuclear transcription factor-kB (NF-kB). Biochimie, **93:** 921-930.

- Bander, N. H., Yao, D., Liu, H., Chen, Y. T., Steiner, M., Zuccaro, W. and Moy, P. (1997). MHC class I and II expression in prostate carcinoma and modulation by interferon-alpha and -gamma. Prostate, **33 (4):** 233-239.

- Banks, R. E., Gearing, A. J. H., Hemingway, I. K., Norfolk, D. R., Perren, T. J. and Selby, P. J. (1993). Circulating intercellular adhesion molecule-1 (ICAM-1), E-selectin and vascular cell adhesion molecule-1 (VCAM-1) in human malignancies. British Journal of Cancer, **68:** 122-124.

- Basson, M. D. (2008). An intracellular signal pathway that regulates cancer cell adhesion in response to extracellular forces. Cancer Research, 68: 2-4.

- Batson, O. V. (1995). Detection of circulating tumour cells in patients with localised and metastatic prostatic carcinoma: clinical implications. Journal of Clinical Oncology, **13**: 1195–1200.

- Bayer-Garner, I. B. And Smoller, B. (2000). Androgen receptors: a marker to increase sensitivity for identifying breast cancer in skin metastasis of unknown primary site. Modern Pathology, **13 (2):** 119–122.

- Beitz, J. and Calabresi, P. (1993). P. Calabresi, P. Schein (Eds.), Medical Oncology, McGraw-Hill Inc., New York (1993).

- Berx, G. and Roy, F. V. (2009). Involvement of members of the cadherin superfamily in cancer. Cold Spring Harbor Perspectives in Biology, **1:** 1-27.

- Bianco, R., Melisi, D., Ciardiello, F. and Tortora. G. (2006). Key cancer cell signal transduction pathways as therapeutic targets. European Journal of Cancer, **42:** 290-294.

- Bild, T., Jose, J. and Hartmann, R. W. (2004). Discovery of Inhibitors of MCF-7 tumour cell adhesion to endothelial cells and investigation on their mode of action. Archiv der Pharmazie, **337 (12):** 687-694.

- Bjornsti, M. A. and Houghton, P. J. (2004). The TOR pathway: a target for cancer therapy. Nature Review Cancer, **4:** 335–348.

- Bookstein, R., MacGrogan, D., Hilsenbeck, S. G., Sharkey, F.and D. C. Allred. (1993). p53 Is Mutated in a Subset of Advanced-Stage Prostate Cancers. Cancer Research, **53:** 3369-3373.

- Bourdillon, M.C., Poston, R.N., Covacho, C., Chignier, E., Bricca, G. and McGregor, J. L. (2000). ICAM-1 deficiency reduces atherosclerotic lesions in double-knockout mice (ApoE$^{-/-}$/ICAM-1$^{-/-}$) fed a fat or a chow diet. Arteriosclerosis, Thrombosis and Vascular Biology, **20:** 2630–2635.

- Bowen, C., Bubendorf, L., Voeller, H. J., Slack, R., Willi, N., Sauter, G., Gasser, T. C., Koivisto, P., Lack, E. E., Kononen, J., Kallioniemi, O. P. and Gelmann, E. P. (2000). Loss of NKX3.1 expression in human prostate cancers correlates with tumor progression. Cancer Research, **60**: 6111–6115.

- Box, C., Rogers, S. J., Mendiola, M. and Eccles, S. A. (2010). Tumour-microenvironmental interactions: paths to progression and targets for treatment. Seminars in Cancer biology, **20 (3):** 128-138.

- Brahimi-Horn, C. and Pouyssegur, J. (2006). The role of the hypoxia-inducible factor in tumour metabolism growth and invasion. Bulletin du Cancer, **93 (8):** 10073-10080.

- Brodie, A. M. H. And Lih-Yuh, W. (1987). *In vitro* and *in vivo* studies with aromatase inhibitor 4-hydroxyandrostenedione. Stroids, **50 (1–3)**: 89–103.

- Brooks, S. A., Browne, H. J. L., Carter, T. M., Kinch, C. E. And Hall, D. M. S. (2010). Molecular interactions in cancer cell metastasis. Acta Histochemica, **112:** 3-25.

- Brueggemeier, R. W., (2004). Aromatase inhibitors: New endocrine treatment of breast cancer. Seminars in Reproductive Medicine, **22(1):** 31-43.

- Brueggemeier, R. W., Hackett, J. C. and Diaz-Cruz, E. S. (2005). Aromatase inhibitors in the treatment of breast cancer. Endocrine Reviews, **26(3):** 331–345.

- Bruno, R. D., and Njar, V. C. O. (2007). Targeting cytochrome P450 enzymes: A new approach in anti-cancer drug development. Bioorganic and Medicinal Chemistry, **15:** 5047-5060.

- Budinsky, A. C., Brodowicz, T., Wiltschke, C., Czerwenka, K., Michl, I., Krainerand, M. and Zielinski, C. C. (1997). Decreased expression of ICAM-1 and its induction by tumor necrosis factor on breast-cancer cells in vitro. International Journal of Cancer, **71:** 1086–1090.

- Buitrago, D., Keutgen, X. M., Crowley, M., Filicori, F., Aldailami, H., Hoda, R., Liu, Y. F., Hoda, R. S., Scognamiglio, T., Jin, M. Fahey, T. J. and Zarnegar, R. (2011). Intercellular adhesion molecule-1 (ICAM-1) is upregulated in aggressive papillary thyroid carcinoma. Annals of Surgical Oncology, **19:** 973–980.

- Buul, J. D. V. and Hordijk, P. L. (2004). Signaling in leukocyte transendothelial migration. Arteriosclerosis, Thrombosis, and Vascular Biology, **24:** 824-833.

- Byrne, G. J., Ghellal, A., Iddon, J., Blann, A. D., Venizelos, V., Kumar, S., Howell, A., Bundred, N. J. (2000). Serum soluble vascular cell adhesion molecule-1: role as a surrogate marker of angiogenesis. Journal of the National Cancer Institute, **92 (16):** 1329-1336.

- Calia, R., Appel, J. Z. and Lefer, A. M. (1998). Leukocyte-endothelium interaction during the early stages of hypercholesterolemia in the rabbit: Role of P-selectin, ICAM-1, and VCAM-1. Arteriosclerosis, Thrombosis and Vascular Biology, **18:** 1093–1100.

- Cancer Research UK (2012).

- Cano, P., Godoy, A., Escamilla, R., Dhir, R. and Onate, S. A. (2007). Stromal–epithelial cell interactions and androgen receptor-coregulator recruitment is altered in the tissue microenvironment of prostate cancer. Cancer Research, **67 (2):** 511- 519.

- Cantley, L. C. (2002). The phosphoinositide 3-kinase pathway. Science, **296:** 1655–1657.

- Carracedo, A., Alimonti, A. and Pandolfi, P. P. (2011). PTEN level in tumour suppression: How much is too little. Cancer Research, **71:** 629-633.

- Catz, S. D. and Johnson, J. L. (2003). BCL-2 in prostate cancer: A minireview. Apoptosis, **8:** 29–37.

- Cavallaro. U. and Christofori, G. (2004). Cell adhesion and signalling by cadherins and Ig-CAMs in cancer. Nature Reviews, **4:** 118-132.

- Chambers, A. F., Groom, A. C. And MacDonald, I. C. (2002). Dissemination and growth of cancer cells in metastatic site. Nature Reviews, **2:** 563-572.

- Chan, F. C. Y., Potter, G. A., Barrie, S. E., Haynes, B. P., Rowlands, M. G., Houghton, J. and Jarman, M. (1996). 3- and 4-pyridylalkyl adamantanecarboxylates: Inhibitors of human cytochrome P45017α (17α-hydroxylase/ C-17, C-20-lyase). Potential non-steroidal agents for the treatment of prostatic cancer. Journal of Medicinal Chemistry, **39:** 3319-3323.

- Chen, C. C. and Manning, A. M. (1995). Transcriptional regulation of endothelial cell adhesion molecules: A dominant role for NF-kappa B. Agents and Actions Supplements, **47:** 135–141.

- Chen, C., Mobley, J. L., Dwir, O., Shimron, F., Grabovsky, V., Lobb, R. R., Shimizu, Y. and Alon, R. (1999). High affinity very late antigen-4 subsets expressed on T Cells are mandatory for spontaneous adhesion strengthening but not for rolling on VCAM-1 in Shear Flow. Journal of Immunology, **162:** 1084-1095.

- Chen, C. D., Welsbie, D. S., Tran, C., Baek, S. H., Chen, R., Vesella, R., Rosenfeld, M. G. And Sawyers, C. L. (2004). Molecular determinants of resistance to antiandrogen therapy. Nature Medicine, **10:** 33 – 39.

- Chen, J. T., Liang, J. B., Chou, C. L., Chien, M. W., Shyu, R. C., Chou, P. I. and Lu, D. W. (2006). Glucosamine sulfate inhibits TNF-α and IFN-γ induced production of ICAM-1 in human retinal pigment epithelial cells in vitro. Investigative Ophthalmology and Visual Science, **47:** 664–672.

- Chen, Y. C., Lu, P. H., Hsu, J. L., Yu, C. C. and Guh, J. H. (2011). ICAM-1 and AMPK regulate cell detachment and apoptosis by N-methyl-N'-nitro-N-nitrosoguanidine, a widely spread environmental chemical, in human hormone-refractory prostate cancers. Toxicology and Applied Pharmacology, **257:** 412–419.

- Chotard-Ghodsnia, R., Haddad, O., Leyrat, A., Drochon, A., Verdier, C. and Duperray, A. (2007). Morphological analysis of tumour cell/ endothelial cell interactions under shear flow. Journal of Biomechanics, **40 (2):** 335-344.

- Christiansen, J. J. and Rajasekaran, A. Y. (2006). Reassessing epithelial to mesenchymal transition as a prerequisite for carcinoma invasion and metastasis. Cancer Research, **66 (17):** 8319-8326.

- Christofori, G. and Semb, H. (1999). The role of the cell-adhesion molecule E-cadherin as a tumour-suppressor gene. Trends in Biochemical Sciences, **24(2):** 73-76.

- Christofori, G. (2006). New signals from the invasive front. Nature, **441:** 444-450.

- Chumsri, S., Howes, T., Bao, T., Sabnis, G. and Brodie, A. (2011). Aromatase, aromatase inhibitors, and breast cancer. Journal of Steroid Biochemistry & Molecular Biology, **125:** 13-22.

- Cinamon, G., Shinder, V., Shamri, R. and Alon, R. (2004). Chemoattractant signals and β2 occupancy at apical endothelial contacts combine with shear stress signals to promote transendothelial neutrophil migration. Journal of Immunology, **173**: 7282–7291.

- Colleoni, M., Gelber, S., Goldhirsch, A., Aebi, S., Castiglione-Gertsch, M., Price, K. N., Coates, A. S. and Gelber, R.D. (2006). Tamoxifen after adjuvant chemotherapy for premenopausal women with lymph node-positive breast cancer: International Breast Cancer Study Group Trial 13-93. Journal of Clinical Oncology, **24(9):** 1332–1341.

- Collins, I. and Garrett, M. D. (2005). Targeting the cell division cycle in cancer: CDK and cell cycle checkpoint kinase inhibitors. Current Opinion in Pharmacology, **5:** 366–373.

- Constantinou, A. I., Krygier, A. E. and Mehta, R. R. (1998). Genistein induces maturation of cultured human breast cancer cells and prevents tumor growth in nude mice. American Journal of Clinical Nutrition, **68:** 1426–1430.

- Constantin, G., Majeed, M., Giagulli, C., Piccio, L., Kim, J. Y., Butcher, E. C., and Laudanna. C. (2000). Chemokines trigger immediate β2 integrin affinity and mobility changes: Differential regulation and roles in lymphocyte arrest under flow. Immunity, **13:** 759–769.

- Coombes, R. C., Kilburn, L. S., Snowdon, C. F., Paridaens, R., Coleman, R. E., Jones, S. E., Jassem, J., Van de Velde, C. J.H., Delozier, T., Alvarez, I., Del Mastro, L., Ortmann, O., Diedrich, K., Coates, A. S., Bajetta, E., Holmberg, S. B., Dodwell, D., Mickiewicz, E., Andersen, J., Lønning, P. E., Cocconi, G., Forbes, F., Castiglione, M., Stuart, N., Stewart, A., Fallowfield, L. J., Bertelli, G., Hall, E., Bogle, R. G., Carpentieri, M., Colajori, E., Subar, M., Ireland, E. and Bliss, J. M. (2007). Survival and safety of exemestane versus tamoxifen after 2–3 years tamoxifen treatment (Intergroup Exemestane Study): a randomised controlled trial. Lancet, **369:** 559–570.

- Cooper, C. R., Bhatia, J. K., Muenchen, H. J., McLean, I., Hayasaka, S., Taylor, J., Poncza, P. J. and Pienta, K. J. (2002). The regulation of prostate cancer cell adhesion to human bone marrow endothelial cell monolayers by androgen dihydrotestosterone and cytokines. Clinical and Experimental Metastasis, **19 (1):** 25-33.

- Cornish-Bowden, A. (1974). Statistical considerations in the estimation of enzyme kinetic parameters by the direct linear plot and other methods. Biochemical Journal, **139:** 721-730.

- Cristofanilli, M., Valero, V., Mangalikm A., Royce, M., Rabinowitz, I., Arena, F. P., Kroener, J. F., Curcio, E., Watkins, C., Bacus, S., Cora, E. M., Anderson, E. and Magill, P.J. Phase II, randomized trial to compare anastrozole combined with gefitinib or placebo in postmenopausal women with hormone receptor-positive metastatic breast cancer. Clinical Cancer Research,**16(6):** 1904-1914.

- Culig, Z., Hobisch, A., Cronauer, M. V., Radmayr, C., Trapinan, J., Ilittniair, A., Bartsch, G. and Klocker, H. (1994). Androgen receptor activation in prostatic tumor cell lines by insulin-like growth factor-I, keratinocyte growth factor, and epidermal growth factor. Cancer Research, **54:** 5474-5478.

- Cuzick, J., Forbes, J. F., Sestak, I., Cawthorn, S., Hamed, H., Holli, K. and Howell, A. (2007). Long-term results of tamoxifen prophylaxis for breast cancer- 96-month follow-up of the randomized IBIS-I trial. Journal of National Cancer Institute, **99(4):** 272-282.

- Cuzick, J., Sestak, I., Baum, M., Buzdar, A., Howell, A., Dowsett, M. and Forbes, J. F. (2010). Effect of anastrozole and tamoxifen as adjuvant treatment for early-stage breast cancer: 10-year analysis of the ATAC trial. Lancet Oncology, **11:** 1135–1141.

- Dano, K., Behrendt, N., Hoyer-Hansen, G., Johnsen, M., Lund, L. R., Ploug, M. and Romer, J. (2005). Plasminogen activation and cancer. Journal of Thrombosis and Haemostasis, **93:** 676 – 681.

- Day, J. M., Tutill, H. J., Purohit, A. and Reed, M. J. (2008). Design and validation of specific inhibitors of 17β-hydroxysteroid dehydrogenases for therapeutic application in breast and prostate cancer, and in endometriosis. Endocrine-Related Cancer, **15:** 665–692.

- Day, J. M., Tutill, H. J., Foster, P. A., Bailey, H. V., Heaton, W. B., Sharland, C. M., Vicker, N., Potter, B. V. L., Purohita, A. and Reed, M. J. (2009). 'Development of hormone-dependent prostate cancer models for the evaluation of inhibitors of 17β-hydroxysteroid dehydrogenase Type 3'. Molecular and Cellular Endocrinology, **301:** 251–258.

- De Bono, J., Nazir, S., Ruparelia, N., Bashir, Y., Betts, T. and Rajappan, K. (2010). Prednisone plus cabazitaxel or mitoxantrone for metastatic castration-resistant prostate cancer progressing after docetaxel treatment: a randomised open-label trial. Lancet, **376:** 1147–1154.

- Defazio, G., Trojano, M., Ribatti, D., Nico, B., Giorelli, M., De Salvia, R. Russo, G., Roncali, L. and Livrea, P. (1998). Journal of Neuroimmunology, **88:** 13–20.

- De Jong, K. P., Gouw, A. S., Peeters, P. M., Bulthuis, M., Menkema, L., Porte, R. J., Slooff, M. J., Van Goor, H. and Van den Berg, A. (2005). P53 mutation analysis of colorectal liver metastases: relation to actual survival, angiogenic status, and p53 overexpression. Clinical Cancer Research, **11(11):** 4067-73.

- Del Re, M., Michelucci, A., Simi, P. and Danesi, R. (2011). Pharmacogenetics of anti-estrogen treatment of breast cancer Cancer Treatment Reviews, **38 (5):** 442-450.

- Denisov, I. G., Makris, T. M., Sligar, S. G. and Schlichting, I. (2005). Structure and chemistry of cytochrome P450. Chemical Reviews, **105:** 2253–2278.

- Deong, M. M., Nolte, I. M., Meerman, G. J. T. Van der Graaf, W. T.A., Oosterwijk, J. C., Kleibeuker, J. H., Schaapveld, M. and De Vries, E. G. E. (2002). Genes other than BRCA1 and BRCA2 involved in breast cancer susceptibility. Journal of Medical Genetics, **39:** 225–242.

- Deryugina, E. I. and Quigley, J. P. (2006). Matrix metalloproteinases and tumor metastasis. Cancer and Metastasis Reviews, **25:** 9–34.

- Ding, Y. B., Chen, G. Y., Xia, J. G., Zang, X. W., Yang, H. Y. and Yang, L. (2003). Association of VCAM-1 overexpression with oncogenesis, tumor angiogenesis and metastasis of gastric carcinoma. World Journal of Gastroenterology, **9(7):** 1409-1414.

- Dorgan, J. F. Stanczyk, F. Z., Kahle, L. L. and Brinton, L. A. (2010). Prospective case-control study of premenopausal serum estradiol and testosterone levels and breast cancer risk. Breast Cancer Research, 12 (R98): 1-8.

- Dustin, M. L. and Springer, T. A. (1988). Lymphocyte function associated antigen-1 (LFA-1) interaction with intercellular adhesion molecule-1 (ICAM-1) is one of at least three mechanisms for lymphocyte adhesion to cultured endothelial cells. Journal of cell Biology, **107**: 321-331.

- Dymicka-Piekarska, V. And kemona, H. (2009). Does colorectal cancer clinical advancement affect adhesion molecules (sP- selectin, sE- selectin and ICAM-1) concentration? Thrombosis Research, **124 (1)**: 80–83.

- Eadie, G. S. (1942). The inhibition of cholinesterase by physostigmine and prostigmine. Journal of Biological Chemistry, **146:** 85–93.

- Eales, L. J. Immunology for life student: a basic introduction: a student-centred learning approach, Chichester, New-York, John Wiley and sons, 1997.

- Early Breast Cancer Trialists' Collaborative Group (EBCTCG). (2005). Effects of chemotherapy and hormonal therapy for early breast cancer on recurrence and 15-year survival: an overview of the randomised trials. The Lancet, **365 (9472)**: 1687 – 1717.

- Early Breast Cancer Trialists' Collaborative Group (EBCTCG). (2011). Relevance of breast cancer hormone receptors and other factors to the efficacy of adjuvant tamoxifen: patient-level meta-analysis of randomised trials. Lancet, **378:** 771–84.

- Effert, P., McCoy. R., Abdel–Hamid. M., Flynn.K., Zhang. Q., Busson. P., Tursz. T., Liu. E. and Raab–Traub, N. (1992). Alterations of the p53 gene in nasopharyngeal carcinoma. Journal of Virology, **66:** 3768–3775.

- Elgie, A. W., Sargent, J. M., Taylor, C. G., and Williamson, C. (1996). An in vitro study of blast cell metabolism in acute myeloid leukaemia using that MTT assay. Leukemia Research, **20 (5):** 407-413.

- Eliassen, A. H., Missmer, S. A., Tworoger, S. S., Spiegelman, D., Barbieri, R. L., Dowsett, M. and Hankinson, S. E. (2006). Endogenous steroid hormone concentrations and risk of breast cancer among premenopausal women. Journal of the National Cancer Institute, **98 (19):** 1406- 1415.

- Engelman, J. A., Luo, J. and Cantley, L. C. (2006). The evolution of phosphatidylinositol 3-kinases as regulators of growth and metabolism. Nature Reviews Genetics, **7:** 606–619.

- Evans R. M. (1988). The steroid and thyroid hormone receptor superfamily. Science, **240:** 889–95.

- Feldman, B. J. and Feldman, D. (2001). The development of androgen-independent prostate cancer. Nature Review Cancer, **1:** 34- 45.

- Feng, S., Cen, J., Huang, Y., Shen, H., Yao, L., Wang, Y. and Chen, Z. (2011).Matrix metalloproteinase-2 and 9 secreted by leukemic cells increase the permeability of blood-brain barrier by disrupting tight junction proteins. PLoS ONE **6(8):** e20599.

- Ferrara, N. and Davis-Smyth, T. (1997). The biology of vascular endothelial growth factor. Endocrine Reviews, **18:** 4-25.

- Ferrara, N. (2002). Role of vascular endothelial growth factor in physiologic and pathologic angiogenesis: Therapeutic implications. Seminars in Oncology, **29 (6)**: 10–14.

- Fidler, I. J. (2003). The pathogenesis of cancer metastasis: the 'seed and soil' hypothesis revisited. Nature Reviews, **3:** 1-6.

- Filling, C., Berndt, K. D., Benach, J., Knapp, S., Prozorovski, T., Nordling, E., Ladenstein, R., Jornvall, H. and Oppermann, U. (2002). Critical residues for structure and catalysis in short-chain dehydrogenases/reductases. The Journal of Biological Chemistry, **277 (28):** 25677–25684.

- Fink, B. E., Gavai, A. V., Tokarski, J. S., Goyal, B., Misra, R., Xiao, H. Y., Kimball, S. D., Han, W. C., Norris, D., Spires, T. E., You, D., Gottardis, M. M., Lorenzi, M. V., and Vite, G. D. (2006). Identification of a novel series of tetrahydrodibenzazocines as inhibitors of 17β-hydroxysteroid dehydrogenase type 3. Bioorganic and Medicinal Chemistry Letters, **16:** 1532–1536.

- Fischera, D., Lib, Y., Ahlemeyerc, B., Krieglsteinc, J. and Kissel, T. (2003). In vitro cytotoxicity testing of polycations: influence of polymer structure on cell viability andhemolysis. Biomaterials, **24:** 1121–1131.

- Folkman, J. (1995). Angiogenesis in cancer, vascular, rheumatoid and other disease. Nature Medicine, **1**: 27-30.

- Folkman, J. (2006). Angiogenesis. Annual Review of Medicine, **57:** 1-18.

- Forsythe J. A., Jiang, B. H., Iyer, N. V., Agani, F., Leung, S. W., Koos, R. D. and Semenza, G. L. (1996). Activation of vascular endothelial growth factor gene transcription by hypoxia-inducible factor 1. Molecular and Cellular Biology, **16:** 4604-4613.

- Francavilla, C., Maddaluno, L. and Cavallaro, U. (2009). The functional role of cell adhesion molecules in tumour angiogenesis. Seminars in Cancer Biology, **19:** 298–309.

- Fraser, H. M. and Lunn, S. F (2000). Angiogenesis and its control in the female reproductive system. British Medical Bulletin, **56:** 787-797.

- Freimoser, F. M., Jakob, C. A., Aaebi, M., and Tuor, U. The MTT [3-(4, 5-dimethylthiazol-2-yl)-2, 5-diphenyltetrazolium Bromide] assay is a fast and reliable method for colorimetric determination of fungal cell densities. Applied and Environmental Microbiolgy, **65 (8):** 3727–3729.

- Gallicchio, M., Rosa, A. C., Dianzani, C., Brucato, L., Benetti, E., Collino, M. And Fantozzi, R. (2008). Celecoxib decreases expression of the adhesion molecules ICAM-1 and VCAM-1 in a colon cancer cell line (HT29). British Journal of Pharmacology, **153 (5):** 870-878.

- Gassmann, P, Kang, M. L., Mees, S. T. and Haier, J. (2010). In vivo tumour cell adhesion in the pulmonary microvasculature is exclusively mediated by tumour cell-endothelial cell interaction. BMC cancer, **10 (177):** 1-11.

- Gelmann, E. P. (2002). Molecular biology of the androgen receptor. Journal of Clinical Oncology, **20 (13):** 3001-3015.

- Geng J. G. (2003). Interaction of vascular endothelial cells with leukocytes, platelets and cancer cells in inflammation, thrombosis and cancer growth and metastasis. Acta Pharmacologica Sinica, **24:** 1297–1300.

- Georgolios, A. Batistatou, N. Bonitsism, D. Stagikas, L and Charalabopoulos, M. K (2006). The role of intercellular adhesion molecule-1 in head and neck cancer. A. Experimental Oncology, **28 (4):** 270–274.

- Gho, Y. S., Kim, P. N., Li, H. C., Elkin, M. and Kleinman, H. K. (2001). Stimulation of tumor growth by human soluble intercellular adhesion molecule-1. Cancer Research, **61:** 4253–4257.

- Ghossein, R.A., Scher, H.I., Gerald, W.L., Kelly, W.K., Curley, T., Amsterdam, A., Zhang, Z.F. and Rosai, J. (1967). The vertebral system of veins as a means for cancer dissemination. Progress in Clinical Cancer, **3:** 1-18.

- Giavazzi, R., Chirivi, R. G. S., Garofalo, A., Rambaldi, A., Hemingway, I., Pigott, R. and Gearing, A. J. H. (1992). Soluble intercellular adhesion molecule 1 is released by human melanoma cells and is associated with tumor growth in nude mice1. Cancer Research, **52:** 2628-2630.

- Gibson, G. G. and Skett, P. Introduction to drug metabolism, 3rd edition, Cheltenham; Nelson Thornes, 2001.

- Giovannucci, E., Liu, Y., Platz, E. A., Stampfer, M., J. and Willett, W. C. (2007). Risk factors for prostate cancer incidence and progression in the health professionals follow-up study. International Journal of Cancer, **121(7):** 1571–1578.

- Gobbi, G., Cavalli, A., Negri, M., Schewe, K. E., Belluti, F., Piazzi, L., Hartmann, R. W., Recanatini, M. and Bisi, A. (2007). Imidazolylmethylbenzophenones as highly potent aromatase inhibitor. Journal of Medicinal Chemistry, **50 (15):** 3420–3422.

- Golias, C., Charalabopoulos, A., Peschos, D., Maritsi, D., Charalabopoulas, K and Batistatou, A. (2005). Adhesion molecules in cancer invasion and metastasis. Hippokratia, 9 (3): 106-114.

- Gout, S. and Huot, J. (2008). Role of cancer microenvironment in metastasis: Focus on colon cancer. Microenvironment, **1:** 69–83.

- Grantab, R., Sivananthan, S. And Tannock, I. F. (2006).The penetration of anticancer drugs through tumour tissue as a function of cellular adhesion and packing density of tumour cells. Cancer Research, **66:** 1033–1039.

- Gregory, C. W., Johnson, R. T., Mohler, J. L., French, F. S. and Wilson, E. M. (2001). Androgen receptor stabilization in recurrent prostate cancer is associated with hypersensitivity to low androgen. Cancer Research, **61:** 2892-2898.

- Haass, N. K., Smalley, k. S., Li, L. and Herlyn, M. (2005). Adhesion, migration and communication in melanocytes and melanoma. Pigment Cell Research, **18 (3):** 150–159.

- Habermann, B. F. (2003). Integrin adhesion receptors in tumour metastasis. Clinical & Experimental Metastasis, **20:** 203–213.

- Haddad, O., Chotard-Ghodsnia, R., Verdier, C. and Duperray, A. (2010). Tumor cell/endothelial cell tight contact upregulates endothelial adhesion molecule expression mediated by NFkappaB: differential role of the shear stress. Experimental Cell Research, **316 (2):** 615-626.

- Haidar, S., Ehmer, P. B., Barassin, S., Hartmann, C. B. and Hartmann, R. W. (2003). Effects of novel 17α-hydroxylase/C17, 20-lyase (P450 17, CYP 17) inhibitors on androgen biosynthesis in vitro and in vivo. Journal of Steroid Biochemistry and Molecular Biology, **84:** 555–562.

- Haider, S. M., Patel, J. S., Poojari, C. S. and Neidle, S. (2010). Molecular modeling on inhibitor complexes and active-site dynamics of cytochrome P450 C17, a target for prostate cancer therapy. Journal of Molecular Biology, **400:** 1078–1098.

- Hakki, T. and Bernhardt, R. (2006). CYP17 and CYP1B-dependant steroid hydroxylases as drug development targets. Pharmacology, **111:** 27-52.

- Halbleib, J. M. and Nelson, W. J. (2006). Cadherins in development: cell adhesion, sorting, and tissue morphogenesis. Genes and Development, **20:** 3199-3214.

- Hanahan, D. and Weinberg, R. A. (2000). The hallmarks of cancer. Cell, **100:** 57–70.

- Hanahan, D. and Weinberg, R. A. (2011). Hallmarks of cancer: The next generation. Cell, **144:** 646- 674.

- Hanes, C. S. (1932). Studies on plant amylases: The effect of starch concentration upon the velocity of hydrolysis by the amylase of germinated barley. Biochemical Journal, **26 (5):** 1406–1421.

- Hanley, W. D., Napier, S. L., Burdick, M. M., Schnaar, R. L., Sackstein, R. and Konstantopoulos, K. (2006). Variant isoforms of CD44 are P- and L-selectin ligands on colon carcinoma cells. The Journal of the Federation of American societies for Experimental Biology, **20:** 337-339.

- Hanlon, D. M. O., Fitzsimons, H., Lynch, J., Tormey, S., Malone, C. and Given, H. F. (2002). Soluble adhesion molecules (E-selectin, ICAM-1 and VCAM-1) in breast carcinoma. European Journal of Cancer, **38:** 2252–2257.

- Harada, K., Kubo, H., Tanaka, A. and Nishioka, K. (2012). Identification of oxazolidinediones and thiazolidinediones as potent 17β hydroxysteroid dehydrogenase type 3 inhibitors. Bioorganic and Medicinal Chemistry Letters, **22:** 504–507.

- Harbeck, N., Salem, M., Nitz, U., Gluz, O. and Liedtke, C. (2010). Personalized treatment of early-stage breast cancer: present concepts and future directions Cancer Treatment Reviews, **36 (8):** 584-594.

- Hartmann, R. W., Ehmer, P. B., Haider, S., Hector, M., Jose, J., Klein, C. D. P., Seidel, S. B., Sergejew, T. F., Wachall, B. G., Wachter, G. A. and Zhuang, Y. (2002). Inhibition of CYP 17, a New Strategy for the Treatment of Prostate Cancer. Archiv der Pharmazie, **335 (4):** 119-128.

- Harrington, K. J. (2011). Biology of cancer. Medicine, **39 (12):** 689- 692.

- Harris, R. C., Chung, E. and Coffey, R. J. (2003). EGF receptor ligands. Experimental Cell Research, **284:** 2–13.

- Hashimoto, K., Kataoka, N., Nakamura, E., Asahara, H., Ogasawara, Y., Tsujioka, K.and Kajiya, F. (2004). Direct observation and quantitative analysis of spatiotemporal dynamics of individual living monocytes during transendothelial migration. Atherosclerosis, **177 (1):** 19-27.

- Hayes S. H. and Seigel, G. M. (2009). Immunoreactivity of ICAM-1 in human tumors, metastasis and normal tissues. International Journal of Clinical and Experimental Pathology, **2:** 553–60.

- Heidenberg, H.B., Sesterhenn, I.A., Gaddipati, J.P., Weghorst, C.M., Buzard, G.S., Moul, J.W. and Srivastava S. (1995) Alteration of the tumour suppressor gene p53 in a high fraction of hormone refractory prostate cancer. Journal of Urology, **154:** 414–421.

- Henderson, B. E., Ross, R. K., Judd, H. L., Krailo, M. D. and Pike, M. C. (1985). Do Regular Ovulatory Cycles Increase Breast Cancer Risk. Cancer **56:** 1206-1208.

- Hennessy, B. T., Smith, D. L., Ram, P. T., Lu, Y. and Mills, G. B. (2005). Exploiting the PI3K/AKT pathway for cancer drug discovery. Nature Reviews Drug Discovery, **4:** 988–1004.

- Henriksen, G., Breistol, K. and Bruland, O. S. (2002). Significant antitumor effect from bone-seeking, alpha-particle-emitting (223) Ra demonstrated in an experimental skeletal metastases model. Cancer Research, **62:** 3120–3125.

- Herbst, R. Y. (2004). Review of epidermal growth factor receptor biology. International Journal of Radiation Oncology Biology Physics, **59 (2):** S21–S26.

- Hermann, U., Hutter, E., Voglauer, R., Grillari, J., Voth, M., Bereiter-Hahn, J., Jansen-Durr, P. Jendrach, M. (2007). Identification of cultivation-independent markers of human endothelial cell senescence in vitro. Biogerontology, **8:** 383–397.

- Hideshima, T., Chauhan, D., Schlossman, R., Richardson, P. and Anderson, K. C. (2001). The role of tumor necrosis factor a in the pathophysiology of human multiple myeloma: therapeutic applications. Oncogene, **20:** 4519- 4527.

- Higano, C. S., Schellhammer, P. F., Small, E. J., Burch, P. A., Nemunaitis, J., Yuh, L., Provost, N. and Frohlich, M. W. (2009). Integrated data from 2 randomized, double-blind, placebo-controlled, phase 3 trials of active cellular immunotherapy with sipuleucel-T in advanced prostate cancer. Cancer, **115:** 3670–3679.

- Higano, C. S. (2012). New treatment options for patients with metastatic castration-resistant prostate cancer. Cancer treatment reviews, **38 (5)**: 340–345.

- Hood, J. D. and Cheresh, D. A. (2002). Role of integrins in cell invasion and migration. Nature Reviews Cancer, **2:** 91-100.

- Howell, A., Robertson, J. F. R., Albano, J. Q., Aschermannova, A., Mauriac, L., Kleeberg, U. R., Vergote, I., Erikstein, B., Webster, A. and Morris, C. (2002). Fulvestrant, formerly ICI 182,780, is as effective as anastrozole in postmenopausal women with advanced breast cancer progressing after prior endocrine treatment Journal of Clinical Oncology, **20 (16):** 3396-3403.

- Hu, N., Westra, J., Rutgers, A., Der Meer, B. D. V., Huitema, M. G., Stegeman, C. A., Abdulahad, W. H., Satchell, S. C., Mathieson, P. W., Heeringa, P. and Kallenberg, C. G. M. (2011). Decreased CXCR1 and CXCR2 expression on neutrophils in anti-neutrophil cytoplasmic autoantibody-associated vasculitides potentially Increases neutrophil adhesion and impairs migration. Arthritis Research and Therapy, **13:** R201.

- Hu, R., Dawood, S., Holmes, M. D., Collins, L. C., Schnitt, S. J., Cole, K., Marotti, J.D., Hankinson, S. E., Colditz, G. A. and Tamimi, R. M. (2011). Androgen receptor expression and breast cancer survival in postmenopausal women. Clinical Cancer Research, **17:** 1867-1874.

- Huang, Q., Shen, H. M., Shui, G., Wenk, M. R. and Ong, C. N. (2006). Emodin inhibits tumor cell adhesion through disruption of the membrane lipid raft-associated integrin signaling pathway. Cancer Research, **66:** 5807-5815.

- Hubbard, A. K. and Rothlein, R. (2000). Intercellular adhesion molecule-1 (ICAM-1) expression and cell signaling cascades. Free Radical Biology and Medicine, **28**: 1379–1386.

- Huggins, C., Stevens, R. E., Hodges, C. V. (1941). Studies on prostatic cancer: The effects of castration on advanced carcinoma of the prostate gland. Archives of Surgery, **43(2):** 209-223.

- Huh, S. J., liang, S., Sharma, A., Dong, C. and Robertson, G. P. (2010). Transiently entrapped circulating tumor cells interact with neutrophils to facilitate lung metastasis development. Cancer Research, **70:** 6071-6082.

- Hynes, R. O. (2002). Integrins: Bidirectional, allosteric signaling machines. Cell, **110:** 673–687.

- Iiizumi, M., Mohinta, S., Bandyopadhyay, S. and Watabe, K. (2007). Tumor–endothelial cell interactions: Therapeutic potential. Microvascular Research, **74:** 114–120.

- Ikuta, S., Kirby, J. A., Shenton, B. K., Givan, A. L. and Lennard, T.W.J. (1991). Human endothelial cells: effect of TNF-α on peripheral blood mononuclear cell adhesion. Immunology, **73:** 71-76.

- Inoue, T. and Ogawa, O. (2011). Role of signaling transduction pathways in development of castration-resistant prostate cancer. Prostate Cancer, **2011:** 1-7.

- International Breast Cancer Study Group. (2006). Tamoxifen after adjuvant chemotherapy for premenopausal women with lymph node–positive breast cancer: International breast cancer study group trial 13-93. Journal of Clinical Oncology, **24 (9):** 1332- 1341.

- Ismael, G. F. V., Rosa, D. D., Mano, M. S. and Awada, A. (2008). Novel cytotoxic drugs: Old challenges, new solutions. Cancer Treatment Reviews, **34:** 81- 91.

- James, N.D., Sydes, M.R., Clarke, N.W., Mason, M.D., Dearnaley, D.P., Anderson, J., Popert, R.J., Sanders, K., Morgan, R.C., Stansfeld, J., Dwyer, J., Masters, J. and Parmar, (2008). Systemic Therapy for Advancing or Metastatic Prostate Cancer (STAMPEDE): a multi-arm multi-stage randomised controlled trial. Journal of Clinical oncology, **20:** 577-581.

- Jefcoate, C. R. (1978). Measurement of substrate and inhibitor binding to microsomal cytochrome P-450 by optical-difference spectroscopy. Methods in Enzymology, **52**: 58–279.

- Jemal, A., Siegel, R., Ward, E., Hao, Y., Xu, J., Murray, T. And Thun, M. J. (2008). Cancer Statistics. Cancer Journal of Clinicians, **58:** 71–96.

- Jemal, A., Bray, F., Center, M. M., Ferlay, J., Ward, E. and Forman, D. (2011). Global Cancer Statistics. Cancer Journal for Clinicians, **61:** 69–90.

- Jiang, B. H. and Liu, L. H. (2008). PI3K/PTEN signaling in tumorigenesis and angiogenesis. Biochimica et Biophysica Acta - Proteins and Proteomics, **1784 (1)**: 150–158.

- Jornvall, H., Persson, B., Krook, M., Atrian, S., Gonzalez-Duarte, R., Jeffery, J. and Ghosh, D. (1995). Short-chain dehydrogenases/reductases (SDR). Biochemistry, **34:** 6003–6013.

- Kaaks, R., Rinaldi, S., Key, T. J. Berrino, F., Peeters, P. H. M., Biessy, C., Dossus, L., Lukanova, A., Bingham, S., Khaw, K. T., Allen, N. E. Bueno-de-Mesquita, H. B., Van Gils, C. H., Grobbee, D., Boeing, H., Lahmann, P. H., Nagel, G., Chang-Claude, J., Clavel-Chapelon, F., Fournier, A., Thie'baut, A., Gonza'lez, C. A., Quiro's, J. R., Tormo, M. J. and Ardanaz, E., Amiano, P. Krogh, V., Palli, D., Panico, S., Tumino, R., Vineis, P., Trichopoulou, A., Kalapothaki, V., Trichopoulos, D., Ferrari,P., Norat, T., Saracci, R. and Riboli, E. (2005). Postmenopausal serum androgens, oestrogens and breast cancer risk: the European prospective investigation into cancer and nutrition. Endocrine-Related Cancer, **12:** 1071–1082.

- Kammerer, S., Roth, R. B., Reneland, R., Marnellos, G., Hoyal, C. R., Markward, N. J., Ebner, F., Kiechle, M. Schwarz-Boeger, U., Griffiths, L. R., Ulbrich, C., Chrobok, K., Forster, G., Praetorius, G. M., Meyer, P., Rehbock, J., Cantor, J. R., Nelson, M. R. and Braun, A. (2004). Large-Scale Association Study Identifies ICAM Gene Region as Breast and Prostate Cancer Susceptibility Locus. Cancer Research, **64:** 8906-8910.

- Kannagi, R., Izawa, M., Koike, T., Miyazaki, K. and Kimura, N. (2004). Carbohydrate mediated cell adhesion in cancer metastasis and angiogenesis. Cancer Science, **95:** 377– 384.

- Kansas, G. S. (1996). Selectins and their ligands: Current concepts and controversies. Blood, **88 (9):** 3259-3287.

- Katchy, A., Edvardsson, K., Aydogdu, E. and Williamsa, C. (2012). Estradiol-activated estrogen receptor does not regulate mature microRNAs in T47D breast cancer cells. Journal of Steroid Biochemistry and Molecular Biology, **128:** 145–153.

- Kate, M. T., Hofland, L. J., Grevenstein, W. M. U. V., Koetsveld, P. V. V., Jeekel, J. and Eijck, C. H. J. V. (2004). Influence of proinflammatory cytokines on the adhesion of human colon carcinoma cells to lung microvascular endothelium. International Journal of Cancer, **112:** 943–950.

- Keam, S. J. and Scott, L. J. (2006). Letrozole: In postmenopausal hormone-responsive early-stage breast cancer. Drugs, **66 (3):** 353-362.

- Kilsdonk, J. W. J. V., Kempen, L. C. L. T. V., Muijen, G. N. P. V., Ruiter, D. J. and G. W. M. Swart. (2010).Soluble adhesion molecules in human cancers: Sources and fates. European Journal of Cell Biology, **89:** 415–427.

- Kim, H. S., Han, S. Y., Kim, T. S., Kwack, S. J., Lee, R. D., Kim, I. Y., Seok, J. H., Lee, B. M., Yoo, S. D. and Park, K. L. (2002). No androgenic/anti-androgenic effects of bisphenol-A in Hershberger assay using immature castrated rats. Toxicology Letters, **135:** 111-123.

- Kim, Y. S., Ahn, Y., Hong, M. H., Joo, S. Y., Kim, K. H., Sohn, S., Park, H. W., Hong, Y. J., Kim, J. H., Kim, W., Jeong, M. H., Cho, J. G., Park, J. C. and Kang, J. C. (2007). Curcumin attenuates inflammatory responses of TNF-α stimulated human endothelial cells. Journal of Cardiovascular and Pharmacology, **50 (1):** 41-49.

- Koch, A. W., Manzur, K. L. and Shan, W. (2004). Structure-based models of cadherin-mediated cell adhesion: the evolution continues. Cellular and Molecular Life Sciences, **6:** 1884–1895.

- Koh, E., Noda, T., Kanaya, J. and Namiki, M. (2002). Differential expression of 17β-hydroxysteroid dehydrogenase isozyme genes in prostate cancer and noncancer tissues. Prostate, **53:** 154–159.

- Koivunen, J., Aaltonen, V. and Peltonen, J. Protein kinase C (PKC) family in cancer progression. (2006). Cancer Letters, **235:** 1–10.

- Koochekpour, S. (2010). Androgen receptor signaling and mutations in prostate cancer. Asian Journal of Andrology, 12: 639–657.

- Kotsopoulos, J. and Narod, S. A. (2005). Towards a dietary prevention of hereditary breast cancer. Cancer Causes Control, **16(2):** 125-38.

- Koutsilieris, M. (1995). Skeletal metastases in advanced prostate cancer: Cell biology and therapy. Critical Reviews in Oncology/Hematology, **18:** 51-64.

- Kristensen, V. N., Harada, N., Yoshimura, N., Haraldsen, E., Lonning, P. E., Erikstein, B., Karesen, R., Kristensen, T. and Borresen-Dale, A. L. (2000). Genetic variants of CYP19 (aromatase) and breast cancer risk. Oncogene, **1919:** 1329 – 1333.

- Kruti, S., Jandu, B., Abdullah, A. and Ahmed, S. (2011). Synthesis, biochemical evaluation and rationalisation of the inhibitory activity of a range of derivatives of 2-imidazol-1-yl-1-phenyl-ethanone as potential novel inhibitors of 17α-hydroxylase/17, 20-lyase (P-45017α). Letters in Drug and Discovery, **8 (6):** 516-522.

- Labrie, F., Dupont, A., Belager, A., Lacoursiere, Y., Raynaud, J. P., Husson, J. M., Gareau, J., Fazekas, A. T. A., Sandow, J., Monfette, G., Girard, J. G., Emond, J., Houle, J. G. (1983). New approach in the treatment of prostate cancer: complete instead of partial withdrawal of androgens. Prostate, **4:** 579-594.

- Laplante, Y. and Poirier, D. (2008). Proliferative effect of androst-4-ene-3, 17-dione and its metabolites in the androgen-sensitive LNCaP cell line. Steroids, **73:** 266-271.

- Lassila, O. and Komi, J. (2000). Toremifene increases the expression of intercellular adhesion molecule-1 (ICAM-1) on MCF-7 breast cancer cells and jurkat cells. Scandinavian Journal of Immunology, **51:** 73–78.

- Laubli, H. and Borsig, L. (2010). Selectins promote tumour metastasis. Seminars in Cancer Biology, **20:** 169–177.

- Laughton, C. A. and Neidle, S. (1990). Inhibitors of the P450 enzymes aromatase and lyase-crystallographic and molecular modelling studies suggest structural features of pyridylacetic acid-derivatives responsible for difference enzyme inhibitory activity. Journal of Medicinal Chemistry, **33:** 3055-3060.

- Laughton, C. A., McKenna, R., Neidle, S., Jarman, M., McCague, R. And Rowlandst, M. G. (1990). Crystallographic and molecular modeling studies on 3-ethyl-3-(4-pyridyl) piperidine-2,6-dione and its butyl analogue, inhibitors of mammalian aromatase. Comparison with natural substrates: prediction of enantioselectivity for n-alkyl derivatives. Journal of Medicinal Chemistry, **33:** 2673-2679.

- Lawson, C. and Wolf, S. (2009). ICAM-1 signaling in endothelial cells. Pharmacological Reports, **61:** 22–32.

- Lee, J. W., Soung, Y. H., Kim, S. Y., Lee, H. W., Park, W. S., Nam, S. W., Kim, S. H., Lee, J. Y., Yoo, N. J. and Lee, S. H. (2005). PIK3CA gene is frequently mutated in breast carcinomas and hepatocellular carcinomas. Oncogene, **24:** 1477–1480.

- Lee, H. M., Choi, E. J., Kim, E. J. Kim, T. D. Kim, Y. K. Kang, C. and Gho, Y. S. (2010). A membranous form of ICAM-1 on exosomes efficiently blocks leukocyte adhesion to activated endothelial cells. Biochemical and Biophysical Research Communications, **397:** 251–256.

- Lee-Robichaud, P., Akhtar, M. E. and Akhtar, M. (1998). Control of androgen biosynthesis in the human through the interaction of Arg^{347} and Arg^{358} of CYP17 with cytochrome b_5. Biochemical Journal, **332:** 293-296.

- Lehr, J. E. And Pienta, K. J. (1998). Preferential adhesion of prostate cancer cells to a human bone marrow endothelial cell line. Journal of the National Cancer Institute, **90 (2):** 118-123.

- Le Lain, R., Nicholls, P. J., Smith, H. J. and Maharlouie, F. H. (2001). Inhibitors of human and rat testes microsomal 17β-hydroxysteroid dehydrogenase (17β-HSD) as potential agents for prostatic cancer. Journal of Enzyme Inhibition, **16:** 35–45.

- Leroux, F. (2005). Inhibition of P450 as a new strategy for the treatment of prostate cancer. Journal of Medicinal Chemistry, **12:** 1623-1629.

- Lewis, D. F. V., and Lee-Robichaud, P. (1998). Molecular modelling of steroidogenic cytochromes P450 from families CYP11, CYP17, CYP19 and CYP21 based on the CYP102 crystal structure. Journal of Steroid Biochemistry and Molecular Biology, **66 (4):** 217-233.

- Ley, K. (2003). The role of selectins in inflammation and disease. Trends in Molecular Medicine, **9 (6):** 263-268.

- Lieu, C. and Kopetz, S. (2010).The Src family of protein tyrosine kinases: a new and promising target for colorectal cancer therapy. Clinical Colorectal Cancer, **9 (2):** 89-94.

- Limonta, P., Marelli, M. M. And Moretti R. M. (2001). LHRH analogues as anticancer agents: pituitary and extrapituitary sites of action. Expert Opinion on Investigational Drugs, **10:** 709–720.

- Lineweaver, H. and Burk, D. (1934). The determination of enzyme dissociation constants. Journal of the American Chemical Society, **56 (3):** 658–666.

- Liu, A. V. (2000). Differential expression of cell surface molecules in prostate cancer cells. Cancer Research, **60:** 3429-3434.

- Liu, Z. Z. (2005). Molecular mechanism of TNF signaling and beyond. Cell Research, **15(1):** 24-27.

- Lombardo, M.E., Hakky, S. I. and Hudson, P. B. (1993). *In vitro* studies on the inhibition of testosterone synthesis in the human testis by atamestane. Journal of Steroid Biochemistry and Molecular Biology, **44:** 287–290.

- Lonning, P. E., Bajetta, E., Murray, R., Tubiana-Hulin, M., Eisenberg, P. D., Mickiewicz, E., Celio, I., Pitt, P., Mita, M., Aaronson, N. K., Fowst, C., Arkhipov, A., Salle, E. D., Polli, A. and Massimini, G. (2000). Activity of exemestane in metastatic breast cancer after failure of nonsteroidal aromatase inhibitors: a phase II trial. Journal of Clinical Oncology, **18(11):** 2234-2244.

- Lota, R. K., Dhanani, S., Owen, C. P. and Ahmed, S. (2006). Synthesis, biochemical evaluation and rationalisation of the inhibitory activity of a series of 4-hydroxyphenyl ketones as potential inhibitors of 17β-hydroxysteroid dehydrogenase type 3 (17β-HSD3). Bioorganic and Medicinal Chemistry Letters, **16:** 4519–4522.

- Lota, R. K., Olusanjo, M. S., Dhanani, S., Owen, C. P. and Ahmed, S. (2008). Synthesis, biochemical evaluation and rationalisation of the inhibitory activity of a range of 4-hydroxyphenyl ketones as potent and specific inhibitors of the type 3 of 17β-hydroxysteroid dehydrogenase (17β-HSD3). The Journal of Steroid Biochemistry and Molecular Biology, **111 (1–2):** 128-137.

- Lowry O. H., Rosebrough N.J., Farr A.L. and Randall RJ. (1951). Protein measurement with the Folin phenol reagent. Journal of Biological Chemistry, **193:** 265-75.

- Lu, X., Mu, E., Wei, Y., Riethdorf, S., Yang, Q., Yuan, M., Yan, J.,Hua, Y., Tiede, B. J., Lu, X., Haffty, B. G., Pantel, K., Massague, J., and Kang, Y. (2011). VCAM-1 promotes osteolytic expansion of indolent bone micrometastasis of breast cancer by engaging α4β1-positive osteoclast progenitors. Cancer Cell, **20:** 701-714.

- Lukacik, P., Kavanagh, K. L. and Oppermann, U. (2006). Structure and function of human 17β-hydroxysteroid dehydrogenases. Molecular and Cellular Endocrinology, **248:** 61–71.

- Luu-The, V., Belanger, A. and Labrie. (2008). Androgen biosynthetic pathways in the human prostate. Journal of Clinical Endocrinology and Metabolism, **22:** 207-221.

- Mackay, H. J. and Twelves, C. J. (2003). Protein kinase C: a target for anticancer drugs. Endocrine Related Cancer, **10:** 389–396.

- Maddika, S., Ande, S. R., Panigrahi, S., Paranjothy, T., Weglarczyk, K., Zuse, A., Eshraghi, M., Manda, K. D., Wiechec, E. and Los, M. (2007). Cell survival, cell death and cell cycle pathways are interconnected: Implications for cancer therapy. Drug Resistance Updates, **10:** 13–29.

- Maehama, T. and Dixon, J. E. (1998). The Tumor Suppressor, PTEN/ MMAC1, dephosphorylates the lipid second messenger, phosphatidylinositol 3, 4, 5 -trisphosphate. Journal of Biological Chemistry, **273 (22):** 13375–13378.

- Makrilia, N., Kollias, A., Manolopoulos, L. and Syrigos, K. (2009). Cell adhesion molecules: role and clinical significance in cancer. Cancer Investigation, **27(10):** 1023-37.

- Maltais, R., Luu-The, V. and Poirier, D. (2001). Parallel solid-phase synthesis of 3β-peptido-3α-hydroxy-5α- androstan-17-one derivatives for inhibition of Type 3 17β-hydroxysteroid dehydrogenase. Bioorganic and Medicinal Chemistry, **9:** 3101–3111.

- Maltais, R. Luu-The, V. and Poirier, D. (2002). Synthesis and optimization of a new family of Type 3 17β-hydroxysteroid dehydrogenase inhibitors by parallel liquid-phase chemistry. Journal of Medicinal Chemistry, **45 (3):** 640–653.

- Maltais, R., Fournier, M. A. and Poirier, D. (2011). Development of 3-substituted-androsterone derivative as potent inhibitors of 17β-hydroxsteroid dehydrogenase type 3. Bioorganic and Medicinal Chemistry, **19:** 4652-4668.

- Marchais-Oberwinkler, S., Henna, C., Moller, G., Klein, T., Negri, M., Oster, A., Spadaro, A., Werth, R., Wetzel, M., Xu, K., Frotscher, M., Hartmann, R. W., Adamski, J. (2011). 17β-Hydroxysteroid dehydrogenases (17β-HSDs) as therapeutic targets: Protein structures, functions, and recent progress in inhibitor development. Journal of Steroid Biochemistry & Molecular Biology, **125:** 66–82.

- Marcom, P. K., Isaacs, C., Harris, L., Wong, Z. W., Kommarreddy, A., Novielli, N., Mann, G., Tao, Y., Ellis, M. J. (2007). The combination of letrozole and trastuzumab as first or secondline biological therapy produces durable responses in a subset of HER2 positive and ER positive advanced breast cancers. Breast Cancer Research Treatment, **102:** 43–49.

- Marieb, E. N. Human Anatomy and Physiology, 5th Ed, 2001, Addison Wesley Longmann, San Francisco.

- Marin, V., Kaplanski, G., Gres, S., Farnarier, C., Bongrand, P. (2001). Endothelial cell culture: protocol to obtain and cultivate human umbilical endothelial cells. Journal of Immunological Methods, **254:** 183–190.

- Mason, H. S. (1957). Mechanisms of oxygen metabolism. Advances in Enzymology and Related Subjects of Biochemistry, **19:** 79-233.

- Mason, M. D., Davies, G. And jiang, W. G. (2002). Cell adhesion molecules and adhesion abnormalities in prostate cancer. Critical Reviews in Oncology/Hematology, **41 (1)**: 11–28.

- Mastro, L. D., Levaggi, A., Giraudi, S. and Pronzato, P. (2011). Luteinising hormone releasing hormone agonists (LH-RHa) in premenopausal early breast cancer patients: Currrent role and future perspectives. Cancer Treatment Reviews, **37:** 208-211.

- Matsuyama H., Pan Y., Skoog L., Tribukait B., Naito K., Ekman P., Lichter P., Bergerheim U.S. (1994). Deletion mapping of chromosome 8p in prostate cancer by fluorescence in situ hybridization. Oncogene, **9:** 3071–3076.

- McCrohon, J. A., Jessup, W., Handelsman, D. J. and Celermajer, D. S. (1999). Androgen exposure increases human monocyte adhesion to vascular endothelium and endothelial cell expression of vascular cell adhesion molecule-1. Circulation, **99:** 2317-2322.

- McDonald, D. M. And Baluk, P. (2002). Significance of blood vessel leakiness in cancer. Cancer Research, **62:** 5381–5385.

- McDonald, B., Spicer, J., Giannais, B., Fallavollita, L., Brodt, P. and Ferri, L. E. (2009). Systemic inflammation increases cancer cell adhesion to hepatic sinusoids by neutrophil mediated mechanisms. International Journal of Cancer, **125:** 1298–1305.

- McDonnell, T.J., Troncoso, P., Brisbay, S. M., Logothetis, C., Chung, L. W., Hsieh, J. T., Tu, S. M. and Campbell, M. L. (1992). Expression of the protooncogene bcl-2 in the prostate and its association with emergence of androgen-independent prostate cancer. Cancer Research, **52 (24):** 6940-6944.

- McEver, R. P. (1997) Selectin-carbohydrate interactions during inflammation and metastasis. Glycoconjugate Journal, **14:** 585-591.

- McEver, R. P. (2002). Selectins: Lectins that initiate cell adhesion under flow. Current Opinion in Cell Biology, **14:** 581–586.

- McKeever, B.M., Hawkins, B.K., Geissler, W. M., Wu, L., Sheridan, R.P., Mosley, R.T, and Andersson, S. (2002). Amino acid substitution of arginine 80 in 17 beta-hydroxysteroid dehydrogenase type 3 and its effect on NADPH cofactor binding and oxidation/reduction kinetics. Biochimica et Biophysica Acta, **1601:** 29–37.

- McMahon, G. (2000). VEGF receptor signaling in tumor angiogenesis. The Oncologist, **5(1):** 3-10.

- Melotti, P., Nicolis, E., Tamanini, A., Rolfini, R., Pavirani, A., and Cabrini, G. Activation of NF-kB mediates ICAM-1 induction in respiratory cells exposed to an adenovirus-derived vector. Gene Therapy, 8: 1436–1442.

- Michell, M. J. (2010). Breast Cancer. Cambridge University Press, USA. ISBN: 978052151950

- Miles, F. L., Pruitt, F. L., Golen, K. L. V. and Cooper, C. R. (2008). Stepping out of the flow: capillary extravasation in cancer metastasis. Clinical and Experimental Metastasis, **25:** 305–324.

- Miller W. R. (1997). Aromatase inhibitors and breast cancer. Cancer Treatment Reviews, **23:** 171-187.

- Mindnich, R., Haller, F., Halbach, F., Moeller, G., Angelis, M. H. D., and Adamski, J. (2005). Androgen metabolism via 17β-hydroxysteroid dehydrogenase type 3 in mammalian and non-mammalian vertebrates: comparison of the human and the zebrafish enzyme. Journal of Molecular Endocrinology, **35:** 305–316.

- Missmer, S. A., Eliassen, A. H., Barbieri, R. L. and Hankinson, S. E. (2004). Endogenous estrogen, androgen, and progesterone concentrations and breast cancer risk among postmenopausal women. Journal of the National Cancer Institute, **96 (24):** 1856-1865.

- Mizokami, A., Koh, E., Fujita, H., Maeda, Y., Egawa, M., Koshida, K., Seijiro, H., Keller, E. T., and Namiki, M. (2004). The adrenal androgen androstenediol is present in prostate cancer tissue after androgen deprivation therapy and activates mutated androgen receptor. Cancer Research, **64:** 765-771.

- Morales, L., Canney, P., Dyczka, J., Rutgers, E., Coleman, R., Cufer, T., Welnicka-Jaskiewicz, M., Nortier, J., Bogaerts, J., Therassei, P. and Paridaensa, R. (2007). Postoperative adjuvant chemotherapy followed by adjuvant tamoxifen versus nil for patients with operable breast cancer: A randomised phase III trial of the European Organisation for Research and Treatment of Cancer Breast Group. European Journal of Cancer, **43:** 331-340.

- Moreira, V. M. A., Vasaitis, T. S., Njar, V. C. O. and Salvador, J. A. R. (2007). Synthesis and evaluation of novel 17-indazole androstene derivatives designed as CYP17 inhibitors. Steroids, **72:** 939–948.

- Moreira, V. M. A., Vasaitis, T. S., Guo, Z. Njar, V. C. O. and Salvador, J. A. R. (2008). Synthesis of novel C17 steroidal carbamates studies on CYP17 action, androgen receptor binding and function, and prostate cancer cell growth. Steroids, **73:** 1217–1227.

- Moser, C., Lang, S. A. and Stoeltzing, O. (2009). Heat-shock protein 90 (Hsp90) as a molecular target for therapy of gastrointestinal cancer. Anticancer Research, **29:** 2031-2042.

- Mosmann, T. (1983). Rapid colorimetric assay for cellular growth and survival: application to proliferation and cytotoxicity assays. Journal of Immunological Methods, **65:** 55–63.

- Murphy, L. C. and Watson, P. (2002). Steroid receptors in human breast tumorigenesis and breast cancer progression. Biomedicine and Pharmacotherapy, **56:** 65-77.

- Murray, A. J. (2009). The genetics of breast cancer. Surgery, **28 (3):** 103-106.

- Nakajin, S., Hall, P. F. and Onoda, M. (1981). Testicular microsomal cytochrome P450 for C_{21} steroid side chain cleavage. Spectral and binding studies. Journal of Biological Chemistry, **256:** 6134-6139.

- Najy, A. J., Day, K. C. and Day, M. L. (2008). ADAM15 supports prostate cancer metastasis by modulating tumour cell–endothelial cell Interaction. Cancer Research, **68:** 1092-1099.

- Nebel, J. C. (2006). Generation of 3D templates of active sites of proteins with rigid prosthetic groups. Bioinformatics, **22 (10):** 1183–1189.

- Ngatch, B. T., Luu-The, V. and Poiriera, D. (2000). Androsterone 3β-substituted derivatives as inhibitors of type 3 17β-hydroxysteroid dehydrogenase. Bioorganic and Medicinal Chemistry Letters, **10**: 2533-2536.

- Nieswandt, B., Hafner, M., Echtenacher, B., & Mannel, D.N. (1999). Lysis of tumor cells by natural killer cells in mice is impeded by platelets. Cancer Research, **59:** 1295-1300.

- Nilsson, S., Larsen, R. H., Foss, S. D., Balteskard, L. Borch, K. W., Westlin, J. E., Salberg, G. And Bruland, Y. S. (2005). First clinical experience with α-emitting radium-223 in the treatment of skeletal metastases. Clinical Cancer Research, **11:** 4451-4459.

- Nilsson, S., Franzen, L., Parker, C., Tyrrell, C., Blom, R., Tennvall, J., Lennernas, B., Petersson, U., Johannessen, D.C., Sokal, M., Pigott, K., Yachnin, J., Garkavij, M., Strang, P., Harmenberg, J., Bolstad, B., Bruland, O.S. (2007). Bone-targeted radium-223 in symptomatic, hormone-refractory prostate cancer: a randomised, multicentre, placebo-controlled phase II study. Lancet Oncology, **8 (7):** 587-594.

- Njar, V. C. O, Hector, M. and Hartmann, R. W. (1996). 20-Amino and 20, 21-aziridinyl pregnene steroids: Development of potent inhibitors of 17α-hydroxylase/C17, 20-lyase ($P450_{17\alpha}$). Bioorganic and Medicinal chemistry, **4:** 1447-1453.

- Nnane, I. P., Njar, V. C. O. Liu, Y., Lu, Q. and Brodie, A. M. H. (1999). Effects of novel 17-azolyl compounds on androgen synthesis in vitro and in vivo. Journal of Steroid Biochemistry and Molecular Biochemistry, **71:** 145-152.

- Nunez, R. (2001). Flow cytometry: Principles and instrumentation. Current Issues in Molecular Biology, **3(2):** 39-45.

- Nussbaumer, S., Bonnabry, P., Veuthey, J. L. and Souverain, S. F. (2011). Analysis of anticancer drugs: A review. Talanta, **85:** 2265– 2289.

- Ogawa, Y., Hirakawa, K., Nakata B., Fujihara, T., Sawada, T., Kato,Y., Yoshikawa, K and Sowa, M. (1998). Expression of intercellular adhesion molecule-1 in invasive breast cancer reflects low growth potential, negative lymph node involvement, and good prognosis. Clinical Cancer Research, **4:** 31–36.

- Ogawa, Y., Hai, E., Ikeda, K. M. K., Tokunaga, S., Sakurai, H. N. K., Inoue, T., Nishiguchi Y. (2008). Androgen receptor expression in breast cancer: relationship with clinicopathological factors and biomarkers. International Journal of Clinical Oncology, **13:** 431–435.

- Ogden, J. (2004). Understanding Breast Cancer. John Whiley and Sons Ltd, UK. ISBN: 0470855967.

- Okumura, N., Yoshida, H., Kitagishi, Y., Nishimura, Y. and Matsuda, S. (2011). Alternative splicings on p53, BRCA1 and PTEN genes involved in breast cancer. Biochemical and Biophysical Research Communications, **413:** 395–399.

- Oldenburg, R. A., Meijers-Heijboer, H., Cornelisse, C. J. and Devilee, P. (2007). Genetic susceptibility for breast cancer: How many more genes to be found. Critical Reviews in Oncology/Hematology, **63:** 125–149.

- Olsson, A. K., Dimberg, A., Kreuger, J. and Claesson-Welsh, L. (2006). VEGF receptor signalling in control of vascular function. Nature Reviews Molecular Cell Biology, **7:** 359-371.

- Osborne, C. K., Neven, P. Dirix, L. Y., Mackey, J. R., Robert, J., Underhill, C., Schiff, R., Gutierrez, C., Migliaccio, I., Anagnostou, V. S., Rimm, D. L., Magill, P. and Sellers, M. (2011). Gefitinib or Placebo in combination with tamoxifen in patients with hormone receptor-positive metastatic Breast Cancer: a randomized phase II study. Clinical Cancer Research, **17(5):** 1147–1159.

- Owen, C. P., Nicholls, P. J., Smith, H. J. and Whomsley, R. (1999). Inhibition of aromatase (P450 (Arom) by some 1-(benzofuran-2-ylmethyl) imidazoles. Journal of Pharmacy and Pharmacology, **51:** 427-433.

- Owen, C. P and Ahmed, S. (2004). The derivation of a potential transition state for the reduction reaction catalysed by 17β-hydroxysteroid dehydrogenase—an approximate representation of its active site for use in drug design and discovery. Biochemical and Biophysical Research Communications, **318(1):** 131-134.

- Owen, C. P., Dhanani, S., Patel, C. H., Shahid, I. and Ahmed, S. (2006). Synthesis and biochemical evaluation of a range of potent benzyl imidazole-based compounds as potential inhibitors of the enzyme complex 17α-hydroxylase/17, 20-lyase ($P450_{17\alpha}$). Bioorganic & Medicinal Chemistry Letters, **16 (15):** 4011-4015.

- Owen, C. P., Shahid, I., Olusanjo, M. S., Patel, C.H., Dhanani, S. and Ahmed, S. (2008). Synthesis, biochemical evaluation and rationalisation of the inhibitory activity of a range of phenyl alkyl imidazole-based compounds as potent inhibitors of the enzyme complex 17α-hydroxylase/17, 20-lyase ($P450_{17\alpha}$). The Journal of Steroid Biochemistry and Molecular Biology, **111(1–2):** 117-127.

- Paget, S. (1889). The distribution of secondary growths in cancer of the breast. Lancet, **1:** 571–573.

- Pantel, K., Schlimok, G., Angstwurm, M., Passlick, B., Izbicki, J. R., Johnson, J. P. and Riethmuller, G. (1995) Early metastasis of human solid tumours: expression of cell adhesion molecules. Ciba Foundation Symposium, **189**, 157-176.

- Paprocka, M. Dus, D., Mitterrand, M. Lamerant-Fayel, N. and Kieda, C. (2008). Flow cytometric assay for quantitative and qualitative evaluation of adhesive interactions of tumor cells with endothelial cells. Microvascular Research, **76:** 134–138.

- Park, J. S., Kim, K. M., Kim, M. H., chang, H. J., Baek, M. K., Kim, S. M. and Jung, Y. D. (2009). Resveratrol inhibits tumour cell adhesion to endothelial cells by blocking ICAM-1 expression. Anticancer Research, **29:** 355-362.

- Paschos, K. A., Canovas, D. and Bird, N. C. (2009). The role of cell adhesion molecules in the progression of colorectal cancer and the development of liver metastasis. Cellular Signalling, **21:** 665–674.

- Payne, A. H. and Hales, D. B. (2004). Overview of steroidogenic enzymes in the pathway from cholesterol to active steroid hormones. Endocrine Review, **25 (6):** 947-970.

- Pechurskaya, T. A., Lukashevich, O. P., Gilep, A. A., and Usanov, S. A. (2008). Engineering, expression, and purification of "soluble" human cytochrome P45017a and its functional characterization. Biochemistry, **73 (7):** 806-811.

- Penning, T. M. (1996). 17β-Hydroxysteroid dehydrogenase: inhibitors and inhibitor design. Endocrine-Related Cancer, **3:** 41-56.

- Penning, T. M., Bennett. M. J. Hoog, S. S., Schlegel, B. P. Jez, J. M. and Lewist, .M. (1997). Structure and function of 3α-hydroxysteroid dehydrogenase. Steroids, **62:** 101-111.

- Penning, T. M., Jin, Y., Rizner, T. L., and Bauman, D. R. (2008). Pre-receptor regulation of the androgen receptor. Molecular and Cellular Endocrinology, **281**: 1-8.

- Penning, T. M. (2011). Human hydroxysteroid dehydrogenases and pre-receptor regulation: Insights into inhibitor design and evaluation. Journal of Steroid Biochemistry and Molecular Biology, **125:** 46–56.

- Perl, A. K., Wilgenbus, P., Dahl, U., Semb, H. and Christofori, G. (1998). A causal role for E-cadherin in the transition from adenoma to carcinoma, Nature, **392:** 190–193.

- Peters, A. A., Buchanan, G., Ricciardelli, C., Bianco-Miotto, T., Centenera, M. M., Harris, J. M., Jindal, S., Segara, D., Jia, L., Moore, N. L., Henshall, S. M., Birrell, S. N., Coetzee, G. A., Sutherland, R. L., Butler, L. M. and Tilley, W. D. (2009). Androgen receptor inhibits estrogen receptoralpha activity and is prognostic in breast cancer. Cancer Research, **69:** 6131–6140.

- Petrylak, D. P., Tangen, C. M., Hussain, M. H. A., Lara Jeffrey, P. N., Jones, J. A., Taplin,, M. E., Burch, P. A., Berry, D., Moinpour, C., Kohli, M., Benson, M. C., Small, E. J., Raghavan, D. and Crawford, E. D. (2004). Docetaxel and Estramustine Compared with Mitoxantrone and Prednisone for Advanced Refractory Prostate Cancer. The New England Journal of Medicine, **351:** 1513-20.

- Pezaro C, J., Mukherji, D., and Bono, J. S. D. (2011). Abiraterone acetate: redefining hormone treatment for advanced prostate cancer. Drug Discovery Today, **17(5-6):** 221-6.

- Pienta, K. J. and Bradley, D. (2006). Mechanisms underlying the development of androgen-independent prostate cancer. Clinical Cancer Research, **12:** 1665-1671.

- Pittaway, D. E. (1983). Inhibition of testosterone synthesis in the canine testis *in vitro*. Contraception, **27:** 431–436.

- Pletnev, V. Z. And Duax, W. L. Rational proteomics IV: modeling the primary function of the mammalian 17beta-hydroxysteroid dehydrogenase type 8. (2005). Journal of Steroid Biochemistry and Molecular Biology, **94:** 327–335.

- Poirier, D. (2003). Inhibitors of 17β-hydroxysteroid dehydrogenases. Current Medicinal Chemistry, **10 (6):** 453-477.

- Poirier, D. (2010). 17β-Hydroxysteroid dehydrogenase inhibitors: a patent review. Expert Opinion on Therapeutic Patents, **20(9):** 1123-45.

- Pokutta, S. and Weis, W. I. (2007). Structure and Mechanism of Cadherins and Catenins in Cell-Cell Contacts. Annual Review of Cell and Development Biology, **23:** 237–261.

- Polychronis, A., Sinnett, H. D., Hadjiminas, D., Singhal, H., Mansi, J. L. Shivapatham, D., Shousha, S., Jiang, J., Peston, D., Barrett, N., Vigushin, D., Morrison, K., Beresford, E., Ali, S., Slade, M. J. and Coombes, R. C. (2005). Preoperative gefitinib versus gefitinib and anastrozole in postmenopausal patients with oestrogen-receptor positive and epidermal-growth-factor-receptor-positive primary breast cancer: a double-blind placebo-controlled phase II randomised trial. Lancet Oncology, **6:** 383–91.

- Pond, G. R., Armstrong, A. J., Galsky, M.D., Wood, B. A., Leopold, L. and Sonpavde, G. (2012). Efficacy of docetaxel-based chemotherapy following ketoconazole in metastatic castration-resistant prostate cancer: Implications for prior therapy in clinical trials. Urologic Oncology. In Press, Corrected Proof.

- Potter, G. A., Barrie, S. E. And Jarman, M. (1995). Novel steroidal inhibitors of human cytochrome P450, 17-α hydroxylase, 17, 20 lyase- potential agents for the treatment of prostatic cancer. Journal of Medicinal Chemistry, **38**: 2463-2471.

- Prehn, C., Mollera, G. and Adamski, J. (2009). Recent advances in 17 beta-hydroxysteroid dehydrogenases. Journal of Steroid Biochemistry and Molecular Biology, **114:** 72–77.

- Preston, D. M., Torrens, J. I., Harding, P., Howard, R. S., Duncan, W. E. and Mcleod, D. G. (2002). Androgen deprivation in men with prostate cancer is associated with an increased rate of bone loss. Prostate Cancer and Prostatic Diseases, **5:** 304–310.

- Price, J. T. and Thompson, E. W. (2002). Mechanisms of tumour invasion and metastasis: emerging targets for therapy. Expert opinion on Therapeutic Targets, **6(2):** 217-33.

- Prins, G. S. and Korach, K. S. (2008). The role of estrogens and estrogen receptors in normal prostate growth and disease. Steroids, **73:** 233-244.

- Puhalla, S., Brufsky, A. and Davidson, N. (2009). Adjuvant endocrine therapy for premenopausal women with breast cancer. The Breast, **3:** 122-130.

- Pujol, P., Daures, J. P., Thezenas, S., Guilleux, F., Rouanet, P. and Grenier, J. (1998). Changing estrogen and progesterone receptor patterns in breast carcinoma during the menstrual cycle and menopause. Cancer, **83 (4):** 698-705.

- Puranen, T. J., Poutanen, M. H., Peltokrto, H. E., Vihko, P. T. And Vihko, R. K. (1994). Site-directed mutagenesis of the putative active site of human 17β-hydroxysteroid dehydrogenase type 1. Biochemical Journal, **304:** 289-293.

- Quigley, J. P. and Armstrong, P. B. (1998). Tumor cell intravasation *Alu*-cidated: The chick embryo opens the window level. Cell, **94:** 281–284.

- Rahman, M., Kuhn, I., Rahman, M., Liljequist, B. O. and Mollby, R. (2004). Evaluation of a scanner-assisted colorimetric MIC method for susceptibility testing of gram-negative fermentative bacteria. Applied and Environmental Microbiology, **70 (4):** 2398–2403.

- Rainger, G. E. and Nash, G. B. Cellular pathology of atherosclerosis: smooth muscle cells prime cocultured endothelial cells for enhanced leukocyte adhesion. Circulation Research, **88:** 615-622.

- Rathinam, R. and Alahari, S. K. (2010). Important role of integrins in the cancer biology. Cancer Metastasis Review, **29:** 223–237.

- Regan, M. M., Neven, P., Giobbie-Hurder, A., Goldhirsch, A., Ejlertsen, B., Mauriac, L., Forbes, J. F., Smith, I., Lang, I., Wardley, A., Rabaglio, M., Price, K. N., Gelber, R. D., Coates, A. S. and Thurlimann, B. (2011). Assessment of letrozole and tamoxifen alone and in sequence for postmenopausal women with steroid hormone receptor-positive breast cancer: the BIG 1-98 randomised clinical trial at 8·1 years median follow-up. Lancet Oncology, **12:** 1101–1108.

- Reich, R., Thompson, E. W., Iwamoto, Y., Martin, G. R., Deason, J. R., Fuller, G. C. and Misktn, R. (1988). Effects of inhibitors of plasminogen activator, serine proteinases, and collagenase IV on the invasion of basement membranes by metastatic cells. Cancer Research, **48:** 3307-3312.

- Reid, A. H. M., Attard, G., Barrie, E., and De Bono, J. S. (2008). CYP17 inhibition as a hormonal strategy for prostate cancer. Nature Reviews Urology, **5:** 610-620.

- Reynolds, L. P. and Redmer, D. A. (2001). Angiogenesis in the placenta. Biology of Reproduction, **64(4):** 1033-1040.

- Rice, G. E., Gimbrone, M. A. and Bevilacqua, M. P. (1988). Tumor cell-endothelial interactions increased adhesion of human melanoma cells to activated vascular endothelium. American Journal of Pathology, **133 (2):** 204- 210.

- Richmond, P.J.M., Karayiannakis, J.A., Nagafuchi, A., Kaisary, A.V. and Pignatelli, M. (1997). Aberrant E-cadherin and α-catenin expression in prostate cancer: correlation with patient survival. Cancer Research, **57:** 3189–3193

- Rokhlin, O. W. and Cohen, M. B. (1996). Soluble forms of CD44 and CD54 (ICAM-1) cellular adhesion molecules are released by human prostatic cancer cell lines. Cancer Letters, **107:** 29-35.

- Roland, C. L., Haken, A. H., Sarr, M. G. And Barnett, C. C. (2007). Evidence-based surgical hypothesis ICAM-1 expression determines malignant potential of cancer. Surgery, **441 (6):** 705-707.

- Rosenberg, J. E., Weinberg, V. K., Kelly, W. K., Michaelson, D., Hussain, M. H., Wilding, G., Gross, M., Hutcheon, D. and Small, E. J. (2007). Activity of second-line chemotherapy in docetaxel-refractory hormone-refractory prostate cancer patients randomized phase 2 study of ixabepilone or mitoxantrone and prednisone. Cancer, **110 (3):** 556- 563.

- Rosette, C., Roth, R. B., Oeth, P., Braun, A., Kammerer, S., Ekblom, J. and Denissenko, M. F. (2005). Role of ICAM1 in invasion of human breast cancer cells. Carcinogenesis, **26 (5):** 943—950.

- Roskoski, R. (2005). Src kinase regulation by phosphorylation and dephosphorylation. Biochemical and Biophysical Research Communications, **33: 1–14.**

- Rosol, T. J., Tannehill-Gregg, S. H., LeRoy, B. E., Mandl, S, Contag, C. H. (2003). Animal models of bone metastasis. Cancer, **97 (3):** 748-757.

- Rossouw, J. E., Prentice, R. L., Manson, J. E., Wu, I. L., Barad, D., Barnabei, V. M., Ko, M., LaCroix, A. z., Margolis, K. L. and Stefanick, M. L. (2002). Postmenopausal hormone therapy and risk of cardiovascular disease by age and years since menopause. The Journal of the American Medical Association, **297 (13):** 1465-1477.

- Ruoslahti E, Rajotte D. (2000). An address system in the vasculature of normal tissues and tumors. Annual Reviews in Immunology, **18:** 813–827.

- Sadelain, M., Riviere, I. And Brentjens, R. (2003). Targeting tumours with genetically enhanced T lymphocytes. Nature Reviews Cancer, **3:** 35–45.

- Sahai, E. (2005). Mechanisms of cancer cell invasion. Current Opinion in Genetics & Development, **15:** 87–96.

- Sahai, E. (2007). Illuminating the metastatic process. Nature Reviews Cancer, **7:** 737-749.

- Sansal, I. and Sellers, W. R. (2004). The biology and clinical relevance of the PTEN tumour suppressor pathway. Journal of Clinical Oncology, **22:** 2954–2963.

- Sasaki, M., Ostanin, D., Elrod, J. E., Oshima, T., Jordan, P., Itoh, M., Joh, T., Minagar, A., and Alexander, J. S. (2003). TNF-α-induced endothelial cell adhesion molecule expression is cytochrome P-450 monooxygenase dependent. American Journal of Physiology- Cell Physiology, **284:** C422–C428.

- Scalia, R., Appel, J. Z., Lefer, A. M. (1998). Leukocyte-endothelium interaction during the early stages of hypercholesterolemia in the rabbit role of P-Selectin, ICAM-1, and VCAM-1. Arteriosclerosis, Thrombosis and Vascular Biolody, **18:** 1093-1100.

- Schenkman, J. B., Cinti, D. L. Orrenius, S., Moldeus, P. and Kraschnitzs, R. (1972). The nature of the reverse type 1 (modified type 11) spectral change in liver microsomest. Biochemistry, **(11) 23:** 4243-4250.

- Schiller, J. (2010). Prostate Cancer. Emilie M. Smyth, USA. ISBN: 145368235X

- Schluter, H., Moll, I., Wolburg, H., Franke, W. W. (2007). The different structures containing tight junction proteins in epidermal and other stratified epithelial cells, including squamous cell metaplasia. European Journal of Cell Biology, **86 (11–12):** 645–655.

- Schneider, J. G., Amend, S. R. and Weilbaecher, K. N. (2011). Integrins and bone metastasis: Integrating tumour cell and stromal cell interactions. Bone, **48:** 54–65.

- Schover, L. R. (2008). Premature ovarian failure and its consequences: vasomotor symptoms, sexuality, and fertility. Journal of Oncology, **26 (5):** 753-758.

- Schroder, C., Witzel, I., Muller, V., Krenkel, S., Wirtz, R. M., Janicke, F., Schumacher, U. and Milde-Langosch, K. (2011). Prognostic value of intercellular adhesion molecule (ICAM)-1 expression in breast cancer. Journal of Cancer Research and Clinical Oncology, **137(8):** 1193-201.

- Schuster, D., Kowalik, D., Kirchmair, J., Laggner, C., Markt, P., Gumy, C.A., Strohle, F., Möller, G., Wolber, G., Wilckens, T., Langer, T., Odermatt, A. and Adamski, J. (2011). Identification of chemically diverse, novel inhibitors of 17_-hydroxysteroid dehydrogenase type 3 and 5 by pharmacophore-based virtual screening. Journal of Steroid Biochemistry and Molecular Biology, **125:** 148–161.

- Schwartz, M. A., Schaller, M. D. and Ginsberg, M. H. (1995). Integrins: Emerging paradigms of signal transduction. Annual Review of Cell and Developmental Biology, **11:** 549-599.

- Scott, L. J., Clarke, N. W. George, N. J. R., Shanks, J. H., Testa, N. G. and Lang, S. H. (2001). Interactions of human prostatic epithelial cells with bone marrow endothelium: binding and invasion. British Journal of Cancer, **84(10):** 1417–1423.

- Scott, H. M., Mason, J. I. and Sharpe, R. M. (2009). Steroidogenesis in the fetal testis and its susceptibility to disruption by exogenous compounds. Endocrine Reviews, **30(7):** 883–925.

- Secreto, G., Venturelli, E., Meneghini, E., Greco, M., Ferraris, C., Gion, M., Zancan,M., Fabricio, A. S. C., Berrino, F., Cavalleri, A. and Micheli, A. (2009). Testosterone and biological characteristics of breast cancers in postmenopausal women. Cancer Epidemiology Biomarkers and Prevention, **18:** 2942-2948.

- Setlur, S. R. and Rubin, M. A. (2005). Current thoughts on the role of the androgen receptor and prostate cancer progression. Advances in Anatomic Pathology, **12:** 265–270.

- Setty, B. N. Y. and Betal, S. G. (2008). Microvascular endothelial cells express a phosphatidylserine receptor: a functionally active receptor for phosphatidylserine-positive erythrocytes. Blood, **111:** 905-914.

- Shah, K., Jandu, B., Abdullah, A. and Ahmed, S. (2011). Synthesis, biochemical evaluation and rationalisation of the inhibitory activity of a range of derivatives of 2-imidazol-1-yl-1-phenyl-ethanone as potential novel inhibitors of 17α-hydroxylase/17, 20-lyase (p-$450_{17\alpha}$). Letters in Drug Design and Discovery, **8 (6):** 516-522.

- Shahid, I., Patel, C. H., Dhanani, S. Owen, C. P., Ahmed, S. (2008). Synthesis, biochemical evaluation of a range of potent 4-substituted phenyl alkyl imidazole-based inhibitors of the enzyme complex 17α-Hydroxylase/17, 20-Lyase (P45017α). Journal of Steroid Biochemistry and Molecular Biology, **110:** 18–29.

- Sheikh, S., Rahman, M., Gale, Z., Luu, N. T., Stone, P. C. W., Matharu, N. M., Rainger, G. E. L. and Nash, G. B. (2005). Differing mechanisms of leukocyte recruitment and sensitivity to conditioning by shear stress for endothelial cells treated with tumour necrosis factor-α or interleukin-1β. British Journal of Pharmacology, **145 (8):** 1052-1061.

- Sheski, F. D., Natarajan, V. Pottratz, S. T. (1999). Tumor necrosis factor-α stimulates attachment of small cell lung carcinoma to endothelial cells. Journal of Laboratory and Clinical Medicine, **133 (3)**: 265–273.

- Shi, R. and Lin, S. X. (2004). Cofactor hydrogen bonding onto the protein main chain is conserved in the short chain dehydrogenase/reductase family and contributes to nicotinamide orientation. Journal of Biological Chemistry, **279 (16):** 16778–16785.

- Shields, J. M., Pruitt, K. McFall, A., Shaub, A. and Der, C. J. (2000). Understanding Ras: 'it ain't over 'til it's over'. Trends in Cell Biology, **10:** 147–154.

- Siegel, R., Naishadham, D. and Jemal, A. (2012). Cancer Statistics. Cancer Journal for Clinicians, **62:** 10–29.

- Simpson, E. R. (2003). Sources of estrogen and their importance. Journal of Steroid Biochemistry and Molecular Biology, **86:** 225–230.

- Simpson, M. A., Reiland, J., Burger, S. R. Furcht, L. T., Spicer, A. P. Oegema, T. R. and McCarthy, J. B. (2001). Hyaluronan synthase elevation in metastatic prostate carcinoma cells correlates with hyaluronan surface retention, a prerequisite for rapid adhesion to bone marrow endothelial cells. The Journal of Biological Chemistry, **276 (21):** 17949–17957.

- Singh, M. S., Francis, P. A. and Michael, M. (2011). Tamoxifen, cytochrome P450 genes and breast cancer clinical outcomes. The Breast, **20:111-118.**

- Skubitz, A. P. (2002). Adhesion molecules. Cancer Treatment and Research, **107:** 305-29.

- Slack-Davis, J. K., Atkins, K. A., Harrer, C., Hershey, E. D. and Conaway, M. (2009). Vascular cell adhesion molecule-1 is a regulator of ovarian cancer peritoneal metastasis. Cancer Research, **69:** 1469-1476.

- Sonne-Hansen, K. And Lykkesfeldt, A. E. (2005). Endogenous aromatization of testosterone results in growth stimulation of the human MCF-7 breast cancer cell line. The Journal of Steroid Biochemistry and Molecular Biology, **93 (1)**: 25–34.

- Sordella, R., Bell, D. W., Haber, D. A., Settleman, J. (2004). Gefitinib-Sensitizing EGFR Mutations in Lung Cancer Activate Anti-Apoptotic Pathways. Science, **305:** 1163- 1167.

- Spano, D., Heck, C., De Antonellis, P., Christofori, G. and Zollo, M. (2012). Molecular networks that regulate cancer metastasis, Seminars in Cancer Biology, **22 (3):** 234–249.

- Stanbrough M., Bubley G.J., Ross K., Golub, T. R., Rubin, M. A., Penning, T. M., Febbo, P. G. And Balk, S. P. (2006). ncreased expression of genes converting adrenal androgens to testosterone in androgen-independent prostate cancer. Cancer Research, **66:** 2815–2825.

- Stearns, V., Johnson, M. D., Rae, J. M., Morocho, A., Novielli, A., Bhargava, P., Hayes, D. F., Desta, Z., Flockhart, D. A. (2003). Active tamoxifen metabolite plasma concentrations after coadministration of tamoxifen and the selective serotonin reuptake inhibitor paroxetine. Journal of the National Cancer Institute, **95 (23):** 1758-1764.

- Stoletov, K., Kato, H., Zardouzian, E., Kelber, J., Yang, J., Shattil, S. And Klemke, R. (2010). Visualizing extravasation dynamics of metastatic tumor cells. Journal of Cell Science, **123:** 2332-2341.

- Strell, C., Lang, K., Niggemann, B., Zaenker, K. S. and Entschladen, F. (2007). Surface molecules regulating rolling and adhesion to endothelium of neutrophil granulocytes and MDA-MB-468 breast carcinoma cells and their interaction. Cellular and Molecular Life Sciences, **64:** 3306-3316.

- Strell, C. and Entschladen, F. (2008). Extravasation of leukocytes in comparison to tumour cells. Cell Communication and Signalling, **6: 1-13.**

- Suryadevara, P. K., Olepu, S., Lockman, J. W., Ohkanda, J., Karimi, M., Verlinde, C. L. M. J., Kraus, J. M., Schoepe, J., Voorhis, W. C. V., Hamilton, A. D., Buckner, F. S. and Gelb, M. H. (2009). Structurally simple inhibitors of lanosterol 14α-demethylase are efficacious in a rodent model of acute chagas disease. Journal of Medicinal Chemistry, **52 (12):** 3703–3715.

- Swalwell, J. I., Vocke, C. D., Yang, Y., Walker, J. R., Grouse, L., Myers, S. H., Gillespie, J. W., Bostwick, D. G., Duray, P. H., Linehan, W. M. and Emmert-Buck, M. R. (2002). Determination of a minimal deletion interval on chromosome band 8p21 in sporadic prostate cancer. Genes Chromosomes Cancer, **33:** 201–205.

- Swiney, D. C. and Mak, A. Y. (1994). Androgen formation by cytochrome P450 CYP17. Solvent isotope effect and pL studies suggest a role for protons in the regulation of oxene versus peroxide chemistry. Biochemistry, **33:** 2185-2190.

- Takagi, J. (2007). Structural basis for ligand recognition by integrins. Current Opinion in Cell Biology, **19:** 557–564.

- Takahashi, M. Ikeda, U., Masuyama, J. I. Kitagawa, S. I., Kasahara, T., Shimpo, M. Kano, S. and Shimada, K. Monocyte-endothelial cell interaction induces expression of adhesion molecules on human umbilical cord endothelial cells. Cardiovascular Research, **32:** 422-429.

- Takizawa, K., Kamijo, R., Ito, D., Hatori, M., Sumitani, K. and Nagumo, M. (1999).Synergistic induction of ICAM-1 expression by cisplatin and 5-fluorouracil in a cancer cell line via a NF-kB independent pathway. British Journal of Cancer, **80(7):** 954–963.

- Tammela, T. (2004). Endocrine treatment of prostate cancer. Journal of Steroid Biochemistry and Molecular Biology, **92:** 287-295.

- Tannock, I. F., De Wit, R., Berry, W. R., Horti, J., Pluzanska, A., Chi, K. N., Oudard, S., Theodore, C., James, N. D., Turesson, I., Rosenthal, M. A. and Eisenberger, M. A. (2004). Docetaxel plus Prednisone or Mitoxantrone plus Prednisone for Advanced Prostate Cancer. The New England Journal of Medicine, **351:** 1502-12.

- Tchedam-Ngatcha, B., Luu-The, V. and Poirier, P. (2000). Androstene 3β-substituted derivataves as inhibitors of type 3 17β-hydroxysteroid dehydorgenase. Bioorganic and Medicinal Chemistry Letters, **10 (22):** 2533-2536.

- Tchedam-Ngatcha,. B., Laplante, Y., Labrie, F., Luu-The, V., Poirier, D. (2006). 3β-Alkyl-androsterones as inhibitors of type 3 17β-hydroxysteroid dehydrogenase: Inhibitory potency in intact cells, selectivity towards isoforms 1, 2, 5 and 7, binding affinity for steroid receptors, and proliferative/antiproliferative activities on AR^+ and ER^+ cell lines. Molecular and Cellular Endocrinology, **248:** 225–232.

- Thamilselvan, V., Basson, M. D. (2005). The role of the cytoskeleton in differentially regulating pressure-mediated effects on malignant colonocyte focal adhesion signaling and cell adhesion. Carcinogenesis, **26:**1687-1697.

- Thamilselvan, V., Craig, D. H. and Basson, M. D. (2007). FAK association with multiple signal proteins mediates pressure-induced colon cancer cell adhesion *via* a Src-dependent PI3K/Akt pathway. The Journal of Federation of American Societies for Experimental Biology, **21:** 1730-1741.

- Thompson, D. and Easton, D. (2001). Variation in cancer risks, by mutation position, in BRCA2 mutation carriers. American Journal of Human Genetics, **68:** 410–419.

- Thompson, D. and Easton, D. (2004). The genetic epidemiology of breast cancer genes. Journal of Mammary Gland Biology and Neoplasia, **(9) 3:** 221-236.

- Titus, M. A., Schell, M. J., Lih, F. B., Tomer, K. B. and Mohler, J. L. (2005). Testosterone and dihydrotestosterone tissue levels in recurrent prostate cancer. Clinical Cancer Research, **11:** 4653-4657.

- Trachtenberg, J. and Zadra, J. (1988). Steroid-synthesis-inhibition by ketoconazole-site of action. Clinical and Investigative Medicine, **11:** 1-5.

- Tunney, M. M. Ramage, G., Field, T. R. Moriarty, T. F. and Storey, D. G. (2004). Rapid colorimetric assay for antimicrobial susceptibility testing of pseudomonas aeruginosa. Antimicrobial agents and chemotherapy, **48 (51):** 1879–1881.

- Ulukaya E., Ozdikicioglu, F., Oral, A. Y. and Demirci, M. (2008). The MTT assay yields a relatively lower result of growth inhibition than the ATP assay depending on the chemotherapeutic drugs tested. Toxicology in Vitro, **22:** 232–239.

- Unterluggauer, H., Hutter, E., Voglauer, R., Grillari, R., Voth, M., Bereiter-Hahn, J. Jansen-Durr, P. and Jendrach, M. (2007). Identification of cultivation-independent markers of human endothelial cell senescence in vitro. Biogerontology, **8:** 383–397.

- Urbanits, S., Griesmacher, A., Hopfinger, G., Stockhammer, G., Karimi, A., Muller, M. M., Pittermann, E. and Grisold, W. (2002). FACS analysis—a new and accurate tool in the diagnosis of lymphoma in the cerebrospinal fluid. Clinica Chimica Acta, **317:** 101–107.

- Urso, B., Brown, R. A., O'Rahilly, S., Shepherd, P. R. and Siddle, K. (1999). The alpha-isoform of class II phosphoinositide 3-kinase is more effectively activated by insulin receptors than IGF receptors, and activation requires receptor NPEY motifs. Federation of European Biochemical Societies, **460:** 423–426.

- Valentino, L. and Pierre, J. (2006). JAK/STAT signal transduction: Regulators and implication in hematological malignancies. Biochemical Pharmacology, **71:** 713-721.

- Vara, J. A. F., Casado, E., Castro, J. D., Cejas, P., Belda-Iniesta, C. and Gonzalez-Baron, M. (2004). PI3K/Akt signalling pathway and cancer. Cancer Treatment Reviews, **30:** 193–204.

- Vasaitis, T. S., Bruno, R. D. and Njara, V. C. O. (2011). CYP17 inhibitors for prostate cancer therapy. Journal of Steroid Biochemistry and Molecular Biology, **125:** 23–31.

- Vaughn, D. E. and Bjorkman, P. J. (1996). The (Greek) key to structures of neural adhesion molecules. Neuron, **16:** 261–267.

- Vicker, N., Sharland, C. M., Heaton, W. B., Gonzalez, A. M. R., Bailey, H. V., Smith, A., Springall, J. S., Day, J. M., Tutill, H. J., Reed, M. J., Purohit, A. and Pottera, B. V. L. (2009). The design of novel 17β-hydroxysteroid dehydrogenase type 3 inhibitors. Molecular and Cellular Endocrinology, **301:** 259–265.

- Vihko, P., Herrala A., Harkonen, P., Isomaa, V., Kaija, H., Kurkela, R. and Pulkka, A. (2006). Control of cell proliferation by steroids: The role of 17HSDs Molecular and Cellular Endocrinology, **248:** 141–148.

- Vlietstra, R. J., Alewijk, D. C. V., Hermans, K. G., Steenbrugge, G. J. V. and Trapman J. (1998). Frequent inactivation of PTEN in prostate cancer cell lines and xenografts. Cancer Research, **58:** 2720–2723.

- Wang, J., Milner, R. (2006). Fibronectin promotes brain capillary endothelial cell survival and proliferation through alpha5beta1 and alphavbeta3 integrins via MAP kinase signalling. Journal of Neurochemistry, **96:** 148–59.

- Webb, D. S. A., Mostowski, H. S. and Gerrard, T. L. (1999). Cytokine-induced enhancement of ICAM-1 expression results in increased vulnerability of tumor cells to monocyte-mediated lysis. Journal of Immunology, **146:** 3682–3686.

- Wilson, J. K., Sargent, J. M., Elgie, A. W., Hill, J. G. and Taylor, C. J. (1990). A feasibility study of the MTT assay for chemosensitivity testing in ovarian malignancy. British Journal of Cancer, **62:** 189-194.

- Wirth, M., Tyrrell, C., Delaere, Sanchez-Chapado, M., Ramon, J., Wallace, D. M. A., Hetherington, J., Pina, F., Heyns, C. F., Navani, S. and Armstrong, J. (2007). Bicalutamide (Casodex) 150 mg plus standard care in early non-metastatic prostate cancer: results from Early Prostate cancer Trial 24 at a median 7 years' follow-up. Prostate Cancer and Prostatic Diseases, **10:** 87-93.

- Wojtalla, A. and Arcaro, A. (2011). Targeting phosphoinositide 3-kinase signalling in lung cancer. Critical Reviews in Oncology/Hematology, **80 (2)**: 278–290.

- Woodward, J. (2008). Crossing the endothelium: E-selectin regulates tumour cell migration under flow conditions. Cell Adhesion and Migration, **2 (3):** 151-152.

- Wozniak, M. A., Modzelewska, K., Kwong, L. and Keely, P. J. (2004). Focal adhesion regulation of cell behaviour. Biochimica et Biophysica Acta, **1692:** 103– 119.

- Wozniak, A. (2012). Challenges in the current antiangiogenic treatment paradigm for patients with non-small cell lung cancer. Critical Reviews in Oncology/ Hematology, **82:** 200- 212.

- Wyckoff, J. B., Wang, Y., Lin, E. Y., Li, J, F., Goswami, S., Stanley, E. R., Segall, J. E., Pollard, J. E. And Condeelis, J. (2007). Direct visualization of macrophage-assisted tumor cell intravasation in mammary tumors. Cancer Research, **67:** 2649-2656.

- Yadav, M. R., Sabale, P. M., Giridhar, R., Zimmer, C., Haupenthal, J. and Hartmann, R. W. (2011). Synthesis of some novel androstanes as potential aromatase inhibitors. Steroids, **76:** 464-470.

- Yano, S., Nishioka, Y., Goto, H. and Sone, S. (2003). Molecular mechanisms of angiogenesis in non-small cell lung cancer, and therapeutics targeting related molecules. Cancer Science, **94 (6):** 479–485.

- Yap, T. A., Carden, C. P., Attard, G. and Bono, J. S. D. (2008). Targeting CYP17: established and novel approaches in prostate cancer. Current Opinion in Pharmacology, **8:** 449-457.

- Yarden, Y. and Sliwkowski, M. X. (2001). Untangling the ErbB signalling network Nature Reviews Molecular Cell Biology, **2:** 127–137.

- Yeh, S. Hu, Y. C., Wang, P. H. Xie, C., Xu, Q., Tsai, M. Y., Dong, Z., Wang, R. S., Lee, T. H. and Chang, C. (2003). Abnormal mammary gland development and growth retardation in female mice and mcf7 breast cancer cells lacking androgen receptor. Journal of Experimental Medicine, **198 (12):** 1899–1908.

- Yilmaz, M., Christofori, G. And Lehembre, F. (2007). Distinct mechanisms of tumour invasion and metastasis. Trends in Molecular Medicine, **13 (12):** 535-541.

- Yoon, J. J., Lee, Y. J., Kim, J. S., Kang, D. G., Lee, H. S. (2010). Protective role of betulinic acid on TNF-α induced cell adhesion molecules in vascular endothelial cells. Biochemical and Biophysical Research Communications, **391(1):** 96–101.

- Zurek, J., Foloppe, N., Harvey, J. N. and Mulholland, A. J. (2006). Mechanisms of reaction in cytochrome P450: hydroxylation of camphor in P450cam. Organic and Biomolecular Chemistry, **4:** 3931-3937.

10. APPENDICES

APPENDIX 1

Compounds	Structures	% Inhibition ± SEM ([I]=100 μM) 17αOHase	% Inhibition ± SEM ([I]=100 μM) 17, 20 lyase	IC_{50} (μM)
KTZ	-	81.55 ± 0.23	67.87±1.39	89.41 ± 4.81
370	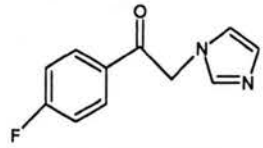	64.0 ± 2.19	59.32±2.78	67.30 ± 5.65
385	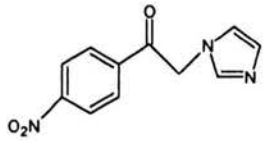	66.04 ± 3.08	67.64±2.01	98.86 ± 1.14
388	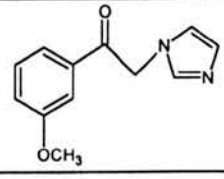	72.03 ± 0.92	71.00±1.25	34.22 ± 0.34
389	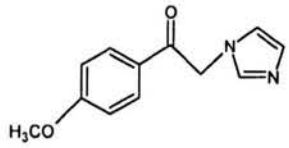	56.82 ± 1.95	68.10±1.69	NC
391	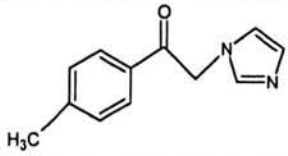	77.44 ± 2.08	69.38± 2.44	NC
399	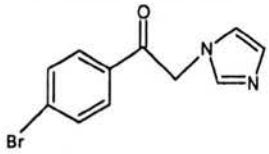	78.28 ± 1.61	59.49± 0.94	16.92 ± 1.74
400	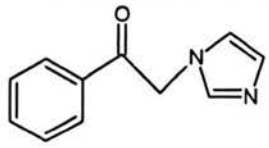	41.85 ± 4.53	64.90± 2.82	NC

402	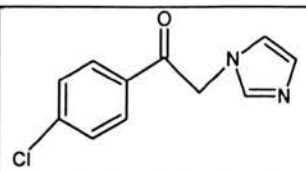	73.71± 1.73	73.44± 1.71	63.09 ± 0.95
406	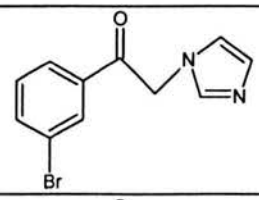	83.56 ± 2.35	72.35± 5.96	7.91 ± 0.42
410	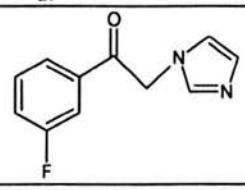	67.09 ± 5.86	69.30± 2.29	NC

Summary of the screening of some imidazole-based substituted phenyl ethanone compounds against the enzyme 17α-OHase. *The compounds were tested along reference drug ketoconazole (KTZ) at a concentration of 100 μM. The* IC_{50} was calculated using graphpad prism software. *The data is the mean ± SEM of three different experiments (n =3).NC = Not calculated*

APPENDIX 2

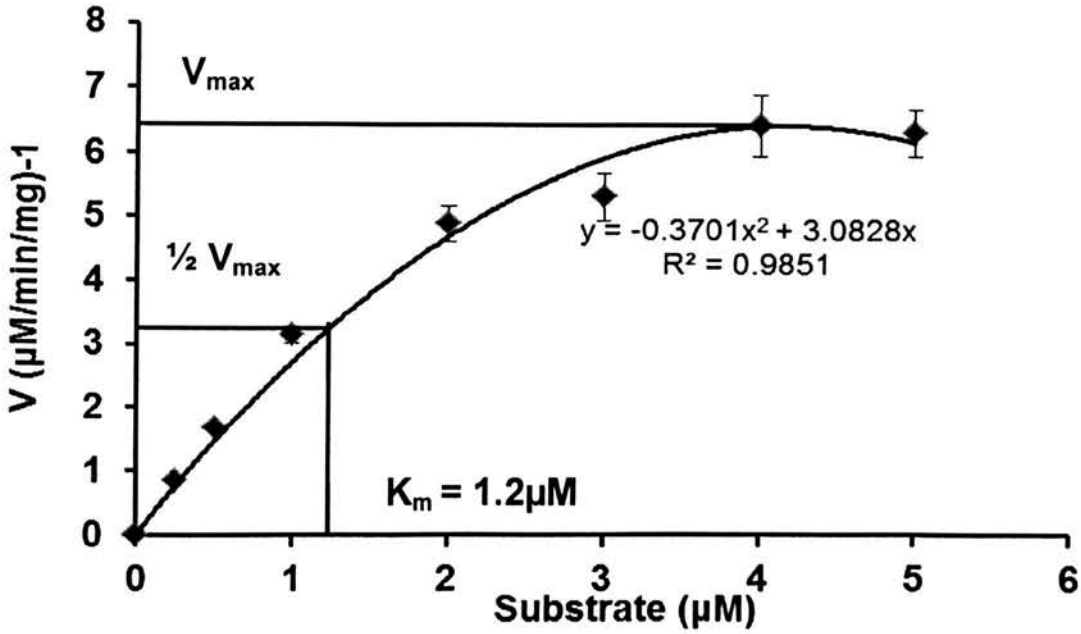

Michaelis Menten plot for 17, 20 lyase enzyme. *The V_{max} was found to be 6.5 $(\mu M.min/mg)^{-1}$. The substrate concentration at ½ V_{max} = 3.25 $(\mu M.min/mg)^{-1}$ was calculated as k_m = 1.2 µM. The data is the mean ± SEM of three different experiments (n =3).*

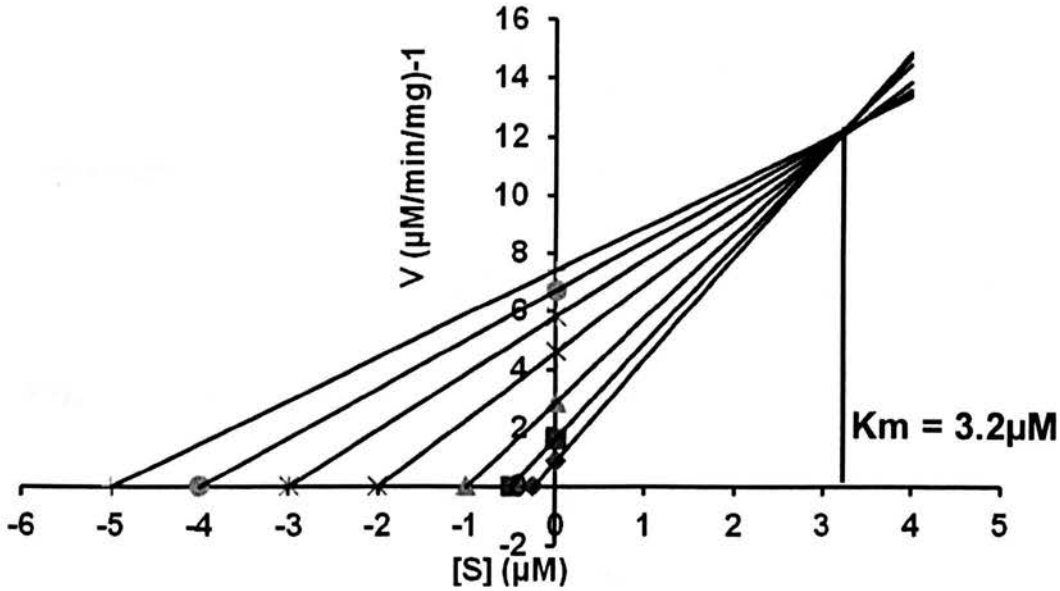

Direct linear plot for 17, 20 lyase enzyme. *The point of intersection of all data sets is K_m. The data is the mean ± SEM of three different experiments (n =3).*

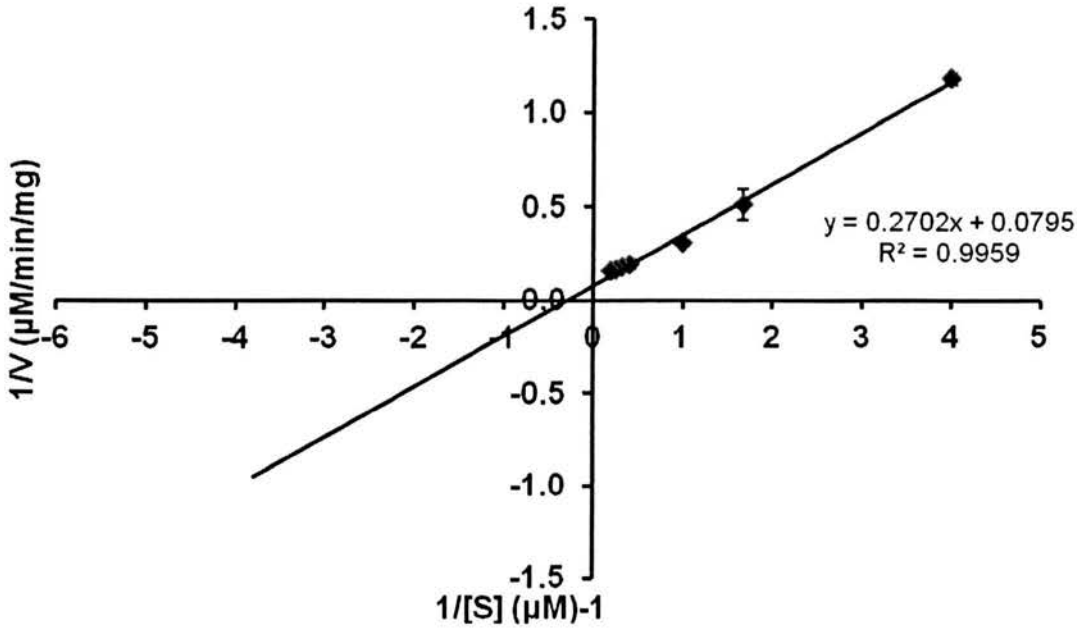

Lineweaver-Burk plot for 17, 20 lyase. *The data is the mean ± SEM of three different experiments (n =3).*

According to the Lineweaver-Burk equation:

$$\frac{1}{V} = \frac{Km}{Vmax} \times \frac{1}{S} + \frac{1}{Vmax}$$

From the graph; $y = 0.270x + 0.079$

So; $\frac{1}{Vmax} = 0.079$ or $Vmax = \frac{1}{0.079} = 12.658$

Similarly; $\frac{Km}{Vmax} = 0.270$

So; $K_m = 0.270 \times 12.658$

K_m = 1.33 µM

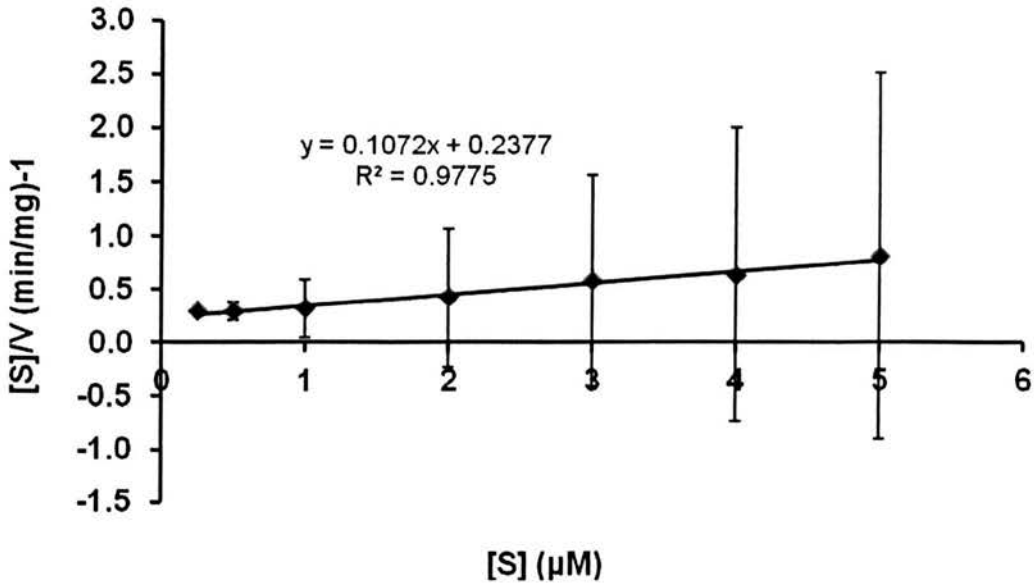

Hanes-Woolf plot for 17, 20 lyase. *The data is the mean ± SEM of three different experiments (n =3).*

According to the Hanes-Woolf equation:

$$\frac{S}{v} = \frac{Km}{Vmax} + \frac{1}{Vmax} \times S$$

From the graph; $y = 0.107x + 0.237$

Or $y = 0.237 + 0.107x$

So; $\frac{1}{Vmax} = 0.107$ or $Vmax = \frac{1}{0.107} = 9.346$

Similarly; $\frac{Km}{Vmax} = 0.237$

So; $K_m = 0.237 \times 9.346$

K_m = 2.21 μM

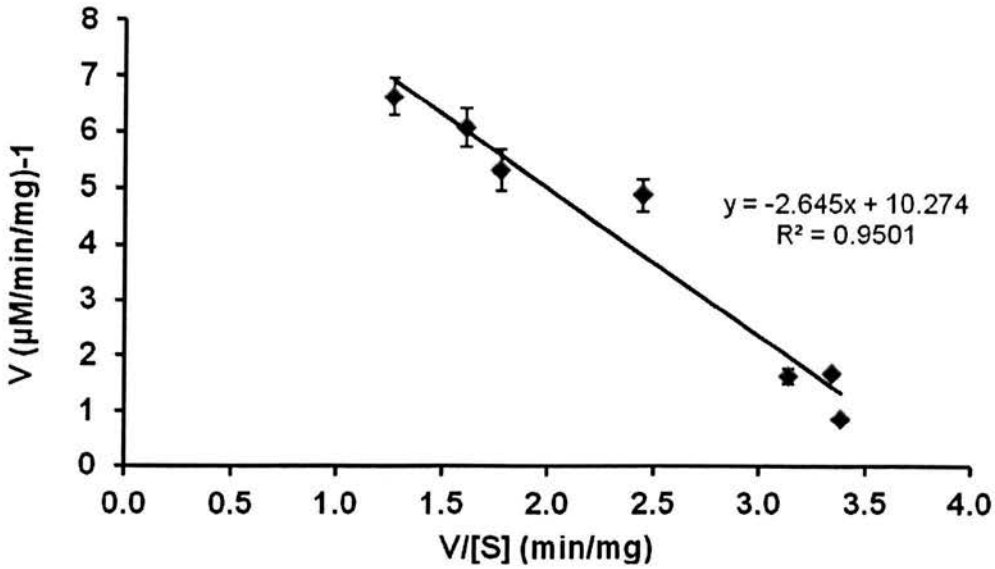

Eadie-Hofstee plot for 17, 20 lyase. *The data is the mean ± SEM of three different experiments (n =3).*

According to the Eadie-Hofstee equation:

$$V = -K_m \times \frac{v}{s} + V_{max}$$

From the graph; $y = -2.645 + 10.27$

Therefore; **K_m = 2.645 µM**

APPENDIX 3

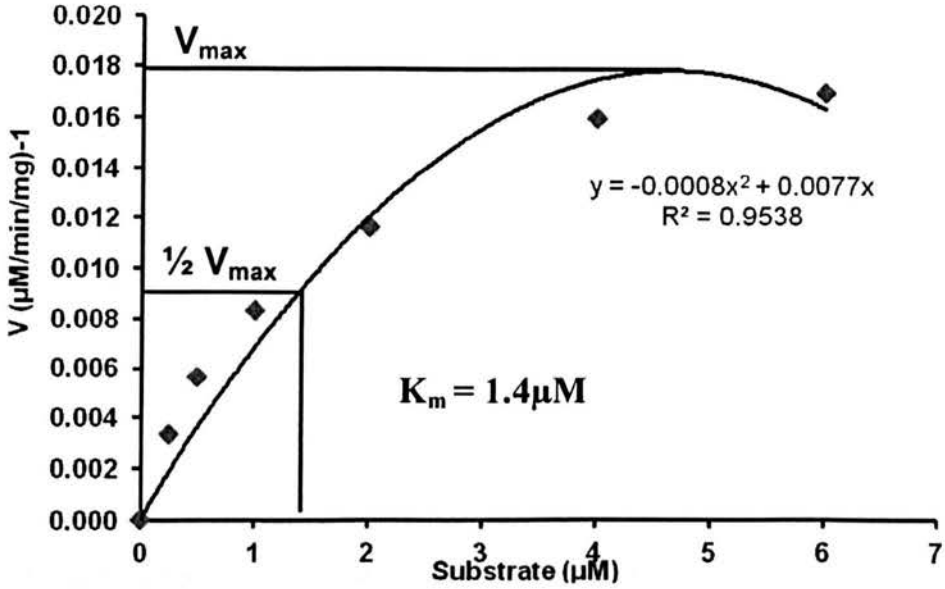

Michaelis Menten plot for 17β-HSD 3 enzyme. The V_{max} was found to be 0.018 (µM.min/mg)$^{-1}$. *The substrate concentration at ½ V_{max} = 0.009 (µM.min/mg)$^{-1}$ was calculated as k_m = 1.4 µM. The data is the mean ± SEM of three different experiments (n =3).*

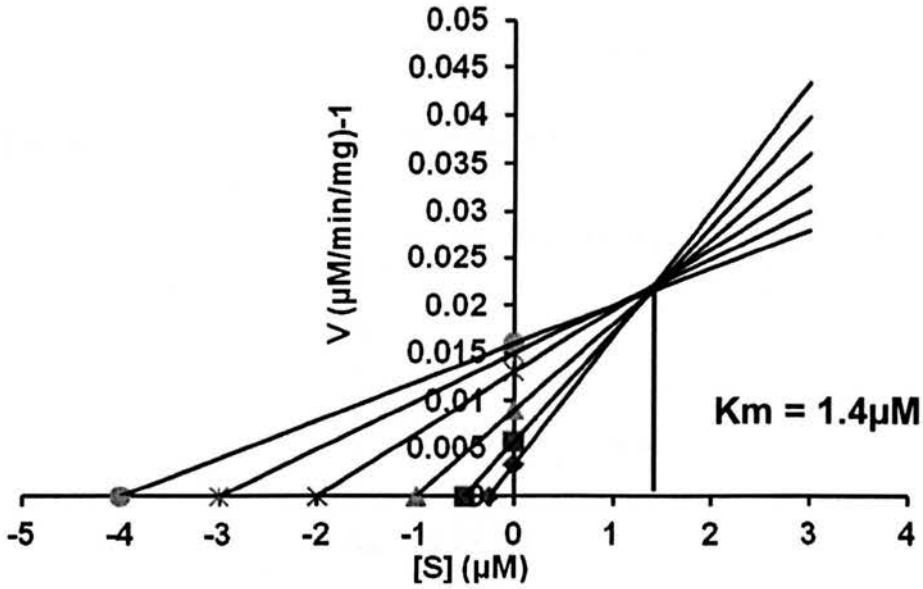

Direct linear plot for 17β-HSD 3 enzyme. The point of intersection of all data sets is K_m. *The data is the mean ± SEM of three different experiments (n =3).*

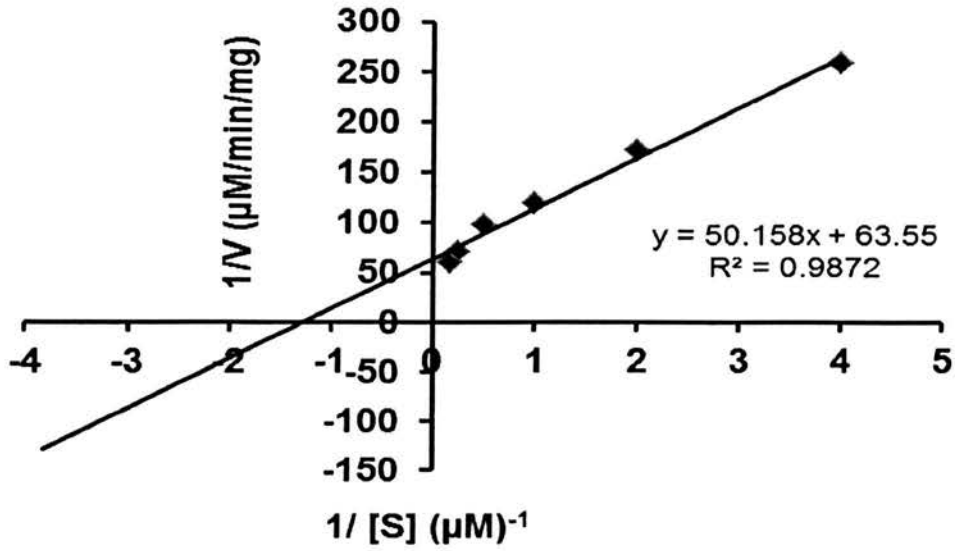

Lineweaver-Burk plot for 17β-HSD 3. *The data is the mean ± SEM of three different experiments (n =3).*

According to the Lineweaver-Burk equation:

$$\frac{1}{V} = \frac{Km}{Vmax} \times \frac{1}{S} + \frac{1}{Vmax}$$

From the graph; $y = 50.158x + 63.55$

So; $\frac{1}{Vmax} = 63.55$ or $Vmax = \frac{1}{63.55} = 0.0157$

Similarly; $\frac{Km}{Vmax} = 50.158$

So; $K_m = 50.158 \times 0.0157$

K_m = 0.79 µM

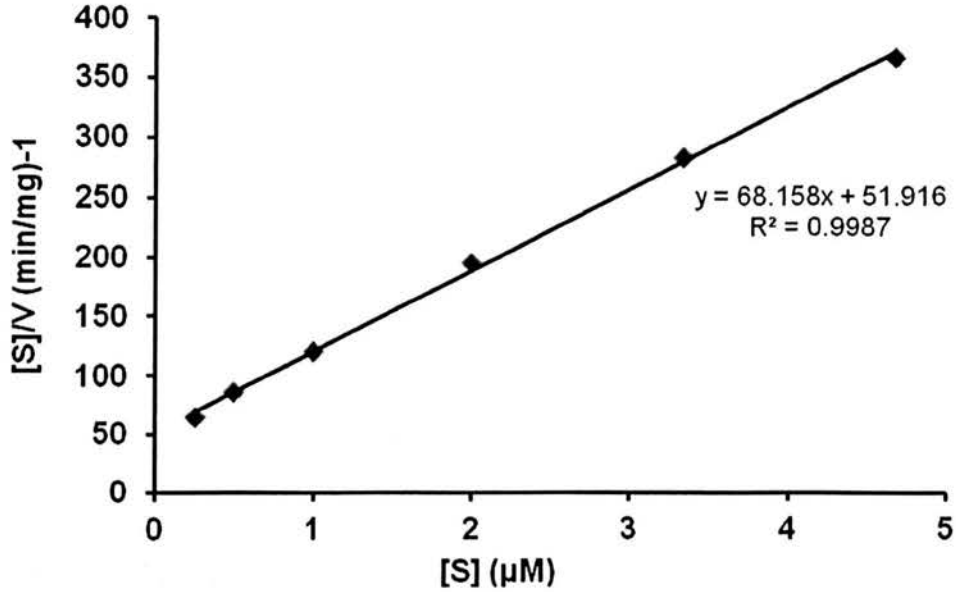

Hanes-Woolf plot for 17β-HSD 3. *The data is the mean ± SEM of three different experiments (n =3).*

According to the Hanes-Woolf equation:

$$\frac{S}{v} = \frac{Km}{Vmax} + \frac{1}{Vmax} \times S$$

From the graph; $y = 68.158x + 51.916$

Or $y = 51.916x + 68.158$

So; $\frac{1}{Vmax} = 68.158$ or $Vmax = \frac{1}{68.158} = 0.0147$

Similarly; $\frac{Km}{Vmax} = 51.916$

So; $K_m = 51.916 \times 0.0147$

K_m = 0.76 µM

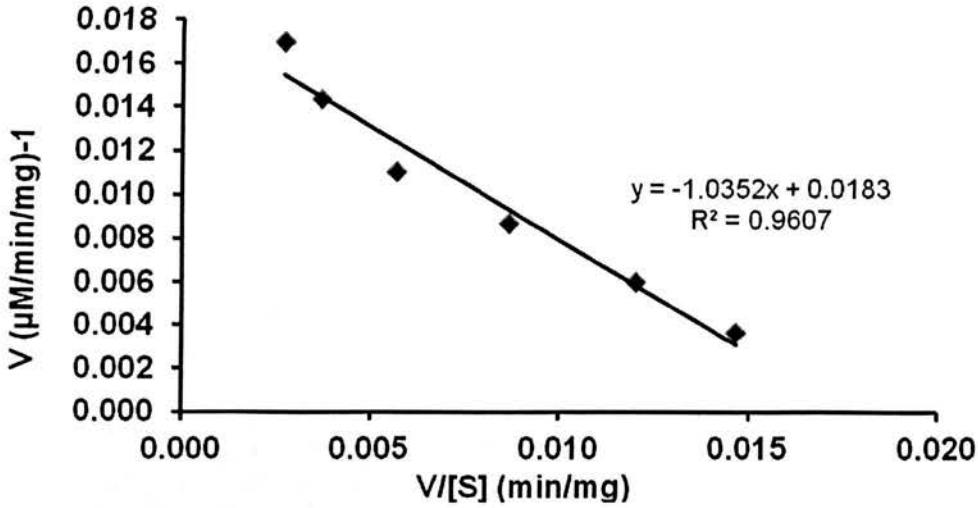

Eadie-Hofstee plot for 17β-HSD 3. *The data is the mean ± SEM of three different experiments (n =3).*

According to the Eadie-Hofstee equation:

$$V = -K_m \times \frac{v}{s} + V_{max}$$

From the graph; $y = -1.0352x + 0.0183$

Therefore; $\mathbf{K_m = 1.04\ \mu M}$

APPENDIX 4

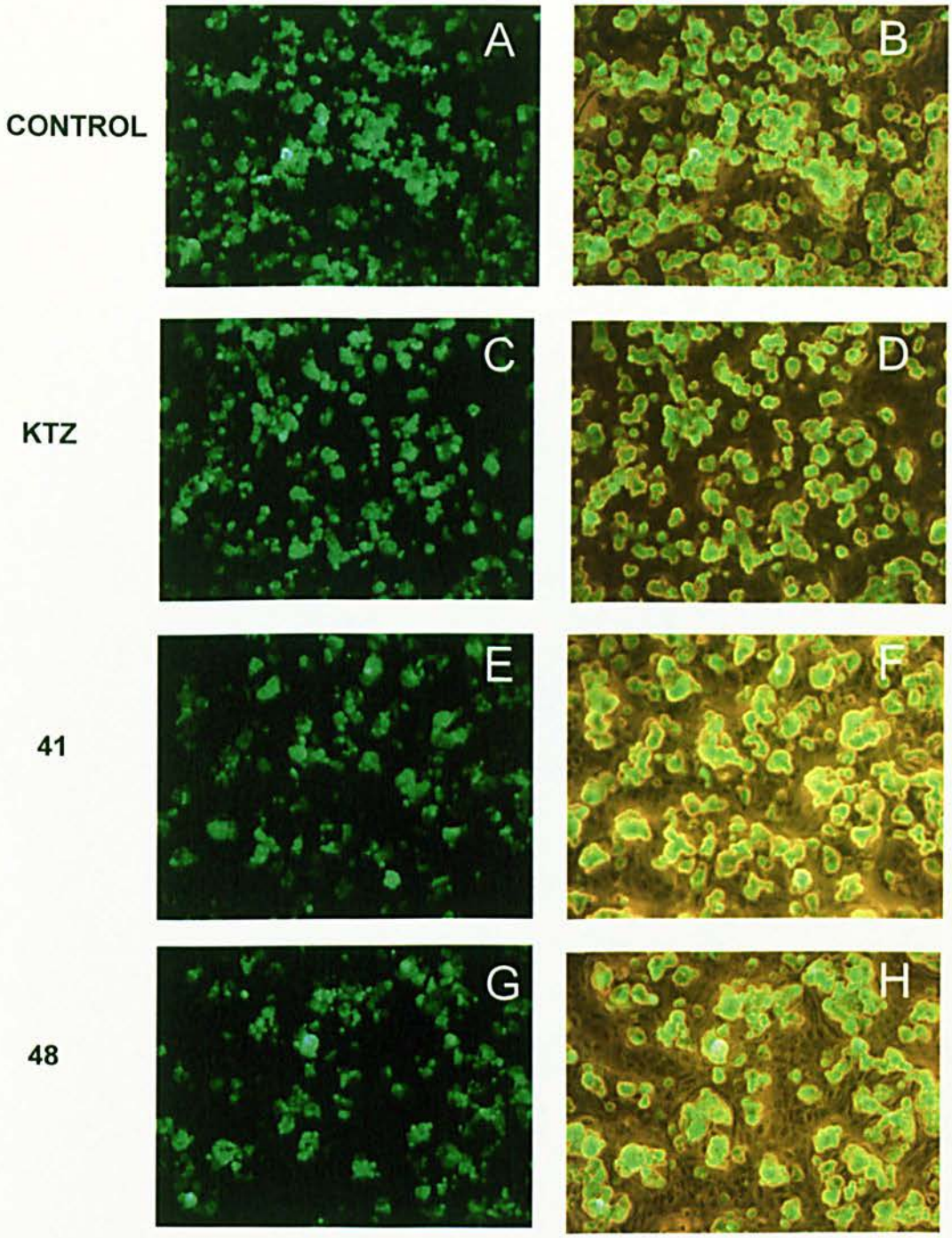

Fluorescence and phase-contrast-microscopy of DU145 cells attached to non-treated HUVEC monolayers. *DU145 cells were treated with CYP17 inhibitors for 24 hours. Fluorescently labelled DU145 cells (green) are attached to HUVEC monolayer (Right). (A-B) Un-treated DU145 cells (C-D) DU145 cells treated with KTZ (E-F) DU145 cells treated with compound 41 (G-H) DU145 cells treated with compound 48. Images were acquired using a fluorescent microscope at X100 magnification. The images are qualitatively representative of three different experiments (n=3).*

APPENDIX 5

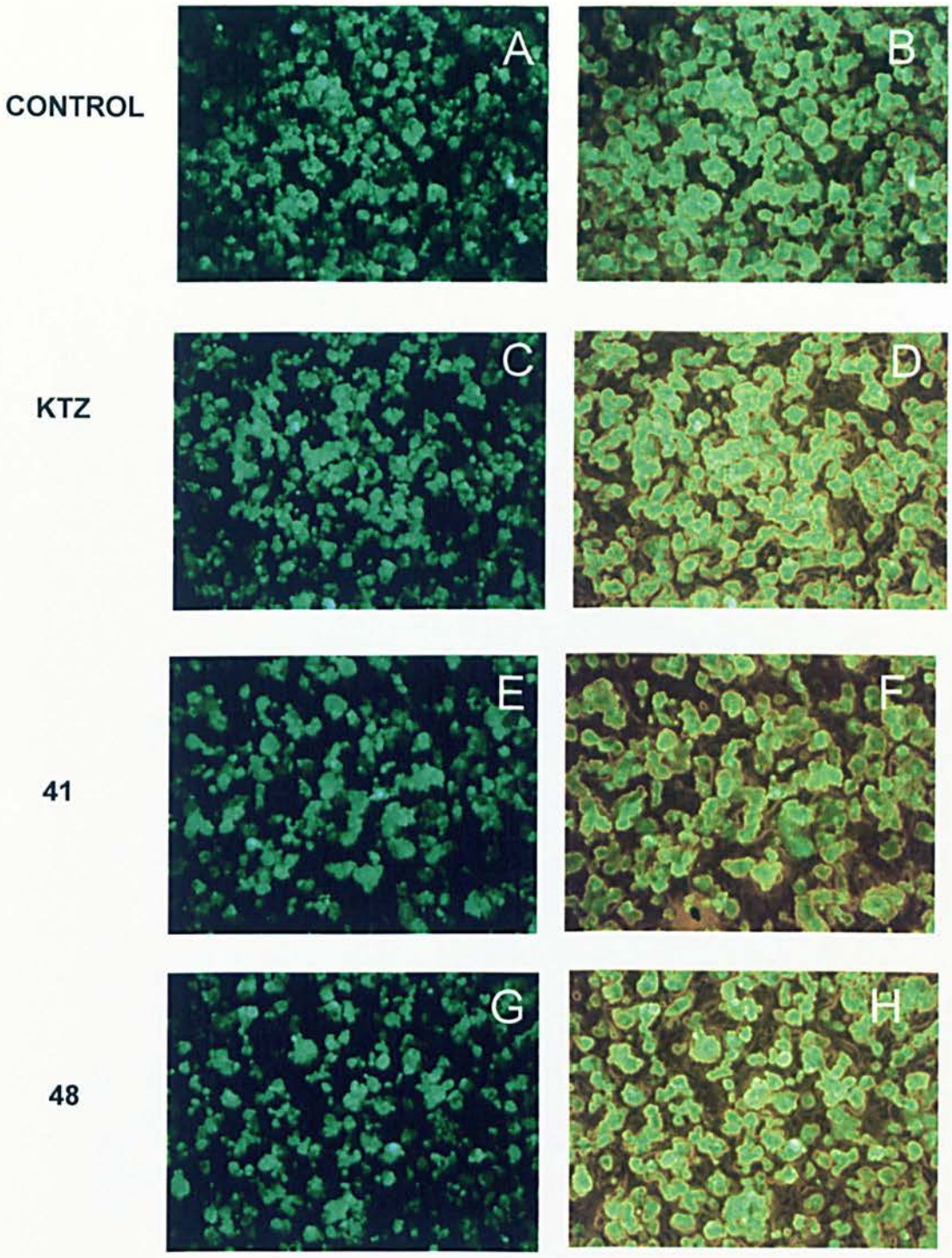

Fluorescence and phase-contrast-microscopy of DU145 cells attached to TNF-α treated HUVEC monolayers *DU145 cells were treated with CYP17 inhibitors for 24 hours. Fluorescently labelled DU145 cells (green) are attached to HUVEC monolayer (Right). (A-B) Un-treated DU145 cells (C-D) DU145 cells treated with KTZ (E-F) DU145 cells treated with compound 41 (G-H) DU145 cells treated with compound 48. Images were acquired using a fluorescent microscope at X100 magnification. The images are qualitatively representative of three different experiments (n=3).*

APPENDIX 6

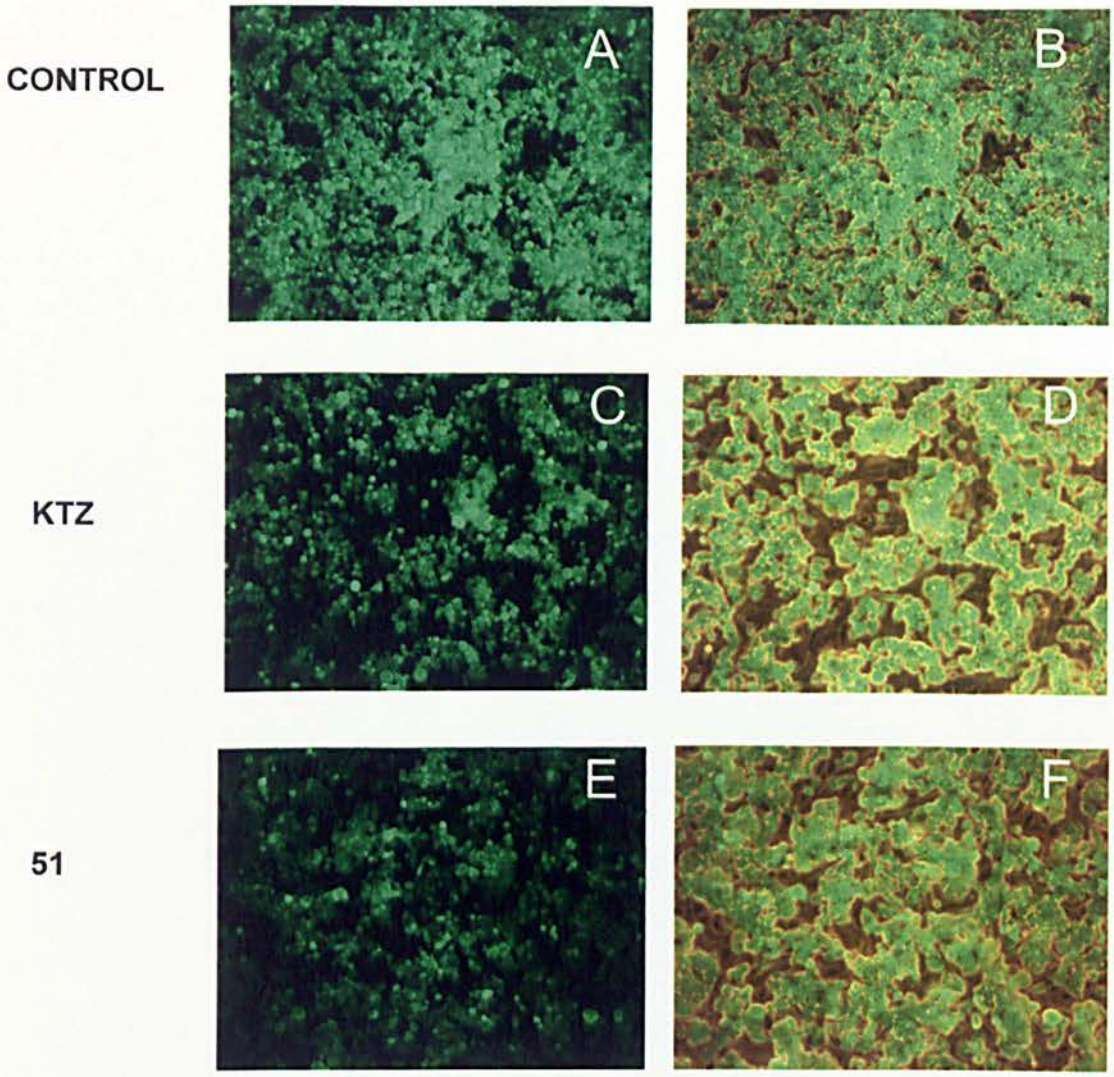

Fluorescence and phase-contrast-microscopy of PC3 cells attached to non-treated HUVEC monolayers. *PC3 cells were treated with CYP17 inhibitors for 24 hours. Fluorescently labelled PC3 cells (green) are attached to HUVEC monolayer (Right). (A-B) Un-treated PC3 cells (C-D) PC3 cells treated with KTZ (E-F) PC3 cells treated with compound 51. Images were acquired using a fluorescent microscope at X100 magnification. The images are qualitatively representative of three different experiments (n=3).*

APPENDIX 7

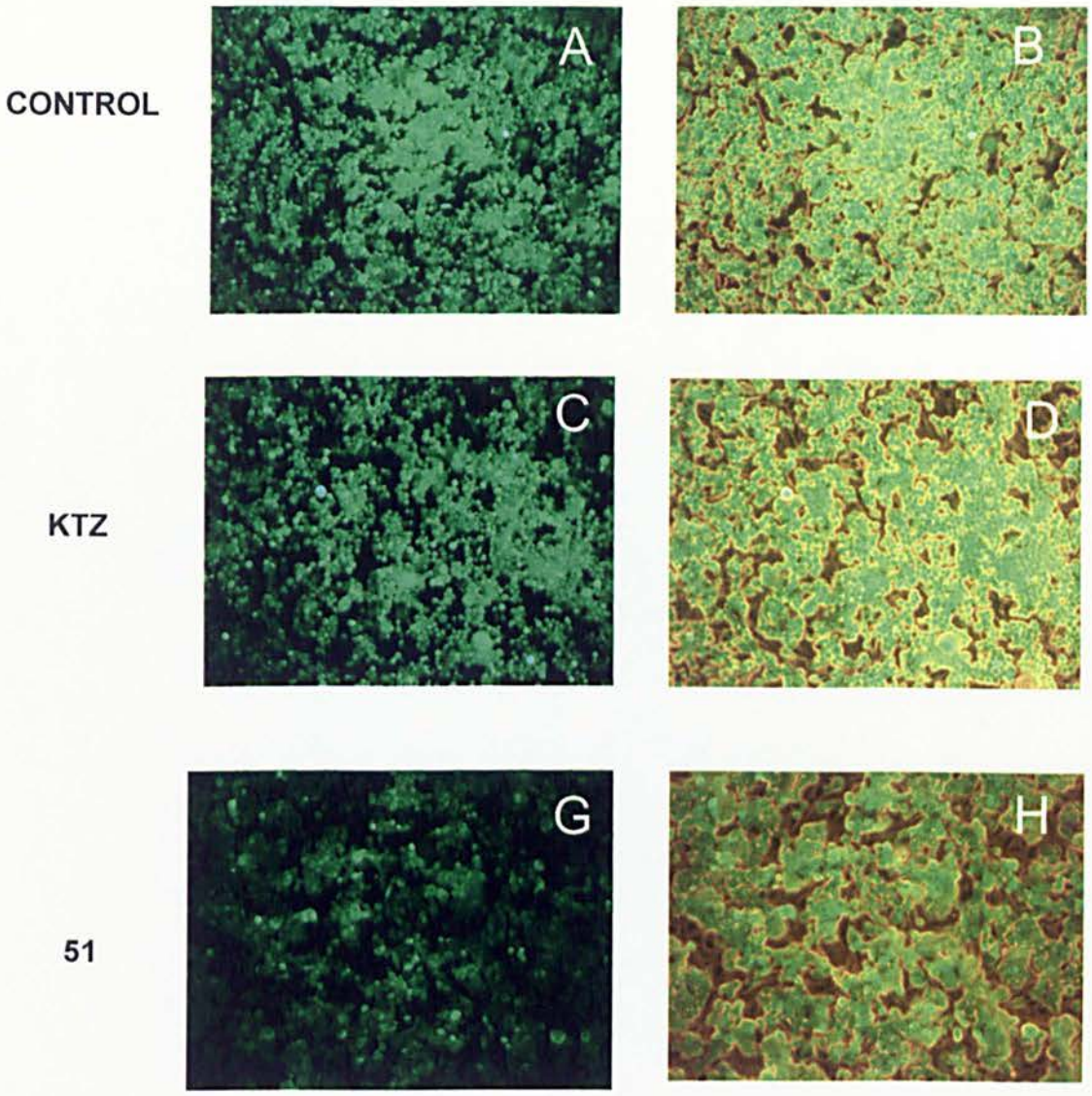

Fluorescence and phase-contrast-microscopy of PC3 cells attached to TNF-α-treated HUVEC monolayers. *PC3 cells were treated with CYP17 inhibitors for 24 hours. Fluorescently labelled PC3 cells (green) are attached to HUVEC monolayer (Right). (A-B) Un-treated PC3 cells (C-D) PC3 cells treated with KTZ (E-F) PC3 cells treated with compound 51. Images were acquired using a fluorescent microscope at X100 magnification. The images are qualitatively representative of three different experiments (n=3).*

APPENDIX 8

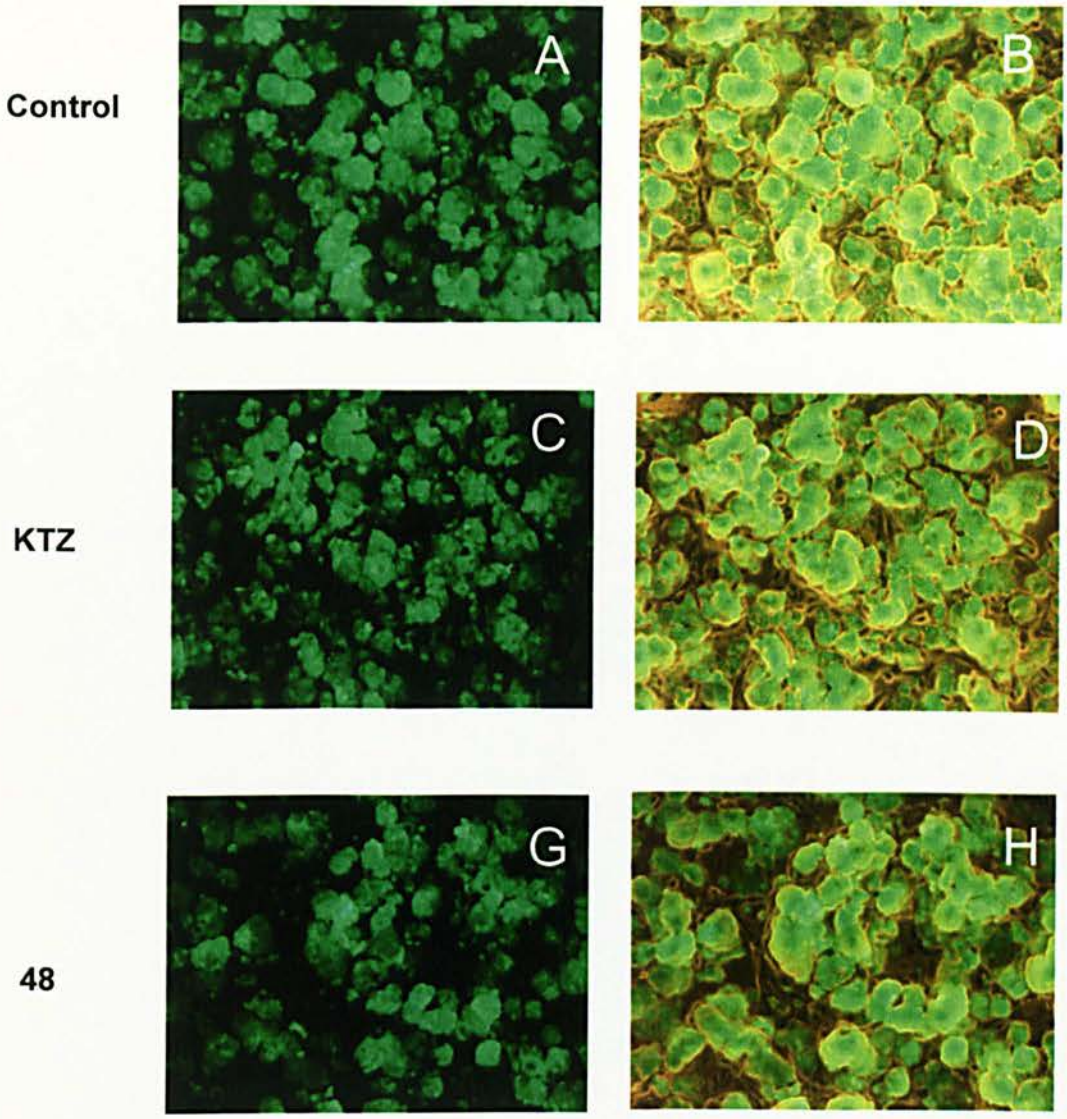

Fluorescence and phase-contrast-microscopy of MCF7 cells attached to non-treated HUVEC monolayers. *MCF7 cells were treated with CYP17 inhibitors for 24 hours. Fluorescently labelled PC3 cells (green) are attached to HUVEC monolayer (Right). (A-B) Un-treated MCF7 cells (C-D) MCF7 cells treated with KTZ (E-F) MCF7cells treated with compound 51. Images were acquired using a fluorescent microscope at X100 magnification. The images are qualitatively representative of three different experiments (n=3).*

APPENDIX 9

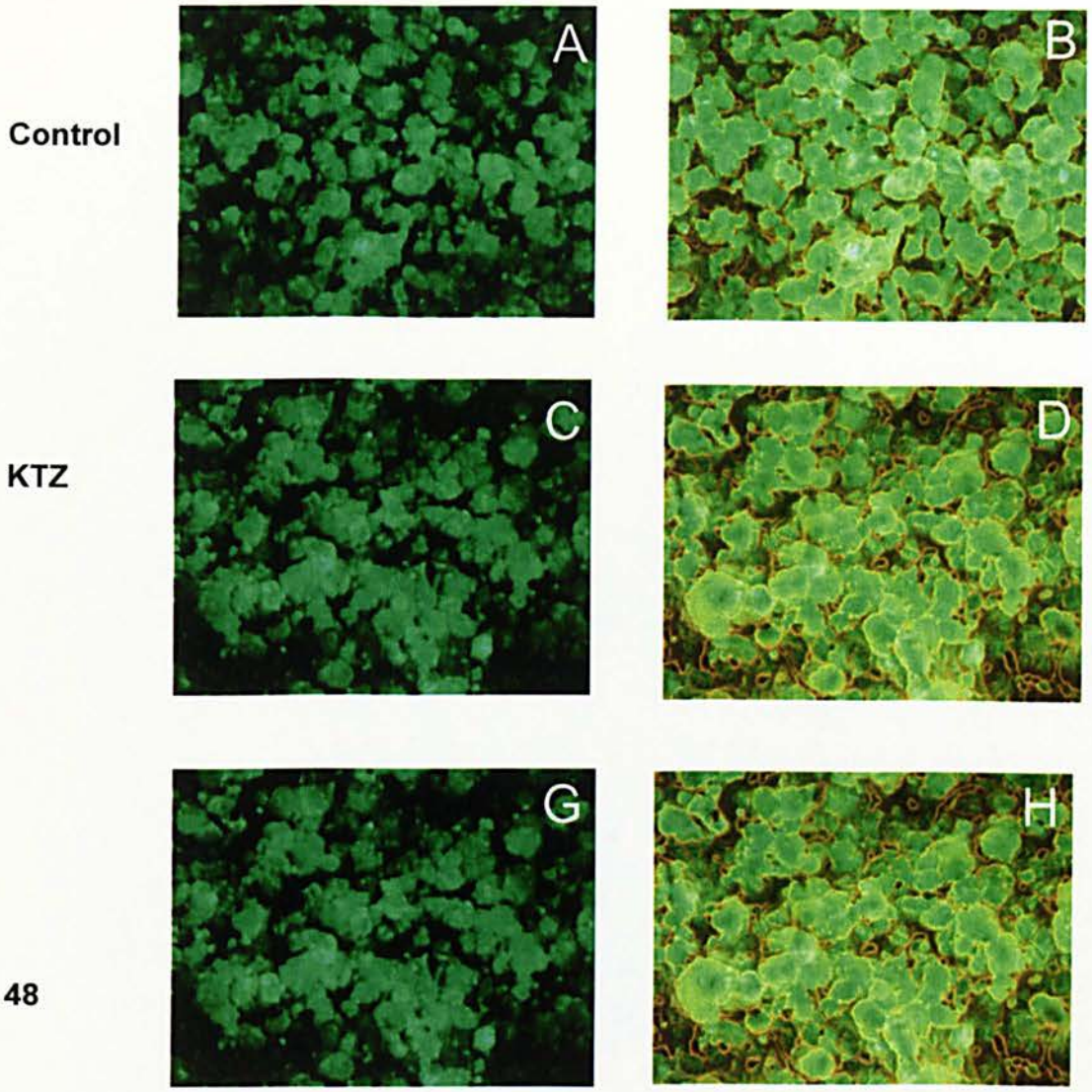

Fluorescence and phase-contrast-microscopy of MCF7 cells attached to TNF-α-treated HUVEC monolayers. *MCF7 cells were treated with CYP17 inhibitors for 24 hours. Fluorescently labelled PC3 cells (green) are attached to HUVEC monolayer (Right). (A-B) Un-treated MCF7 cells (C-D) MCF7 cells treated with KTZ (E-F) MCF7cells treated with compound 51. Images were acquired using a fluorescent microscope at X100 magnification. The images are qualitatively representative of three different experiments (n=3).*

APPENDIX 10

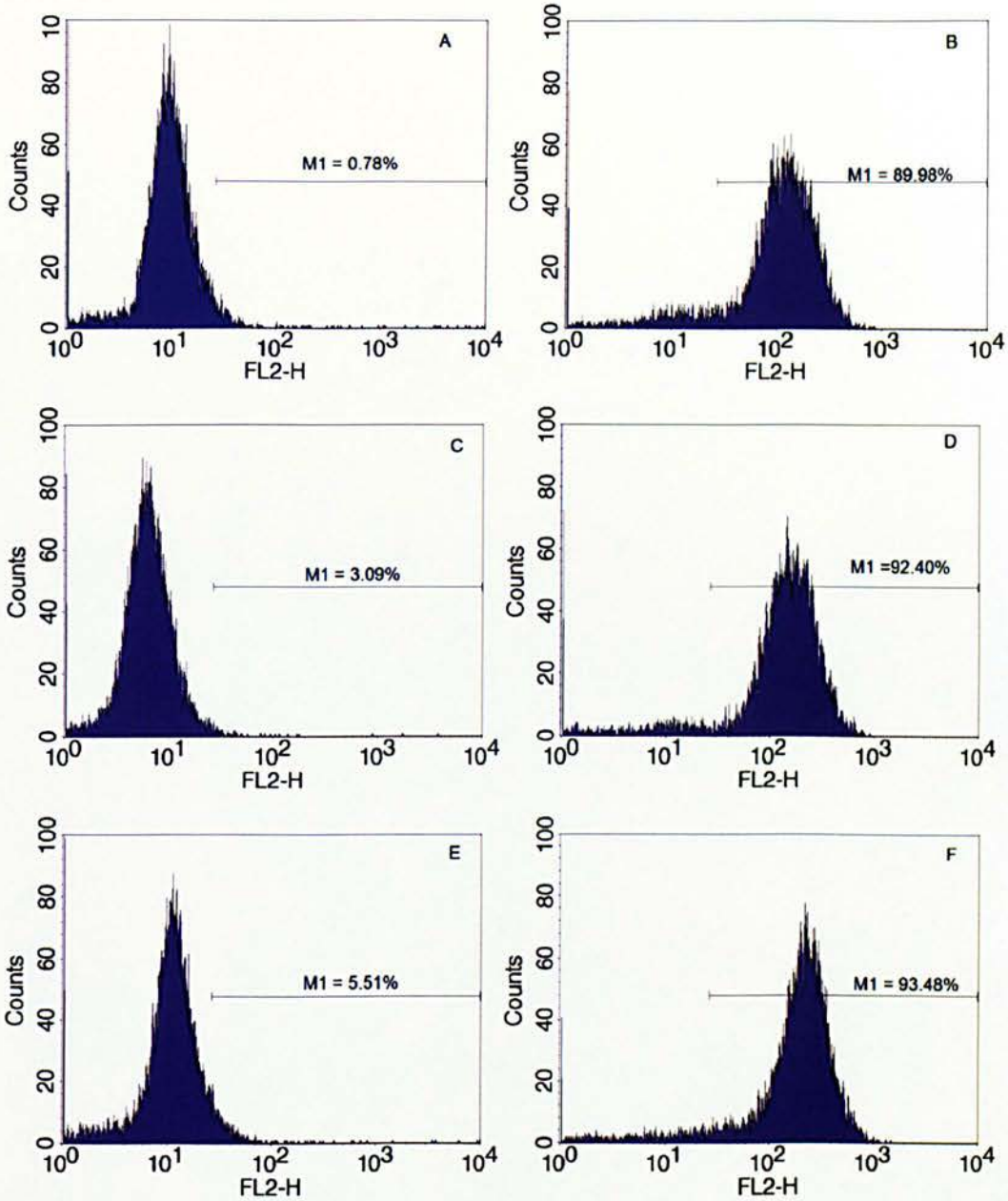

Titration of PE-Isotype control (left) and CD144 antibody (right). *The Isotype control and CD144 antibody was added in different dilutions for an hour. (A) Isotype control 1:100 (B) CD144 1: 100 (C) Isotype control 1:50 D) CD144 1:50 E) Isotype control 1:15 D) CD144 1:15. The marker, M1 values represent the percentage of 10,000 gated events.*

APPENDIX 11

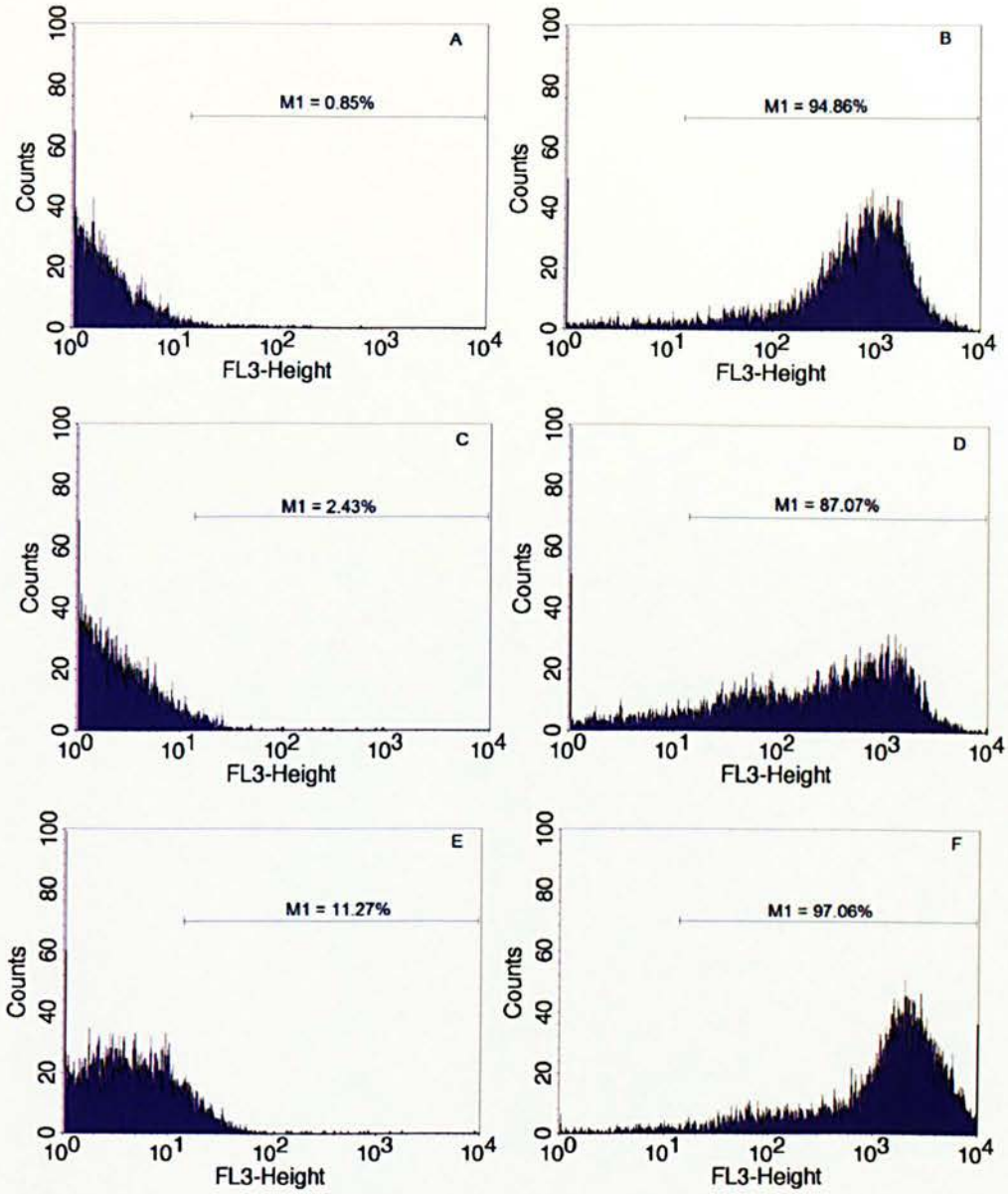

Titration of Isotype control (left) and CD54 (right). *The isotype control and CD54 antibody was used in different dilutions. (A) Isotype control 1:100 (B) CD54 1: 100 (C) Isotype control 1:50 D) CD 54 1:50 E) Isotype control 1:10 D) CD144 1:10. The marker, M1 values represent the percentage of 10,000 gated events.*